

Journal of Polymer Science

Part A-1: Polymer Chemistry

Contents

V. P. ZUBOV, L. I. VALUEV, V. A. KABANOV, and V. A. KARGIN: Effects of Complexing Agents in Radical Copolymerization	833
CHONGWON NAM, TETSUO KOSHIJIMA, EINOSUKE MURAKI, and TAKAMARO MAKU: Graft Copolymerization of Methyl Methacrylate onto Lignosulfonate by H_2O_2 -Fe(II) Redox System. I. Preparation and Characterization of the Graft Copolymer	855
KATSUKIYO ITO: Cross-Termination Rate Constants in Copolymerizations of Some Methacrylates and Styrene	867
TSUYOSHI MATSUMOTO, JUNJI FURUKAWA, and HIROHISA MORIMURA: Polymerization of Butadiene and Vinyl Ether with Catalyst Prepared from π -Allyl Nickel Halide and Organic Peroxide	875
HIDEMASA YAMAGUCHI, HIROSHI UENO, and YUJI MINOURA: Optically Active Copolyamides by Melt and Solution Condensation Polymerization	887
HIDEMASA YAMAGUCHI, HIROSHI UENO, and YUJI MINOURA: Optically Active Copolyamides by Interfacial Condensation Polymerization	897
HARUHIKO WATANABE and MASAO MURANO: γ -Ray-Induced Polymerization of α -Haloacrylic Acids	911
N. GRASSIE and J. G. SPEAKMAN: Thermal Degradation of Poly(alkyl Acrylates). I. Preliminary Investigations	919
N. GRASSIE, J. G. SPEAKMAN, and T. I. DAVIS: Thermal Degradation of Poly(alkyl Acrylates). II. Primary Esters: Ethyl, <i>n</i> -Propyl, <i>n</i> -Butyl, and 2-Ethylhexyl	931
N. GRASSIE and J. G. SPEAKMAN: Thermal Degradation of Poly(alkyl Acrylates). III. A Secondary Ester: Isopropyl Acrylate	949
HOWARD C. HAAS, RUBY L. MACDONALD, and ALAN N. SCHULER: Synthetic Thermally Reversible Gel Systems. VII	959
CHARLES E. CARRAHER, JR., and LARRY TORRE: Modification of Poly(vinyl Alcohol) Through Reaction with Phosphorus-Containing Reactants	975
CHARLES E. CARRAHER, JR., and GARY A. SCHERUBEL: Production of Organometallic Polymers by the Interfacial Technique. XX. Synthesis of Polyoxytannylalkylenes	983
R. BACSKAI, L. P. LINDEMAN, and J. Q. ADAMS: Preparation and Structure of Chlorinated Poly(vinyl Fluoride)	991

(continued inside)

ห้องสมุด ภาควิชาเคมี

Board of Editors: H. Mark • C. G. Overberger • T. G. Fox

Advisory Editors:

R. M. Fuoss • J. J. Hermans • H. W. Melville • G. Smets

Editor: C. G. Overberger **Associate Editor:** E. M. Pearce

Advisory Board:

T. Alfrey, Jr.	N. D. Field	R. W. Lenz	C. C. Price
W. J. Bailey	F. C. Foster	Eloisa Mano	B. Rånby
John Boor, Jr.	H. N. Friedlander	C. S. Marvel	J. H. Saunders
F. A. Bovey	K. C. Frisch	F. R. Mayo	C. Schuerch
J. W. Breitenbach	N. G. Gaylord	R. B. Mesrobian	W. H. Sharkey
W. J. Burlant	W. E. Gibbs	Donald Metz	V. T. Stannett
G. B. Butler	A. R. Gilbert	H. Morawetz	J. K. Stille
S. Bywater	M. Goodman	M. Morton	M. Szwarc
W. L. Carrick	J. E. Guillet	J. E. Mulvaney	A. V. Tobolsky
H. W. Coover, Jr.	George Hulse	S. Murahashi	E. J. Vandenberg
W. H. Daly	Otto Kauder	G. Natta	Herbert Vogel
F. Danusso	J. P. Kennedy	K. F. O'Driscoll	L. A. Wall
F. R. Eirich	W. Kern	S. Okamura	O. Wichterle
E. M. Fettes	J. Lal	P. Pino	F. H. Winslow

Contents (continued)

DINABANDHU PRAMANICK and SANTI R. PALIT: Studies in Some New Initiator Systems for Vinyl Polymerization. IV. Amino Acids as the Reducing Component.	1005
M. M. ISHANOV, U. A. AZIZOV, M. S. NIGMANKHODZHAYEVA, and KH. U. USMANOV: Radiation-Induced Crosslinking of Cellulose with Acrolein.	1013
V. V. KORSHAK, M. M. TEPLYAKOV, and R. D. FEDOROVA: Synthesis and Investigation of Polybenzimidazoles Containing Alkyl Substituents in Aromatic Nuclei.	1027
L. W. FROST and G. M. BOWER: Polyimidazopyrrolones and Related Polymers. I. Dianhydrides and o-Acetamidodiamines.	1045
KARL O. KNOLLMUELLER, ROBERT N. SCOTT, HERBERT KWASNIK, and JOHN F. SIECKHAUS: Icosahedral Carboranes. XVI. Preparation of Linear Poly-m-carboranylenesiloxanes.	1071

(continued on inside back cover)

The Journal of Polymer Science is published in four sections as follows: Part A-1, Polymer Chemistry, monthly; Part A-2, Polymer Physics, monthly; Part B, Polymer Letters, monthly; Part C, Polymer Symposia, irregular.

Published monthly by Interscience Publishers, a Division of John Wiley & Sons, Inc., covering one volume annually. Publication Office at 20th and Northampton Sts., Easton, Pa. 18042. Executive, Editorial, and Circulation Offices at 605 Third Avenue, New York, N. Y. 10016. Second-class postage paid at Easton, Pa. Subscription price, \$325.00 per volume (including Parts A-2, B, and C). Foreign postage \$15.00 per volume (including Parts A-2, B, and C).

Copyright © 1971 by John Wiley & Sons, Inc. All rights reserved. No part of this publication may be reproduced by any means, nor transmitted, or translated into a machine language without the written permission of the publisher.

Effects of Complexing Agents in Radical Copolymerization*

V. P. ZUBOV, L. I. VALUEV, V. A. KABANOV, and V. A. KARGIN,
Lomonosov State University, Moscow, USSR

Synopsis

Radical copolymerization of methyl methacrylate (MMA, M_1) with various monomers has been studied in presence of modifiers, i.e., complexing agents (CA): $ZnCl_2$, $AlCl_3$, $AlBr_3$, $Al(C_2H_5)_2Cl$, forming coordinate complexes with ester group of the monomer and of the propagating radical. The comonomers of the first group form complexes of similar structure and stability as MMA, methyl acrylate, or butyl acrylate. The comonomers of the second group do not form complexes with the modifiers (vinylidene chloride, 2,6-dichlorostyrene, *p*-chlorostyrene, styrene). For all systems studied the copolymer composition follows the Mayo-Lewis equation. In the first group of the systems the effective reactivity ratios (r_1 , r_2) approach unity with increase of the CA molar content ($r_1 = r_2 \approx 1$ at $[CA]/[MMA] + [MA] \geq 0.3$). In the second group of the systems the values of r_1 either increase to a limit value (at $[CA]/[MMA] \geq 0.3$), pass through maximum, or decrease to a limiting value with the CA molar content. The values of r_2 decrease in all systems. The character of variation of r_1 and r_2 has been explained in terms of effects of the CA's on reactivity of MMA and PMMA radical. The equations for the copolymer compositions in these systems have been derived.

The salts of nontransition metals ($LiCl$, $MgCl_2$, $ZnCl_2$, $AlCl_3$, $AlBr_3$) forming complexes with functional groups of vinyl monomers considerably effect the rate of radical polymerization and composition of the copolymers.¹⁻¹² The present paper deals with the studies of the mechanism of these processes. For this purpose methyl methacrylate (MMA), a monomer having a functional group can interact with the complexing agents (CA) like $ZnCl_2$, $AlBr_3$, $Al(C_2H_5)_2Cl$, was copolymerized with other monomers of different types. In the first group of the systems, the comonomers form complexes of similar structure and stability as MMA [methyl acrylate (MA), butyl acrylate (BA)]. The ability to form complexes in the second group of comonomers [vinylidene chloride (VDC), styrene (St), *p*-chlorostyrene (*p*-CST), and 2,6-dichlorostyrene (2,6-DCST)] is much lower than that of MMA.

EXPERIMENTAL

The monomers were purified according to accepted techniques, then carefully dried first over metallic calcium and then over calcium hydride

* This paper was presented at the IUPAC International Symposium on Macromolecular Chemistry, Budapest, 1969.

in vacuo. AlBr_3 was purified by multiple vacuum distillation, AlCl_3 by multiple distillation in argon atmosphere. ZnCl_2 and $\text{Al}(\text{C}_2\text{H}_5)_2\text{Cl}$ were reagent grade materials and were used without further purification. The criterion of purity of the reagents was formation of colorless complex on mixing of the monomers with the complexing agents. The mixing was carried out in an all-glass apparatus *in vacuo*. Polymerization was initiated either photochemically ($\lambda = 313 \text{ m}\mu$) or by thermal decomposition of azobisisobutyronitrile (AIBN). Preparation of the reaction systems was carried out in the dark because in some of the systems diffusing light causes polymerization to occur. In the dark, the uninitiated reaction was not observed. The polymerization rates were measured dilatometrically and gravimetrically. The polymers were separated from the complexing agents by pouring the reaction mixture into a mixture of methanol and hydrochloric acid and then reprecipitated several times. Compositions of the copolymers MMA-VDC, MMA-*p*-CST and MMA-2,6-DCST were determined by analysis for chlorine by Schöniger's method.¹³ The composition of MMA-MA copolymers was determined by means of infrared spectroscopy by the ratio of optical densities of deformation modes of CH_3 - and $-\text{CH}_2$ - groups¹⁴ at 1486 and 1451 cm^{-1} and the composition of the MMA-BA copolymers by a NMR method based on the ratio of the areas under the peaks of $-\text{O}-\text{CH}_3$ and $-\text{O}-\text{CH}_2-$ protons.¹⁵ The compositions of the MMA-St copolymers were determined by elementary analysis and from the NMR spectra on the basis of the ratio of the areas under the peaks of benzene ring protons to the total area under the spectrum.¹⁶ The NMR spectra were recorded on a NMR spectrometer (JNM-C-60-HL, JEOL) in 8% solution in CCl_4 and in 6% solutions of the MMA-BA copolymers in CHCl_3 .

In all cases the dependence of the copolymer composition on the composition of the feed formally obeyed Mayo-Lewis' equation. The copolymerization reactivity ratios (r_1, r_2) were determined by graphical¹⁷ and analytical¹⁸ methods.

RESULTS

Compositions of the MMA-MA copolymers prepared in the presence of ZnCl_2 and AlBr_3 approach the composition of the monomeric mixture with increase of the complexing agent (CA) content in the reaction system and become practically equal to it at comparatively small CA content, i.e.; $[\text{CA}]/[\text{MMA}] + [\text{MA}] \geq 0.2-0.3$, when a considerable fraction of the monomer molecules is still uncomplexed. In other words, the apparent copolymerization reactivity ratios become equal to unity and remain unchanged at further increase of CA concentration (Table I, Fig. 1). A similar result has been observed in the MMA-BA system (Table I). Establishment of the limit values of the copolymerization constants at $[\text{CA}]/[\text{M}_1] + [\text{M}_2] \simeq 0.2-0.3$ indicates that above this ratio practically all the propagation occurs by a mechanism involving CA participation.

TABLE I. Copolymerization of MMA (M_1) with MA and BA in Presence of CA's

CA	M_2	Polymerization conditions	M_2 (mole fraction)			r_1	r_2
			$\frac{[CA]}{[M_1] + [M_2]}$	in the monomer mixture	m_2 in the copolymer		
ZnCl ₂	MA	[AIBN] = 5×10^{-3} mole/l., 50°C	0	0.10	0.05	2.23 ± 0.13	0.36 ± 0.1
				0.20	0.10		
				0.25	0.13		
				0.30	0.16		
				0.40	0.23		
				0.50	0.32		
			0.15	0.10	0.08	1.33 ± 0.03	0.70 ± 0.03
				0.20	0.16		
				0.30	0.24		
				0.40	0.32		
				0.50	0.43		
				0.60	0.53		
			0.33	0.10	0.09	1.11 ± 0.10	1.09 ± 0.12
				0.20	0.19		
				0.30	0.29		
				0.40	0.40		
				0.50	0.50		
				0.45	0.11		
			0.45	0.20	0.20	0.91 ± 0.03	0.88 ± 0.09
				0.30	0.30		
				0.40	0.39		
				0.50	0.49		
				0.64	0.11		
				0.20	0.20		
0.64	0.30	0.30	0.99 ± 0.05	0.93 ± 0.1			
	0.40	0.41					
	0.50	0.50					
	0.10	0.05					
	0.20	0.10					
	0.30	0.16					
AlBr ₃	MA	UV ($\lambda = 313$ $m\mu$), 48°C	0.075	0.10	0.06	2.30 ± 0.15	0.45 ± 0.15
				0.20	0.13		
				0.30	0.20		
				0.40	0.29		
				0.50	0.40		
				0.15	0.09		
			0.15	0.20	0.19	1.75 ± 0.04	0.78 ± 0.05
				0.30	0.28		
				0.50	0.48		
				0.40	0.11		
				0.20	0.20		
				0.30	0.30		
0.40	0.50	0.51	1.11 ± 0.04	0.91 ± 0.10			
	0.20	0.20					
	0.30	0.30					
	0.50	0.51					
	0.96	0.96					
	0.05	0.11					
ZnCl ₂	BA	[AIBN] = 5×10^{-3} mole/l., 50°C	0	0.40	0.25	0.96 ± 0.05	0.96 ± 0.11
			0.15	0.40	0.33		
			0.33	0.40	0.35		
			0.45	0.40	0.39		
			0.50	0.51			

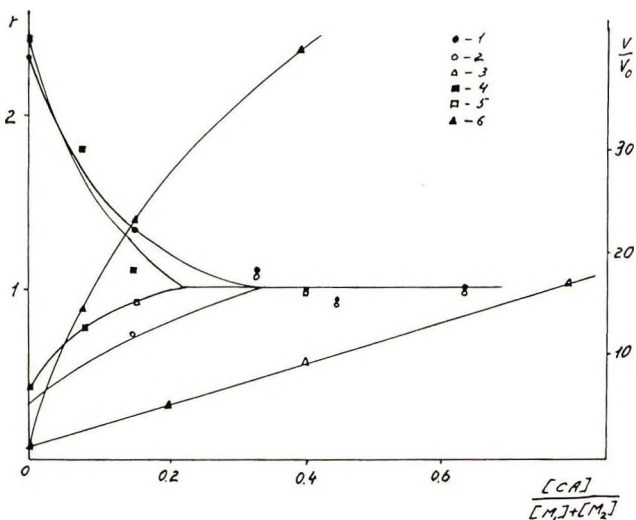


Fig. 1. Dependence of the copolymerization parameters and relative copolymerization rate (V/V_0) where V_0 is the rate of polymerization without CA in the system MMA(M_1)-MA in presence of CA's on the ratio $[CA]/([MMA] + [MA])$: (1) r_1 , (2) r_2 , and (3) V/V_0 at $[MMA]:[MA] = 1:1$, 50°C , $[AIBN] = 5 \times 10^{-3}$ mole/l., CA = ZnCl_2 ; (4) r_1 , (5) r_2 , and (6) V/V_0 at $[MMA]:[MA] = 1:1$, 48°C , UV ($\lambda = 313\text{m}\mu$), CA = AlBr_3 .

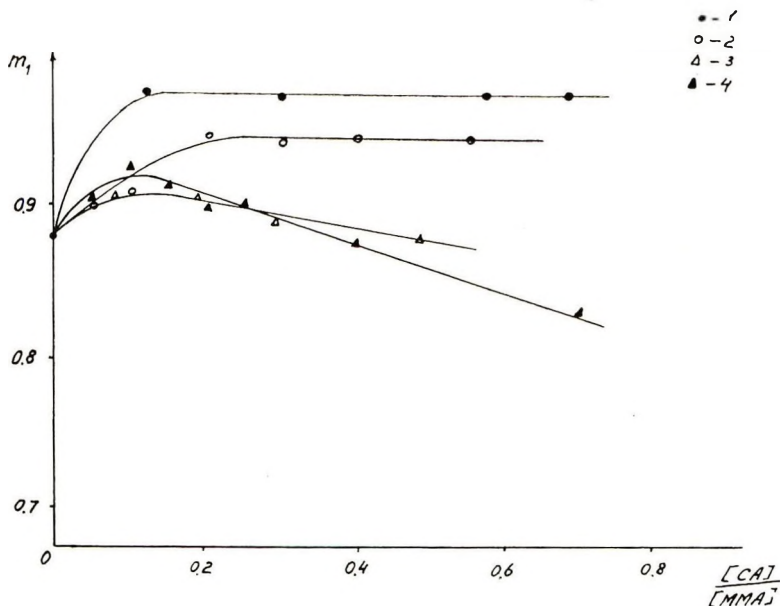


Fig. 2. Dependence of MMA content in MMA-VDC copolymer on the ratio $[CA]/[MMA]$: (1) CA = ZnCl_2 , 50°C , $[AIBN] = 5 \times 10^{-3}$ mole/l.; (2) CA = $\text{Al}(\text{C}_2\text{H}_5)_2\text{Cl}$, UV ($\lambda = 313\text{m}\mu$), 20°C ; (3) CA = AlBr_3 , UV ($\lambda = 313\text{m}\mu$), 20°C ; (4) CA = AlCl_3 , UV ($\lambda = 313\text{m}\mu$), 20°C .

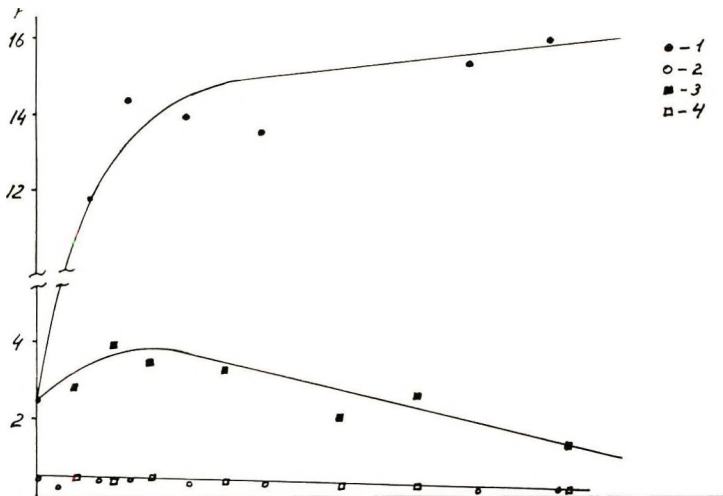


Fig. 3. Dependence of the copolymerization parameters in system MMA(M_1)-VDC on the ratio $[CA]/[MMA]$: (1) r_1 and (2) r_2 at 50°C, $[AIBN] = 5 \times 10^{-3}$ mole/l., CA = $ZnCl_2$; (3) r_1 and (4) r_2 at 20°C, UV ($\lambda = 313m\mu$), CA = $AlCl_3$.

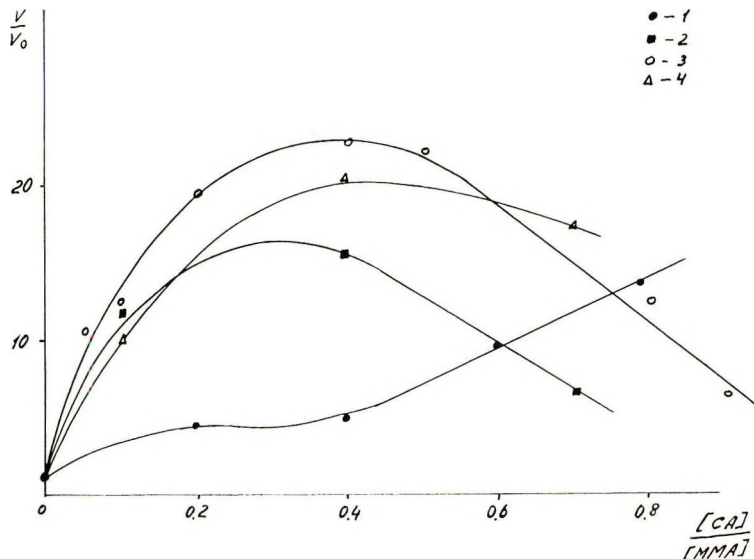


Fig. 4. Dependence of the relative copolymerization rate in system MMA-VDC on the ratio $[CA]/[MMA]$: (1) $[MMA]:[VDC] = 2:1$, CA = $ZnCl_2$; (2) $[MMA]:[VDC] = 10:1$, CA = $AlCl_3$; (3) $[MMA]:[VDC] = 3:1$, CA = $AlCl_3$; (4) $[MMA]:[VDC] = 1:1$, CA = $AlCl_3$.

Figure 1 also shows the relative rates of the copolymerization in the MMA-MA (1:1) system. In the region of the smaller CA content, the change in relative rate is paralleled by a change in the copolymerization constants. At higher CA contents, the copolymerization rates continue to

TABLE II
 Copolymerization of MMA (M_1) with VDC in Presence of CA's

CA	Polymerization conditions	M_2 (mole fraction) $\frac{[CA]}{[MMA]}$	m_1 in monomer mixture	m_2 in co-polymer	r_1	r_2
ZnCl ₂	[AIBN] = 5×10^{-3} mole/l., 50°C	0	0.10	0.05	2.54 ± 0.20	0.5 ± 0.15
			0.17	0.08		
			0.25	0.12		
			0.29	0.14		
			0.30	0.15		
			0.33	0.17		
		0.50	0.30			
		0.03	0.10	0.02	5.3 ± 0.4	0.18 ± 0.17
			0.20	0.04		
			0.30	0.08		
			0.45	0.14		
			0.55	0.21		
		0.07	0.10	0.01	11.8 ± 0.8	0.41 ± 0.22
			0.20	0.02		
			0.30	0.04		
			0.40	0.07		
		0.12	0.10	0.01	14.5 ± 2.5	0.4 ± 0.2
			0.20	0.01		
			0.25	0.03		
			0.29	0.03		
			0.38	0.04		
		0.20	0.10	0.01	13.9 ± 0.9	0.21 ± 0.07
			0.20	0.01		
			0.30	0.03		
			0.40	0.05		
			0.45	0.07		
		0.30	0.10	0.02	13.5 ± 2.4	0.3 ± 0.2
			0.20	0.02		
			0.29	0.03		
			0.33	0.04		
			0.50	0.10		
		0.57	0.10	0.02	15.7 ± 1.2	0.1 ± 0.2
			0.20	0.02		
			0.29	0.03		
			0.33	0.04		
			0.50	0.08		
		0.68	0.10	0.02	16.0 ± 3.0	0.2 ± 0.2
			0.20	0.02		
			0.29	0.03		
			0.33	0.04		
			0.50	0.09		

TABLE II (continued)
 Copolymerization of MMA (M_1) with VDC in Presence of CA's

CA	Polymerization conditions	M_2 (mole fraction)		r_1	r_3	
		$\frac{[CA]}{[MMA]}$	$\frac{m_2}{m_1}$ in monomer mixture			
AlCl ₃	UV ($\lambda = 313 \text{ m}\mu$), 20°C	0	0.09	0.04	2.5 ±	0.4 ±
			0.25	0.12		
			0.40	0.21		
			0.50	0.29		
			0.60	0.37		
		0.05	0.75	0.54	0.1	0.05
			0.15	0.06		
			0.28	0.13		
			0.45	0.24		
			0.65	0.44		
		0.10	0.09	0.03	2.82 ±	0.54 ±
			0.25	0.07		
			0.40	0.12		
			0.50	0.18		
			0.60	0.26		
		0.15	0.75	0.41	0.06	0.04
			0.13	0.04		
			0.25	0.09		
			0.50	0.25		
			0.65	0.39		
		0.25	0.13	0.04	3.5 ±	0.52 ±
			0.25	0.10		
			0.50	0.24		
			0.65	0.37		
			0.37	0.37		
		0.40	0.13	0.04	3.3 ±	0.37 ±
			0.25	0.10		
			0.50	0.24		
			0.65	0.37		
			0.37	0.37		
		0.50	0.08	0.04	0.2	0.09
			0.25	0.13		
			0.40	0.21		
			0.50	0.27		
			0.60	0.34		
		0.70	0.75	0.44	2.02 ±	0.13 ±
			0.13	0.05		
			0.25	0.11		
			0.50	0.23		
			0.65	0.37		
		0.50	0.13	0.05	0.07	0.03
			0.25	0.11		
			0.50	0.23		
			0.65	0.37		
			0.37	0.37		
		0.70	0.09	0.07	2.6 ±	0.22 ±
			0.25	0.17		
			0.40	0.22		
0.50	0.32					
0.60	0.37					
0.70	0.75	0.46	0.1	0.03		
	0.09	0.07				
	0.25	0.17				
	0.40	0.22				
	0.50	0.32				

increase despite the constancy of r_1 and r_2 . The increase in the rate in the region of high $[CA]/[M_1] + [M_2]$ ratios is probably due to a decrease of the termination constants similarly as described by Lachinov et al.¹⁹

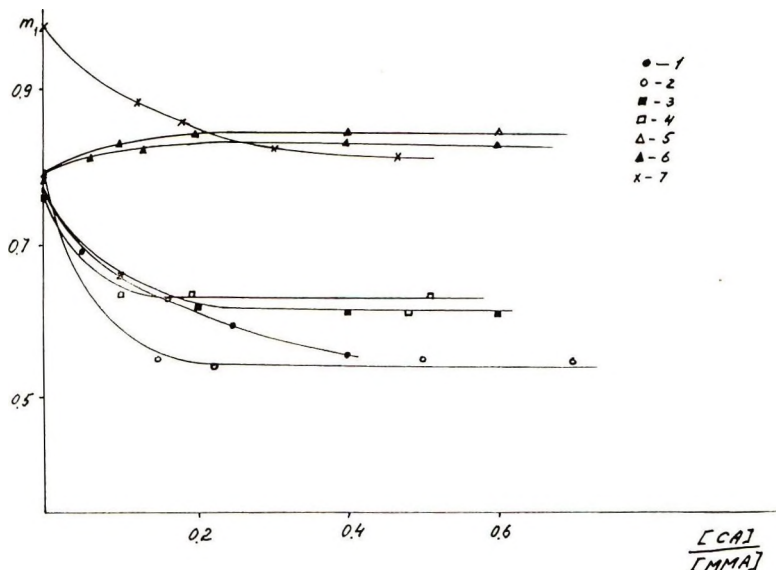


Fig. 5. Dependence of MMA content in the MMA(M_1) copolymers on the ratio $[CA]/[MMA]$: (1) $M_2 = St$, $[M_1]:[M_2] = 5.67$, $CA = ZnCl_2$, $[AIBN] = 5 \times 10^{-3}$ mole/l., $50^\circ C$; (2) $M_2 = St$, $[M_1]:[M_2] = 3.0$, $CA = Al(C_2H_5)_2Cl$, UV ($\lambda = 313m\mu$), $20^\circ C$; (3) $M_2 = p\text{-CSt}$, $[M_1]:[M_2] = 5.67$, $CA = ZnCl_2$, $[AIBN] = 5 \times 10^{-3}$ mole/l., $50^\circ C$; (4) $M_2 = p\text{-CSt}$, $[M_1]:[M_2] = 5.67$, $CA = Al(C_2H_5)_2Cl$, UV, ($\lambda = 313m\mu$), $20^\circ C$; (5) $M_2 = 2,6\text{-DCSt}$, $[M_1]:[M_2] = 1.28$, $CA = ZnCl_2$, $[AIBN] = 5 \times 10^{-3}$ mole/l., $50^\circ C$; (6) $M_2 = 2,6\text{-DCSt}$, $[M_1]:[M_2] = 1.5$, $CA = Al(C_2H_5)_2Cl$, UV ($\lambda = 313m\mu$), $20^\circ C$; (7) $M_2 = 2,6\text{-DCSt}$, $[M_1]:[M_2] = 5.57$, $CA = AlCl_3$, UV ($\lambda = 313m\mu$), $20^\circ C$.

Figure 2 shows the dependence of the copolymer composition in the system MMA(M_1)–VDC at fixed monomer mixture composition (MMA:VDC = 3:1) on CA content. One can see that the effects depend on the nature of CA. Introduction of $ZnCl_2$ and $Al(C_2H_5)_2Cl$ brings about an increase of MMA content in the copolymer, which attains a constant value at $[CA]/[MMA] = 0.2\text{--}0.3$. But in the case of aluminum halides, the MMA content in the copolymer first increases and then decreases, passing through a maximum. The apparent values of r_1 and r_2 for the typical systems MMA–VDC– $ZnCl_2$ and MMA–VDC– $AlCl_3$ are shown in Table II and in Figure 3. As can be seen, r_1 similarly increases and then either remains constant ($ZnCl_2$) or decreases ($AlCl_3$) with CA content; r_2 decreases in the whole range of CA concentrations. The nonlinear character of r_1 variation with $ZnCl_2$ content in the system MMA–VDC– $ZnCl_2$ shows that linear extrapolation of the results obtained at low $[ZnCl_2]$ to the 1:1 complex, based on the assumption that the only effect of $ZnCl_2$ is activation of MMA,⁴ is invalid.

The character of r_1 variation indicates that in these systems all additions to MMA radicals also occur with CA participation at CA concentrations lower than stoichiometric (Fig. 4). At low CA content, the copolymeri-

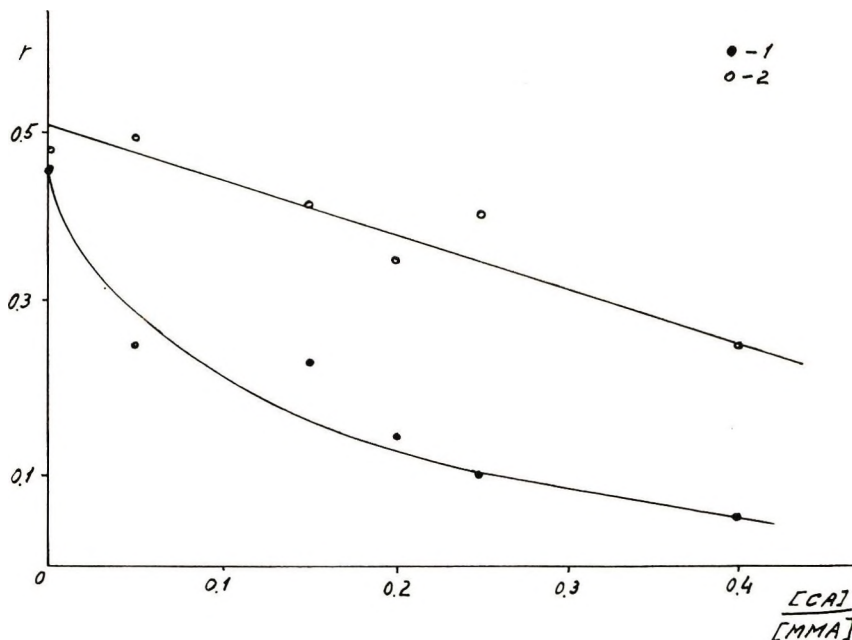


Fig. 6. Dependence of the copolymerization parameters in system MMA(M_1)-St on the ratio $[CA]/[MMA]$. $1-r_1$, $2-r_2$, $[AIBN] = 5 \cdot 10^{-3}$ mole/l., $t = 50^\circ\text{C}$, $CA = \text{ZnCl}_2$.

zation rates are changed (increased) in a parallel way with r_1 . In the region of high CA content the copolymerization rates are either decreased, though at somewhat higher CA concentrations than r_1 is decreased (when CA is AlCl_3) or continuously increased (when CA is ZnCl_2). The difference again is probably due to the effects of CA on termination constants.

In order to clarify further the mechanism of the process it was also of interest to investigate the role of the nature of the second monomer on the parameters of radical copolymerization in presence of CA. The copolymerization of MMA with styrene, *p*-chlorostyrene and 2,6-dichlorostyrene as the monomers of the similar structure but different polarization of the double bond has been studied. The e values for St and *p*-CSt are equal to -0.8 and -0.3 , respectively.²⁰ The accepted e value for 2,6-DCSt is ~ 0.1 (close to the value of 2,5-dichlorostyrene), because calculation from the copolymerization constants in the system MMA(M_1)-2,6-DCSt ($r_1 = 2.05$, $r_2 = 0.12$) gives too high a value ($e_2 = +2$) due to steric hindrance in homopropagation for 2,6-DCSt,²¹ which are not taken into account in the Q- e scheme.

Figure 5 shows the dependence of the copolymer composition for the monomer pairs MMA-St, MMA-*p*-CSt, and MMA-2,6-DCSt on CA concentration at fixed composition of the feed. In the systems MMA-2,6-DCSt- ZnCl_2 and MMA-2,6-DCSt- $\text{Al}(\text{C}_2\text{H}_5)_2\text{Cl}$, the molar MMA content in the copolymer increases with an increase in CA concentration; in the other systems [MMA-St- ZnCl_2 , MMA-St- $\text{Al}(\text{C}_2\text{H}_5)_2\text{Cl}$, MMA-

TABLE III
Copolymerization of MMA(M₁) with St in Presence of ZnCl₂

Polymerization conditions	$\frac{[\text{ZnCl}_2]}{[\text{MMA}]}$	M ₂ (mole fraction) in monomer mixture	m ₂ in copolymer	r ₁	r ₂	r ₁ r ₂
[AIBN] = 5 × 10 ⁻³ mole/l., 50°C	0	0.05	0.10	0.45 ± 0.01	0.47 ± 0.03	0.212
		0.10	0.18			
		0.15	0.23			
		0.20	0.27			
		0.25	0.33			
		0.29	0.35			
		0.40	0.43			
		0.50	0.50			
	0.05	0.05	0.15	0.25 ± 0.02	0.49 ± 0.03	0.122
		0.10	0.25			
		0.15	0.31			
		0.65	0.61			
		0.70	0.67			
	0.15	0.05	0.26	0.23 ± 0.05	0.41 ± 0.1	0.094
		0.10	0.31			
		0.15	0.37			
		0.65	0.63			
		0.70	0.65			
	0.20	0.14	0.36	0.15 ± 0.02	0.37 ± 0.06	0.056
		0.20	0.39			
		0.25	0.45			
		0.29	0.45			
		0.40	0.50			
		0.50	0.54			
	0.25	0.05	0.26	0.10 ± 0.01	0.40 ± 0.08	0.040
		0.10	0.35			
		0.15	0.41			
		0.65	0.61			
0.70		0.63				
0.40	0.05	0.36	0.056 ± 0.003	0.25 ± 0.03	0.014	
	0.10	0.42				
	0.14	0.45				
	0.15	0.45				
	0.20	0.44				
	0.25	0.47				
	0.29	0.49				
	0.50	0.55				
	0.65	0.59				
	0.70	0.61				

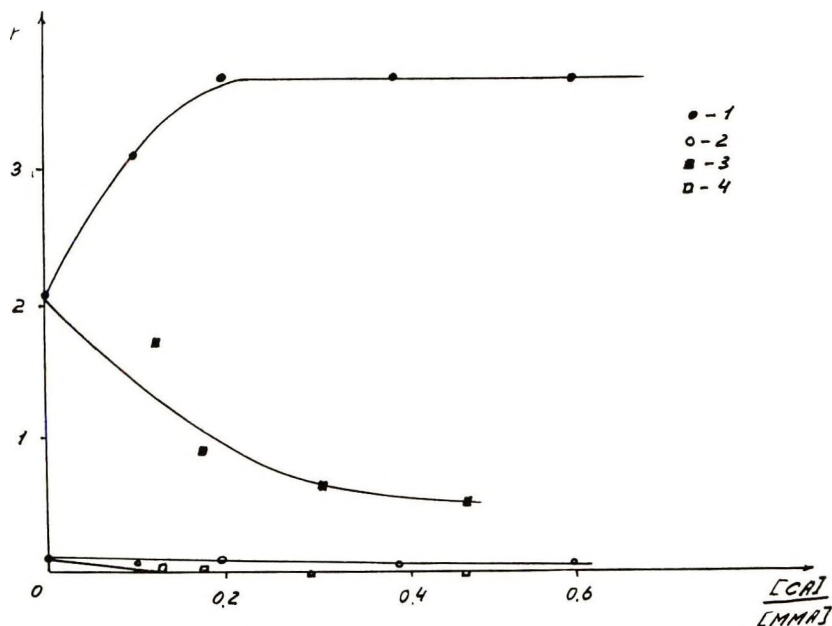


Fig. 7. Dependence of the copolymerization parameters in the system MMA(M_1)-2,6-DCSt on the ratio $[CA]/[MMA]$: (1) r_1 and (2) r_2 at CA = ZnCl₂, [AIBN] = 5×10^{-3} mole/l., 50°C; (3) r_1 and (4) r_2 at CA = AlCl₃, UV ($\lambda = 313 \text{ m}\mu$), 20°C.

p -CSt-ZnCl₂, MMA-2,6-DCSt-AlCl₃] it decreases. Despite the differences in the direction of the changes of the copolymer compositions, in all cases the latter approach limiting values at relatively low CA content.

Attempts to copolymerize MMA with St and p -CSt in presence of aluminum halides failed because these compounds cause fast cationic polymerization of St and p -CSt even in the presence of an excess of MMA.

The copolymerization parameters have been determined in the characteristic systems MMA-St-ZnCl₂, MMA-2,6-DCSt-ZnCl₂, and MMA-2,6-DCSt-AlCl₃ (MMA = M_1 , see Tables III and IV and Figs. 6 and 7).

The r_1 and r_2 are in MMA-St system decrease with decreasing ZnCl₂ and the product $r_1 r_2$ becomes very low; this is usually related to a high alternating tendency in the copolymer. The structure of the copolymers has been checked by means of NMR. Figure 8 shows the spectra of the copolymers prepared in presence of ZnCl₂ (Fig. 8a) and Al(C₂H₅)₂Cl (Fig. 8b). For the sake of comparison NMR spectra of the practically alternating copolymer prepared¹¹ in presence of Al(C₂H₅)_{1.5}Cl_{1.5} (Fig. 8c) and of a conventional radical copolymer (Fig. 8d) are reproduced. All the copolymers have 1:1 composition. As can be seen from Figure 8, the spectra of the copolymers prepared with ZnCl₂ and Al(C₂H₅)Cl differ from the conventional random copolymer and show characteristic splitting of the α -methyl and methoxyl protons similar to that in the alternating copolymer. The copolymerization rates are strongly increased with ZnCl₂ in the system (Fig. 9).

TABLE IV
Copolymerization of MMA (M_1) with 2,6-DCSt in Presence of CA's

CA	Polymerization conditions	$\frac{[CA]}{[MMA]}$	M_2 in monomeric mixture	m_{12} copolymer	r_1	r_2		
ZnCl ₂	[AIBN] = 5×10^{-3} mole/l, 50°C	0	0.20	0.10	2.05 ± 0.04	0.12 ± 0.02		
			0.28	0.13				
			0.33	0.15				
			0.44	0.21				
		0.1	0.20	0.07	3.10 ± 0.24	0.05 ± 0.01		
			0.28	0.10				
			0.33	0.12				
			0.44	0.17				
		0.2	0.20	0.06	3.72 ± 0.04	0.09 ± 0.01		
			0.28	0.09				
			0.33	0.11				
			0.44	0.16				
		0.4	0.20	0.06	3.68 ± 0.1	0.09 ± 0.03		
			0.28	0.09				
			0.33	0.11				
			0.44	0.16				
		0.6	0.20	0.06	3.68 ± 0.1	0.09 ± 0.03		
			0.28	0.09				
			0.33	0.11				
			0.44	0.16				
		AlCl ₃	UV ($\lambda = 313$ $m\mu$), 20°C	0.126	0.15	0.11	1.76 ± 0.44	0.42 ± 0.30
					0.21	0.16		
					0.47	0.32		
					0.60	0.35		
0.18	0.16			0.15	0.89 ± 0.12	-0.04 ± 0.24		
	0.26			0.23				
	0.46			0.36				
	0.62			0.35				
0.31	0.15			0.18	0.62 ± 0.07	-0.18 ± 0.17		
	0.28			0.24				
	0.49			0.34				
	0.56			0.37				
0.47	0.15			0.19	0.49 ± 0.16	-0.30 ± 0.17		
	0.40			0.35				
	0.52			0.22				
	0.60			0.38				

TABLE V
Effects of CA on C=O Band in the Infrared Spectrum of the MMA Complex

CA	ν , cm^{-1}	$\Delta\nu$, cm^{-1}
—	1725	0
Al(C ₂ H ₅)Cl	1625	-100
ZnCl ₂	1612	-113
AlCl ₃	1580	-145
AlBr ₃	1590	-135

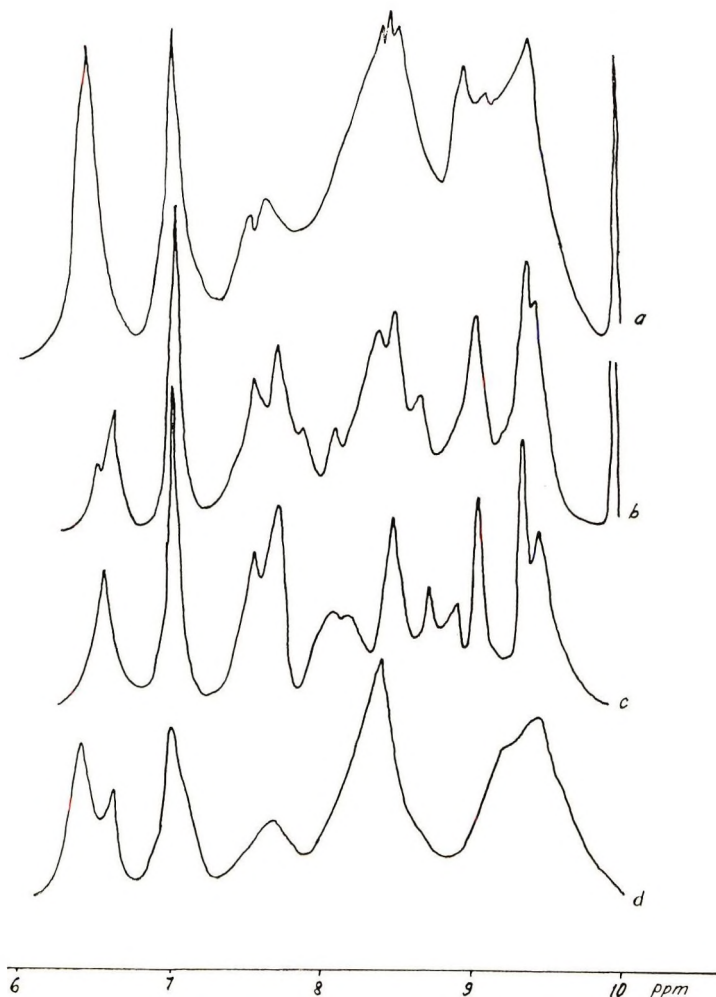


Fig. 8. NMR spectra of the (1:1) MMA-St copolymer prepared by polymerization in presence of: (a) ZnCl_2 at $[\text{ZnCl}_2]/[\text{MMA}] = 0.6$; (b) $\text{Al}(\text{C}_2\text{H}_5)_2\text{Cl}$ at $[\text{Al}(\text{C}_2\text{H}_5)_2\text{Cl}]/[\text{MMA}] = 0.7$; (c) $\text{Al}(\text{C}_2\text{H}_5)_{1.5}\text{Cl}_{1.5}$; and (d) conventional radical copolymer. The spectra have been recorded in 15% solution in *o*-dichlorobenzene at 150°C with octamethylcyclotetrasiloxane as a reference (9.95 ppm).

The apparent copolymerization reactivity ratios in the system MMA-2,6-DCSt- ZnCl_2 (see Fig. 7 and Table IV) are varied in a way similar to that in the system MMA-VDC- ZnCl_2 (r_1 increase and approaches a limiting value, r_2 decreases) but the change in r_1 is much less than in the MMA-VDC system. When AlCl_3 is used instead of ZnCl_2 , r_1 and r_2 are changed in a way similar to that in the system MMA-St- ZnCl_2 (both are decreased to limiting values at CA content lower than stoichiometric).

As far as different CA's act in different ways in the copolymerization, it is of interest to compare their ability to form complexes with MMA.

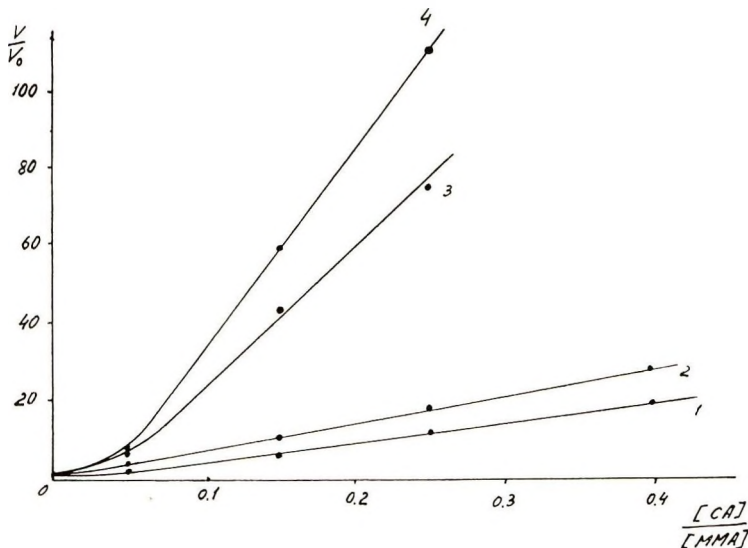


Fig. 9. Dependence of the relative copolymerization rate in the system MMA-St on the ratio $[CA]/[MMA]$: (1) $[MMA]:[St] = 19$; (2) $[MMA]:[St] = 9$; (3) $[MMA]:[St] = 0.55$; (4) $[MMA]:[St] = 0.43$. $[AIBN] = 5 \times 10^{-3}$ mole/l, $t = 50^\circ\text{C}$, $CA = \text{ZnCl}_2$.

The measure of the relative strength of the complex is the shift of the $\text{C}=\text{O}$ valent frequency.²² The data are shown in Table V. The data show that all the complexes are stable enough. The complexing and polarizing power of ZnCl_2 and $\text{Al}(\text{C}_2\text{H}_5)\text{Cl}$ are somewhat lower than those of AlCl_3 and AlBr_3 .

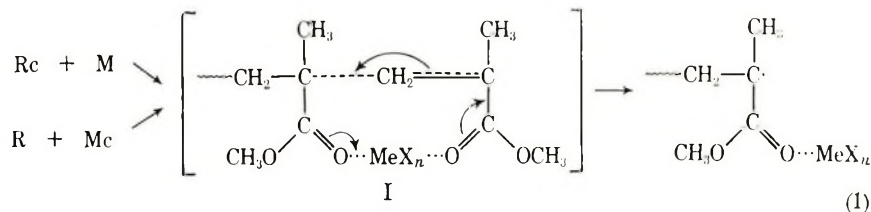
Finally it has been shown that ZnCl_2 does not affect the rates of photo-induced homopolymerization of two representative monomers in the second group such as VDC and St, dissolved in ethyl acetate- ZnCl_2 (1:0.4) complex as compared to polymerization in pure ethyl acetate.

DISCUSSION

Before discussing the results on copolymerization in presence of different CA's, let us first briefly consider the effects of these compounds in radical homopolymerization of MMA, a monomer in which the functional group forms a complex with the CA's. These effects have to be of primary importance for understanding the copolymerization behavior, because, as shown above, the polymerization rates of the comonomers not forming complexes with the modifiers (and thus the activity of the monomers and of the radicals) remain unchanged in presence of these compounds.

It is known that introduction of relatively small amounts of ZnCl_2 and AlBr_3 ^{6,19} ($[CA]/[MMA] \simeq 0.2$) causes considerable increase of propagation rate constant, but the termination constant remains practically unchanged. At higher molar content of AlBr_3 the termination constant decreases

sharply and k_p passes through a maximum. As we had shown earlier,^{8-10,23} ESR spectra of PMMA radicals complexed with some of the metal halides differ from those of ordinary PMMA radicals. The difference is attributed to contact interaction of the impaired electron with the metal atom in the CA molecule. In other words there is certain density of the odd electron on the metal atom. On the basis of this, the propagation mechanism involving a CA molecule has been proposed:



According to the mechanism, the monomer addition occurs by electron transfer through the metal atom in the cyclic transition complex. The efficiency of the process is higher than of ordinary homolytic opening of the double bond. The decrease of k_p at $[\text{AlBr}_3]/[\text{MMA}] > 0.4$ that has been interpreted assuming that, when the monomer and the radical both bound to the CA, the transition state I is not realized or probably requires dissociation of one of the coordination bonds with the modifier (with monomer or with the radical).

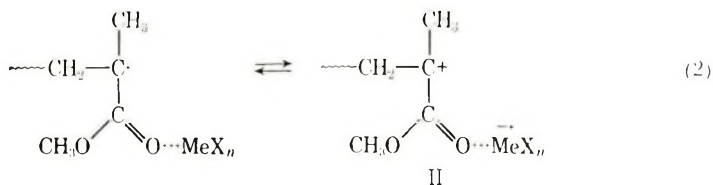
This scheme can readily account for the results on copolymerization of MMA with MA or BA (monomers with ideal radical reactivity lower than that of MMA, but forming similar complexes with the modifiers). If the propagation occurs as shown on the scheme, the differences in the relative activities of the double bonds may disappear, and thus the copolymer composition becomes equal to the composition of the monomeric mixture, and apparent values of r_1 and r_2 approach unity.

In the copolymerization of MMA (M_1) with monomers which are not complexed with the modifiers one may expect that variation in values of r_1 is determined on the one hand by the effect of CA on k_{11} , which is independent of the nature of the second monomer, and on the other hand by the effect of CA on the reactivity of the complexed PMMA radical towards the second monomer, which does depend on the nature of the second monomer. The character of r_2 variation depends on the effect of CA on the activity of MMA in the addition to the radical of the second monomer.

The increase of r_1 in the systems MMA-VDC-ZnCl₂ corresponds to an increase in k_{11} in the presence of ZnCl₂.^{6,26} From the approach of r_1 to constant value at $[\text{ZnCl}_2]/[\text{MMA}] \simeq 0.25$, it may be concluded that further increase of ZnCl₂ (and thus of complexed MMA) concentration does not considerably effect the k_{11} value (in accord with the data of Ref. 26). The same type of behavior is observed in the presence of Al(C₂H₅)₂Cl. In the system MMA-VDC-AlCl₃(AlBr₃), the r_1 value passes through maximum with increase of $[\text{AlX}_3]/[\text{MMA}]$. This behavior correlates quite well with

character of variation of k_p in the system MMA-AlBr₃¹⁹ and with the character of variation of the copolymerization rate in system (see Fig. 4) with AlCl₃ content.

Now by using the values of r_1 (our data) and literature values^{6,26} of k_p at given CA content it is possible to estimate semiquantitatively the effects of CA on the reactivity of PMMA radicals to VDC. At $[\text{ZnCl}_2]/[\text{MMA}] = 0.16$ $r_1 \simeq 13$ ($r_1^0 = 2.5$), $r_1/r_1^0 = 5.2$ and $k_{11}/k_{11}^0 = 2.4$; thus $k_{12}/k_{12}^0 \simeq 0.5$ (where superscript zero refers to the system without CA). Though these data correspond to the intermediate content of the CA where free and complexed PMMA radicals are present and therefore cannot be directly used for separate description of the reactivity of the complexed radical, one can see that the reactivity of the complexed PMMA radical of VDC is lower than that of the free radical. In the system MMA-VDC-AlBr₃ r_1 has not been determined, but as can be seen from Figure 2 the character of variation of r_1 with $[\text{CA}]/[\text{MMA}]$ has to be quite similar to that in the system MMA-VDC-AlCl₃, where r_1 increases only slightly with increasing $[\text{AlCl}_3]/[\text{MMA}]$ (in the range $[\text{AlCl}_3]/[\text{MMA}] \leq 0.2$). As far as $k_{11}/k_{11}^0 \simeq 3$ at $[\text{AlBr}_3]/[\text{MMA}] = 0.2$, this means that $k_{12}/k_{12}^0 > 1$; thus the reactivity of the PMMA radical complexed with AlX₃ to VDC molecule is higher than that of free PMMA radical. The different effects of ZnCl₂ and AlX₃ on the reactivity of PMMA radical can be understood, if one takes into account that complexation brings about higher delocalization of the impaired electron (including the metal atom) and thus decreases its ideal radical reactivity. At the same time, the radical attains some cationic character that may enhance its reactivity to the other monomer due to polar effects. The limit resonance structures are represented by the scheme (2):

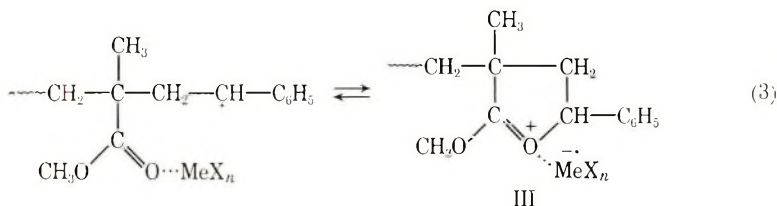


In the case of MMA-ZnCl₂-VDC system, the polar effects apparently do not play an important role, but in the case of the stronger polarizing agents AlCl₃ and AlBr₃ (see Table V) they probably become predominant in the reactivity of the complexed PMMA radical to VDC. The proposed mechanism is further corroborated by the results on the copolymerization with 2,6-DCSt and St. Introduction of ZnCl₂ brings about an increase of r_1 at copolymerization with 2,6-DCSt ($e \simeq 0.1$) through at $[\text{ZnCl}_2]/[\text{MMA}] = 0.16$, $r_1/r_0 = 1.7$ and $k_{12}/k_{12}^0 = 1.4$. In copolymerization with St ($e = -0.8$), r_1 is already decreased; $r_1/r_0 = 0.4$, at $[\text{ZnCl}_2]/[\text{MMA}] = 0.16$, $k_{12}/k_{12}^0 = 7$. Therefore though k_{11} is varied in a similar way in all the systems, the variation in k_{12} changes from a decrease to (VDC) to a progressive increase as the e value of the comonomer becomes more negative.

Introduction of AlCl_3 brings about a decrease of r_1 even in copolymerization with 2,6-DCSt. The decrease of r_1 corresponds to increasing importance of ionic structures in the transition state for addition of the second monomer to the complexed PMMA radical.

In the presence of all CA's the values of r_2 decrease with CA concentration. This means that activity of complexed MMA increases as compared to that of pure MMA. The MMA activation in reaction with the radical of the second monomer may be attributed to higher conjugation in the monomer complex (the band for the $\pi \rightarrow \pi^*$ transition in the ultraviolet spectra is shifted to the longer waves by about 700 cm^{-1} ²⁴ and to the polar effect (because complex formation causes subsidiary negative polarization of the electron density in the monomer).

The other and perhaps most important reason of appearance of the marked tendency to alternation in copolymerization (e.g., with styrene) in presence of CA's probably lies in supplemental stabilization of the radical formed after addition of the second monomer to the complexed PMMA radical. It can be described by the structures, one which contains a five-membered oxonium ring (III).



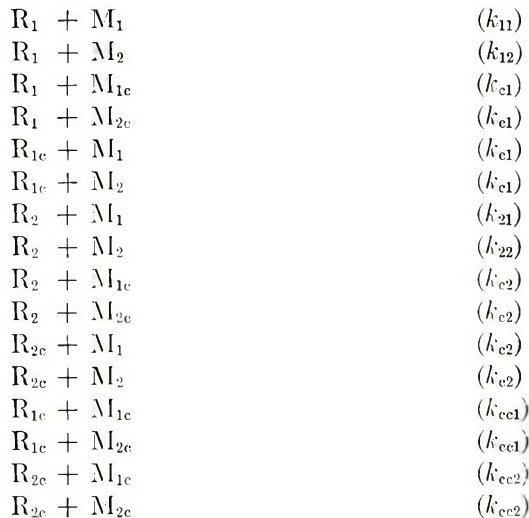
Formation of the ring facilitates addition of one styrene molecule. Addition of the next styrene molecules would however break the supplemental stabilization, because in this case a seven-membered oxonium cycle has to be formed.

A similar mechanism is probably operating in alternating copolymerization of methyl acrylate, acrylonitrile, and MMA with α -olefins in presence of alkylaluminum halides.¹¹ The presence of CA in these systems provides not only alternating effect but permits preparation of high molecular weight products. In absence of CA, radical polymerization and copolymerization of α -olefins is practically impossible due to degradative chain transfer to the α -olefin. Stabilized radicals like II and III are probably less active in abstraction of hydrogen atoms from α -olefins. Finally, the inability to form unstrained oxonium cycles due to sterical hindrance may be the reason for lack of alternation tendency in copolymerization of vinylpyridines with styrene in presence of zinc salts,²⁵ though polarizing and resonance effects of zinc salts on the vinylpyridine monomer and radical are quite high (especially in 4- and 2-vinylpyridines).^{24,25}

Now let us consider the kinetic scheme describing radical copolymerization in presence of the complexing agents (modifiers).

Case I. Both Monomers Form Similar Complexes with the Modifiers

At the copolymerization in such system, 16 elementary reactions have to be taken into account:



where M_1 , M_2 , M_{1c} , and M_{2c} are free and complexed monomers and R_1 , R_2 , R_{1c} , and R_{2c} are free and complexed radicals of the first and the second monomers. It has been assumed that the rate constants k_{c1} , k_{c2} , k_{cc1} , k_{cc2} are equal to each other for sets of interactions because for these pairs the copolymer composition approaches the composition of the monomeric mixture at CA content lower than stoichiometric ($[CA]/[M_1] + [M_2] \leq 0.2-0.3$) where most of the propagation acts occurring can be expressed by a single reaction. On defining

$$\alpha = [R_c]/[R_0]$$

$$\beta = [M_c]/[M_0]$$

where $[R_0]$, $[M_0]$ are total concentrations of radical and monomer, respectively, one can express

$$[R_c] = \alpha[R_0]$$

$$[R] = (1 - \alpha)[R_0]$$

$$[M_c] = \beta[M_0]$$

$$[M] = (1 - \beta)[M_0]$$

The rates of consumption of the monomers M_1 and M_2 are given by eqs. (4) and (5):

$$\begin{aligned}
 -d[M_{10}]/dt &= k_{11}[R_1][M_1] + k_{c1}[R_1][M_{1c}] + k_{c1}[R_{1c}][M_1] + k_{21}[R_2][M_1] \\
 &+ k_{c2}[R_2][M_{1c}] + k_{cc1}[R_{1c}][M_{1c}] + k_{cc2}[R_{2c}][M_{1c}] + k_{c2}[R_{2c}][M_1] \\
 &= [M_{01}]\{[R_{01}][k_{11}(1-\alpha)(1-\beta) + k_{c1}(1-\alpha)\beta + k_{c1}\alpha(1-\beta) \\
 &+ k_{cc1}\alpha\beta] + [R_{02}][k_{21}(1-\alpha)(1-\beta) + k_{c2}(1-\alpha)\beta + k_{c2}\alpha(1-\beta) \\
 &+ k_{cc2}\alpha\beta]\} \quad (4)
 \end{aligned}$$

$$\begin{aligned}
 -d[M_{20}] &= k_{12}[R_1][M_2] + k_{c1}[R_1][M_{2c}] + k_{c1}[R_{1c}][M_2] + k_{22}[R_2][M_2] \\
 &+ k_{c2}[R_2][M_{2c}] + k_{c2}[R_{2c}][M_2] + k_{cc1}[R_{1c}][M_{2c}] + k_{cc2}[R_{2c}][M_{2c}] \\
 &= [M_{02}]\{[R_{02}][k_{22}(1-\alpha)(1-\beta) + k_{c2}(1-\alpha)\beta + k_{c2}\alpha(1-\beta) \\
 &+ k_{cc2}\alpha\beta] + [R_{01}][k_{12}(1-\alpha)(1-\beta) + k_{c1}(1-\alpha)\beta \\
 &+ k_{c1}\alpha(1-\beta) + k_{cc1}\alpha\beta]\} \quad (5)
 \end{aligned}$$

Diving eqs. (4) by eq. (5) we obtain eq. (6):

$$\begin{aligned}
 d[M_{01}]/d[M_{02}] &= ([M_{01}]/[M_{02}])\{[R_{01}][k_{11}(1-\alpha)(1-\beta) + k_{c1}(1-\alpha)\beta \\
 &+ k_{cc1}\alpha\beta] + [R_{02}][k_{21}(1-\alpha)(1-\beta) + k_{c2}(1-\alpha)\beta + k_{c2}\alpha(1-\beta) \\
 &+ k_{cc2}\alpha\beta]\}/\{[R_{02}][k_{22}(1-\alpha)(1-\beta) + k_{c2}(1-\alpha)\beta \\
 &+ k_{c2}\alpha(1-\beta) + k_{cc2}\alpha\beta] + [R_{01}][k_{12}(1-\alpha)(1-\beta) + k_{c1}(1-\alpha)\beta \\
 &+ k_{c1}\alpha(1-\beta) + k_{cc1}\alpha\beta]\} \quad (6)
 \end{aligned}$$

In the stationary state,

$$\begin{aligned}
 d[R_{01}]/dt &= k_{21}[R_2][M_1] + k_{c2}[R_2][M_{1c}] + k_{c2}[R_{2c}][M_1] + k_{cc2}[R_{2c}][M_{1c}] \\
 &- k_{12}[R_1][M_2] - k_{c1}[R_1][M_{2c}] - k_{c1}[R_{1c}][M_2] - k_{cc1}[R_{1c}][M_{2c}] \quad (7)
 \end{aligned}$$

Thus

$$\begin{aligned}
 [R_{02}] &= \\
 &\frac{[R_{01}][M_{02}]\{k_{12}(1-\alpha)(1-\beta) + k_{c1}(1-\alpha)\beta + k_{c1}\alpha(1-\beta) + k_{cc1}\alpha\beta\}}{[M_{01}]\{k_{21}(1-\alpha)(1-\beta) + k_{c2}(1-\alpha)\beta + k_{c2}\alpha(1-\beta) + k_{cc2}\alpha\beta\}} \quad (8)
 \end{aligned}$$

After substitution of eq. (8) into eq. (6), we obtain:

$$\frac{d[M_{10}]}{d[M_{20}]} = \frac{[M_{10}]}{[M_{20}]} \frac{r_1^{\text{ef}}[M_{01}] + [M_{02}]}{r_2^{\text{ef}}[M_{02}] + [M_{01}]} \quad (9)$$

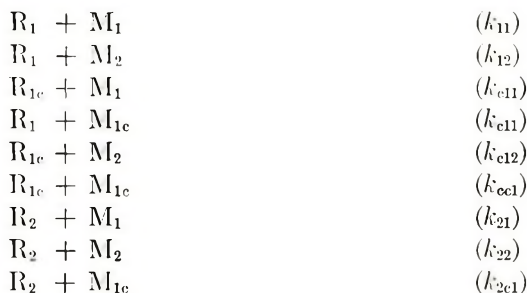
$$\text{where } r_1^{\text{ef}} = \frac{k_{11}(1-\alpha)(1-\beta) + k_{c1}(1-\alpha)\beta + k_{c1}\alpha(1-\beta) + k_{cc1}\alpha\beta}{k_{12}(1-\alpha)(1-\beta) + k_{c1}(1-\alpha)\beta + k_{c1}\alpha(1-\beta) + k_{cc1}\alpha\beta} \quad (9a)$$

$$r_2^{\text{ef}} = \frac{k_{22}(1-\alpha)(1-\beta) + k_{c2}(1-\alpha)\beta + k_{c2}\alpha(1-\beta) + k_{cc2}\alpha\beta}{k_{21}(1-\alpha)(1-\beta) + k_{c2}(1-\alpha)\beta + k_{c2}\alpha(1-\beta) + k_{cc2}\alpha\beta} \quad (9b)$$

Equation (9) is analogous in structure to the Mayo-Lewis equation, but r_1^{ef} and r_2^{ef} are functions of the elementary constants and of the values α and β which depend on CA content and on the stability of the complexes formed between the monomers and the radicals with the modifier (CA). As can be easily seen from eqs. (9a) and (9b), regardless of the absolute values of the elementary constants, r_1^{ef} and r_2^{ef} both approach unity with increasing CA content (when α and β approach unity); this has been found in copolymerization of MMA with MA and BA in the presence of ZnCl_2 and AlBr_3 .

Case II. One of the Monomers (M_1) Forms a Complex with the Modifier

For copolymerization in such systems, 9 types of elementary reactions have to be taken into account:



The rates of consumption of the monomers M_1 and M_2 in course of the copolymerization are given as:

$$\begin{aligned}
 -d[M_{01}]/dt &= k_{11}[R_1][M_1] + k_{c11}[R_{1c}][M_1] + k_{e11}[R_1][M_{1c}] \\
 &\quad + k_{ec1}[R_{1c}][M_{1c}] + k_{21}[R_2][M_1] + k_{2c1}[R_2][M_{1c}] \\
 &= [M_{01}]\{[R_{01}][k_{11}(1-\alpha)(1-\beta) + k_{c11}\alpha(1-\beta) + k_{e11}(1-\alpha)\beta \\
 &\quad + k_{ec1}\alpha\beta] + [R_2][k_{21}(1-\beta) + k_{2c1}\beta]\} \quad (10)
 \end{aligned}$$

$$\begin{aligned}
 -d[M_{02}]/dt &= k_{12}[R_1][M_2] + k_{e12}[R_{1c}][M_2] + k_{22}[R_2][M_2] \\
 &= [M_{02}]\{[R_{01}][k_{12}(1-\alpha) + k_{e12}\alpha] + [R_2]k_{22}\} \quad (11)
 \end{aligned}$$

Then by dividing eq. (10) by eq. (11) substituting R_2 through R_{01} from stationary expression for R_{01} one obtains:

$$d[M_{01}]/d[M_2] = ([M_{01}]/[M_2])(r_1^{\text{ef}}[M_{01}] + [M_2]) / (r_2^{\text{ef}}[M_2] + [M_{01}]) \quad (12)$$

where $r_1^{\text{ef}} =$

$$\frac{[k_{11}(1-\alpha)(1-\beta) + k_{c11}\alpha(1-\beta) + k_{e11}(1-\alpha)\beta + k_{ec1}\alpha\beta]}{[k_{12}(1-\alpha) + k_{e12}\alpha]} \quad (12a)$$

$$r_2^{\text{ef}} = k_{22}/[k_{21}(1-\beta) + k_{2c1}\beta] \quad (12b)$$

Again, the equation for the copolymer composition is analogous in structure to the Mayo-Lewis equation. The parameters r_1^{ef} and r_2^{ef} are variable

functions of the elementary constants and of the values α and β which depend on CA content in the system and on the stability of the complexes formed between the monomer or the radical with the modifier (CA). Equations (12a) and (12b) can qualitatively describe all the observed experimental dependences of r_1^{ef} and r_2^{ef} on CA content (increase or decrease of r_1^{ef} to a limiting value, passing of r_1^{ef} through the maximum; monotonic decrease of r_2^{ef}).

Therefore the results on the copolymerization of MMA with different monomers in presence of some CA's can be expounded by means of a mechanism involving the effect of the modifier on the propagation rate constants with complexed monomers and radicals. The kinetic schemes based on these assumptions (1) explain why these actually multicomponent systems formally obey at all contents of CA the binary copolymerization equation and (2) could be used for quantitative estimation of reactivity of the complexed monomers and radicals. The latter procedure requires first of all the knowledge of the values of k_p for MMA homopolymerization as a function of CA content, which has not yet been determined in the systems most extensively explored in the paper. Thus we now have been limited only to qualitative analysis of the results. On substituting probable values of kinetic constants into the expressions for r_1 [eqs. (9a) and (12a) and putting $\beta \simeq [\text{CA}]/[\text{M}_0]$ or $[\text{CA}]/([\text{M}_1] + [\text{M}_2])$ one can infer that the PMMA or PMA radicals form more stable complexes with the modifiers than the monomers. In other words at $[\text{CA}]/([\text{MMA}] + [\text{MA}])$ or $[\text{CA}]/[\text{MMA}]$ ratios lower than unity, all the propagating radicals are complexed with the modifiers. The conclusion well accounts for the results on copolymerization and is in accord with direct evidence by ESR method.²³

References

1. C. H. Bamford, A. D. Jenkins, and R. Johnston, *Proc. Roy. Soc. (London)*, **A 241**, 364, 1226 (1957).
2. C. H. Bamford, A. D. Jenkins, and R. Johnston, *J. Polym. Sci.*, **29**, 120, 355 (1958).
3. I. Parrod and H. Monteiro, *C. R. Acad. Sci. (Paris)*, **251**, 2026 (1960).
4. M. Imoto, F. Otsu, and S. Shemizu, *Makromol. Chem.*, **65**, 174, 180, 194 (1963).
5. M. Imoto, F. Otsu, B. Yamada, and S. Shemizu, *Makromol. Chem.*, **82**, 277 (1965).
6. C. H. Bamford, S. Brumby, and R. P. Wayne, *Natura*, **209**, 292 (1965).
7. S. Tasuke, K. Tsuji, and T. Vonezawa, paper presented at International Symposium on Macromolecular Chemistry, Tokyo-Kyoto, 1966; *Preprints*, 2.2.07.
8. V. A. Kargin, V. A. Kabanov, and V. P. Zubov, *Vysokomol. Soedin.*, **2**, 765 (1960).
9. V. P. Zubov and M. B. Iachinov, paper presented at International Symposium on Macromolecular Chemistry, Prague, 1965; *Abstracts*, A468.
10. V. P. Zubov, M. B. Iachinov, V. B. Golubev, V. F. Kulikova, V. A. Kabanov, L. S. Polak, and V. A. Kargin, paper presented at International Symposium on Macromolecular Chemistry, Tokyo-Kyoto, 1966; in *Macromolecular Chemistry, Tokyo-Kyoto (J. Polym. Sci. C, 23)*, I. Sakurada and S. Okamura, Eds., Interscience, New York, 1968, p. 149.

11. M. Hirooko, H. Yabuuchi, J. Iseki, and Y. Nakai, *J. Polym. Sci. A-1*, **6**, 1381 (1968).
12. L. I. Valuev, V. P. Zubov, V. A. Kabanov, and V. A. Kargin, *Dokl. Akad. Nauk SSSR*, **185**, 342 (1969).
13. W. S. Schoniger, *Mikrochim. Acta*, **1955**, 123; *ibid.*, **1959**, 670.
14. A. Katera, M. Shima, K. Akiyama, M. Kume, and M. Miyakawa, *Bull. Chem. Soc. Japan*, **39**, 758 (1968).
15. N. Grassie, B. J. D. Terrance, J. D. Fortune, and J. D. Gemmel, *Polymer*, **6**, 653 (1965).
16. H. I. Harwood and W. M. Ritchey, *J. Polym. Sci. B*, **3**, 419 (1965).
17. M. Fineman and S. D. Ross, *J. Polym. Sci.*, **5**, 269, 1950.
18. A. I. Ezrielev, E. L. Brochina, and E. S. Roskin, *Vysokomol. Soedin. A*, **11**, 1670 (1969).
19. M. B. Lachinov, V. P. Zubov, and V. A. Kabanov, *Vysokomol. Soedin. B*, **12**, 4 (1970).
20. J. Brandrup and E. H. Immergut, Eds., *Polymer Handbook*, Interscience, New York, 1967.
21. C. S. Marvel, G. E. Inskeep, R. Deanin, A. E. Juve, C. H. Schroeder, and M. M. Goff, *Ind. Eng. Chem.*, **39**, 1486 (1947).
22. M. F. Lappert, *J. Chem. Soc.*, **1961**, 817; *ibid.*, **1962**, 542.
23. V. B. Golubev, V. P. Zubov, L. I. Valuev, G. S. Naumov, V. A. Kabanov, and V. A. Kargin, *Vysokomol. Soedin., A*, **12**, 2689 (1969).
24. S. Tasuke and S. Okamura, *J. Polym. Sci. B*, **5**, 95 (1967).
25. S. Tasuke and S. Okamura, *J. Polym. Sci. A-1*, **5**, 1083 (1967).
26. V. P. Zubov, V. A. Kabanov, *Vysokomol. Soedin. A*, **14**, No. 5 (1971).

Received April 13, 1970

Graft Copolymerization of Methyl Methacrylate onto Lignosulfonate by H_2O_2 -Fe(II) Redox System. I.

Preparation and Characterization of the Graft Copolymer

CHONGWON NAM,* TETSUO KOSHIJIMA, EINOSUKE MURAKI,
and TAKAMARO MAKU,* *Government Industrial Research Institute
Osaka, Ikeda, Osaka, Japan*

Synopsis

Graft copolymerization of methyl methacrylate onto lignosulfonate in aqueous medium was investigated. It was found that the H_2O_2 -Fe(II) redox system is very effective for the grafting ($E_a = 4.4$ kcal/mole). The $\text{H}_2\text{O}_2/\text{Fe}^{2+}$ ratio was the most important factor in the graft copolymerization and characteristics of the resultant graft copolymers. In most cases, polymerization for 100 min at 30°C was enough to obtain 80% conversion and 50-60% grafting efficiency. The resultant polymer mixture was subjected to extraction alternately with acetone and water, and the graft copolymer was isolated free from homopolymer and unreacted lignosulfonate. With increasing $\text{H}_2\text{O}_2/\text{Fe}^{2+}$ ratio, the grafting ratio showed a maximum at 4, whereas the yield of graft copolymer and number of poly(methyl methacrylate) branches for every building unit of lignosulfonate increased up to a ratio of 4, both values, however, remaining constant above 4. The graft copolymer obtained for the case $\text{H}_2\text{O}_2/\text{Fe}^{2+} = 4$ consisted of one part of lignosulfonate and five parts of poly(methyl methacrylate). The number of branches in the graft copolymer was $6 \times 10^{-3}/\text{OCH}_3$ or one every 167 guaiacyl nuclei.

INTRODUCTION

Lignosulfonic acid, as well as thiolignin is one of the representative lignin derivatives produced in pulp and paper mills as by-product. Investigations on the chemical structure and utilization of lignin have been continued for long time but in spite of a large number of investigations so far reported, only very few successful results have been found in the field of lignin utilization owing to its complicated and variable structure. Thiolignin has been used as a carbon source in the process of recovery of cooking liquor, whereas lignosulfonic acid had been discarded into rivers, thus becoming increasingly a public hazard.

It is of interest to modify the chemical and/or the physical properties of lignin or lignin derivatives by grafting with suitable vinyl monomers. Some of the characteristic properties of hydrochloric acid lignin graft

* Present address: Wood Research Institute, Kyoto University, Kyoto, Japan.

products obtained by graft copolymerization induced by γ -radiation have been reported.¹⁻⁶ In this case, however, many questions remained unsolved, since due to the heterogeneous reaction system the products obtained contained both graft copolymer and unreacted lignin molecules. When liginosulfonic acid is used as backbone polymer, it is possible to carry out the graft copolymerization in aqueous solution and to remove unreacted lignin portions from the reaction products, thus creating more favorable conditions for a thorough study of the grafting. For this reason the graft copolymerization of methyl methacrylate onto liginosulfonate by using the H_2O_2 -Fe(II) redox system was attempted, and it was found that the graft copolymerization took place very readily and with high efficiency, even close to room temperature. In the radiation-induced graft copolymerization of styrene onto hydrochloric acid ligin, phenolic hydroxyl groups in the ligin molecule were found to depress radical grafting¹ as expected, and the grafted side chains were recognized qualitatively to combine directly to C_5 or C_6 of the guaiacyl nuclei in ligin molecules.⁴ The diversity of chemical structure of ligin originates from the different ways in which the guaiacyl glycerol units may be linked together. The linkages may roughly be divided into two main groups: i.e., ether linkage type (C—O—C) and condensation type (C—C). Since only few functional groups are able to participate in graft copolymerization reactions initiated by such a mild conditions, as used here, it seems justified to consider only few groups involved in the guaiacyl glycerol unit as active centers for the grafting reaction. On initiating graft copolymerization by the H_2O_2 -Fe(II) redox system, there is a strong possibility that not only oxidation of ferrous ion to ferric ion with hydrogen peroxide but also participation of liginosulfonate in the redox system takes place. Therefore the influence of varying $\text{H}_2\text{O}_2/\text{Fe}^{2+}$ ratio upon grafting onto liginosulfonate becomes extremely important. The liginosulfonate-methyl methacrylate graft copolymers produced by using the H_2O_2 -Fe(II) redox system were considered to differ from those obtained by γ -irradiation with respect to the number and molecular weight of side branches, and presumably also with respect to the kind of linkage formed on grafting. It is the purpose of this paper to study the influence of the ratio $\text{H}_2\text{O}_2/\text{Fe}^{2+}$ upon the graft copolymerization and on the properties of the resultant graft copolymer.

EXPERIMENTAL

Barium Liginosulfonate

Commercial calcium liginosulfonate powder prepared from softwood was dialyzed by Tailor's equipment for 4 days, when the removal of ash was complete. It was then deionized by Amberlite IR-120, neutralized with barium carbonate, and refined by precipitating two times from ethanol; the methoxy content was 10.95%, phenolic hydroxyl⁷ 1.72%, \bar{M}_n 9.4×10^3 (as free acid). In order to measure number-average molecular weight, the

TABLE I
Graft Copolymerization of Methyl Methacrylate onto Lignosulfonate by H_2O_2 -Fe(II) Redox System^a

H_2O_2 , Fe ²⁺ , mole/mole	Yield, g/g lignosulfonate		Ligno- sulfonate content of graft copolymer, %		Graft- ing ratio, 100 (100 - a)/a ^b	\bar{M}_n of poly- (methyl meth- acrylate) branches, $\times 10^{-4}$	Number of branches per OCH ₃ of ligno- sulfonate, $\times 10^3$	Conversion of methyl methacrylate, %	
	Graft copolymer	Homo- polymer	Unreacted lignosulfonate						
1	0.23	0.37	0.99	49.2	103	18.5	2.42	24.2	10.5
2	1.36	0.49	0.61	26.5	278	16.1	4.60	67.0	31.8
3	2.45	1.45	0.38	21.7	361	18.1	5.65	57.0	72.0
4	2.77	1.71	0.34	18.4	443	16.5	7.62	57.4	85.8
5	3.01	2.07	0.23	23.2	351	13.8	6.82	52.8	93.5
6	3.00	1.79	0.33	26.9	272	13.3	5.80	55.1	85.0
7	2.74	1.86	0.25	25.1	298	12.8	6.62	52.4	83.5
8	2.83	1.94	0.23	28.9	246	11.4	6.14	50.8	84.4
10	2.81	1.93	0.23	28.9	246	9.6	7.24	50.9	83.9
1/none	0	0	0.99	—	—	—	—	—	—
5/none	0	0	1.00	—	—	—	—	—	—

^a Graft copolymerization conditions: barium lignosulfonate, 1 g; methyl methacrylate, 5 ml (0.047 mole); FeSO_4 , 1×10^{-4} mole in acetate buffer (pH 4.6, 5 ml); H_2O_2 , $1-10 \times 10^{-4}$ mole in acetate buffer (pH 4.6, 5 ml); reaction temperature, 30°C; reaction time, 100 min.

^b a = barium lignosulfonate content of graft copolymer.

dicyclohexylamine salt of lignosulfonic acid was prepared according to the method of Tachi and Nakai,⁸ the results showed $\bar{M}_n = 1.3 \times 10^4$; N = 2.15%.

Graft Copolymerization

Commercial methyl methacrylate was washed successively with saturated aqueous solution of sodium hydrogen sulfite, 5% sodium hydroxide, and 20% sodium chloride solution and dried over anhydrous sodium sulfate. The methyl methacrylate was distilled with addition of sulfur, and the distillate was collected at 42.5–43.5°C/90 mm Hg. In a 40-ml glass tube, 1 g barium lignosulfonate, 1×10^{-4} mole ferrous sulfate dissolved in 5 ml acetate buffer (pH 4.6), 4.7 g methyl methacrylate, and various amounts of hydrogen peroxide diluted with 5 ml acetate buffer (pH 4.6) were added in that order. Before addition of the hydrogen peroxide the content of the glass tube was cooled below 0°C. Immediately after addition of hydrogen peroxide, the mixture in the glass tube was frozen by Dry Ice-acetone, degassed in the usual way, and sealed *in vacuo*. Polymerization was usually carried out by shaking the sealed ampoules in a water bath controlled at $30 \pm 0.1^\circ\text{C}$ for the intended time. The results are summarized in Table I.

Fractionation of Polymer Mixture

The content of the ampoules was poured into 200 ml water containing 0.5% hydroquinone, the suspension being dialyzed through a gel cellophane tube for 5 days to remove remaining initiators and then fractionated by alternate extraction as shown in Figure 1. The extraction of the polymer mixture with solvents (200 ml) by stirring for 3 hr, followed by decantation of supernatant after allowing to stand overnight was repeated until no polymer is detectable in the solvent. Each fraction was concentrated, precipitated from ethanol, washed with petroleum ether, and dried under reduced pressure. The water-soluble part was unreacted lignosulfonate,

TABLE II
Elementary Analyses of Fractionated Polymers

Fraction	Polymer	Analysis		Grafting ratio	
		C, %	H, %	From elementary analysis	From lignosulfonate content
Water-soluble	Lignosulfonate	41.86	4.51		
Water- and acetone insoluble	Graft copolymer	52.80	6.40	154	158
Acetone-soluble	Poly(methyl methacrylate)	59.85	8.23		

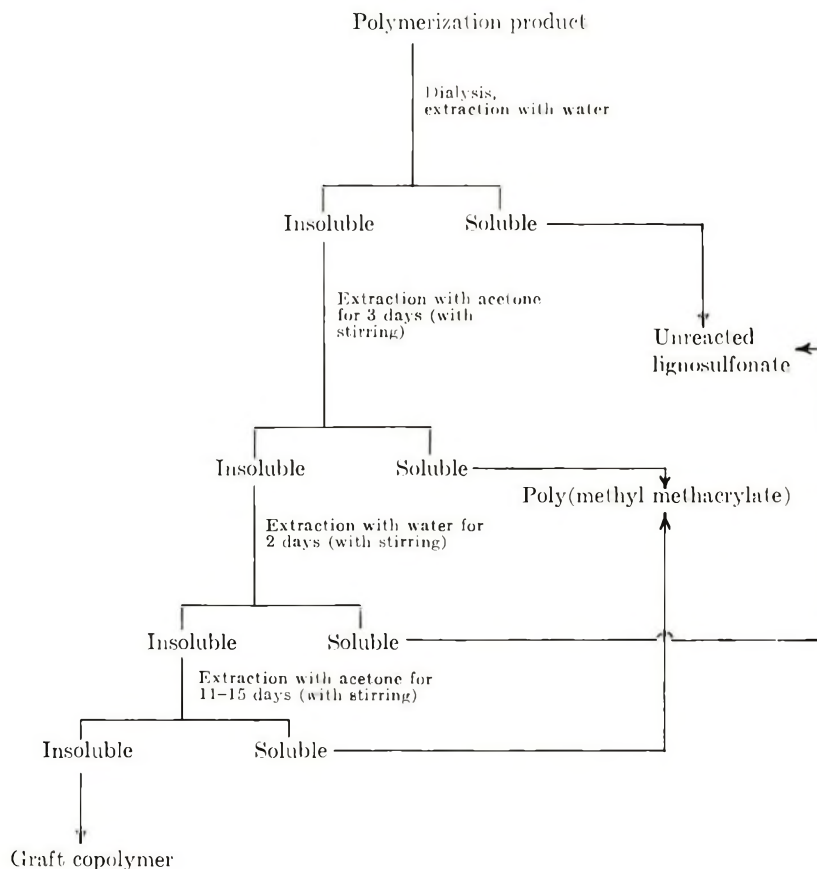


Fig. 1. Fractionation of polymerization products.

the acetone-soluble part was poly(methyl methacrylate) homopolymer, and the material insoluble in both water and acetone was considered to be graft copolymer (see Table II).

Determination of Grafting Ratio of Graft Copolymer

Grafting ratio was calculated from the lignosulfonate content, which was determined spectrophotometrically on the acetyl bromide-acetic acid solution of graft copolymer according to the method of Johnson et al.⁹ The absorptivity of barium lignosulfonate in solution at $280\text{ m}\mu$ was 15.2, which we used throughout our experiments for the determination of the lignin contents. When the lignin content of the graft copolymer was a (in per cent), grafting ratios were calculated as $100(100 - a)/a$.

Separation of Poly(Methyl Methacrylate) Branches from Graft Copolymer

The graft copolymer containing one part of lignosulfonate was suspended in 200 parts of water heated to 75°C , and then 4 parts of sodium chlorite

and 8 parts of acetic acid were added to the suspension, which was maintained at 75°C for 1 hr with occasional stirring. By repeating the oxidation eight times, separated branches became soluble in acetone. For osmotic pressure measurements, the separated poly(methyl methacrylate) branches were refined by precipitation from acetone solution with ethanol. There were no changes before and after the oxidation in number-average molecular weight of poly(methyl methacrylate).

Determination of Number-Average Molecular Weight

Number-average molecular weights (\bar{M}_n) were determined by using a Mechrolab membrane osmometer, Model 502. Measurements in the case of poly(methyl methacrylate) were carried out with the use of 1,2-dichloroethane as solvent at 30°C, and in the case of the dicyclohexylamine salt of liginosulfonic acid, by use of water-saturated 1-butanol at 20°C.

Determination of Apparent Activation Energy of the Graft Copolymerization

Polymerization of methyl methacrylate (5 ml) was carried out in the presence of barium liginosulfonate (1 g), at 10, 20, 30, and 40°C and at pH 4.6, by use of a redox system consisting of 1×10^{-5} mole ferrous sulfate and 2×10^{-5} mole hydrogen peroxide. An aliquot of the reaction mixture was sampled periodically at given time intervals, and the graft copolymer was isolated from the polymer mixture by fractionation as described above. The overall polymerization rates of methyl methacrylate branches were calculated from the yields of the graft copolymer. The apparent activation energy was 4.4 kcal/mole which was obtained from the usual Arrhenius plot of the rate versus polymerization temperature. Periodic changes of graft copolymer yield and grafting ratio at 20°C are shown in Figure 2.

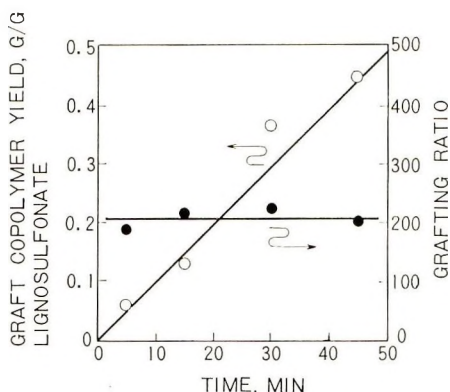
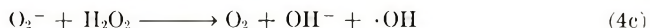
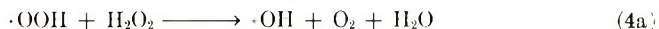
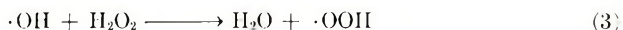


Fig. 2. Changes of graft copolymer yields and grafting ratios with time. Graft polymerization conditions: liginosulfonate, 1 g; methyl methacrylate, 5 ml; FeSO_4 , 10^{-4} mole; H_2O_2 , 2×10^{-4} mole; 20°C; pH 4.6 (acetate buffer).

RESULTS AND DISCUSSION

The reaction mechanism of the interactions between hydrogen peroxide and ferrous ion was suggested by Haber and Weiss^{10,11} to be shown in eqs. (1)–(4).



Ferrous ion is oxidized to ferric ion by hydrogen peroxide, which is decomposed to hydroxyl radical and hydroxyl ion. The resultant hydroxyl radical reacts again with ferrous ion to yield ferric ion (2) or reacts with hydrogen peroxide to produce hydroperoxy radical (3), which liberates oxygen molecules on successive reactions (4). Reactions (1) and (2) indicate one mole of hydrogen peroxide reacts with two moles of ferrous ions. When excess of hydrogen peroxide and vinyl monomer were present,



Baxendale¹² found that not only did polymerization take place but also oxygen was not evolved, indicating the occurrence of reaction (2a) and the depression of reactions (3) and (4). In general, reaction (2) competes with (2a) in the presence of monomer, and one mole of hydrogen peroxide oxidizes one or two moles of ferrous ions, depending upon the concentrations of monomer and ferrous ion and monomer reactivities. In the case of graft copolymerization of vinyl monomers onto lignosulfonate, however, the hydroxyl radical is considered to initiate not only polymerization of methyl methacrylate but also graft copolymerization, presumably by hydrogen abstraction from lignin molecules. Furthermore, it seems likely that ferric ion generated by reaction (1) is reduced by lignosulfonate to ferrous ion, which again forms the H_2O_2 -Fe(II) redox system with the remaining hydrogen peroxide molecules. Therefore, considerably large values would be expected for the optimum ratio of $\text{H}_2\text{O}_2/\text{Fe}^{2+}$ (mole/mole) in order for effective grafting onto lignosulfonate to take place. The correlation between $\text{H}_2\text{O}_2/\text{Fe}^{2+}$ ratio and graft copolymerization was therefore investigated in the present paper in great detail.

Figure 3 indicates the yields of graft copolymer and poly(methyl methacrylate) homopolymer produced under the conditions presented in Table I. With increasing $\text{H}_2\text{O}_2/\text{Fe}^{2+}$ ratio, the graft copolymer yields increased until the ratio reached a value of 4, above which the yields became constant. As shown in Table II, the grafting ratio of 154 calculated from elementary analyses of the graft copolymer, homopolymer, and lignosulfonate agreed with the value of 158 derived from lignin content of the graft copolymer.

Infrared spectra of the graft copolymer show absorbance due to ester

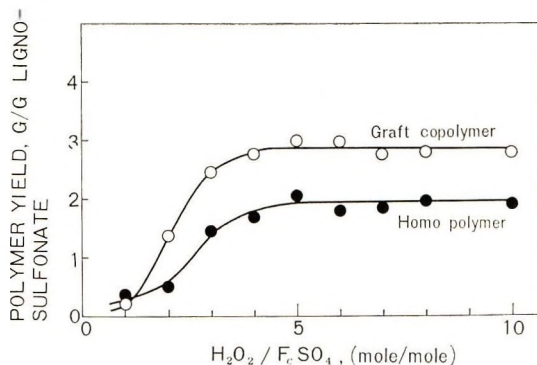


Fig. 3. Yields of graft copolymer and homo polymer.

carbonyl of poly(methyl methacrylate) at 1725 cm^{-1} , those of benzene ring at 1605 and 1520 cm^{-1} , and characteristic absorbances of the ester single bond of poly(methyl methacrylate) at 1270 , 1240 , 1190 , and 1150 cm^{-1} . Thus it was shown that the acetone- and water-insoluble part of reaction mixture was graft copolymer consisting of lignin and poly(methyl methacrylate).

With increasing $\text{H}_2\text{O}_2/\text{Fe}^{2+}$ ratio, the grafting ratio reached its maximum at a ratio of 4, where the value was 443 (Fig. 4). When the $\text{H}_2\text{O}_2/\text{Fe}^{2+}$ ratio attained a value of 2 or more, the grafting efficiency exceeded 50%, meaning more than half the polymerized monomer was grafted to lignin molecules (Fig. 5). The \bar{M}_n of poly(methyl methacrylate) branches of graft copolymer was in the range of $1 \times 10^5 \sim 2 \times 10^5$, as shown in Figure 6, indicating the \bar{M}_n of branches is 10–20 times that of lignosulfonate. This is unreasonable, because the grafting ratio of a backbone polymer having one branch is more than 1000. It is well known that lignosulfonic acid has broad molecular weight distribution extending from approximately 10^3 to 10^5 . The explanation of this apparent discrepancy is given when one assumes that grafting takes place predominantly on large lignosulfonate molecules owing to its low content of phenolic hydroxyl which is considered to be located at the end of the lignin molecule. With increasing ratio of $\text{H}_2\text{O}_2/\text{Fe}^{2+}$, the \bar{M}_n of the side branches is proportionally reduced by increasing termination reactions due to excess of hydroxyl radicals. \bar{M}_n of homopolymer produced by the $\text{H}_2\text{O}_2\text{-Fe(II)}$ (5:1) redox system was 90,000 which was considerably less than \bar{M}_n (138,000) of branches of corresponding graft copolymer.

The building unit of lignin molecules has been confirmed to be guaiacyl glycerol, carrying one methoxyl group per unit. The number of branches per methoxyl groups was calculated, as indicated in Figure 7. As shown, the number was actually unchanged above a ratio of 4 for $\text{H}_2\text{O}_2/\text{Fe}^{2+}$, meaning that there was a restriction in number of active points in lignosulfonate for graft copolymerization of vinyl monomer under the conditions

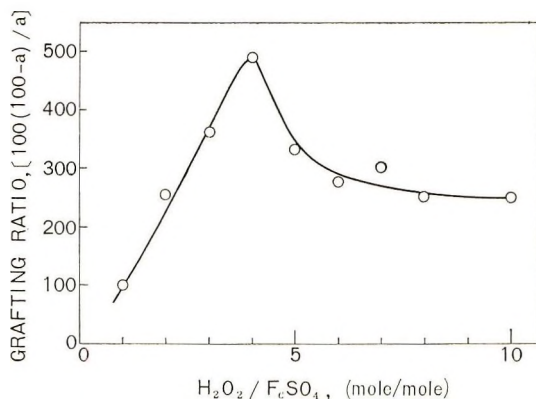


Fig. 4. Grafting ratios of lignosulfonate-methyl methacrylate graft copolymers.

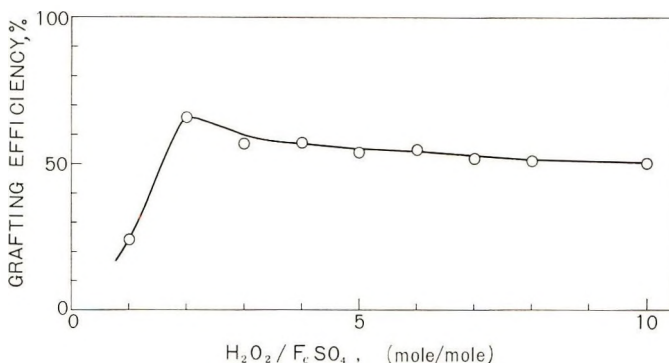


Fig. 5. Grafting efficiencies of the graft copolymerization.

used. The number is $6 \times 10^{-3}/\text{OCH}_3$, namely one poly(methyl methacrylate) branch for every 167 methoxyls or approximately for every 167 guaiacyl glycerol units.

The grafting mode of lignosulfonate was considered from the results described above as follows. Up to a ratio of 4 for $\text{H}_2\text{O}_2/\text{Fe}^{2+}$, the grafting yield and the grafting ratio increase with increasing $\text{H}_2\text{O}_2/\text{Fe}^{2+}$ ratio owing to the increase of active points formed on the building units of lignosulfonate, and the backbone polymer carries relatively long branches having \bar{M}_n of $16.5 \times 10^4 \sim 18.5 \times 10^4$. At $\text{H}_2\text{O}_2/\text{Fe}^{2+} = 4$, the number of the active centers for grafting reaches a saturation point, and the number of branches which each building unit of lignosulfonate carries does not change with increasing the ratio further. On the contrary, the grafting ratio is depressed when $\text{H}_2\text{O}_2/\text{Fe}^{2+}$ ratios of more than 4 are used. The fact that graft copolymer yield is not being reduced may be explained by assuming that the amount of reactive lignosulfonate increases with increasing amount of hydroxyl radical. Actually, Figure 8 indicates that the yield of graft

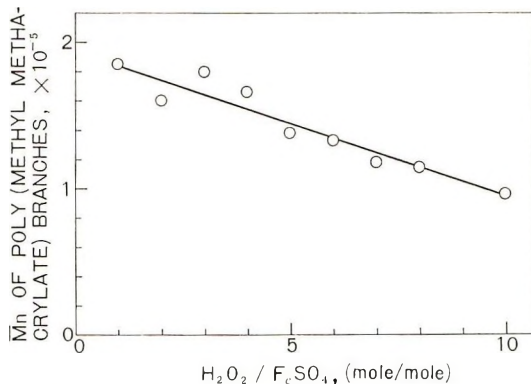


Fig. 6. Number-average molecular weights of poly(methyl methacrylate) branches of graft copolymers.

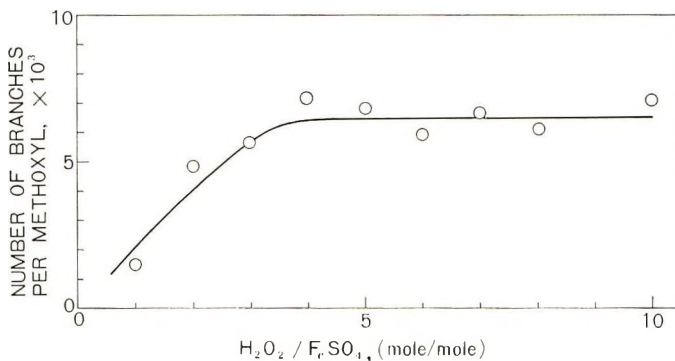


Fig. 7. Number of branch polymers per lignosulfonate unit.

copolymer increases acceleratively with increasing total amount of $H_2O_2 + Fe^{2+}$ when H_2O_2/Fe^{2+} ratio is kept at 4. Namely, increasing amounts of hydroxyl radical lead to an increase in the graft copolymer yield. Therefore, the assumption that an analogous reaction will take place when sufficient amounts of lignosulfonate and excess of hydrogen peroxide are present is considered to be reasonable (see below). On the other hand, neither graft copolymer nor poly(methyl methacrylate) is obtained without lignosulfonate (see Table I), but oxidation of ferrous ion to ferric ion was observed. This means that lignosulfonate itself accelerates redox polymerization very effectively, not only serves as backbone polymer in graft copolymerization. In addition, the optimum ratio of hydrogen peroxide to ferrous ion is 4, as shown in Figures 3, 4, and 7, indicating that lignosulfonate also participates in the redox reaction, probably through repeating such a cycle in which ferric ion in eq. (1) is reduced to ferrous ion by lignosulfonate, and the latter forms a new redox system with remaining hydrogen peroxide. As seen in Figure 9, both the yields of graft copolymer and of homopolymer increase with increasing ratio of lignosulfonate to

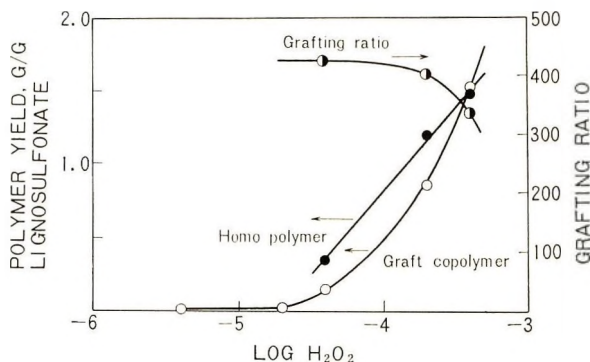


Fig. 8. Effects of hydrogen peroxide on the graft copolymerization ($\text{H}_2\text{O}_2/\text{Fe}^{2+} = 4$). Amount of hydrogen peroxide used is expressed by logarithm of mole. Graft copolymerization conditions: lignosulfonate, 1 g; methyl methacrylate, 5 ml; 30°C ; 30 min; pH 4.6 (acetate buffer).

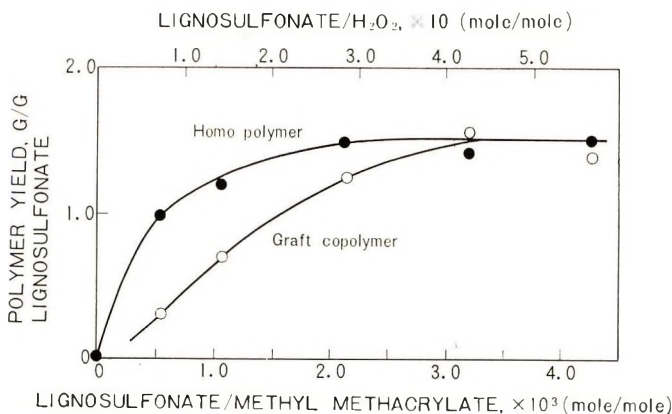


Fig. 9. Dependence of polymer yield on the amount of lignosulfonate. Graft copolymerization conditions: methyl methacrylate, 5 ml; FeSO_4 , 10^{-4} mole; H_2O_2 , 4×10^{-4} mole; 30°C ; 25 min; pH 4.6 (acetate buffer).

methyl methacrylate but remain unchanged after the ratios go up to 3×10^{-3} mole/mole, where the contribution of the lignosulfonate to the polymerization reaction would reach a saturation point. It is of interest to know the apparent activation energy of this very rapidly advancing graft copolymerization of methyl methacrylate onto lignosulfonate. The activation energy of 4.4 kcal/mole seems to be too small, and nevertheless, explains why the graft copolymerization proceeds very easily. Figures 2, 3, and 8 indicate the grafting ratio depends largely upon the ratio $\text{H}_2\text{O}_2/\text{Fe}^{2+}$.

Attempts have been made to graft vinyl acetate and acrylamide, as well as methyl methacrylate, onto lignosulfonate by using the H_2O_2 -Fe(II) redox system. Graft copolymerization has been examined also for the methyl methacrylate-lignosulfonate system with the use of Ce^{4+} ion or benzoyl peroxide systems. In all of the cases, experiments were un-

successful, as separation of graft copolymer from reaction mixture was difficult or only homopolymerization occurred. It is noteworthy, however, that in many cases, the presence of barium lignosulfonate was found to accelerate polymerization of the monomers, when the H_2O_2 -Fe(II) redox system was used in aqueous solution.

CONCLUSION

Graft copolymerization of methyl methacrylate onto barium lignosulfonate from softwood was carried out in aqueous medium. It was found that the H_2O_2 -Fe(II) redox system was extremely effective for the purpose. Particularly, the ratio of $\text{H}_2\text{O}_2/\text{Fe}^{2+}$ was the most important factor determining reaction rates, yields, and composition of the resultant graft copolymers. In the graft copolymerization system, lignosulfonate was thought to participate in the redox system as reducing agent, not only backbone polymer.

References

1. T. Koshijima and E. Muraki, *J. Japan Wood Res. Soc.*, **10**, 110, 116 (1964).
2. T. Koshijima and E. Muraki, *J. Japan Wood Res. Soc.*, **12**, 139 (1966).
3. T. Koshijima, *J. Japan Wood Res. Soc.*, **12**, 144 (1966).
4. T. Koshijima and E. Muraki, *J. Polym. Sci. A-1*, **6**, 1431 (1968).
5. T. Koshijima and E. Muraki, *J. Soc. Materials Sci.*, **16**, 834 (1967).
6. T. Koshijima, E. Muraki, K. Naito, and K. Adachi, *J. Japan Wood Res. Soc.*, **14**, 52 (1968).
7. O. Goldschmid, *Anal. Chem.*, **26**, 1421 (1954).
8. I. Tachi, A. Nakai, and Y. Kojima, *J. Japan. Tech. Assoc. Pulp Paper Ind.*, **14**, 534, 586 (1960).
9. D. Johnson, W. E. Moore, and L. C. Zank, *Tappi*, **44**, 793 (1961).
10. F. Haber and J. Weiss, *Naturwiss.*, **20**, 948 (1932).
11. F. Haber and J. Weiss, *Proc. Roy. Soc. (London)*, **A147**, 332 (1934).
12. J. Baxendale, M. Evans, and G. Park, *Trans Faraday Soc.* **42**, 155 (1946).

Received June 19, 1970

Revised September 21, 1970

Cross-Termination Rate Constants in Copolymerizations of Some Methacrylates and Styrene

KATSUKIYO ITO, *Government Industrial Research Institute of Nagoya, Kita-ku, Nagoya, Japan*

Synopsis

Cross-termination rate constants in the copolymerization of some methacrylates with styrene were determined. The rate constants obtained decrease with increasing r_1 and increase with decreasing r_2 . The relationship between the cross-termination and propagation rate constants was discussed on theoretical and experimental bases.

INTRODUCTION

In the preceding paper,¹ Arlman's treatment² for cross-termination processes in copolymerization was modified. This modified treatment can be analyzed for the cross-termination processes (1):



where A and B are monomer units, k_{ijmn} ($i, j, m, n = A$ or B) are the various cross-termination rate constants, and \bar{k}_{tab} is the geometric mean of two termination rate constants k_{ta} and k_{tb} in homopolymerizations ($\bar{k}_{\text{tab}} = k_{\text{ta}}k_{\text{tb}}$). Relationships between $f_1 (= [B]/[A])$ and $l (= k_{\text{tab}}/\bar{k}_{\text{tab}}, k_{\text{tab}})$; an apparent cross-termination rate constant) are

$$\phi = K_1 + K_2/r_1r_2 + K_3f_1/r_1 \quad K_3f_1r_1 \gg K_4/r_2f_1 \quad (2)$$

$$\phi = K_1 + K_2/r_1r_2 + K_4/r_2f_1 \quad K_3f_1r_1 \ll K_4/r_2f_1 \quad (3)$$

where ϕ is calculated by

$$\phi = (1 + f_1/r_1)(1 + 1/r_2f_1)l \quad (4)$$

and $r_1 = k_{\text{paa}}/k_{\text{pab}}$ and $r_2 = k_{\text{pbb}}/k_{\text{pba}}$ for the propagation rate constants.

On the application of these equations to the various copolymerization systems, $K_1 + K_2/r_1r_2$, K_3 , and K_4 were calculated. Especially, $K_1 + K_2/r_1r_2$ could be related to r_1r_2 by the equation:

$$K_1 + K_2/r_1r_2 = 18/r_1r_2 \quad (5)$$

In this paper, the cross-termination rate constants in copolymerizations of some methacrylates are analyzed by eqs. (2) and (3). The cross-termination rate constants obtained are mainly discussed by relating them to the propagation rate constant.

EXPERIMENTAL

Materials

2,2'-Azobisisobutyronitrile (AIBN), styrene (St), ethyl methacrylate (EMA), *n*-butyl methacrylate (nBMA), and isobutyl methacrylate (iBMA) were commercial products. Phenyl methacrylate (PMA) was obtained from Isequ Co. All monomers were purified by distillation. Their boiling points were: St, 43°C/20 mm Hg; EMA, 48°C/60 mm Hg; nBMA, 54°C/14 mm Hg; iBMA, 43.5°C/13 mm Hg; PMA, 75°C/4-5 mm Hg. AIBN was recrystallized three times from ethanol. All materials were stored in the dark at -28°C.

Procedures

All reaction mixtures were prepared and sealed under an air pressure of about 10^{-4} mm Hg.

Polymerization rates studied at different monomer feed compositions at $[AIBN] = 0.025$ mole/l. were observed by gravimetric determination of the polymer yield, samples of each run being analyzed at three or more different times. After reaction at $60.0 \pm 0.02^\circ\text{C}$ (water thermostat bath), the contents of the ampoule were poured into a large excess of cold methanol. The precipitated polymer was separated by centrifuging, dried *in vacuo*, and weighed. In no case was the conversion greater than 10%. Yields obtained deviated from a smooth curve by less than 2%.

RESULTS

Polymerization rates R_p for given polymerization systems are given in Table I. The values of l were calculated by using conventional equation:³

$$\frac{R_p[\text{St}]_0}{R_{ps}[\text{St}]} = \frac{r^2 + 2f_1/r_2 + f_1^2}{(r^2\alpha^2 + 2lr\alpha f_1 + f_1^2)^{1/2}} \quad (6)$$

where

$$r = r_1/r_2$$

$$\alpha = ([M]_0/[St]_0)(R_{ps}/R_{pm})$$

where R_{pm} and R_{ps} ($= 1.25 \times 10^{-4}$ mole/l.-sec), respectively, are the bulk polymerization rates of methacrylates and St and $[M]_0$ and $[St]_0$, respectively, are the concentrations of methacrylates and St in the bulk polymerizations. The results obtained are given in Table I.

TABLE I
 Values of f_1 , R_p , and l in Various Copolymerization Systems
 ($R_{ps} = 1.25 \times 10^{-4}$ mole/l.-sec)

System	f_1	$R_p \times 10^4$	l
nBMA-St	0	5.18	
	0.0727	2.28	6.57
	0.1536	1.63	10.0
	0.243	1.37	12.9
	0.365	1.17	19.3
	1.38	0.860	34.6
	2.07	0.835	46.6
	3.06	0.800	63.0
	5.53	0.844	64.2
	iBMA-St	0	4.58
0.0736		2.95	3.09
0.1553		2.23	4.59
0.246		1.72	6.98
0.370		1.17	15.3
1.40		0.840	37.9
2.10		0.703	58.0
3.26		0.861	67.2
EMA-St	0	4.03	
	0.0575	2.48	6.22
	0.0885	2.20	6.22
	0.121	1.99	6.77
	0.192	1.59	9.44
	0.288	1.41	10.3
	1.04	0.930	26.1
	1.63	0.933	26.4
	2.50	0.860	35.0
PMA-St	0	18.5	
	0.0710	9.65	1.20
	0.150	8.53	1.82
	0.239	6.90	2.70
	0.318	5.80	3.36
	0.555	4.40	4.64
	0.902	3.50	6.26
	1.35	2.90	8.72
	2.03	2.10	12.5
	3.15	1.80	14.3

TABLE II
 Values of r_1 , r_2 , $K_1 + K_2/r_1r_2$, K_3 and K_4 for the
 Copolymerization of Methacrylates and Styrene^a

System	r_1	r_2	$K_1 + K_2/r_1r_2$	K_3	K_4
nBMA-St	0.40	0.56	170	6.0	134
iBMA-St	0.40	0.55	95	1.0	114
EMA-St	0.41	0.53	100	4.6	65
MMA-St	0.46	0.52	80 ^b	8.5 ^b	24.3 ^b
PMA-St	0.60	0.30	25	1.0	20

^a r_1 , r_2 are data of Ōtsu et al.⁴

^b Data of the preceding paper.¹

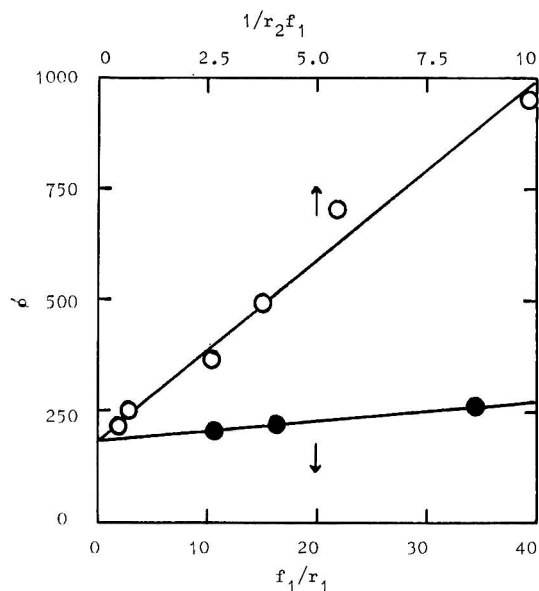


Fig. 1. Relationship between ϕ and f_1/r_1 or $1/r_2 f_1$ in copolymerization of nBMA-St at 60°C: (●) f_1/r_1 vs. ϕ ; (○) $1/r_2 f_1$ vs. ϕ .

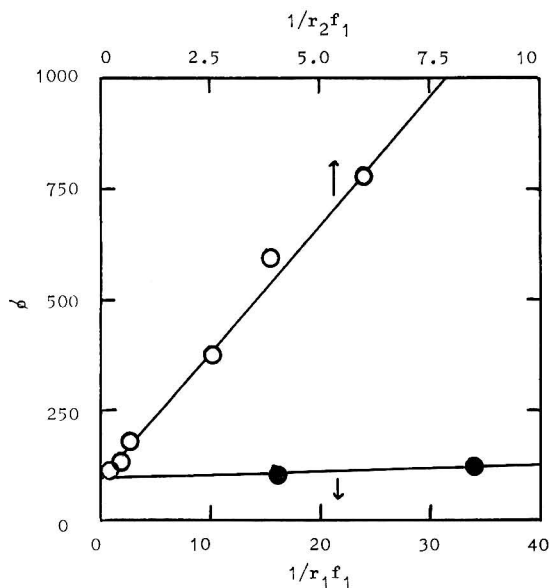


Fig. 2. Relationship between ϕ and f_1/r_1 or $1/r_2 f_1$ in copolymerization of iBMA-St at 60°C: (●) f_1/r_1 vs. ϕ ; (○) $1/r_2 f_1$ vs. ϕ .

On the applications of eqs. (2) and (3) to the various values in Table I and the values of r_1 and r_2 (Table II), various linear relationships could be obtained (Figs. 1-4). From these linear relationships, the values of $K_1 + K_2/r_1 r_2$, K_3 and K_4 were calculated and are given in Table II.

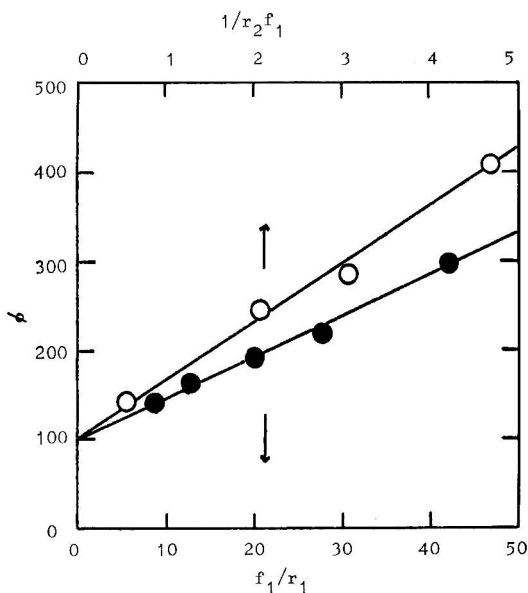


Fig. 3. Relationship between ϕ and f_1/r_1 or $1/r_2 f_1$ in copolymerization of EMA-St at 60°C: (●) f_1/r_1 vs. ϕ ; (○) $1/r_2 f_1$ vs. ϕ .

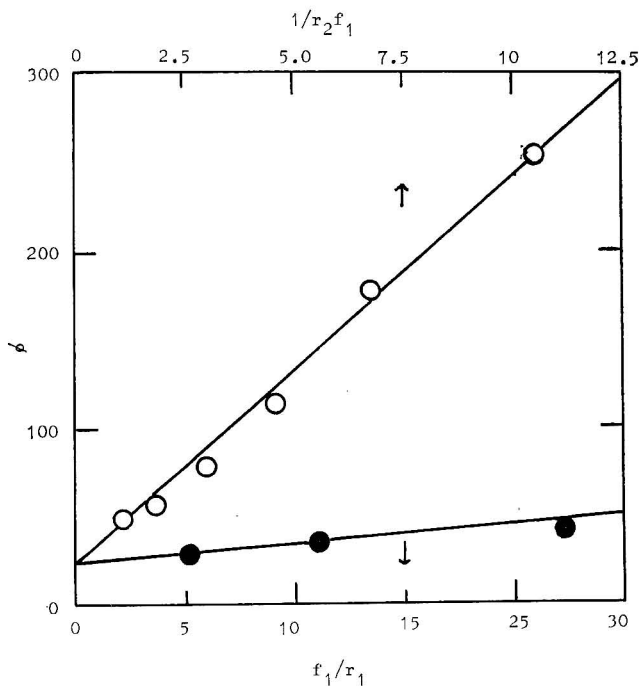


Fig. 4. Relationship between ϕ and f_1/r_1 or $1/r_2 f_1$ in copolymerization of PMA-St at 60°C: (●) f_1/r_1 vs. ϕ ; (○) $1/r_2 f_1$ vs. ϕ .

DISCUSSION

In the preceding paper,¹ eq. (5) is experimentally formulated by assuming that:



In this experiment, eq. (5) is applicable to the copolymerizations of iBMA ($K_1 + K_2/r_1r_2 = 21$) and EMA with St ($K_1 + K_2/r_1r_2 = 22$), but is not applicable to the copolymerization of nBMA-St ($K_1 + K_2/r_1r_2 = 38$) and PMA-St ($K_1 + K_2/r_1r_2 = 4.5$). Thus, this equation is not always applicable. $K_1 + K_2/r_1r_2$ may be qualitatively related to r_1 and r_2 by the increase and decrease of $K_1 + K_2/r_1r_2$ with the decrease of r_1 and the increase of r_1 , respectively (Table II).

K_3 denotes $\text{---BB}^* + \text{*AB} \text{---}$; here, B is St and A is methacrylate and variable. On the variation of A, K_3 values are scattered (Table II) and should not be related to r_1 and r_2 .

K_4 denotes $\text{---AA}^* + \text{*BA} \text{---}$. On the variation of A, K_4 values decrease and increase with increasing r_1 and decreasing r_2 , respectively.

In the preceding paper,¹ K_x is given by

$$K_x = L \exp\{(L_m - L)/R\}/L_m(1 - \exp\{-L/R\}) \quad (7)$$

where L is the distance between the radical chain ends for the thermal energy equalling the coulombic energy of interaction of the net electric charges, L_m is the value of L for the geometric mean \bar{k}_{tab} , and R is the average distance of approach of the radical chain ends for bimolecular reaction. This equation is so complex that a linear relationship between K_x and L over a wide range of L can not be obtained. Further, the experimental results in the preceding paper¹ and this paper are not valid. Thus, the examination of the experimental results were not quantitatively carried out by using Eq. (7).

Following Alfrey and Price,⁵ the familiar propagation rate constant given by eq. (8) is determined by assuming that the actual electric charge $*c$ exists not only on the radical chain end but also on the monomer:

$$k_p = PQ \exp\{-*c^2/R\gamma kT\} \quad (8)$$

where P is characteristic of the radical chain end, Q is the mean reactivity of the monomer, γ is the effective dielectric constant, k is the Boltzmann constant, and T is the absolute temperature.

In a previous paper,⁶ on assuming that:

$$1 \gg \exp\{-L/R\} \quad (9)$$

the chain-termination rate constant was given by:

$$k_t = \text{const. } DL \exp\{-L/R\} \quad (10)$$

where D is the diffusion constant of the radical chain end. When the change of L is small, eq. (10) is rewritten:

$$k_t = \text{const. } D \exp\{-L/R\} \quad (11)$$

By evaluating the distance L by:⁷

$$L = \sigma^* c^2 / \gamma k T \quad (11)$$

we obtain:

$$k_t = \text{const. } D k_p \quad (12)$$

On the application of this equation to the cross-termination and propagation rate constants for a small influence of the penultimate unit, we obtain:

$$l^2 = \text{const.} / r_1 r_2 \quad (13)$$

In the past, by using eq. (13), a relationship between the cross-termination and propagation rate constants has been discussed.^{8,9} However, eqs. (8), (12), and (13) are not correct on the following theoretical and experimental grounds: (1) it may not be possible that an actual electric charge exists on the monomer; (2) the cross-termination rate constant depends strongly on the penultimate unit, but the propagation rate constant is independent of it; (3) the change of K_x compares favorably with the change of r_1 or r_2 . This large change can not be evaluated by eq. (13).

In the bulk polymerizations of some methacrylates, the chain termination rate constant and the propagation rate constant at 30°C are, respectively:^{10,11}

$$k_t = \text{const. } D \times 10^{-1.4\sigma^*} \quad (14)$$

and

$$k_p = \text{const. } 10^{-0.7\sigma^*} \quad (15)$$

where σ^* is the Taft polar constant. The dependence of the Taft polar constant on the chain termination constant is larger than the dependence on the propagation rate constant, and this relationship can not be evaluated by eq. (12).

At least, eq. (13) can not provide a quantitative interpretation for the relationship between the cross-termination and propagation rate constants.

References

1. K. Ito, *J. Polym. Sci. A-1*, **8**, 2819 (1970).
2. E. Arlman, *J. Polym. Sci.*, **17**, 375 (1955).
3. C. Walling, *J. Amer. Chem. Soc.*, **71**, 1930 (1949).
4. T. Ōtsu, T. Ito, and M. Imoto, *J. Polym. Sci. B*, **3**, 113 (1965).
5. T. Alfrey and C. C. Price, *J. Polym. Sci.*, **2**, 101 (1947).

6. K. Ito, *J. Polym. Sci. A-1*, **8**, 1823 (1970).
7. P. Debye, *Tran. Electrochem. Soc.*, **82**, 265 (1942).
8. E. P. Bonsall, L. Valentine, and H. W. Melville, *J. Polym. Sci.*, **7**, 39 (1952).
9. I. N. Duling and C. C. Price, *J. Amer. Chem. Soc.*, **84**, 578 (1962).
10. K. Ito, *J. Polym. Sci.*, **7**, 2247 (1969).
11. K. Yokota, M. Kani, and Y. Ishii, *J. Polym. Sci. A-1*, **6**, 573 (1968).

Received August 24, 1970

Polymerization of Butadiene and Vinyl Ether with Catalyst Prepared from π -Allyl Nickel Halide and Organic Peroxide

TSUYOSHI MATSUMOTO,* JUNJI FURUKAWA,
and HIROHISA MORIMURA,

Department of Synthetic Chemistry, Kyoto University, Kyoto, Japan

Synopsis

The π -allyl nickel halide-organic peroxide system has been found to be active as catalyst for the stereospecific polymerization of butadiene and polymerization of vinyl ether. Benzoyl peroxide is most effective. The catalyst from π -allyl nickel chloride or π -allyl nickel bromide and benzoyl peroxide yields predominantly *cis*-1,4 polymer with high activity, whereas the catalyst from π -allyl nickel iodide affords predominantly *trans*-1,4 polymer. The catalyst system can be divided into two parts, a benzene-soluble and a essentially insoluble component. It is concluded that the catalyst activity originates essentially from the insoluble nickel complex which is composed of halogen atom, benzoyloxy group of conjugated structure, allyl group, and nickel. A structure is proposed for the complex.

INTRODUCTION

The authors have investigated the stereospecific polymerization of butadiene with various nickel catalysts (reduced nickel on a carrier, Raney nickel with metal halide, and nickel compound with metal halide-organometal)¹⁻³ and reported a mechanistic study on the polymerization with π -allyl nickel halide.⁴

The present investigation, which was partly reported in letter form previously,^{5,6} is concerned with new metal complex catalysts prepared from π -allyl nickel halides and organic peroxides and was employed for the stereospecific polymerization of butadiene and the polymerization of vinyl ether.

The reaction product of π -crotyl nickel chloride with benzoyl peroxide was effective as a catalyst for *cis*-1,4 polymerization and was found to be composed of nickel atom, benzoyloxy group, chlorine atom, and crotyl group, in molar ratios of about 1 : 1 : 1 : 0.03-0.05.

Little was reported on the reaction of organic peroxide with transition metal complex before our previous reports. Hagihara et al. prepared tetra-*tert*-butoxychromium from di-*tert*-butyl peroxide and dibenzene chromium.⁷

* On leave of absence from Japan Synthetic Rubber Co., Ltd., Kyobashi, Tokyo, Japan.

Dicyclopentadienyltitanium dibenzoate was prepared from dicyclopentadienyltitanium and benzoyl peroxide by Razuev et al.⁸

Very recently, dicyclopentadienylvanadium was reported by Razuev et al.⁹ to react with peroxides to yield trivalent and tetravalent vanadium benzoate. Scott and Wilke reported the preparation of di-*tert*-butoxy nickel and dibenzoyloxy nickel from ethylenebis(triphenylphosphine)nickel and peroxides.¹⁰

No nickel complex having a benzoyloxy group and halogen has been reported, and our investigation might be the first report to preparation of a stereospecific polymerization catalyst from a transition metal complex and a peroxide.

EXPERIMENTAL

Materials

π -Allyl or π -crotyl nickel halides were prepared from nickel carbonyl and allyl or crotyl halides according to the method of Fisher.¹¹ Organic peroxides were commercial products and were purified by ordinary methods. Benzene was freed of oxygen and water by distillation over the metal ketyl from benzophenone and sodium. Butadiene of BR (butadiene rubber) grade was provided by Japan Synthetic Rubber Company and dried over molecular sieves.

Polymerization

Polymerizations were carried out in glass reaction vessels in a nitrogen atmosphere. Dry butadiene was introduced by distillation to the vessels by using a vacuum-nitrogen apparatus. Polymerizations were terminated by addition of methanol containing aqueous hydrochloric acid.

Reaction of π -Allyl Nickel Halide with Benzoyl Peroxide

A benzene solution of benzoyl peroxide was added to π -allyl nickel halide dissolved in benzene at room temperature with shaking. The reaction mixture was aged about 30 min at room temperature. A precipitate was formed within a few minutes after addition of benzoyl peroxide. In the cases when the reaction mixture was used as catalyst, the above procedure was done in polymerization vessels. The solid nickel complexes which were insoluble in benzene were isolated by filtering the above reaction mixtures in nitrogen atmosphere, followed by washing several times with benzene and drying *in vacuo*. They were transferred to polymerization vessels in a nitrogen box.

Infrared Spectroscopy, Magnetic Susceptibility Measurement, and Elemental Analysis of Nickel Complexes

For these measurements, the samples were prepared under nitrogen atmosphere in a dry box. The infrared spectra were recorded on a Hitachi

grating spectrometer EPI-G. Elemental analysis was done with independent samples for each element.*

Hydrolysis of Nickel Complexes

Nickel complexes were placed in a flask equipped with two necks, one connected with a gas buret and a vacuum-nitrogen apparatus and the other closed with a rubber stopper. Aqueous hydrochloric acid was added by a syringe through the rubber stopper. Gas evolved was identified by vapor-phase chromatography by using activated charcoal.

Microstructure of the Polymers

The polymers were examined in carbon disulfide solution. The method of analysis is that reported by Morero et al.¹²

RESULTS AND DISCUSSION

Polymerization

π -Crotyl nickel chloride itself is poorly active for *cis*-1,4-polymerization of butadiene, but the addition of organic peroxide was found to enhance the activity, as shown in Table I.

Benzoyl peroxide was most effective. In order to clarify whether or not the peroxide acts as a radical initiator for the polymerization, other radical initiators were employed. Azobisisobutyronitrile (AIBN) had no influence on the catalyst activity but decreased the *cis*-1,4 content of the resulting polymer. Di-*tert*-butyl peroxide was much less effective. Lauroyl peroxide was quite effective. Therefore, benzoyl peroxide in the catalyst system does not function merely as a simple radical initiator.

Other oxygen compounds capable of coordinating to the nickel atom, such as phenol, acetylacetone, maleic anhydride, and silver acetate, were found to be ineffective.

As described later, the nickel complex from π -crotyl nickel chloride and benzoyl peroxide was found to contain a benzoyloxy group. Unlike benzoyl peroxide and lauroyl peroxide, other benzoyloxy derivatives such as benzoic acid, benzoic anhydride, and sodium benzoate were much less active.

This fact suggests that the effective ligand is not benzoate anion but benzoyloxy radical.

The reaction of π -crotyl nickel chloride with di-*tert*-butyl peroxide in benzene afforded a transparent, dark-red solution similar to π -crotyl nickel chloride solution, whereas that with benzoyl or lauroyl peroxide yielded a precipitate. The former solution was subjected to infrared spectroscopy after aging for 1 hr in a solution of higher concentration than that used for polymerization. All bands for di-*tert*-butyl peroxide and π -crotyl nickel

* Magnetic susceptibility was measured by the Gouy method with a balance of Sartorius 2514 type and an electromagnet of Nihonkomitsu 100 type.

TABLE I
Polymerization of Butadiene with Catalysts Systems Containing
 π -Crotyl Nickel Chloride^a

No.	Co-catalyst		Poly- merization time, hr	Poly- mer yield, %	<i>cis</i> - 1,4, %	<i>trans</i> - 1,4, %	1,2, %
	Type	mmole					
1	—		60	5	76	20	4
2	—		88	6	79	18	3
3	Benzoyl peroxide	0.5	14	94	86	10	3
4	Benzoyl peroxide	0.5	1	85	89	7	4
5	Benzoyl peroxide	1.0	1	90	90	7	3
6	Lauroyl peroxide	1.0	11	80	79	16	5
7	Lauroyl peroxide	1.0	3	40	80	15	5
8	Di- <i>tert</i> -butyl peroxide	0.5	60	30	77	20	3
9	Di- <i>tert</i> -butyl peroxide	1.0	33	42	76	20	4
10	AIBN	0.3	64	7	45	43	3
11	AIBN	0.5	64	8	0	78	22
12	Benzoic anhydride	1.0	60	35	77	19	4
13	Benzoic anhydride	2.0	3	2	—	—	—
14	Benzoic acid	1.0	60	10	82	13	5
15	Na benzoate	1.0	60	1	—	—	—
16	Phenol	1.0	60	1	—	—	—
17	Ag acetate	1.0	60	11	18	64	18
18	Maleic anhydride	0.6	64	8	74	21	5
19	Acetylacetone	0.5	64	9	78	21	1
20	Acetylacetone	1.0	64	9	72	24	5

^a Conditions: catalyst, $[\pi\text{-C}_4\text{H}_7\text{NiCl}]_2$, 1.0 mmole (except run 2), 2.3 mmole (run 2); butadiene, 7.2 g; benzene, 16 ml; polymerization temperature, 40°C; reaction between two components, room temperature, ca. 15–30 min.

chloride were observed and none of new band could be detected. Therefore, di-*tert*-butyl peroxide hardly reacted with π -crotyl nickel chloride.

Further studies were done with benzoyl peroxide. Table II summarizes the results of polymerization by catalysts with various amounts of added peroxide. The optimum mole ratio of benzoyl peroxide to π -crotyl nickel chloride for activity was 1.0. The *cis*-1,4 contents of polymers were almost the same. This means that the same active site was formed, regardless of the amount of added peroxide, although the molecular weight of the polymer increased with increasing mole ratio.

A precipitate was formed when π -crotyl nickel chloride was mixed with benzoyl peroxide in benzene. The reaction mixture was divided into a benzene-insoluble and a benzene-soluble part, and the activities of these components were investigated, as summarized in Table III. The activity of the system for *cis*-1,4 polymerization was found to originate from the solid complex insoluble in benzene. Experiment 4 of Table III shows the activity of the catalyst in a large-scale run. The addition of 1.0 mole of benzoyl peroxide to π -crotyl nickel chloride resulted in the quantitative formation of the active, benzene insoluble complex, whereas a 0.5 mole of peroxide

TABLE II
Effect of Mole Ratio of Benzoyl Peroxide to π -Crotyl Nickel Chloride^a

No.	(C ₆ H ₅ - CO ₂) ₂	Poly- mer- ization time hr	Poly- mer yield, %	<i>cis</i> - 1,4, %	<i>trans</i> - 1,4, %	1,2, %	[η] (toluene, 30°C), dl/g
	[C ₄ H ₇ - NiCl] ₂ ratio						
1	0.50	1.7	35	90	8	2	0.7
2	0.75	1.7	56	91	5	4	0.9
3	1.00	1.7	68	90	7	3	1.1
4	1.25	1.7	42	91	6	3	1.4
5	1.50	15	0	—	—	—	—

^a Conditions: [C₄H₇NiCl]₂, 0.133 mmole; butadiene, 3.6 g; benzene, 8 ml; polymerization temperature, 50°C; reaction between two components, room temperature, 15 min.

yielded a soluble complex together with an insoluble one. The former was slightly active for *cis*-polymerization, unlike the latter. Consequently, the activity of the reaction mixture originated from the benzene-insoluble complex for the most part.

Table IV lists the results of polymerization with π -allyl nickel bromide, which alone yielded *trans*-polymer with low activity. On the contrary, the π -allyl nickel bromide-benzoyl peroxide system initiated *cis*-polymerization with relatively high activity, although the activity was lower than that of the π -crotyl nickel chloride-benzoyl peroxide system. The optimum mole ratio was also 1.0. A brown precipitate was formed when π -allyl nickel bromide was allowed to react with benzoyl peroxide (BPO) in benzene. The insoluble part isolated yielded a polymer of higher *cis* content and higher molecular weight with lower activity than the reaction mixture itself. The benzene-soluble part separated from the reaction mixture was almost inactive for the polymerization under the conditions described in Table IV. The active site in the benzene-insoluble part seems to be the same both when the mole ratio was 0.5 and 1.0, because polymers obtained in both cases were of the same microstructure.

The results with π -allyl nickel iodide are shown in Table V.

π -Allyl nickel iodide alone initiated *trans* polymerization. In contrast to the case with π -allyl nickel bromide, the π -allyl nickel iodide-benzoyl peroxide system was active for *trans* polymerization, although a precipitate was formed by the reaction of π -allyl nickel iodide with benzoyl peroxide. The benzene-insoluble nickel complex separated from the reaction mixture also initiated *trans* polymerization.

The solubility of the complex catalyst prepared from π -crotyl nickel chloride and benzoyl peroxide in a polar solvent was studied in relation to the catalyst activity. It was soluble in methanol, tetrahydrofuran, and methyl ethyl ketone but insoluble in diethyl ether. The complex seems to be soluble in solvents more polar than methyl ethyl ketone. In Table IV, the

TABLE III
Separation of the Reaction Mixture of π -Crotyl Nickel Chloride with Benzoyl Peroxide^a

No.	Catalyst	Polymerization time, hr	Polymer yield, %	<i>cis</i> -1,4, %	<i>trans</i> -1,4, %	1,2, %	$[\eta]$ (toluene, 30°C), dl/g
1	Reaction mixture	1.0	9.5	90	7	3	—
2	Solid complex insoluble in benzene	1.0	9.5	92	4	4	—
3	Filtrate	72	3	—	—	—	—
4	same as No. 2	4.0	50	94	3	3	2.1
5	Reaction mixture	1.0	8.5	89	7	4	—
6	Solid complex insoluble in benzene	1.0	7.8	91	5	4	—
7	Filtrate	12	13	86	11	3	—

^a Conditions: $[\pi\text{-C}_4\text{H}_7\text{NiCl}]_2$ (except run 4), 1.0 mmole; butadiene, 7.2 g; benzene, 16 ml; reaction between components, room temperature, 30 min; polymerization temperature, 40°C. Conditions for run 4, $[\pi\text{-C}_4\text{H}_7\text{NiCl}]_2$, 2.5 mmole; butadiene, 72 g; benzene 160 ml.

TABLE IV
 Polymerization of Butadiene with the Catalyst Prepared from π -Allyl Nickel Bromide and Benzoyl Peroxide^a

No.	$\frac{[\text{C}_6\text{H}_5\text{CO}_2]_2}{[\text{C}_3\text{H}_5\text{NiBr}]_2}$ ratio	Mixture or benzene- insoluble part	Polymerization time, hr	Polymer yield, %	<i>cis</i> -1,4, %	<i>trans</i> -1,4, %	1,2, %	$[\eta]$ (toluene, 30°C), dl/g
1	0	—	87	40	0	89	11	—
2	0.50	mix	3	58	80	13	7	0.6
3	0.75	mix	3	71	87	8	5	—
4	1.00	mix	3	83	88	7	5	0.8
5	1.25	mix	3	53	88	7	5	—
6	1.50	mix	43	0	—	—	—	—
7	0.50	Bz.-insol.	3	37	90	5	5	1.5
8	1.00	Bz.-insol.	3	52	91	4	5	1.4

^a Conditions: $[\text{C}_3\text{H}_5\text{NiBr}]_2$, 1 mmole; butadiene, 7.2 g; benzene, 16 ml; reaction between two components, room temperature, 30 min; polymerization temperature, 40°C.

TABLE V
 Polymerization of Butadiene with the Catalyst Prepared from π -Crotyl Nickel Iodide and Benzoyl Peroxide^a

No.	$\frac{[\text{C}_6\text{H}_5\text{CO}_2]_2}{[\text{C}_4\text{H}_7\text{NiI}]_2}$ ratio	Mixture or benzene- insoluble part	Polymerization time, hr	Polymer yield, %	<i>cis</i> -1,4, %	<i>trans</i> -1,4, %	1,2, %
1	0	—	29	41	0	96	4
2	1.0	mix	29	48	0	96	4
3	1.5	mix	120	48	0	96	4
4	2.0	mix	120	33	0	95	5
5	1.0	Bz.-insol.	48	30	0	95	5
6 ^b	1.0	Bz.-insol.	48	24	0	95	5

^a Conditions: same as described for Table IV.

^b π -Allyl nickel iodide was used.

catalyst preparation was carried out in benzene followed by the addition of polar solvent after aging. With methyl ethyl ketone, the system became heterogeneous when butadiene was added. Methyl ethyl ketone decreased the activity markedly, and tetrahydrofuran changed the microstructure of the polymer from *cis* to *trans*. A significant amount of oligomers was not detected.

TABLE VI
Effect of Polar Solvents^a

No.	Solvent ^b	Poly- merization time, hr	Polymer yield, %	<i>cis</i> - 1,4, %	<i>trans</i> - 1,4, %	1,2, %
1	Benzene	1	90	90	7	3
2	Diethyl ether- benzene (1:1)	2	62	88	8	4
3	Methyl ethyl ketone- benzene (1:1)	120	26	66	29	5
4	Tetrahydrofuran- benzene (1:1)	120	5	0	97	3
5	Methanol-benzene (1:1)	120	Trace	—	—	—

^a Conditions: $[C_4H_7NiCl]_2$, 1.0 mmole; butadiene, 7.2 g; benzoyl peroxide, 1.0 mmole; polymerization temperature, 40°C.

^b Total volume, 16 ml.

The results of polymerization of vinyl monomers with the complex catalyst of this investigation are shown in Table VII. The polymerization was not a radical-type reaction, although peroxide was used as a component of the catalyst. The systems involving π -crotyl nickel chloride or π -allyl nickel bromide were found to be very active catalyst for cationic polymer-

TABLE VII
Polymerization of Vinyl Monomers^a

No.	Catalyst system	Monomer	Poly- merization time, hr	Polymer yield, %	$[\eta]$ (tol- uene, 30°C), dl/g
1	Crotyl NiCl-BPO	Styrene	48	35	—
2	Crotyl NiCl-BPO	Methyl methacrylate	48	Trace	—
3	Crotyl NiCl-BPO	Acrylonitrile	48	Trace	—
4	Crotyl NiCl-BPO	Isobutyl vinyl ether	Instan- taneous	100	0.5
5	Allyl NiBr-BPO	Methyl methacrylate	48	Trace	—
6	Allyl NiBr-BPO	Isobutyl vinyl ether	0.5	95	—
7	Crotyl NiI-BPO	Isobutyl vinyl ether	7	11	—

^a Reaction mixture was used as catalyst and mole ratio of components is 1.0. Conditions are same as in Table IV except that monomer charged was 10 ml.

ization as well as *cis*-1,4 polymerization of butadiene. The catalytic activity for isobutyl vinyl ether was rather higher than for butadiene. The polymer was solid and soluble in methyl ethyl ketone. It is noteworthy that the catalysts for *cis*-1,4 polymerization of butadiene, such as nickel on diatomaceous earth and nickel naphthenate-boron fluoride-triethylaluminum, are also active for cationic polymerization of vinyl ethers.^{1,3} The cationic character of the nickel catalyst for *cis*-1,4 polymerization seems to be general.

Structure of Catalyst

The active solid complex separated as the benzene-insoluble part from the 1:1 reaction mixture of π -crotyl nickel chloride with benzoyl peroxide was subjected to elemental analysis, magnetic susceptibility measurement, infrared spectroscopy, and hydrolysis by aqueous hydrochloric acid.

The solid nickel complex was insoluble in diethyl ether but soluble in tetrahydrofuran; this suggests the complex to be a polar metal complex.

Elemental analysis was done independently for Ni, C, H, O, and Cl; the results are shown in Table VIII.

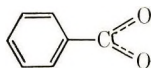
TABLE VIII

	Ni, %	C, %	H, %	O, %	Cl, %
Found	26.8	41.8	3.2	14.0	15.0
Calcd for NiC ₇ H ₅ O ₂ Cl	27.1	38.7	3.3	14.7	16.3

It is suggested that the complex is mainly composed of one benzoyloxy group and one chlorine atom per nickel atom.

The infrared spectrum of the complex is shown in Figure 1. The complex had no band at 1760, 1220, and 990 cm^{-1} characteristic of benzoyl peroxide and no detectable band at 1240, 980, 960, 910, 880, and 817 cm^{-1} assignable to π -crotyl nickel chloride. The sharp, strong band at 1600 cm^{-1} and the sharp band at 1485 cm^{-1} in Figure 1 are assigned to C=C stretching of the aromatic ring. Bands at 720 and 680 cm^{-1} are assigned to C—H out-of-plane deformation of monosubstituted benzene, and several bands at 1200–1000 cm^{-1} to C—H in-plane deformation of monosubstituted benzene. The bands at about 1550 cm^{-1} may be assigned to the O=C=O group, since diacetodiallyldipalladium¹³ has a band at about 1575 cm^{-1} but not at about 1700 cm^{-1} . Generally, carboxyl groups without hydrogen bonding have a strong band at a wavenumber higher than 1700 cm^{-1} , where this complex had only a very weak one.

From infrared spectroscopic data, it is likely that the main organic ligand of the complex is of a conjugated benzoyloxy radical structure (I)

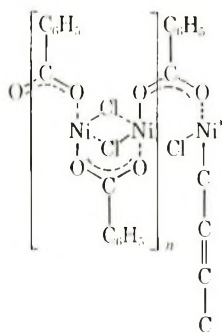


I

The magnetic susceptibility of the complex was 21.6×10^6 at 21°C . Since the nickel content was 26.7%, this means that two unpaired electrons exist per nickel atom or that the nickel atom is divalent.

Decomposition of the complex by aqueous hydrochloric acid gave benzoic acid (63% yield with respect to benzoyl peroxide) and a small amount of butenes (3.4–4.2% yield with respect to crotyl radical, calculated from evolved gas volume). Identification was by infrared and mass spectra and vapor-phase chromatography.

The analytical data lead to the conclusion that the complex involves nearly one benzyloxy group as depicted above, nearly one chlorine atom, and 0.03–0.05 crotyl group per nickel atom. The fact that the complex is paramagnetic suggests that its configuration is not square-planar. A probable structure is shown as II.



II

Infrared spectra of the benzene-insoluble complexes from 1:1 mixtures of benzoyl peroxide and π -allyl nickel bromide or π -crotyl nickel iodide were almost the same as that of the complex from π -crotyl nickel chloride shown in Figure 1. Hydrolysis by aqueous hydrochloric acid of the complex from π -allyl nickel bromide gave also benzoic acid (59% yield with respect to benzoyl peroxide) together with a small amount of propylene (5% yield with respect to allyl radical) but no propane. Nickel content of the complex from π -allyl nickel bromide was 21.6%, which is fairly consistent with 22.5% calculated for $\text{C}_7\text{H}_5\text{O}_2\text{NiBr}$. These data suggest that the benzene-insoluble complex from 1:1 reaction mixture of benzoyl peroxide and π -allyl nickel bromide or iodide is of a similar structure to that from π -crotyl nickel chloride.

The active site in the catalyst is assumed to be the nickel atom (Ni^*) attached to the allyl ligand. It is likely that the allyl ligand exists in a form of σ -allyl, since the complex prepared from π -allyl nickel bromide and oxygen is very active for *cis*-1,4 polymerization and contains σ -allyl.^{5,6} The σ -allyl form may be stabilized by the electron-withdrawing π -interaction of the benzyloxy ligand with nickel. The nickel atom (Ni^*) possesses 10 electrons ($3d^84s^2$) and shares four electrons: two with oxygen, one with chlorine, and one with σ -allyl ligand. Therefore, the nickel atom is capable of coordination with butadiene bidentately, accepting more four electrons to form the krypton shell, contrary to the case of π -allyl ligand.

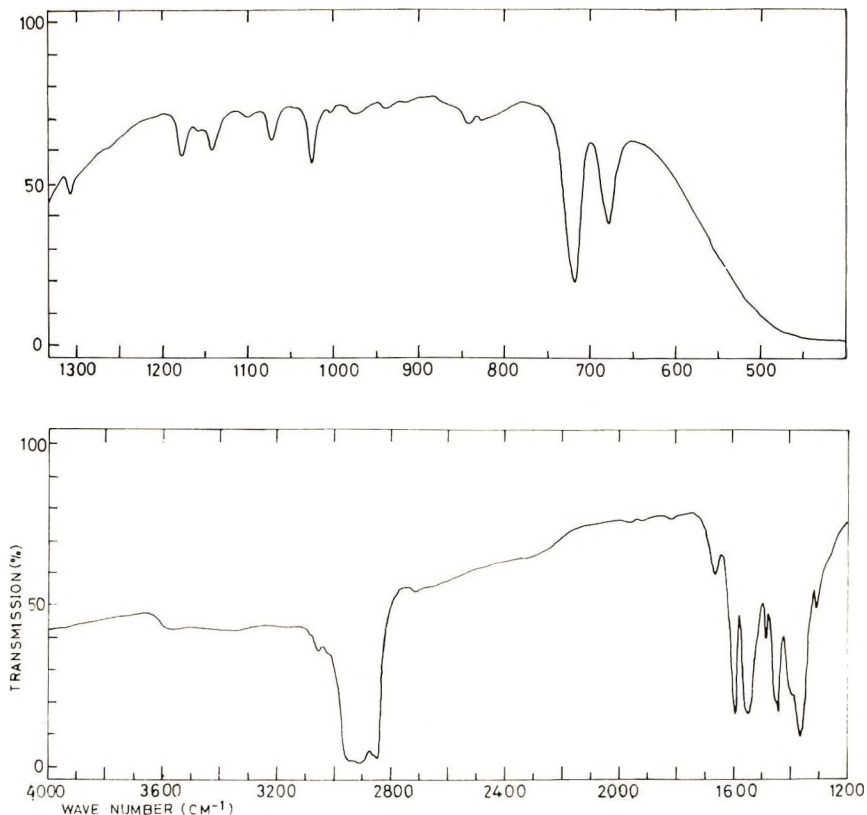


Fig. 1. Infrared spectrum of the benzene-insoluble complex formed by reaction of π -crotyl nickel chloride with benzoyl peroxide (Nujol).

The filtrate in experiment 7 in Table III was found on the basis of infrared data to contain a new nickel complex. It was paramagnetic. Its structure is now being investigated.

The mechanism of *cis* polymerization will be discussed in terms of the results obtained by various catalysts and the quantum chemical calculation in other papers, in which the role of the benzoyloxy ligand in the present catalyst will be explained.

The authors are thankful to Dr. S. Hashimoto and Mr. T. Matsui for elemental analysis and measurement of magnetic susceptibility.

References

1. T. Matsumoto and S. Ohnishi, *Kogyo Kagaku Zasshi*, **71**, 1709 (1968).
2. K. Ueda, S. Ohnishi, T. Yoshimoto, J. Hosono, K. Maeda, and T. Matsumoto, *Kogyo Kagaku Zasshi*, **66**, 1103 (1963).
3. T. Matsumoto and S. Ohnishi, *Kogyo Kagaku Zasshi*, **71**, 2059 (1968).
4. T. Matsumoto and J. Furukawa, *J. Polym. Sci. B*, **5**, 935 (1967).
5. T. Matsumoto, J. Furukawa, and H. Morimura, *J. Polym. Sci. B*, **6**, 869 (1968).
6. T. Matsumoto, J. Furukawa, and H. Morimura, *J. Polym. Sci. B*, **7**, 541 (1969).

7. N. Hagihara and H. Yamazaki, *J. Amer. Chem. Soc.*, **81**, 3160 (1959).
8. G. A. Razuev, V. N. Latyaeva, and L. I. Vyshinskaya, *Dokl. Akad. Nauk SSSR*, **138**, 1126 (1961).
9. G. A. Razuev, V. N. Latyaeva, and A. N. Lineva, *Dokl. Akad. Nauk SSSR*, **187**, 340 (1969).
10. H. Scott and G. Wilke, *Angew. Chem.*, **81**, 896 (1969).
11. O. Fisher and G. Burger, *Z. Naturforsch.*, **16b**, 77 (1961).
12. D. Morero, A. Santambrogio, L. Porri, and F. Ciampelli, *Chim. Ind. (Milan)*, **41**, 758 (1959).
13. S. B. Robinson and B. L. Shaw, *J. Organometal. Chem.*, **3**, 367 (1965).

Received July 20, 1970

Revised October 8, 1970

Optically Active Copolyamides by Melt and Solution Condensation Polymerization

HIDEMASA YAMAGUCHI, HIROSHI UENO, and YUJI MINOURA,
Faculty of Engineering, Osaka City University, Osaka, Japan

Synopsis

The melt and solution condensation copolymerization of nylon salts which were prepared from *d*-camphoric acid and adipic acid with hexamethylenediamine were carried out, and optically active copolyamides were obtained. The copolyamides obtained had a positive specific rotation. The specific rotations for the copolyamides increased with increasing content of *d*-camphoryl units in the copolymers. The optical rotatory dispersion of the copolyamides had positive curves and were found to fit the simple Drude equation. The λ_c values of the polymers obtained by the melt and solution condensation polymerization were 241 $m\mu$ and 245 $m\mu$, respectively.

INTRODUCTION

The copolymerization of vinyl monomers having optically active substituents has been widely studied. Schuerch¹ has copolymerized *l*- α -methylbenzyl methacrylate and *l*- α -methylbenzyl vinyl ether with maleic anhydride to obtain optically active copolymers, which remained to be optically active after the cleavage of optically active side group. Schulz et al.² studied the copolymerization of styrene and menthyl acrylate and reported that the specific rotation of the copolymer increased linearly with increasing content of menthyl acrylate unit. We carried out³ copolymerizations of *N*-bornyl maleimide with styrene, methyl methacrylate, and vinylidene chloride with a free-radical catalyst to obtain optically active copolymers. On the basis of the results that the relation between the specific rotation and the composition of these copolymers was not linear, it was claimed that the asymmetric carbon atoms were newly induced in the polymer main chain.

There have been numerous studies⁴⁻⁸ on optically active polyamides. Overberger and his co-workers^{5,6} obtained optically active polyamides by the ring-opening polymerization of optically active ϵ -caprolactam derivatives and studied their optical behavior. Toy⁷ prepared optically active and inactive polycamphorates and polycamphoramides to compare the melting and crystalline properties of the optically active polymers with those of the corresponding inactive ones. Iwakura et al.^{9,10} prepared optically active polyureas and polyurethanes.

In the previous paper,⁸ we mentioned optically active polyamides synthesized at high temperature by condensation polymerizations of the salt pre-

pared from *d*-tartaric acid with diamines, such as hexamethylenediamine and phenylenediamine.

In the present study, melt and solution condensation copolymerizations of the nylon salts prepared from *d*-camphoric acid and adipic acid with hexamethylenediamine were carried out, and optically active copolyamides were obtained.

EXPERIMENTAL

Materials

Commercially available *d*-camphoric acid and adipic acid were used without further purification. *d*-Camphoric acid has mp 185–186.5°C and $[\alpha]_D^{25} +47.0^\circ$ in EtOH. Hexamethylenediamine was distilled at reduced pressure over potassium hydroxide (bp 94–100°C/20 mm Hg).

Preparation of Hexamethylenediamine *d*-Camphoric Acid Salt and Hexamethylenediamine Adipic Acid Salt

A typical preparation of the hexamethylenediamine *d*-camphoric acid salt used in this work is described below.

d-Camphoric acid (14.4 g, 0.072 mole) dissolved in 60 ml of hot dry ethanol to saturation was added to 24 ml of hot dry ethanol saturated with 8.4 g (0.072 mole) of hexamethylenediamine. Precipitation soon occurred on mixing. After standing overnight at room temperature, the salt was filtered off, washed with cold dry ethanol, and dried *in vacuo*. The salt was obtained in 83% yield (18.9 g), mp 253–254°C.

ANAL. Calcd for $C_{16}H_{22}O_4N_2$: C, 60.75%; H, 10.13%; N, 8.86%. Found: C, 60.95%; H, 10.48%; N, 8.58%.

Similarly, hexamethylenediamine salt of adipic acid was obtained in 96% yield; mp 197–198°C.

Melt Condensation Polymerization of the Nylon Salts

The condensation copolymerizations of the hexamethylenediamine salt of *d*-camphoric acid and the hexamethylenediamine salt of adipic acid were carried out at 260–270°C by the method of melt condensation polymerization. The required amounts of nylon salt were placed in a sealed tube with a side arm to remove water produced; the tube was degassed completely and sealed off. The tube was placed in an oil bath, and the reaction was carried out at 260–270°C for 6 hr. After the polymerization period, the tube was cut and evacuated under reduced pressure to remove water produced in the reaction system, then sealed off again at a reduced pressure and placed on an oil bath for 1 hr. The polymer obtained was dissolved in formic acid and the solution was poured into a large amount of water. The polymer was filtered, washed with hot water, and dried *in vacuo*.

Solution Condensation Polymerization of Nylon Salts

The required amounts of the salt and *m*-cresol were placed in a 50-ml three-necked flask equipped with a reflux condenser, thermometer, and nitrogen gas inlet attachment. The reaction was carried out at 210–220°C on an oil bath under a nitrogen atmosphere. After 1 hr, the reaction mixture was distilled to remove *m*-cresol and water produced. The polymerization was carried further under reduced pressure at 260–270°C on an oil bath for 2 hr. The polymer was purified as detailed for the melt condensation method.

Measurements

The D line optical rotation and optical rotatory dispersion were measured with a Shimadzu model QV-50 polarimeter equipped with xenon source.

The intrinsic viscosity of polymer was measured in 90% formic acid at 25°C with an Ubbelohde viscometer.

Proton magnetic resonance spectra were obtained by a Varian Model, 60 Mcps, nuclear magnetic resonance spectrometer.

RESULTS AND DISCUSSION

Optical Behavior of Nylon Salts

Hydrolysis of the hexamethylenediamine *d*-camphoric acid salts was carried out. An aqueous solution of hydrogen chloride was added to an aqueous solution of the hexamethylenediamine *d*-camphoric acid salt to obtain white precipitates. The products were recrystallized from water, filtered, and dried *in vacuo*. The camphoric acid recovered had a melting point of 187–188°C and $[\alpha]_D$ was +47.0°. The optical rotatory dispersion of the recovered camphoric acid coincided very well with that of the starting

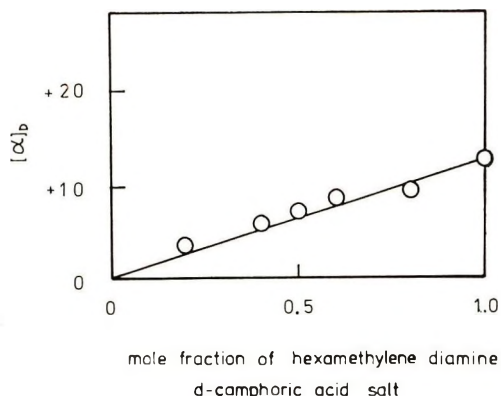


Fig. 1. Relationship between the specific rotation for the mixture of hexamethylenediamine camphoric acid salt and hexamethylenediamine adipic acid salt and the composition.

d-camphoric acid. The result suggests that the optically active nylon salt could be prepared without racemization.

The relationship between the specific rotation of mixtures of hexamethylenediamine *d*-camphoric acid salt and hexamethylenediamine adipic acid salt and the relative proportion of the salts in the mixture is shown in Figure 1.

The specific rotation of the mixture of nylon salts increased linearly with increasing content of the optically active component in the mixture. It is evident from the result that adipic acid does not affect the specific rotation of the mixture.

Copolyamides by Melt and Solution Condensation Polymerization

The reaction conditions and the results of melt and solution condensation polymerizations are summarized in Tables I and II. The polymers obtained were white or pale brown polymers. The copolyamides became fibrous and the melting points and intrinsic viscosities increased with increasing initial mole fraction of adipic acid in the monomer mixture. The melting points and intrinsic viscosities of the copolyamides were somewhat lower than those of polymers obtained by interfacial condensation copolymerizations of *d*-camphoric dichloride and adipic acid dichloride with hexamethylenediamine.¹¹ As the melt and solution condensation polymerizations were reversible reactions and carried out at high temperatures, polymer of high degree of polymerization was not obtained. On the contrary, the interfacial condensation polymerization was an irreversible reaction and carried out at low temperature, and thus no side reactions would occur. It is thought that the interfacial condensation polymerization is able to yield polymers having high degree of polymerization.

TABLE I
Melt Condensation Copolymerization of Hexamethylenediamine Adipic Acid Salt (HAS) and Hexamethylenediamine *d*-Camphoric Acid Salt (HCS)

Run	Copolyamides					
	Molar ratio of nylon salts HCS/HAS	Conversion, %	Molar ratio camphoryl unit/adipyl unit in polymer	Melting point, °C	$[\eta]$, dl/g ^a	$[\alpha]_D^{25}$ ^b
1	10:0	53.8	10:0	77-79	0.021	+14.1°
2	8:2	47.1	6.3:2	85	0.030	+6.1°
3	6:4	48.6	4.7:4	155-156	0.048	+5.8°
4	5:5	59.7	1.8:5	187-190	0.068	+3.2°
5	4:6	66.5	1.6:6	207	0.100	+2.3°
6	2:8	85.7	0.9:8	212-215	0.158	+1.0
7	0:10	90.9	0:10	232-235	0.728	0

^a Measured in 90% formic acid at 20°C.

^b Measured in 90% formic acid at 20-25°C.

TABLE II
Solution Condensation Copolymerization of Hexamethylenediamine Adipic Acid Salt (HAS) and Hexamethylenediamine *d*-Camphoric Acid Salt (HCS)

Run	Copolyamides					
	Molar ratio of nylon salts HCS/HAS	Conversion, %	Molar ratio camphoryl unit/adipyl unit in polymer	Melting point, °C	$[\eta]$, dl/g ^a	$[\alpha]_D^b$
8	10/0	44.6	10/0	77~80	0.024	+14.7
9	8/2	48.0	6.0/2	122~123	0.045	+8.8
10	6/4	50.8	4.0/2	169~171	0.064	+5.3
11	5/5	63.1	3.3/5	191~192	0.084	+8.6
12	4/6	65.3	2.2/6	210~211	0.094	+4.0
13	2/8	82.2	1.0/8	227~229	0.188	+2.6
14	0/10	91.0	0/10	239~242	0.530	0

^a Measured in 90% formic acid at 25°C.

^b Measured in 90% formic acid at 20–25°C.

The molecular weight of the polymers obtained was estimated by using Taylor's equation:¹²

$$\bar{M}_w = 13,000[\eta]^{1.39}$$

The molecular weight of the polymer having $[\eta] = 0.728$ was 8350 and that for $[\eta] = 1.53$ was 24,500.

The NMR spectra for poly(hexamethylene adipamide) and poly(hexamethylene *d*-camphoramide) obtained by the melt and solution condensation polymerizations were measured in formic acid to determine the polymer composition. As shown in Figure 2a for poly(hexamethylene adipamide), the proton signals due to —NH—, and the α , β , and γ methylenes of the hexamethylenediamino unit were observed at 3.5 τ and 6.6 $\tau \sim 8.6 \tau$, respectively. The proton signals due to α , β , and γ methylenes of the adipyl unit were observed at 7.6 τ , 8.3 τ , and 8.3 τ , respectively. On the other hand, as shown in Figure 2c the NMR spectrum of poly(hexamethylene *d*-camphoramide) obtained by the melt condensation polymerization coincided well with that of the polymer obtained by solution condensation polymerization (Fig. 2b). The proton signals due to the —NH— and the α , β , and γ methylenes of hexamethylenediamine unit were observed at 3.5 τ , 6.2 τ , 7.17 τ and 8.6 τ , respectively. The signals due to the methyl protons



and other protons were observed at 9.0, 8.7, and 7.9–7.8 τ , respectively.

The composition of the copolyamides was determined by the NMR spectra. The ratios of the methyl proton intensity of the *d*-camphoryl group

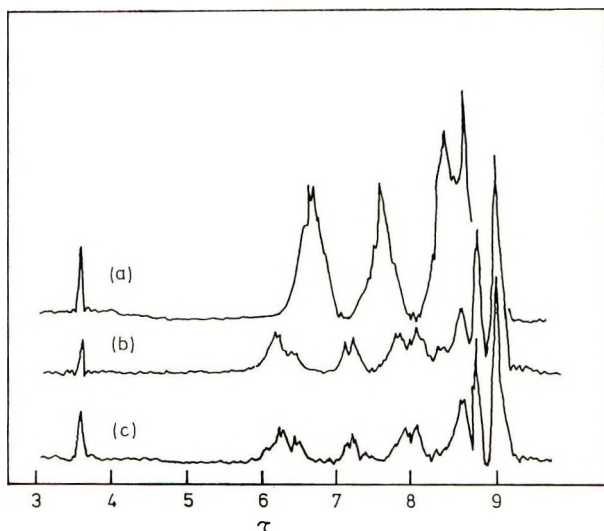


Fig. 2. Proton magnetic resonance spectra (60 Mcps) of: (a) poly(hexamethylene adipamide) and (b) poly(hexamethylene *d*-camphoramide) obtained by melt condensation polymerization; (c) poly(hexamethylene *d*-camphoramide) obtained by solution condensation polymerization.

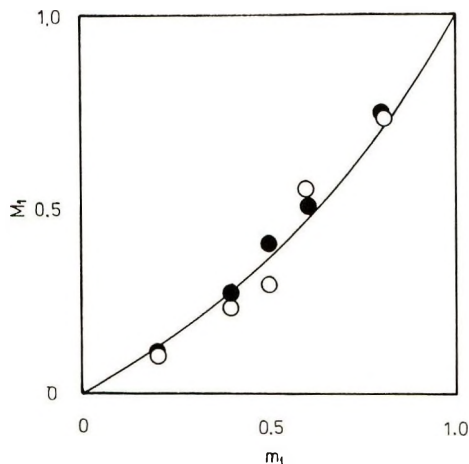


Fig. 3. Relationship between the mole fractions (M_1) of *d*-camphoryl unit in the total acid units of copolyamide and the initial mole fractions (m_1) of *d*-camphoric acid in the mixture of *d*-camphoric acid and adipic acid: (●) melt condensation polymerization; (○) solution condensation polymerization.

(9.0 τ) to the α -proton intensity of the —NH— of the hexamethylenediamine unit (6.2–7.1 τ) of the copolyamides of *d*-camphoric acid and adipic acid with hexamethylenediamine were calculated. The *d*-camphoryl unit content in the copolyamides was determined from the above ratio and the linear relationship between the mole fractions of *d*-camphoryl unit in the

mixture of poly(hexamethylene *d*-camphoramide) and poly(hexamethylene adipamide) and the ratio of the methyl proton intensity of the camphoryl group (9.0 τ) to the α -proton intensity of the $-\text{NH}-$ of hexamethylenediamino (0.2–7.1 τ).

The relationship between the mole fraction (M_1) of *d*-camphoryl units in the copolyamides obtained by the melt and solution condensation polymerization and the initial mole fractions (m_1) of *d*-camphoric acid in the monomer mixtures is shown in Figure 3. The relationship was not a linear one. It is suggested that the hexamethylenediamine adipic acid salt is more reactive than the *d*-camphoric acid derivative in the condensation copolymerization reaction.

Optical Behavior of Copolyamides

The relationship between the specific rotation of the polyamides prepared from hexamethylenediamine *d*-camphoric acid salt and hexamethylenediamine adipic acid salt, and the content of *d*-camphoryl unit is shown in Figure 4.

Downie et al.¹³ synthesized polypeptides from leucine having different degrees of optical purity and reported that the specific rotation of the polypeptide depended on the optical purity of *d*-(or *l*-) leucine used. The same result was reported by Overberger et al.,⁴ who synthesized polymers by interfacial condensation polymerization with amines and 2,2'-dinitro-6,6'-dimethylbiphenyl-4,4'-dicarboxylic acid and 2,2'-dichloro-6,6'-dimethylbiphenyl-4,4'-dicarboxylic acid. We obtained a similar result; at each composition the specific rotation of the copolyamides was increased linearly with increasing content of camphoryl units, although some deviations were observed (Fig. 4).

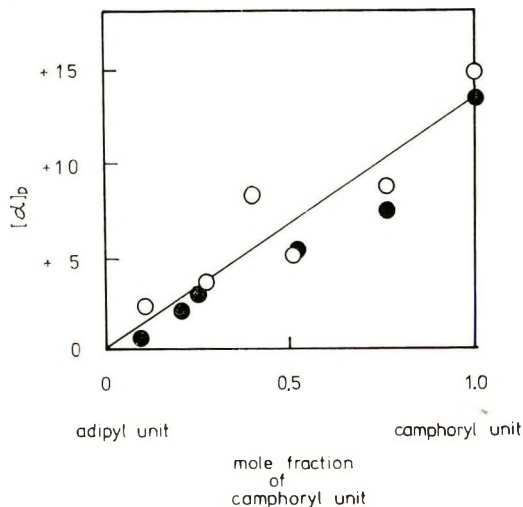


Fig. 4. Relationship between the specific rotation of the copolyamides and the mole fractions of *d*-camphoryl unit in the total acidic units of copolyamide: (●) melt condensation polymerization; (○) solution condensation polymerization.

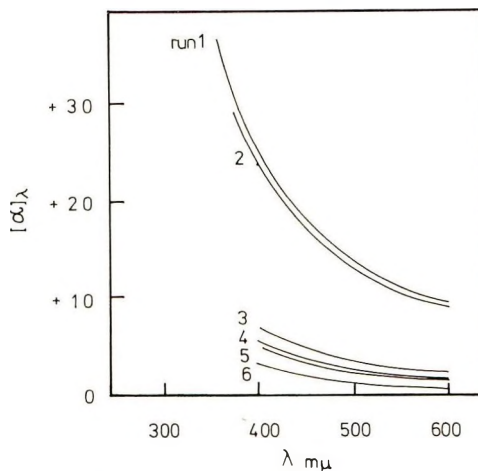


Fig. 5. Optical rotatory dispersion of copolyamides obtained from *d*-camphoric acid hexamethylenediamine salt and adipic acid hexamethylenediamine salt by melt condensation polymerization.

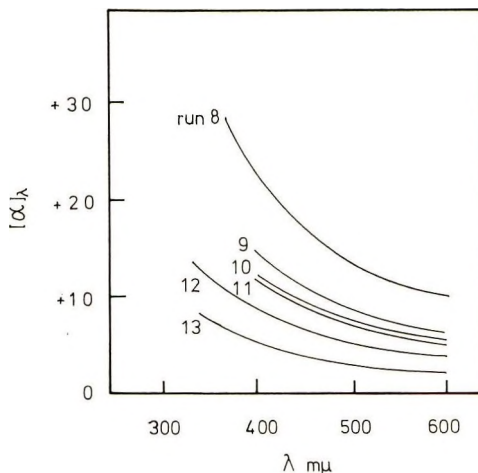


Fig. 6. Optical rotatory dispersion of copolyamides obtained from *d*-camphoric acid hexamethylenediamine salt and adipic acid hexamethylenediamine salt by solution condensation polymerization.

It is believed that the optical activity of *d*-camphoryl units of the polyamides is not affected by the adipyl units in the main chain as the adipyl units are far away from the asymmetric center. The deviations from a linear relationship are believed to be affected by the molecular weight of the copolyamides. Generally the specific rotation of a polymer of high molecular weight does not respond to changes in molecular weight, although it does so easily when the molecular weight is low.

We previously reported¹⁰ that the specific rotation of the polyamides obtained by the condensation polymerization was dependent upon the

molecular weight and that that of poly(*N*-bornyl maleimide)³ obtained by a free-radical polymerization was also dependent upon the molecular weight. It was considered that the specific rotation of these polymers was dependent upon the endgroups.

The optical rotatory dispersion of the copolyamides obtained by the melt and solution condensation polymerizations was measured. As shown in Figures 5 and 6, the optical rotatory dispersion of the copolyamides was positive and fit the simple Drude equation. The λ_c values for the copolyamides were in the range 241–245 $m\mu$, suggesting that the chromophore which caused optical activity was the —CO—NH— group.

The fact that the λ_c values did not depend on the composition of the copolyamide also confirms that the adipyl unit in the main chain does not affect the optical behavior of copolyamides.

References

1. N. Beredjick and S. Schuerch, *J. Amer. Chem. Soc.*, **80**, 1933 (1958).
2. R. C. Schulz and E. Kaiser, *Makromol. Chem.*, **86**, 80 (1965).
3. H. Yamaguchi and Y. Minoura, *J. Polym. Sci. A-1*, **8**, 1467 (1970).
4. C. G. Overberger and T. Yoshimura, paper presented at International Symposium on Macromolecular Chemistry, Tokyo-Kyoto, 1966.
5. C. G. Overberger and H. Jablonen, *J. Amer. Chem. Soc.*, **85**, 3431 (1963).
6. C. G. Overberger and T. Takekoshi, *Macromolecules*, **1**, 7 (1968).
7. M. S. Toy, *J. Polym. Sci. A-1*, **5**, 2481 (1967).
8. Y. Noda, S. Urayama, and Y. Minoura, *J. Polym. Sci. A-1*, **5**, 2441 (1967).
9. Y. Iwakura, K. Hayashi, and I. Inagaki, *Makromol. Chem.*, **104**, 56 (1967); *ibid.*, **110**, 84 (1968).
10. Y. Iwakura, K. Hayashi, and K. Iwata, *Makromol. Chem.*, **93**, 274 (1966); *ibid.*, **108**, 296 (1967); *ibid.*, **112**, 242 (1968); *ibid.*, **116**, 250 (1968).
11. H. Yamaguchi, H. Ueno, and Y. Minoura, *J. Polym. Sci. A-1*, **9**, 897 (1971).
12. G. B. Taylor, *J. Amer. Chem. Soc.*, **69**, 635 (1947).
13. A. R. Downie, A. Elliott, W. E. Hanby, and B. R. Malcolm, *Proc. Roy. Soc. (London)*, **A242**, 325 (1957).

Received August 11, 1970

Revised September 24, 1970

Optically Active Copolyamides by Interfacial Condensation Polymerization

HIDEMASA YAMAGUCHI, HIROSHI UENO and YUJI MINOURA,
*Department of Applied Chemistry, Faculty of Engineering,
Osaka City University, Osaka, Japan*

Synopsis

The polymerization of *d*-camphoryl dichloride with polymethylenediamines ($n = 2, 3, 5, 6, 7, 9$) and copolymerization of hexamethylenediamine with *d*-camphoryl dichloride and adipyl dichloride were carried out by the interfacial condensation method, and optically active copolyamides were obtained. The specific rotation of poly(hexamethylene camphoramide) obtained increased markedly with increasing intrinsic viscosity over the range of 0.05–0.10. The specific rotation for the copolyamides increased linearly with increasing content of *d*-camphoryl units in the polymers. The optical rotatory dispersion of the polyamides and copolyamides had a negative curve which fit the simple Drude equation. The λ_c values of the polyamides and the copolymers obtained were 265 and 273–285 $m\mu$, respectively. In order to investigate the conformation of the polyamides, the effects of solvent on the specific rotation of the polymers were studied.

INTRODUCTION

Some studies^{1,2} of optically active polymers prepared by the condensation polymerization were carried out in order to investigate the physical properties and the behavior of the polymer conformation in solution.

Overberger et al.³ studied the optical rotatory dispersion of optically active polyamides which were synthesized from 2,2'-dinitro-6,6'-dimethylbiphenyl-4,4'-dicarboxylic acid and 2,2'-dichloro-6,6'-dimethylbiphenyl-4,4'-dicarboxylic acid with some amines by interfacial condensation polymerization. Toy⁴ prepared optically active and inactive polycamphorates and polycamphoramides and compared the melting and crystalline properties of optically active polymers with those of inactive ones. Schulz et al.⁵ carried out the interfacial condensation polymerization of (+) 2,2'-diaminobinaphthyl-1,1' with terephthaloyl chloride and obtained an optically active polyamide having molecular asymmetry.

In a previous paper,⁶ optically active polyamides were synthesized from hexamethylenediamine with *d*-tartaric acid, and the effects of the solvent, polymerization time, intrinsic viscosity, and pH on the specific rotation of poly(hexamethylene *d*-tartaramide) were studied. Recently melt and solution condensation copolymerizations of nylon salts prepared from *d*-camphoric acid and adipic acid with hexamethylenediamine, were carried out,

and optically active copolyamides were obtained.⁷ It was found that the specific rotation of the copolyamides increased with increasing content of *d*-camphoryl units in copolyamides.

In this paper, we prepared optically active polyamides by interfacial condensation polymerization of camphoryl dichloride with polymethylenediamine ($n = 2, 3, 5, 6, 7, 9$). Interfacial condensation polymerization of hexamethylenediamine with camphoryl dichloride and adipyl dichloride were also carried out. The relationship between the specific rotation of the copolyamides and the composition was examined. The effects of solvent on the specific rotation were also investigated.

EXPERIMENTAL

Materials

Commercially available *d*-camphoric acid and adipic acid were used without further purification. *d*-Camphoric acid has mp 185–186.5°C and $[\alpha]_D +47.0^\circ$ in EtOH. Hexamethylenediamine was distilled at reduced pressure over potassium hydroxide (bp 94–100°C/20 mm Hg). Commercially available polymethylenediamine ($n = 2, 3, 5, 6, 7, 9$) and piperazine were used without further purification. Benzene was purified by the usual method.

Preparation of *d*-Camphoryl Dichloride

A 300-ml portion of petroleum ether solution of 50 g of *d*-camphoric acid was placed in a 500-ml three-necked flask equipped with a reflux condenser and mechanical stirrer. Phosphorus pentachloride (150 g) was added to the vigorously stirred suspension over a period of 30 min at 0°C. The stirring mixture was allowed to warm to room temperature for 4 hr. This reaction mixture was evacuated on the steam bath under reduced pressure. The residual liquid distilled at 137–138°C/10 mm Hg, yielding 69% (40.8 g) of *d*-camphoryl dichloride, $[\alpha]_D -6.4^\circ$ (lit.⁸ bp 140–141°C/15 mm Hg).

Preparation of Adipyl Dichloride

Adipic acid (40 g) was placed in a 300-ml three-necked flask equipped with a reflux condenser, dropping funnel, and mechanical stirrer. A 200-g portion of thionyl chloride was added to the flask. After 3 hr, unreacted thionyl chloride was distilled off from the reaction mixture. The residual liquid was distilled at a reduced pressure, 110–111°C/10 mm Hg to yield 32.5 g of adipyl dichloride, (lit.⁹ bp 125–128°C/11 mm Hg).

Polymer Procedure

The interfacial condensation polymerization was carried out by the method of Morgan.¹⁰ A benzene solution of camphoryl dichloride and adipyl dichloride was placed in a beaker. Into this beaker was poured gradually an aqueous solution containing polymethyldiamine and sodium

bicarbonate at 0°C with stirring with a magnetic stirrer. A white precipitate of polymer formed at the liquid interface. After 24 hr, the precipitates were filtered and then dissolved in formic acid. The polymer was precipitated in a large amount of water, washed with hot water, and dried *in vacuo*.

Measurements

The D-line optical rotation and optical rotatory dispersion were measured with a Shimadzu model QV-50 polarimeter equipped with xenon source.

The intrinsic viscosity of polymer was measured in ethanol or 90% formic acid at 30°C with an Ubbelohde viscometer.

Proton magnetic resonance spectra were obtained by a Varian Model, 60 Mcps nuclear magnetic resonance spectrometer.

RESULTS AND DISCUSSION

Optical Behavior of *d*-Camphoryl Dichloride

d-Camphoryl dichloride used as a optically active monomer for the interfacial condensation polymerization was synthesized from *d*-camphoric acid. This *d*-camphoryl dichloride had a negative specific rotation, but that prepared by Toy⁴ had a value of $[\alpha]_D +14.0^\circ$ (in benzene). Its optical rotatory dispersion were also measured (Fig. 1). Wreden¹¹ has reported that *d*-camphoric acid was converted to a mixture of *d*-camphoric acid ($[\alpha]_D +47.8^\circ$ in EtOH) and *d*-isocamphoric acid ($[\alpha]_D -47.6^\circ$ in EtOH) by heating with HCl.

To judge from the report, it would be thought that *d*-camphoryl dichloride was partially converted to *d*-isocamphoryl dichloride by hydrogen chloride produced by the reaction of moisture with dichloride when *d*-camphoryl dichloride was distilled. Thus it is thought that the specific rotation becomes negative when the mixture is converted to *d*-isocamphoryl dichloride.

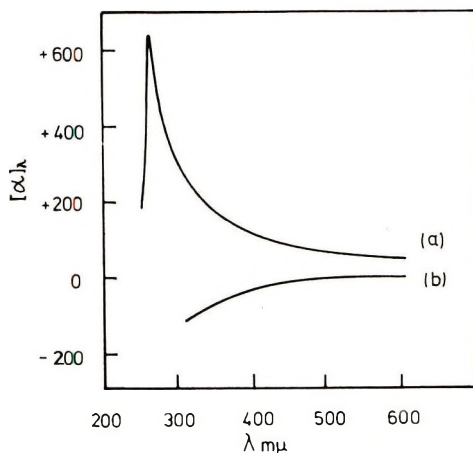


Fig. 1. Optical rotatory dispersion of (a) *d*-camphoric acid and (b) camphoryl dichloride.

The camphoric dichloride obtained was reacted with an aqueous solution of sodium hydroxide. * The camphoric acid recovered had $[\alpha]_D -9.9^\circ$ (in EtOH), mp $173 \sim 175^\circ\text{C}$.

ANAL. Calcd for $\text{C}_{10}\text{H}_{16}\text{O}_4$: C, 60.0%; H, 8.0%. Found: C, 62.0%; H, 7.2%.

The specific rotation of the material recovered clearly confirms that *d*-camphoryl dichloride is partially converted to *d*-isocamphoryl dichloride.

Poly(polymethylene Camphoramide) and Its Optical Behavior

The interfacial condensation polymerization of camphoryl dichloride with polymethylenediamines ($n = 2, 3, 5, 6, 7, 9$) were carried out by the method of Morgan;¹⁰ the reaction conditions and results are summarized in Table I. No relationship between melting point or the specific rotation of these polyamides and the number of methylene was found.

TABLE I
Interfacial Condensation Polymerization of Camphoryl Dichloride with
Polymethylenediamines^a

Run	Number of methylenes of diamine	Polyamides				
		yield, %	Melting point, °C	$[\eta]$, dl/g ^b	$[\alpha]_D^c$	$[M]_D$
1	2	25	139-178	0.157	-17.1	-38.0
2	3	21	81-123	0.052	-9.8	-23.3
3	5	21	102-149	0.074	-22.9	-60.9
4	6	28	127-171	0.100	-19.4	-54.3
5	7	27	119-161	0.102	-31.9	-93.8
6	9	27	121-170	0.182	-28.4	-91.1

^a Interfacial condensation polymerization was carried out at 0°C in benzene- H_2O with Na_2CO_3 as a detergent. Diamine, 0.5 mole/l.; Na_2CO_3 , 1.0 mole/l.; dichloride, 0.5 mole/l.

^b Measured in ethanol at 30°C .

^c Measured in ethanol at $21-22^\circ\text{C}$.

In order to investigate the relationship between the specific rotation and the intrinsic viscosity of polyamides, interfacial condensation polymerizations of camphoryl dichloride with hexamethylenediamine were carried out. Various poly(hexamethylene camphoramides) having intrinsic viscosities in the range 0.055-0.184 were obtained by changing the mole ratio of hexamethylenediamine to camphoryl dichloride (Table II). The relationship between the specific rotation of the poly(hexamethylene camphoramides) and the intrinsic viscosity is shown in Fig. 2. The specific rotation of polyamides increased markedly with increasing intrinsic viscosity over the range of 0.05-0.10; on the contrary, at intrinsic viscosities higher than 0.10, the specific rotation was independent of the intrinsic viscosity.

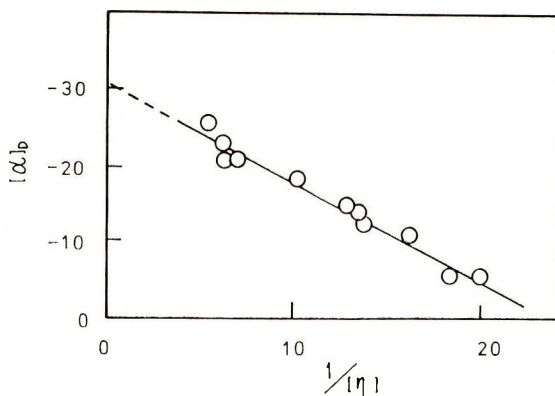


Fig. 2. Relationship between the specific rotation and $1/[\eta]$ for poly(hexamethylene camphoramide).

We have already reported¹² similar results; the specific rotation of poly-*N*-bornylmaleimide obtained by free-radical polymerization was dependent upon the molecular weight, especially in the range of low molecular weight. Schulz and Kaiser¹³ also reported the specific rotation of polymers obtained by free-radical polymerization was dependent upon its intrinsic viscosity. It is thought that the specific rotation of these polymers is dependent upon their endgroups.

TABLE II
Interfacial Condensation Polymerization of Camphoryl Dichloride with
Polymethylenediamines^a

Run	Molar ratio of hexa- methylene- diamine to camphoryl dichloride	Yield, %	Melting point, °C	Polyamides			
				$[\eta]$, dl/g ^b	$1/[\eta]$	$[\alpha]_D^c$	$[M]_D$
7	0.09	31.4	44-78	0.055	18.2	-5.5	-14.3
8	0.21	70.3	54-81	0.050	20.0	-5.5	-14.3
9	0.49	33.1	68-99	0.062	16.2	-11.0	-28.6
10 ^d	0.25	83.3	91-94	0.066	15.2	-13.6	-35.4
11	0.74	25.9	87-128	0.073	13.7	-12.2	-31.7
12	0.99	36.3	110-138	0.079	12.7	-14.4	-37.4
13	1.00	34.7	128-131	0.131	7.6	-21.8	-56.7
14	1.98	69.3	130-167	0.141	7.1	-20.4	-53.0
15	3.95	23.8	154-196	0.184	5.4	-25.2	-65.5
16	9.88	30.0	132-182	0.161	6.2	-20.4	-53.0

^a Interfacial condensation polymerization was carried out at 0°C in benzene-H₂O with the use of Na₂CO₃; diamine, 0.5 mole/l.; Na₂CO₃, 1.0 mole/l.; dichloride 0.05 mole/l. except as otherwise noted.

^b Measured in ethanol at 30°C.

^c Measured in ethanol at 26-27°C.

^d Diamine, 0.17 mole/l.; Na₂CO₃, 0.33 mole/l.; dichloride, 0.67 mole/l.

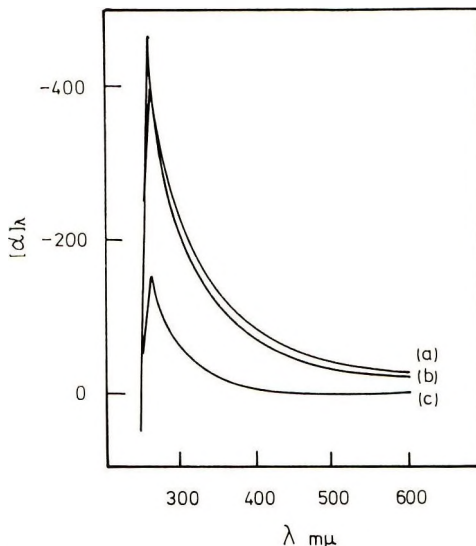


Fig. 3. Optical rotatory dispersion of poly(hexamethylene camphoramide): (a) run 16, $[\eta] = 0.161$; (b) run 4, $[\eta] = 0.100$; (c) run 8, $[\eta] = 0.050$.

The optical rotatory dispersion of poly(hexamethylene camphoramide) are shown in Figure 3. The curves showed a negative Cotton effect and fit a simple Drude equation. The average λ_c values was 265μ .

Copolyamides from Hexamethylenediamine with Camphoryl Dichloride and Adipyl Dichloride

The reaction conditions and the results of the interfacial condensation copolymerization are summarized in Table III. The copolyamides obtained were white or pale brown powders. The copolyamides became fibrous with increasing initial mole fractions of adipyl dichloride in the monomer mixture. The melting point and intrinsic viscosity of the copolyamides increased with decreasing mole fraction of the camphoryl group in the copolymer (Fig. 4).

The melting point and intrinsic viscosity of the copolyamides were higher than those of polymers obtained by melt or solution condensation polymerization.⁷ From the results that the relationship between the melting point and the molecular fractions became linear and did not reach a minimum, it is thought that adipic acid and *d*-camphoric acid are isomorphous.

The melting point and intrinsic viscosity of the copolyamides obtained were higher than those of polymers obtained by melt and solution condensation polymerization of nylon salts from hexamethylenediamine with *d*-camphoric acid and adipic acid.⁷ The interfacial condensation polymerization was not a reversible reaction and was carried out at low temperature, and thus side reactions are minimized. It is found that the interfacial condensation polymerization is able to yield polymers having a high degree of polymerization.

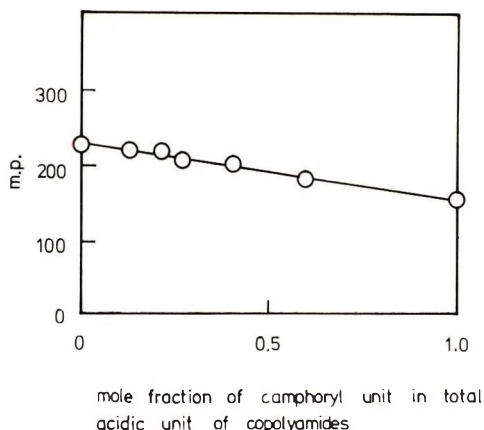


Fig. 4. Relationship between the melting point of copolyamides and the mole fractions (M_1) of camphoryl units in the total acidic units of copolyamide.

The molecular weight of the polymers obtained were estimated conventionally by using Taylor's equation¹⁴ for nylon 6 6:

$$\bar{M}_n = 13000[\eta]^{1.39}$$

The molecular weight of the polymer having $[\eta] = 0.59$ was about 6300.

In order to determine the polymer composition the NMR spectra for poly(hexamethylene adipamide) (Fig. 5a), copolyamide from hexamethylenediamine with camphoryl dichloride and adipic dichloride (Fig. 5b) and poly(hexamethylene *d*-camphoramid) (Fig. 5c) obtained by the interfacial condensation polymerization were measured in formic acid. As shown

TABLE III
Interfacial Condensation Copolymerization of Hexamethylenediamine with Camphoryl Dichloride and Adipyl Dichloride^a

Run	Copolyamides						
	Molar ratio of camphoryl dichloride to adipyl dichloride	Yield, g	Conversion, %	Molar ratio camphoryl units/adipyl units in polymer	Melting point, °C	$[\eta]$, dl/g ^b	$[\alpha]_D^c$
21	10/0	0.83	14.5	10/0	145-147	0.079	-27.9
22	8/2	1.36	34.6	2.9/2	180-182	0.115	-14.7
23	6/4	1.87	47.4	2.7/4	197-198	0.231	-8.1
24	5/5	1.81	46.9	1.8/5	198-200	0.252	-9.5
25	4/6	2.08	55.4	1.6/6	211-212	0.283	-7.8
26	2/8	2.26	62.8	1.2/8	215-217	0.458	-3.4
27	0/10	0.73	21.1	0/10	231-233	0.590	0.0

^a Interfacial condensation polymerization was carried out at 0°C for 24 hr; hexamethylenediamine, 0.304 mole/l.; Na₂CO₃, 0.304 mole/l.; total acid dichloride, 0.152 mole/l.

^b Measured in 90% formic acid at 30°C.

^c Measured in 90% formic acid at 25°C.

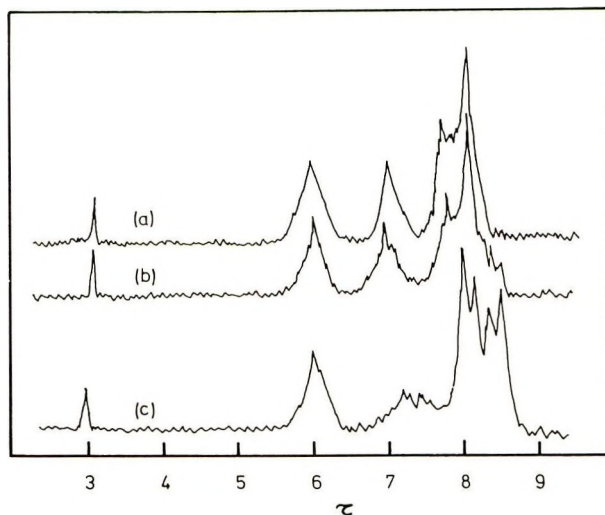


Fig. 5. Proton magnetic resonance spectra (60 Mcps) of (a) poly(hexamethylene adipamide), (b) copolyamides (run 25) prepared from hexamethylenediamine with adipyl dichloride and camphoryl dichloride; (c) poly(hexamethylene camphoramide).

in Figure 5c for poly(hexamethylene camphoramide), the proton signals due to —NH— and α , β , and γ methylenes of the hexamethylenediamino unit were observed at 3.5 τ , 6.4 τ , 8.6 τ , and 8.6 τ , respectively. The proton signals due to the α and β methylenes of the adipyl unit were observed at 7.5 τ and 8.3 τ , respectively.

There were some differences (8.0–8.4 τ) between the NMR spectra of polyamides obtained by melt or solution condensation polymerization and those for polymers obtained by interfacial condensation copolymerization.⁷ Camphoryl dichloride prepared from *d*-camphoric acid with phosphorus pentachloride was partially isomerized and converted to isocamphoryl dichloride. Therefore the NMR spectra of the polyamides obtained by interfacial condensation polymerization differed from those from melt or solution condensation polymerization.

The composition of the copolyamides was determined by the NMR spectral analysis as described in a previous paper.⁷ The ratios of the intensity of the methyl proton of the camphoryl group (8.8–9.1 τ) to that of the α -proton of the —NH— of the hexamethylenediamino group (6.6 τ) of the copolyamides of camphoryl dichloride and adipyl dichloride with hexamethylenediamine were calculated. The contents of camphoryl group in the copolyamides were determined by using these ratios on the basis of the relationship to the mole fractions of camphoryl group in the mixture of poly(hexamethylene adipamide) and poly(hexamethylene camphorylamide) and the ratios.

The relationship between the mole fractions (M_1) of camphoryl units in the total acid unit of copolyamides obtained by the interfacial condensation polymerization and the initial mole fraction (m_1) of camphoryl units in the mixture of acidic monomers is shown in Figure 6. A linear relation was not

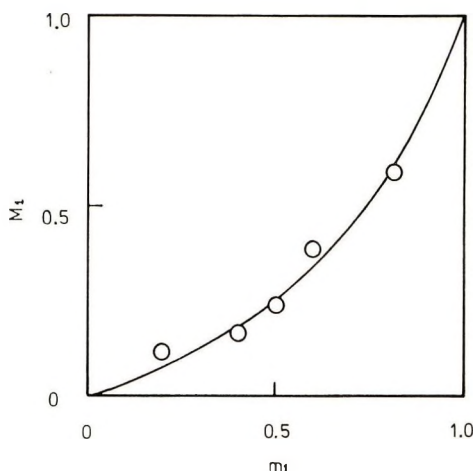


Fig. 6. Relationship between the mole fractions (M_1) of camphoryl units in the total acidic units of copolyamide and initial mole fractions (m_1) of camphoric dichloride in the mixture of camphoric dichloride and adipic dichloride.

found. It is suggested that adipyl dichloride is more reactive to hexamethylenediamine than camphoryl dichloride in the condensation copolymerization reaction.

Optical Behavior of Copolyamides

As shown in Table IV, the copolyamides obtained by the interfacial condensation polymerization had negative optical activity. At each composition the specific rotation of the copolyamides depended linearly on the content of optically active units, as shown in Figure 7. The specific rotation of the copolyamides increased with increasing mole fraction of camphoryl

TABLE IV
Specific Rotation of Polyamide in Various Solvents^a

Solvents	Poly(hexamethylene camphoramide) ^b		Poly(camphoryl piperadine)	
	$[\alpha]_D^c$	$[\alpha]_D^d$	$[\alpha]_D^c$	$[\alpha]_D^d$
Dimethylformamide	-17.9	-13.3	-3.9	-2.9
Ethanol	-19.4	-15.1	-1.8	-1.4
Methanol	-20.2	-16.1	-3.3	-2.6
<i>m</i> -Cresol	-20.4	-14.1	-4.7	-3.6
Formic acid	-31.4	-24.3	-8.7	-6.7
Dichloroacetic acid	-50.7	-36.6	-3.9	-2.8

^a Interfacial condensation polymerization carried out at 0°C in benzene-H₂O with Na₂CO₃ as a detergent; diamine, 0.5 mole/l.; Na₂CO₃, 1.0 mole/l.; dichloride, 0.5 mole/l.

^b Run 4, Table I.

^c Measured at 25.6–26.5°C.

^d $[\alpha]_D = [\alpha]_D [3/(n^2 + 2)]$.

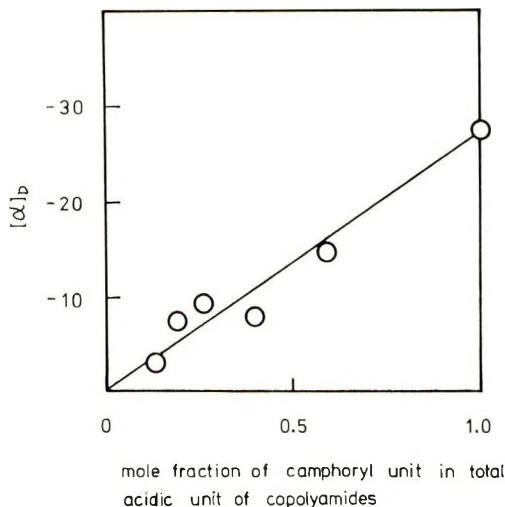


Fig. 7. Relationship between the specific rotation of copolyamides and mole fraction (M_1) of camphoryl units in the total acidic units of copolyamide.

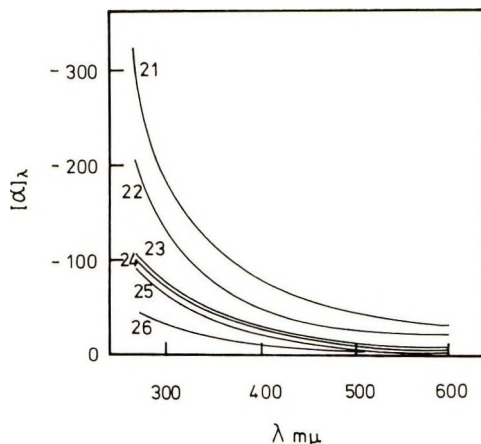


Fig. 8. Optical rotatory dispersion of copolyamides obtained from hexamethylenediamine with camphoric dichloride and adipic dichloride.

units. This linear relationship for the copolyamides obtained by interfacial condensation polymerization coincided very well with that for the copolyamides obtained by melt and solution condensation polymerization.

A linear relationship between the specific rotation of copolymers having optically active centers in the polymer main chain and the mole fraction of optically active unit has been also reported by Downie et al.¹⁵

The optical rotatory dispersions of the copolyamides were negative and fit a simple Drude equation (Fig. 8). The λ_c values for the copolyamides were 273–285 $m\mu$ and suggested the chromophore which caused optical activity was the $-\text{NH}-\text{C}=\text{O}$ group.

Effect of Solving on the Specific Rotation of the Polyamides and Copolyamides

As shown in Table IV, the specific rotation of poly(camphoryl piperazine) did not show large variation in various kind of solvents. It is evident that

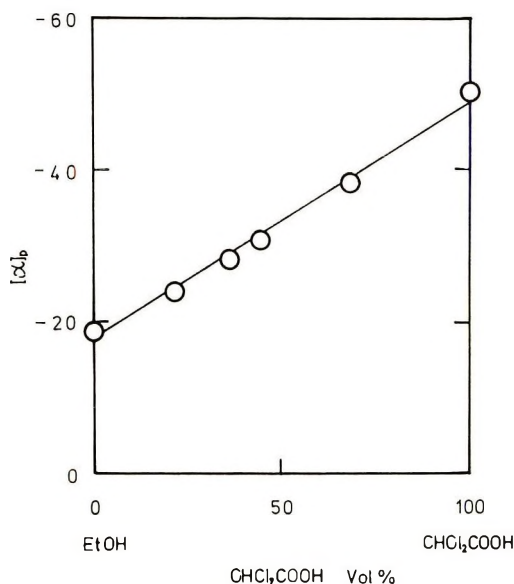


Fig. 9. Relationship between the specific rotation for poly(hexamethylene camphoramide) (run 4) and solvent composition.

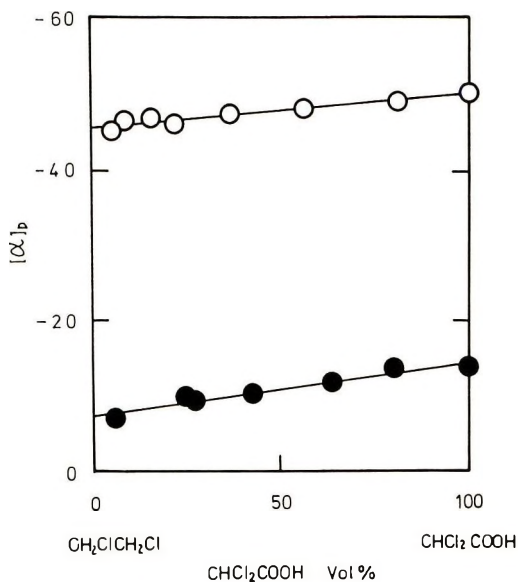


Fig. 10. Relationship between the specific rotation for poly(hexamethylene camphoramide) and solvent composition: (○) run 4, $[\eta] = 0.100$; (●) run 9, $[\eta] = 0.062$.

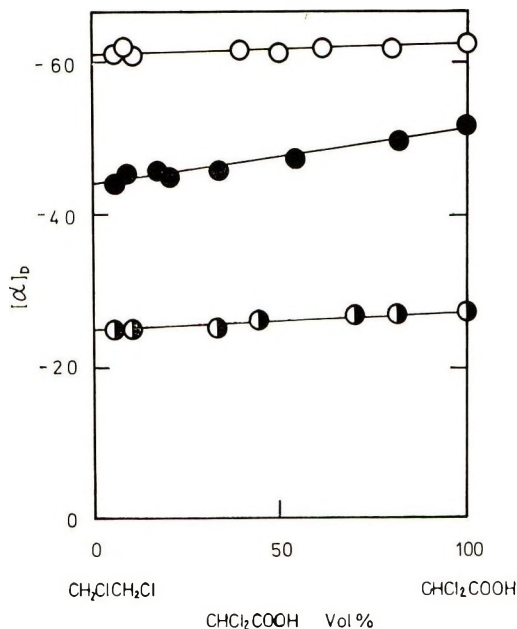


Fig. 11. Relationship between the specific rotation for various polymethylene camphoramides) and solvent composition: (○) $n = 9$, (●) $n = 6$, and (◐) $n = 3$, where n denotes the number of methylenes of the diamine.

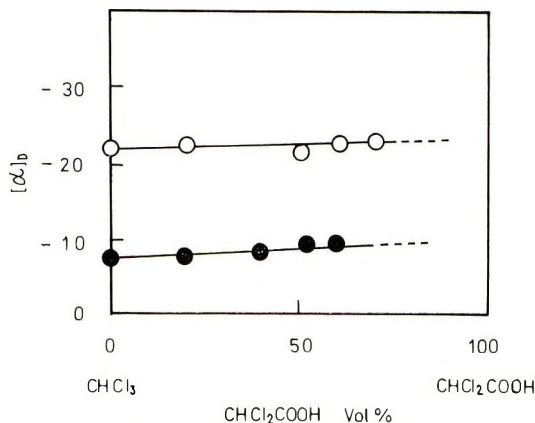


Fig. 12. Relationship between the specific rotation of copolyamides and solvent composition: (○) run 22; (●) run 24.

as poly(camphoryl piperazine) is not able to have intermolecular hydrogen bonding, the specific rotations show similar values in any solvent. On the contrary, the specific rotation of poly(hexamethylene camphoramide) changed markedly, especially in dichloroacetic acid (Table IV). It is thought that poly(hexamethylene camphoramide) forms hydrogen bonds in aprotic solvents such as dimethylformamide but in dichloroacetic acid the hydrogen bonds are destroyed, and thus the specific rotation is low.

It has been reported^{1,16} that some polyamides have a helical conformation

in coil solvents such as chloroform or dichloroethane. In order to investigate whether the polyamides obtained could retain a helical conformation in solution, the specific rotation of the polyamides was measured in dichloroacetic acid-ethanol (Fig. 9) and dichloroacetic acid-dichloroethane mixed solvents (Fig. 10). If the polyamides were to have a helical conformation, the specific rotation would drastically change on addition of dichloroacetic acid, which is a polar solvent and destroys the hydrogen bonding of polyamides. As shown in Figures 9 and 10, the absolute value of the specific rotation for the poly(hexamethylene camphoramide) increased linearly with increasing the addition of dichloroacetic acid, and did not change dramatically. Thus it is thought that the polyamides do not have a helical conformation in EtOH or dichloroethane.

No difference between the behavior of the specific rotation in mixed solvent of poly(hexamethylene camphoramides) of different molecular weights was found, as shown in Figure 10.

The solvent effects of some poly(methylene camphoramides) were measured; results are shown in Figure 11. In spite of the difference in the number of methylenes, the specific rotations in mixed solvent showed similar behavior.

It is evident from these results that the poly(hexamethylene camphoramide) and other poly(methylene camphoramides) do not have a helical conformation in ethanol or dichloroethane.

As shown in Figure 12, a linear relationship between the specific rotation for the copolyamide and the addition of chloroform was obtained. It is found that the copolyamides also do not have a helical conformation in chloroform.

References

1. Y. Iwakura, K. Hayashi, and K. Iwata, *Makromol. Chem.*, **112**, 242 (1968); *ibid.*, **116**, 250 (1968).
2. C. G. Overberger and H. Jabloner, *J. Amer. Chem. Soc.*, **85**, 3431 (1963).
3. C. G. Overberger and T. Yoshimura, paper presented at International Symposium on Macromolecular Chemistry, Tokyo-Kyoto, 1966.
4. M. S. Toy, *J. Polym. Sci. A-1*, **5**, 2481 (1967).
5. R. C. Schulz and R. H. Jung, *Makromol. Chem.*, **116**, 190 (1968).
6. Y. Minoura, S. Urayama, and Y. Noda, *J. Polym. Sci. A-1*, **5**, 2441 (1967).
7. H. Yamaguchi, H. Ueno, and Y. Minoura, *J. Polym. Sci. A-1*, **9**, 887 (1971).
8. J. Scheiber and M. Knothe, *Ber.*, **45**, 2254 (1912).
9. Th. Lieser and K. Macura, *Ann.*, **548**, 226 (1941).
10. P. W. Morgan and S. L. Kwolek, *J. Polym. Sci.*, **40**, 300 (1959); *ibid.*, **62**, 33, 181 (1962).
11. F. Wreden, *Ann.*, **163**, 328 (1872).
12. H. Yamaguchi and Y. Minoura, *J. Polym. Sci. A-1*, **8**, 929 (1970).
13. R. C. Schulz and E. Kaiser, *Makromol. Chem.*, **86**, 80 (1965).
14. G. B. Taylor, *J. Amer. Chem. Soc.*, **69**, 635 (1947).
15. A. R. Downie, A. Elliott, W. E. Hauby, and B. R. Malcolm, *Proc. Roy. Soc. (London)*, **A242**, 325 (1957).
16. P. Doty and J. T. Yang, *J. Amer. Chem. Soc.*, **78**, 498 (1956).

Received September 14, 1970

Revised October 23, 1970

γ -Ray-Induced Polymerization of α -Haloacrylic Acids

HARUHIKO WATANABE and MASAO MURANO,
Katata Research Institute, Toyobo Co. Ltd., Otsu, Japan

Synopsis

The γ -ray induced polymerizations of α -chloroacrylic acid, mp 66°C, and α -bromoacrylic acid, mp 72°C, were investigated in the temperature range from 35°C to 85°C. An analysis of polymerization kinetics was made, and results were similar to those reported in the literature for other vinyl monomers. On heating of the polymer obtained, elimination of hydrogen halide takes place, and intramolecular lactone formation is observed. The rate of lactone formation of poly(α -chloroacrylic acid) obtained in the solid-state polymerization was found to be higher than that in the liquid state, because a highly isotactic configuration of polymers tends to be formed in the solid-state polymerization, and elimination of hydrogen chloride is facilitated with an isotactic 5_2 helix structure.

Introduction

The radiation-induced polymerization of acrylic acid has been reported in the literature.¹ Morawetz et al. have demonstrated that the poly(methacrylic acid) obtained in the solid-state polymerization is highly isotactic.² In the present study, the radiation-induced polymerization of α -chloroacrylic acid and α -bromoacrylic acid was carried out in the temperature range above and below the melting point of the monomers, at an intensity of 5×10^4 r/hr. The structure and configuration of the polymers obtained were elucidated from the infrared absorption spectra and the NMR. The configuration of the polymer obtained in the solid-state polymerization was distinguished from that of polymer obtained in the liquid state.

Experimental

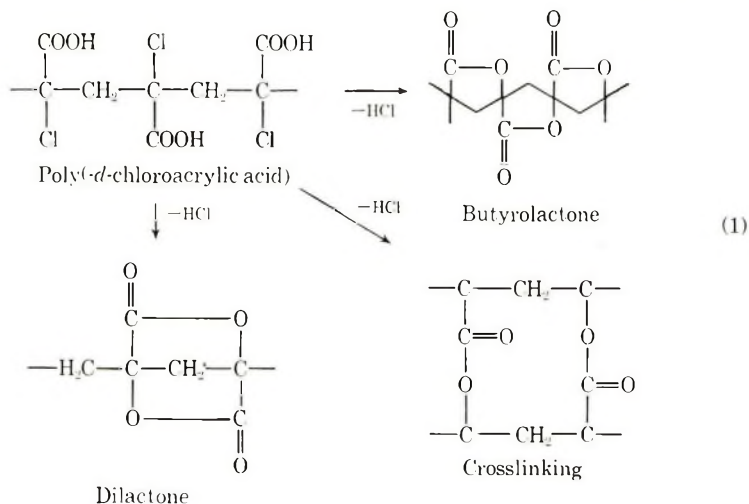
α -Chloroacrylic acid and α -bromoacrylic acid were prepared by the halogenation of methyl acrylate, successive dehydrohalogenation, and hydrolysis with barium oxide.³ The monomers were purified by recrystallizing three times from petroleum ether solution. The monomers were then dried in a vacuum desiccator, yielding pure white crystalline compounds: α -chloroacrylic acid, mp 66°C, and α -bromoacrylic acid, mp 72°C. Then 500-mg. portions of these monomers were sealed under high vacuum in glass ampoules and irradiated by γ -rays from a 1000-Ci ⁶⁰Co source. Irradiations were performed at 35–85°C at intensities of 5×10^4 r/hr. The polymer was isolated by rapid extraction of the residual monomer with dry

ether. The infrared measurements were taken as Nujol paste, and the NMR spectra were measured in pyridine solution at 80°C.

Results and Discussion

Polymerization studies of α -chloroacrylic acid and α -bromoacrylic acid initiated by γ -rays were performed at temperatures above and below the melting points of the monomers. Figure 1 shows yields for polymerization of α -chloroacrylic acid in the temperature range of 35°C to 74°C and Figure 2 indicates data for polymerization of α -bromoacrylic acid from 35°C to 85°C. An Arrhenius plot is presented in Figure 3. The vertical dotted lines indicate the melting point of the two monomers, where the rates of polymerization were changed abruptly. Figure 4 shows the effect of the monomer crystalline structure and of the air on the polymerization rate. It was found that the rate of polymerization of crystals shock-cooled at -196°C is larger than that for crystals made by recrystallization from the petroleum ether solution. In the solid state (below the melting point) the rate of polymerization is not very sensitive to air, that is, the time-conversion curve for solid-state polymerization in the presence of air and at high vacuum are nearly identical; however, no polymerization takes place in the presence of air in the liquid state as shown in Figure 4. The results mentioned above are the same as those for vinyl compounds having melting points above room temperature.¹

When the obtained poly(α -chloroacrylic acid) and poly(α -bromoacrylic acid) were heated, elimination of hydrogen chloride or hydrogen bromide was observed, and the formation of polymers is assumed as shown in eq. (1).



The resulting polymer, having evolved up to 40% hydrogen halide, is soluble in methanol. It is expected that the intermolecular crosslinking reaction does not occur, and the dilactone structure indicated could not be assumed from the restrictions on the bond angles of C and O atom. It is considered

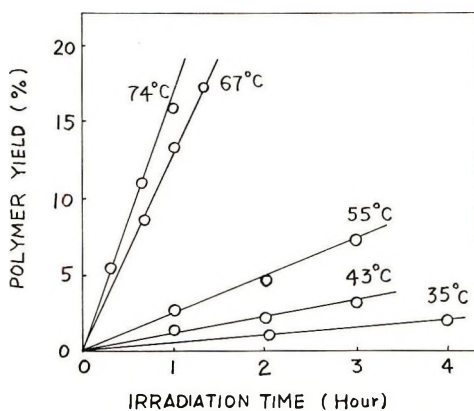


Fig. 1. γ -Ray-induced polymerization of α -chloroacrylic acid *in vacuo* at 5×10^4 r/hr.

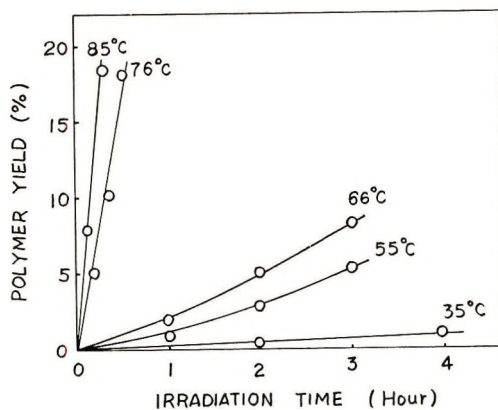


Fig. 2. γ -Ray-induced polymerization of α -bromoacrylic acid *in vacuo* at 5×10^4 r/hr.

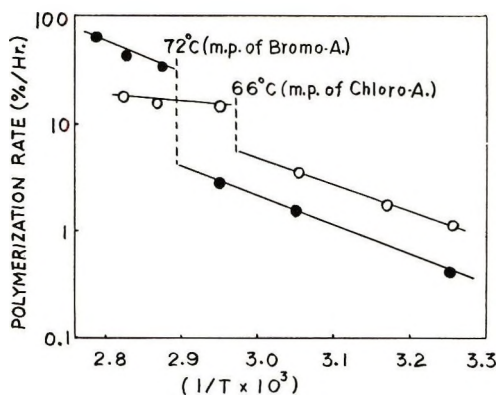


Fig. 3. Arrhenius plots of γ -ray-induced polymerization of α -haloacrylic acids: (—○—) α -chloroacrylic acid (activation energy 3.8 kcal/mole in the liquid state, 10.3 kcal/mole in the solid state); (—●—) α -bromoacrylic acid (activation energy 12.2 kcal/mole in the liquid state, 12.1 kcal/mole in the solid state).

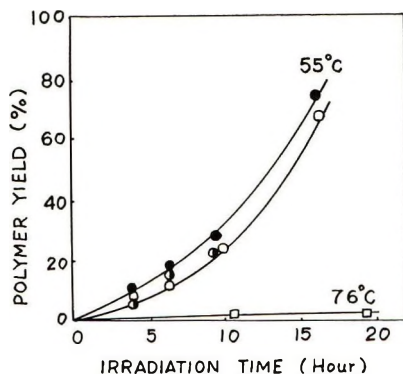


Fig. 4. γ -Ray induced polymerization of α -bromoacrylic acid at 5×10^4 r/hr: (—○—) crystals slowly grown in vacuo; (—●—) crystals slowly grown in air; (—●—) crystals shock-cooled (-196°C) *in vacuo*; (—□—) liquid state in air.

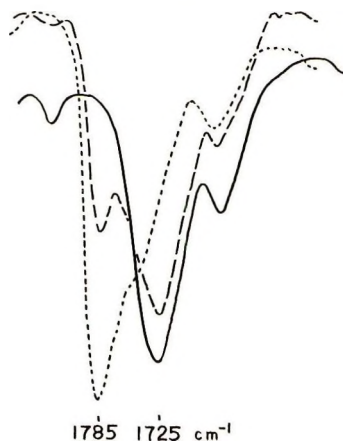


Fig. 5. Change of infrared absorption spectra of poly-(α -chloroacrylic acid) on heating: (—) Poly- α -chloroacrylic acid (--) heating 156°C , 6 min; (- -) heating 206°C , 25 min.

on the basis of the results of infrared spectra, solubility, and polymer structure that the γ -butyrolactone ring formation reaction is facilitated, at least at the initial stage of the reaction. Figure 5 shows the infrared absorption spectra of polymers formed. An absorption of 1725 cm^{-1} attributed to the carboxyl group is converted quantitatively to the 1785 cm^{-1} absorption of the γ -butyrolactone carbonyl group with heating.

Figure 6 shows the lactone yield determined by infrared absorption spectra of poly(α -chloroacrylic acid) and poly(α -bromoacrylic acid) at 156°C in air. The rate of lactonization of poly(α -bromoacrylic acid) is several times larger than that of poly(α -chloroacrylic acid). Even at room temperature, hydrogen bromide is gradually eliminated from poly(α -bromoacrylic acid), and the lactone structure is formed slowly. Hydrogen bromide is so fast liberated from polymer that poly(α -bromoacrylic acid) is unsuitable for in-

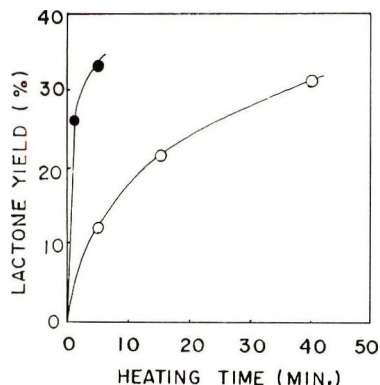


Fig. 6. Rate of lactonization of poly(α -chloroacrylic acid) and poly(α -bromoacrylic acid) at 156°C: (—○—) poly(α -chloroacrylic acid) (80°C, 5×10^4 r/hr, 56 min, yield 16.3%); (—●—) poly(α -bromoacrylic acid) (80°C, 5×10^4 r/hr, 56 min, yield 41.5%).

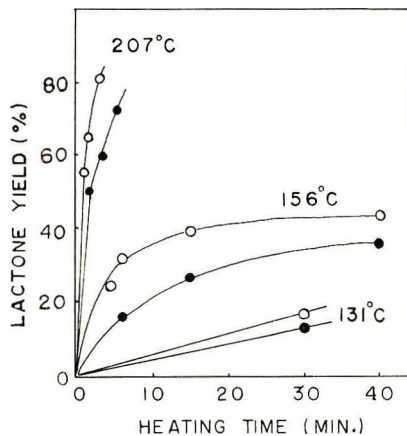


Fig. 7. Rate of lactonization of poly(α -chloroacrylic acid) (The values in the figure represent heating temperature): (—○—) polymer obtained in the solid state (55°C, 5×10^4 r/hr, 4.5 hr, yield 17.5%); (—●—) polymer obtained in the liquid state (88°C, 5×10^4 r/hr, 30 min, yield 12.5%).

investigating the kinetics of the lactonization reaction. The rate of lactone formation of polymers obtained in the solid state is compared with that of polymer formed in the liquid state at various temperatures, as shown in Figure 7; the rate of lactonization of polymer in the solid state is greater than that in the liquid state. It is considered that the rate of lactonization is influenced by the degree of polymerization and the microstructure of resulted polymer. It was difficult to determine the molecular weight of poly(α -chloroacrylic acid) directly by viscometry so that this polymer was esterified with diazomethane and transformed to poly(α -chloromethyl acrylate), dissolved in chloroform, and intrinsic viscosity measured at 30°C. Figure 8 shows the relationship between rate of lactonization and the intrinsic

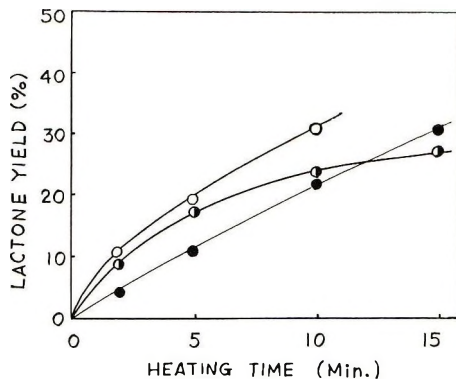


Fig. 8. Relationship between intrinsic viscosity and lactone yield of poly(α -chloroacrylic acid): (—○—) polymer obtained in the solid state (50°C, 5×10^4 r/hr, 3 hr, yield 6.0%, $[\eta] = 1.0$); (—◐—) polymer obtained in the solid state (50°C, 5×10^4 r/hr, 45 hr, yield 64%, $[\eta] = 2.2$); (—●—) polymer obtained in the liquid state (74°C, 5×10^4 r/hr, 1.5 hr, yield 24%, $[\eta] = 2.2$).

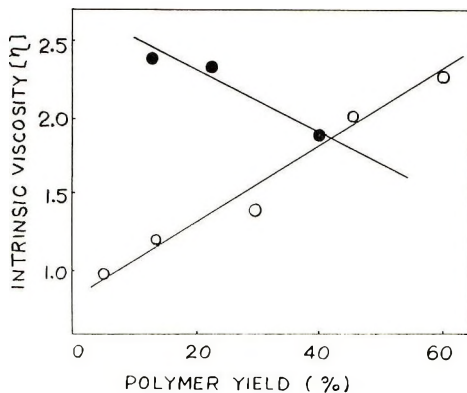


Fig. 9. Relationship between intrinsic viscosity and polymer yield: (—○—) polymer obtained in the solid state; (—●—) polymer obtained in the liquid state.

sic viscosity of polymers obtained in the solid and the liquid state. It is obvious that the rate of lactonization of polymers obtained in the solid state is larger than that of polymers formed in the liquid state at same degree of polymerization. Thus the difference of lactone yield between two polymers is attributable to the polymer structure and not the degree of polymerization. Figure 9 shows intrinsic viscosity of the methyl esters of poly(α -chloroacrylic acid). The molecular weight is proportional to yield of polymerization in the solid state, as reported in the solid-state polymerization of acrylamides,⁸ however, in the liquid-state polymerization, intrinsic viscosity decreases with increasing polymer yield.

The polymer configuration was studied by the use of an NMR technique. To obtain a homogeneous solution for NMR measurement, poly(α -chloroacrylic acid) was esterified as mentioned above to give poly(α -chloromethyl

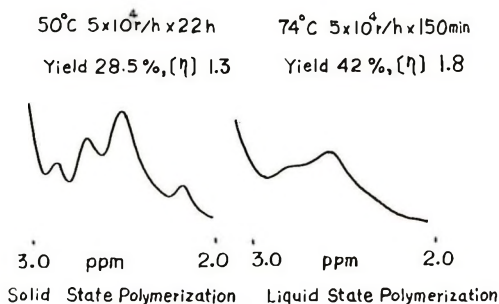


Fig. 10. NMR spectra of poly(α -chloromethyl acrylate) in pyridine at 80°C, obtained from ethyl ester of poly(α -chloroacrylic acid).

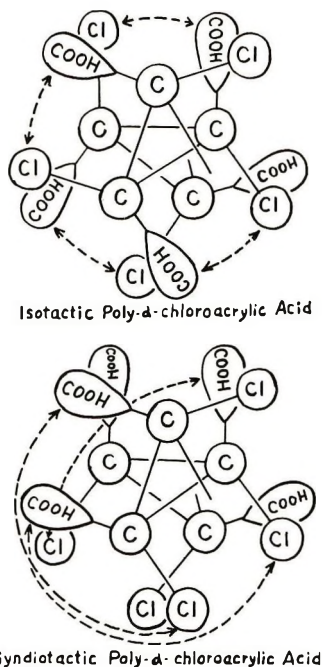


Fig. 11. Projection of the 5_2 helix of isotactic and syndiotactic poly- α -chloroacrylic acid. Dotted lines show the direction of hydrogen chloride elimination.

acrylate). The stereo regularity of poly(methyl methacrylate) was investigated by NMR spectra of the methyl group,⁵ whereas poly(α -chloromethyl acrylate) has no methyl group in the α -carbon atom. The degree of stereo-regularity of poly(α -chloromethyl acrylate) could not be determined directly; however isotactic and syndiotactic configuration could be distinguished by the effect of methylene group. In the chloroform solution we found no difference in NMR spectra between these two type polymers, whereas good distinction were made in pyridine solution. Figure 10 shows typical spectra for pyridine solution at 80°C of poly(α -chloromethyl acry-

late) prepared from poly(α -chloroacrylic acid). The methylene group appears at 2.0–3.0 ppm in spectra of polymers obtained both in solid and liquid state and is affected by the chain conformation. Polymers prepared in the solid state show four prominent peaks, the other peak being less sharp. From the theoretical point of view the methylene protons in the isotactic configuration would be expected because of the effect of the carbonyl group, to be an AB quartet; and the magnetic equivalence of the methylene protons in syndiotactic configuration could be expected to appear single peak. That is, poly(α -chloroacrylic acid) prepared in the solid state is thought to be predominately in an isotactic configuration. This result agrees with the difference between the configuration of poly(methacrylic acid) prepared in the solid and liquid state.²

Considering the planar zigzag structure, the syndiotactic configuration should have advantage for lactone formation, whereas poly(α -chloroacrylic acid) would be expected to be in a 5_2 helix, being similar to poly(methyl methacrylate)⁶; lactone formation is facilitated by the isotactic configuration, as shown in Figure 11.

In the case of polymerization of methacrylic acid salt,⁷ the degree of isotactic configuration decreases with increasing polymer yield. Because of the difficulties of determining the extent of isotactic configuration of poly(α -chloroacrylic acid), the dependence of isotactic configuration on the polymerization time can not be obtained. As shown in Figure 8, the rates of lactonization are nearly equal in the initial heating stage for polymer obtained in the initial polymerization time and final polymerization time; however, in the final heating stage, the lactone yield of the polymer obtained in the final polymerization time becomes smaller compared with that obtained in the initial polymerization time. Because of reasons mentioned above, it is assumed that the degree of isotactic configuration decreases with polymerization time.

References

1. A. J. Restaino, R. B. Mesrobian, H. Morawetz, D. S. Ballantine, G. J. Dienes, and D. J. Metz, *J. Amer. Chem. Soc.*, **78**, 2939 (1956).
2. H. Morawetz and I. D. Robin, *J. Polym. Sci.*, **57**, 687 (1962).
3. C. S. Marvel, *J. Amer. Chem. Soc.*, **62**, 3495 (1940).
4. L. M. Minsk, *J. Amer. Chem. Soc.*, **72**, 2650 (1950).
5. F. A. Bovey and G. V. D. Tiers, *J. Polym. Sci.*, **44**, 173 (1960).
6. J. D. Stroupe and R. E. Hughes, *J. Amer. Chem. Soc.*, **80**, 2341 (1958).
7. J. B. Lando and H. Morawetz, in *Macromolecular Chemistry, Paris 1963* (*J. Polym. Sci. C*, **4**), M. Magat, Ed.
8. T. A. Fadner and H. Morawetz, *J. Polym. Sci.*, **45**, 475 (1960).

Received June 12, 1970

Revised October 23, 1970

Thermal Degradation of Poly(alkyl Acrylates). I. Preliminary Investigations

N. GRASSIE and J. G. SPEAKMAN,*

Department of Chemistry, University of Glasgow, Glasgow W.2, Scotland

Synopsis

A qualitative survey of the thermal degradation reactions which occur in poly(ethyl acrylate), poly(*n*-propyl acrylate), poly(isopropyl acrylate), poly(*n*-butyl acrylate) and poly(2-ethylhexyl acrylate) has been made by using three thermal analytical methods: thermogravimetric analysis (TGA), thermal volatilization analysis (TVA), and the dynamic molecular still (DMS), all combined with infrared and mass spectrometry. Degradation in poly(isopropyl acrylate), which is a secondary ester, becomes discernible at 260°C and proceeds in two stages. The other four polymers, which are all primary esters, are more stable. They degrade in a single-stage process starting at 300°C. The principal volatile products from the primary esters are carbon dioxide and the olefin and alcohol corresponding to the alkyl group. A roughly equivalent quantity of short-chain fragments is also formed. From poly(isopropyl acrylate), carbon dioxide and propylene are the only volatile products in the first phase of the reaction.

In spite of the fact that the chemical structures of polyacrylates and polymethacrylates are so similar, early work suggested that there was a wide divergence in their general thermal degradation characteristics. Thus poly(methyl methacrylate) gives quantitative yields of monomer¹ while the predominating product from poly(methyl acrylate) is a mixture of large chain fragments.² In general terms, this was interpreted as being due to the fact that while the initially formed radicals of poly(methyl methacrylate) depropagate in a reverse polymerization process, poly(methyl acrylate) radicals preferentially undergo inter- and intramolecular transfer reactions. It came to be assumed that polymethacrylates and polyacrylates all behave typically in these two distinct ways.

Subsequently, the thermal degradations of other members of the two series were examined in considerable detail. In particular it was observed that while poly(*n*-butyl methacrylate) yields appreciable amounts of monomer, the reaction is by no means quantitative. Monomer production ceases at 30-50% conversion,³ and at higher temperatures a complex series of reactions occurs in which there is evidence of decomposition of the pendant ester group to give products like butene, methacrylic acid, and anhydride. The behavior of the polyacrylates as a group was also recognized to be more com-

* Present address: Department of Chemistry, University of Mainz, Mainz, West Germany.

plex than originally envisaged. More careful analysis revealed ester decomposition products like carbon dioxide and the corresponding olefins and alcohols as well as traces of monomer.² The behaviors of the two series were observed to coincide in the *tert*-butyl esters, both of which undergo almost quantitative ester decomposition to isobutene and acrylic and methacrylic acids, respectively.^{4,5}

Clearly there is considerable overlap in the thermal degradation behaviors of the two series of polymers, and the purpose of the detailed investigation of a series of poly(alkyl acrylates) which is described in the present series of papers is to provide information which will ultimately allow a unified picture to be presented of the thermal degradation behaviors of these two closely related series of polymers and to correlate the reactions which occur with the structures of the polymers.

EXPERIMENTAL

Preparation of Polymers

Ethyl acrylate (B.D.H. Ltd.), *n*-butyl acrylate (Koch Light Laboratories Ltd.), and 2-ethyl-hexyl acrylate (Union Carbide Ltd.) were available commercially. *n*-Propyl and isopropyl acrylates were prepared by the method of Rehberg and Fisher,^{6,7} which involves ester exchange between methyl acrylate and the appropriate alcohol in presence of a strong acid as catalyst.

The polymerization initiator, azobisisobutyronitrile (Kodak Ltd.), was recrystallized from methanol. The solvents were the corresponding alkyl acetates (Analar grade) except in the case of 2-ethylhexyl acrylate, for which benzene (Analar) was used.

All solvents and monomers were dried over calcium chloride followed by calcium hydride. All except 2-ethylhexyl acrylate were degassed by the conventional freezing and thawing technique after which the solvents were distilled once and the monomers twice, under vacuum, to remove all traces of inhibitor, into a calibrated reservoir. 2-Ethylhexyl acrylate was too involatile for distillation under high vacuum at ambient temperature. It was distilled under reduced pressure (85°C/0.8 cm Hg) directly into the polymerization vessel and degassed as above.

TABLE I
Polymerization Data

Ester	Initiator concn, % (w/v)	Monomer concn, % (v/v)	Conversion, %	Molecular weight × 10 ⁻⁶
Ethyl	0.252	20.0	14	0.87
<i>n</i> -Propyl	0.097	19.4	9	2.30
Isopropyl	0.105	18.4	9	0.65
Butyl	0.105	20.5	16	1.15
2-Ethylhexyl	0.110	17.3	16	0.253

Appropriate amounts of initiator, solvent, and monomer were introduced into dilatometers which were sealed under vacuum. Polymerizations were carried out at $40 \pm 0.1^\circ\text{C}$ to a relatively low conversion. The polymers were precipitated twice by methanol and finally freeze dried from benzene solution. Polymerization data are summarized in Table I.

Preparations were designed to produce polymers with molecular weights of the same order of magnitude. Results in the last column of Table I indicate that this was only partially successful, but, on the other hand, results of subsequent degradation experiments give no reason to suspect that molecular weight differences of this magnitude will have any significant influence on the ultimate conclusions drawn from this work.

A sample of poly(methyl acrylate) was supplied by Dr. I. C. McNeill.

Molecular Weights

Number-average molecular weights were measured by means of a Hewlett-Packard high speed membrane osmometer.

Thermal Analysis

The technique of thermal volatilization analysis (TVA) has been described by McNeill.⁸ Samples of polymer (50 mg) were heated at $10^\circ\text{C}/\text{min}$ under vacuum from ambient temperature to 500°C , the pressure of volatile products evolved being continuously monitored by means of four Pirani gauges associated with traps at 0, -45 , -75 , and -100°C .

Thermal gravimetric analyzes (TGA) were obtained by using the DuPont 950 thermogravimetric analyzer. Samples (10 mg) were heated at $10^\circ\text{C}/\text{min}$ from ambient temperature to 500°C in an atmosphere of nitrogen (oxygen-free).

The dynamic molecular still (DMS) was a modified form of that originally devised by Grassie and Melville.⁹ This provides a convenient and rapid method for the separation and estimation of the three main types of degradation products, namely, products volatile at ambient temperature, chain fragments volatile at degradation temperatures, and involatile residue.

Mass Spectrometry

Mass spectra of volatile products were obtained by using an A.E.I. MS 10 instrument and an LKB 9000 combined gas-chromatograph mass spectrometer. A 10% dinonyl phthalate chromatographic column was used.

Infrared Spectroscopy

Infrared spectra were recorded on a Unicam SP 100 spectrophotometer.

RESULTS AND DISCUSSION

Before embarking on a quantitative study of the thermal degradation of polyacrylates, it is necessary to determine the temperature range in which reaction occurs at a conveniently measurable rate. It is also important to

obtain a qualitative knowledge of the degradation products so that methods may be devised for their quantitative analysis. The present paper describes how this was achieved principally by the application of three thermal analysis techniques: the dynamic molecular still (DMS), thermal volatilization analysis (TVA), and thermal gravimetric analysis (TGA), coupled with infrared and gas chromatography-mass spectrometric (GC-MS) measurements.

Thermal Volatilization Analysis

TVA thermograms of the polymers under investigation, and of a poly-(methyl acrylate) sample for comparison purposes, are illustrated in Figures 1-6. It is immediately clear that poly(isopropyl acrylate), which is a secondary ester, behaves differently from the other polymers, which are all primary esters. Volatilization is discernable in poly(isopropyl acrylate) at 260°C, building up to a maximum at 355°C. A secondary peak occurs at 442°C, and volatile products are still being evolved at 500°C. The other five polymers exhibit a single main peak followed by a low plateau. They are also more stable, volatilization becoming appreciable at 300°C in all but the methyl ester and reaching a maximum in the range 405-415°C. The methyl ester is appreciably more stable than the others with a threshold at 325°C and a maximum at 438°C.

Thermogravimetric Analysis

TGA thermograms for the ethyl, *n*-propyl, isopropyl, and *n*-butyl esters, illustrated in Figure 7, confirm the information derived from TVA. The volatilization of poly(isopropyl acrylate) is obviously a two-stage process beginning at 265°C and leaving an 8% residue at 500°C. The other three polymers degrade in a one-stage process beginning at 300°C and leaving less than 5% of residue at 500°C. The thermograms for the ethyl and *n*-propyl esters are identical.

Dynamic Molecular Still

In view of the close similarity in the behaviors of most of the polymers as revealed by TVA and TGA, these preliminary dynamic molecular still in-

TABLE II
Molecular Still Degradation Data for Poly(*n*-butyl Acrylate)

Temp, °C	Weight, % of original				Molecular weight of soluble residue
	Total residue	Soluble residue	Short-chain fragments	Volatiles	
290	83.2	60.7	12.1	4.7	32,800
300	61.5	51.9	20.4	18.1	19,500
313	39.5	29.4	28.6	31.9	11,200
324	14.1	0	41.8	44.1	Insoluble
347	9.0	0	40.8	50.2	Insoluble
355	10.5	0	43.5	46.0	Insoluble

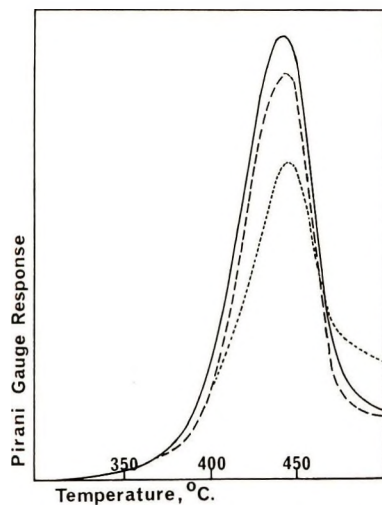


Fig. 1. TVA thermogram of poly(methyl acrylate) at various trap temperatures: (—) 0°C; (---) -45° and -75°C; (· · ·) -100°C.

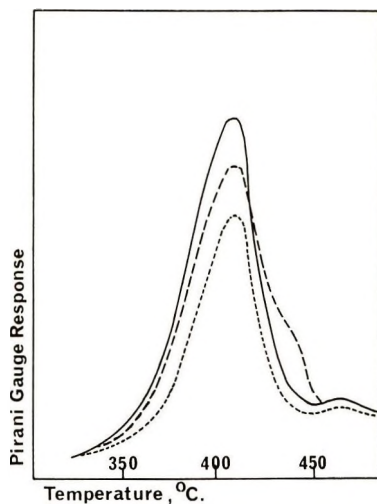


Fig. 2. TVA thermogram of poly(ethyl acrylate) at various trap temperatures: (—) 0 and -45°C; (---) -75°C; (· · ·) -100°C.

vestigations and the identification of the products were concentrated on a single polymer, namely poly(*n*-butyl acrylate). In order to achieve a wide range of extents of volatilization reactions were carried out at increasing temperatures for a standard time of 2 hr. Approximately 200 mg of polymer was used in each experiment. Data are presented in Table II. Some of these results are illustrated in Figure 8.

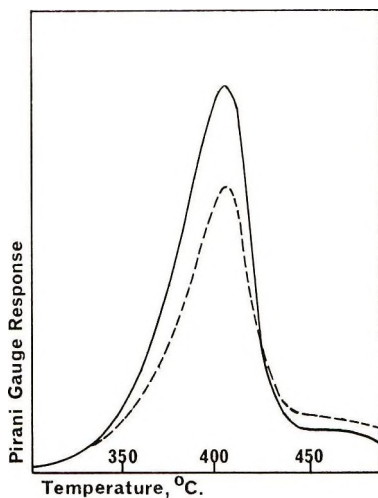


Fig. 3. TVA thermogram of poly(*n*-propyl acrylate) at various trap temperatures: (—) 0 and -45°C ; (---) -75° and -100°C .

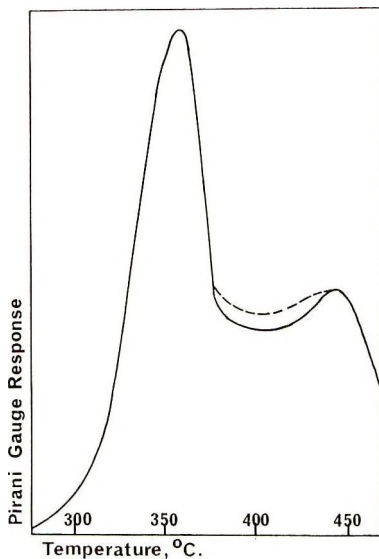


Fig. 4. TVA thermogram of poly(isopropyl acrylate) at various trap temperatures: (—) 0, -45 , and -100°C ; (---) -75°C .

Identification of Products

The volatile products from the experiments summarized in Table II were analyzed by mass spectrometry. The spectra did not change significantly with extent of reaction. Figure 9A shows the spectrum of the products obtained at 355°C . It can be accounted for qualitatively in terms of a mixture of CO_2 , 1-butene, and *n*-butanol, the spectra of which are illustrated in

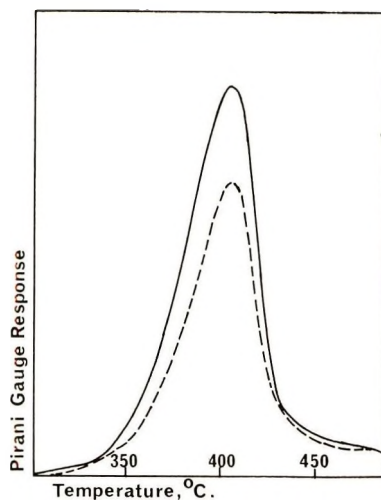


Fig. 5. TVA thermogram of poly(*n*-butyl acrylate) at various trap temperatures: (—) 0 and -45°C ; (---) -75 and -100°C .

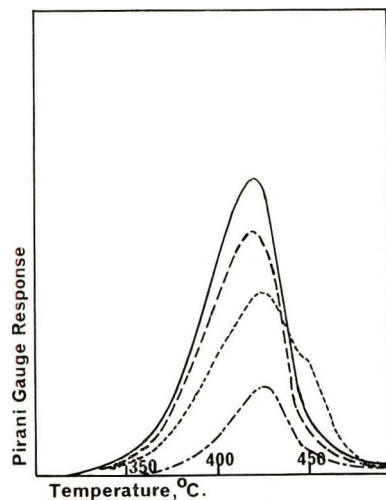


Fig. 6. TVA thermogram of poly(2-ethylhexyl acrylate) at various trap temperatures: (—) 0°C ; (---) -45°C ; (-·-) -75°C ; (- - -) -100°C .

Figures 9B, C, and D, respectively. The infrared spectrum of the most volatile fraction of the volatile products is illustrated in Figure 10, and the assignment of the peaks demonstrates that it can be accounted for satisfactorily as being composed principally of a mixture of CO_2 and butene. The less volatile fraction of the volatile products was analyzed by using GC-MS. The GC-MS chromatogram is shown in Figure 11. The GC-MS mass spectra allowed peaks 1-4 to be assigned to chloroform (solvent), *n*-butanol, *n*-butyl acrylate, and *n*-butyl methacrylate respectively. The mass spectra of the higher molecular weight products were difficult to analyze because,

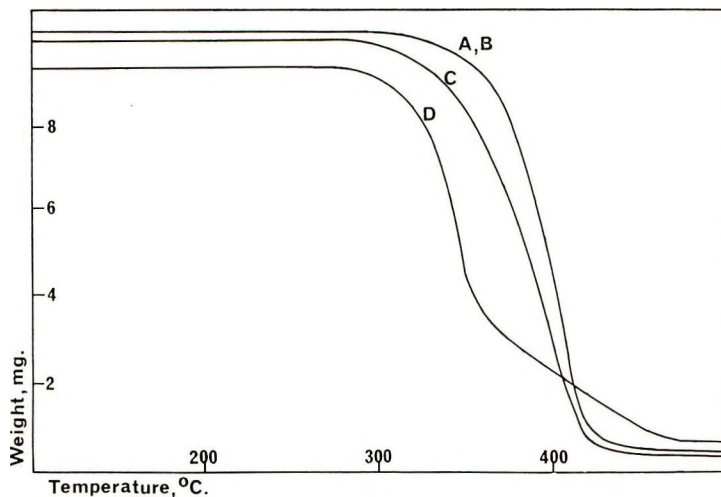


Fig. 7. TGA thermograms for (A) poly(ethyl acrylate); (B) poly(*n*-propyl acrylate); (C) poly(*n*-butyl acrylate); (D) poly(isopropyl acrylate).

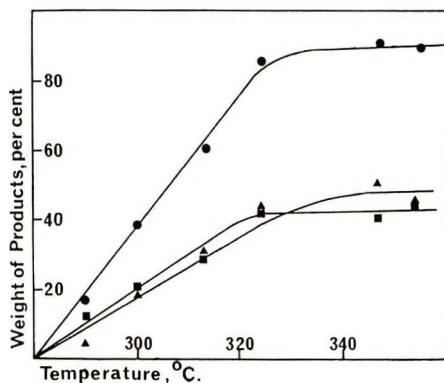


Fig. 8. Extent of degradation of poly(*n*-butyl acrylate) in 2 hr at various temperatures in the dynamic molecular still: (●) total weight loss; (▲) products volatile at room temperature; (■) short-chain fragments.

involving esters, they rarely gave a significant parent peak and because peaks above mass 200 were difficult to assign with absolute certainty. However, Table III lists the main peaks of the more important of the later

TABLE III

Chromatographic Peak	Main mass spectrum peaks
5	134, 117
6	356, 268, 73
7	428, 341, 73
8	502, 415, 281, 147, 73
9	407, 327, 156, 18

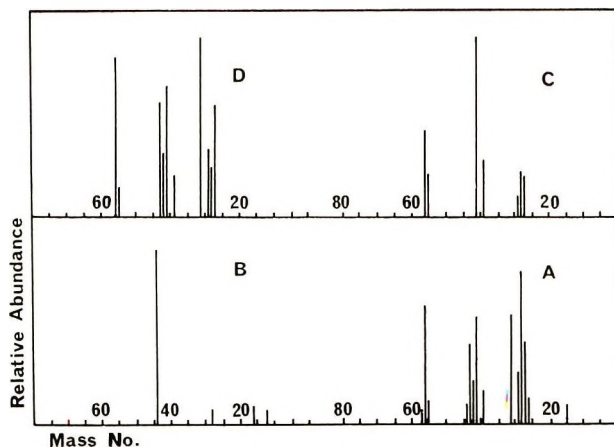


Fig. 9. Mass spectra of: (A) volatile products of degradation of poly(*n*-butyl acrylate) at 355°C; (B) carbon dioxide; (C) 1-butene; (D) *n*-butanol.

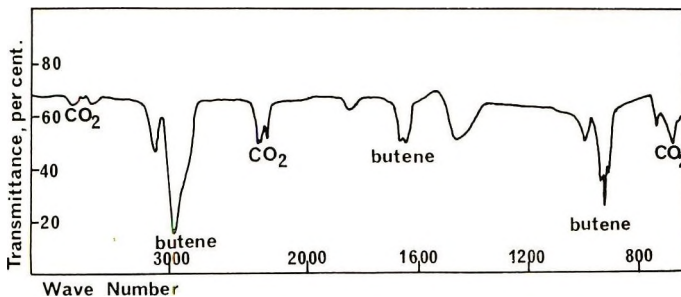


Fig. 10. Infrared spectrum of the most volatile products of degradation of poly(*n*-butyl acrylate).

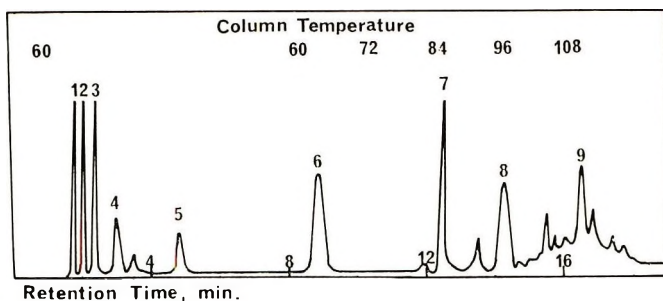


Fig. 11. GC-MS chromatogram of less volatile fraction of the volatile products of degradation of poly(*n*-butyl acrylate).

components in the chromatogram. The appearance of a large peak at mass 73 in three of these spectra would indicate that these components contain butyl ester groups which lose $\text{CH}_3\text{—CH}_2\text{—CH}_2\text{—CH}_2\text{—O}^+$ ions. Component 5 has a large parent peak and is thus probably aromatic in character,

possibly an impurity in the toluene used as solvent to cast the polymer film.

The TVA trace for poly(*n*-butyl acrylate) in Figure 5 is in accord with the occurrence of butene, carbon dioxide, and butanol as the principal volatile products of degradation. The Pirani gauges associated with each of the traps are so adjusted that the responses are identical if the products are not condensed or retarded on passage through the traps. Thus all three products pass through the traps at 0 and -45°C , while butanol is condensed at -75 and -100°C . The difference between the two curves is associated with the butanol content of the products. The close similarity between the TVA thermograms of the *n*-butyl and *n*-propyl esters suggests that an exactly analogous set of products, namely, carbon dioxide, propylene, and propanol, are obtained from poly(*n*-propyl acrylate). Ethanol, on the other hand, is known to be only retarded, not efficiently condensed, at -75°C , resulting in separation of the -75 and -100°C traces. In the thermogram of poly(methyl acrylate) there is a separation of the 0 and -45°C traces, although the -45 and -75°C traces are coincident. From this polymer it is known that carbon dioxide and methanol are the principal volatile products,⁶ so it seems that methanol, in spite of its slightly higher vapor pressure than ethanol at -45°C , is being retarded at this temperature. Although the single peak in the same temperature range in the thermogram of the 2-ethylhexyl ester suggests a similar degradation mechanism with analogous products, their wider range of volatilities accounts for the complete separation of all four traces.

In the TVA thermogram of poly(isopropyl acrylate) all four traces are coincident throughout, indicating that all volatile products in both phases of the reaction are volatile, even at -100°C . In contrast to the other polymers, therefore, there can be no alcohol formed which would cause separation of the 0 and -45°C peaks. Infrared and mass spectral measurements demonstrate that propylene and carbon dioxide are the only volatile products. There are other major differences between the degradation behaviors of poly(isopropyl acrylate) and the primary esters of which the most striking is the fact that chain fragments, which are the major product from the primary esters are not formed from the isopropyl ester. This fact, together with TVA evidence, suggests that the first phase of the reaction consists of ester decomposition of individual units followed, in the second phase, by the complete disintegration of the residue to highly volatile small molecules.

CONCLUSION

Thermal analysis has demonstrated that poly(isopropyl acrylate), a secondary ester, degrades at a lower temperature and in a different manner from the polymers of methyl, ethyl, *n*-propyl, *n*-butyl, and 2-ethylhexyl acrylates, which are all primary esters. These experiments also suggest that a temperature of approximately 265°C would be most suitable for an isothermal

study of the thermal degradation of poly(isopropyl acrylate) while 315°C would be more appropriate for the primary esters.

In order that a detailed study of the mechanisms of these reactions might be carried out it was necessary to devise methods for the efficient separation and analysis of the complex variety of products and of the residue. Investigations of the primary esters and of the isopropyl ester are described, respectively, in the second and third papers of this series.^{10,11}

One of the authors (J. G. S.) is grateful to the Science Research Council for a research scholarship.

References

1. N. Grassie, in *Chemical Reactions of Polymers*, E. M. Fettes, Ed., Interscience New York, 1964, p. 565.
2. G. G. Cameron and D. R. Kane, *Makromol. Chem.*, **113**, 75 (1968).
3. N. Grassie and J. R. MacCallum, *J. Polym. Sci. A*, **2**, 983 (1964).
4. J. R. Schaefgen and I. M. Sarasohn, *J. Polym. Sci.*, **58**, 1049 (1962).
5. D. H. Grant and N. Grassie, *Polymer*, **1**, 445 (1960).
6. C. E. Rehberg and C. H. Fisher, *J. Amer. Chem. Soc.*, **66**, 1203 (1944).
7. C. E. Rehberg, W. A. Faucette, and C. H. Fisher, *J. Amer. Chem. Soc.*, **66**, 1723 (1944).
8. I. C. McNeill, *Europ. Polym. J.*, **6**, 373 (1970).
9. N. Grassie and H. W. Melville, *Proc. Roy. Soc. (London)*, **199A**, 1 (1949).
10. N. Grassie, J. G. Speakman, and T. I. Davis, *J. Polym. Sci. A-1*, **9**, 931 (1971).
11. N. Grassie and J. G. Speakman, *J. Polym. Sci. A-1*, **9**, 949 (1971).

Received September 1, 1970

Revised October 23, 1970

Thermal Degradation of Poly(alkyl Acrylates). II. Primary Esters: Ethyl, *n*-Propyl, *n*-Butyl, and 2-Ethylhexyl.

N. GRASSIE, J. G. SPEAKMAN, and T. I. DAVIS*

Department of Chemistry, University of Glasgow, Glasgow W.2, Scotland

Synopsis

Quantitative analyses of the products of thermal degradation of poly(ethyl acrylate), poly(*n*-propyl acrylate), poly(*n*-butyl acrylate) and poly(2-ethylhexyl acrylate) have been made, principally by the combined application of GLC and mass and infrared spectroscopy. Data are recorded in mass balance tables. The major gaseous products are carbon dioxide and the olefin corresponding to the ester group. The minor gaseous products include the corresponding alkane, the alkane/olefin ratio being of the order of 10^{-2} - 10^{-3} , and traces of carbon monoxide and hydrogen. The alcohol corresponding to the alkyl group is the major liquid product but there are also traces of monomer and the corresponding methacrylate. Alcohol production exhibits autocatalytic properties. The chain fragment fractions of the products are colored yellow and have average chain lengths of 3.2, 3.3, 3.6, and 5.6 for the ethyl, *n*-propyl, *n*-butyl and 2-ethylhexyl esters, respectively. The infrared spectra are similar to those of the parent polymers but with well defined differences. Insolubility develops in the ethyl, *n*-propyl, and *n*-butyl esters, but the residual material from poly(2-ethylhexyl acrylate) remains soluble even at very advanced stages of degradation. All of these products and reaction characteristics are accounted for in terms of radical reactions with a unique initiation step.

In the previous paper¹ it has been shown that there is a close similarity between the thermal degradation behaviors of four poly(primary alkyl acrylates), namely, the ethyl, *n*-propyl, *n*-butyl, and 2-ethylhexyl esters. Thus they all degrade at approximately the same temperature in a one-stage process, and the general pattern of volatile products is similar. In this paper more detailed analyses of the products of reaction are described and mechanisms of degradation discussed.

EXPERIMENTAL

Polymers

The polymers used were these described in the previous paper.¹

* Present address: Department of Chemistry, University of Mainz, Mainz, West Germany.

Degradation Techniques

In the previous paper¹ the use of the dynamic molecular still technique for a preliminary separation of reaction products was described. Grassie and Bain² have discussed its shortcomings when the separation is to be followed by a detailed product analysis and have described an alternative method, the "sealed tube" method,³ which was particularly successful for the separation of the products of degradation of styrene-acrylonitrile copolymers. This method was found to be readily adaptable to the acrylate polymers and was used throughout the investigations described in this paper.

Degradations were carried out at a standard temperature of 315°C, over a range of reaction times, on 100-mg samples of polymer. Products were separated into five fractions, namely, residue, chain fragments, liquids, condensable gases, and non-condensable gases.

Gas-Liquid Chromatography (GLC)

GLC analyses were carried out by using a Microtek 2000 R research chromatograph with a flame ionization detector. A 10% dimonyl phthalate column was normally used, but silica gel and 40% silver nitrate-benzyl cyanide columns were used for gases other than carbon dioxide and the olefins, and a 1% Carbowax 20M column was used for the higher molecular weight products.

Molecular Weights

Number-average molecular weights were measured by means of Hewlett-Packard high-speed membrane and vapor pressure osmometers.

Spectral Measurements

Mass and infrared spectra were recorded as in the previous paper,¹ and ultraviolet spectra by using a Unicam SP 800 instrument.

Sol-Gel Separation

The residual polymer was allowed to stand overnight in 10 ml of toluene. Sol and gel fractions were separated by filtration and estimated by drying to constant weight.

RESULTS

Major Gaseous Products

The major gaseous products were shown in the previous paper¹ to be carbon dioxide and the olefin corresponding to the ester group in the polymer, except in the case of the ethylhexyl ester, when carbon dioxide alone appeared in this fraction. The olefin, being less volatile, in this case appears among the liquid products. Analysis was carried out by the combined application of a constant volume manometer and infrared spectroscopy.

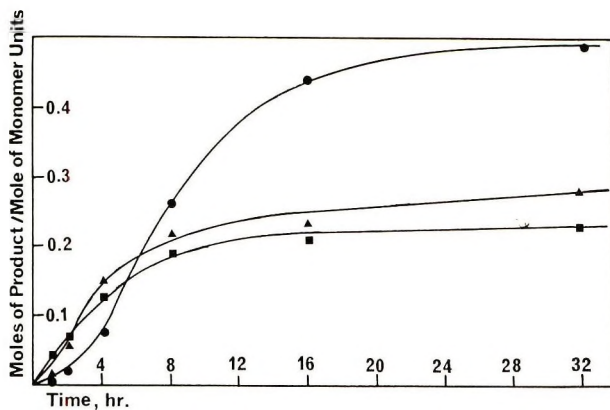


Fig. 1. Production of (▲) carbon dioxide, (■) ethylene, and (●) ethanol during degradation of poly(ethyl acrylate).

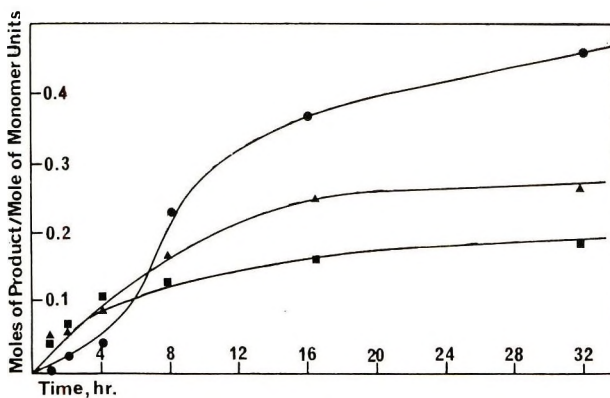


Fig. 2. Production of (▲) carbon dioxide (■) propylene, and (●) *n*-propanol during degradation of poly(*n*-propyl acrylate).

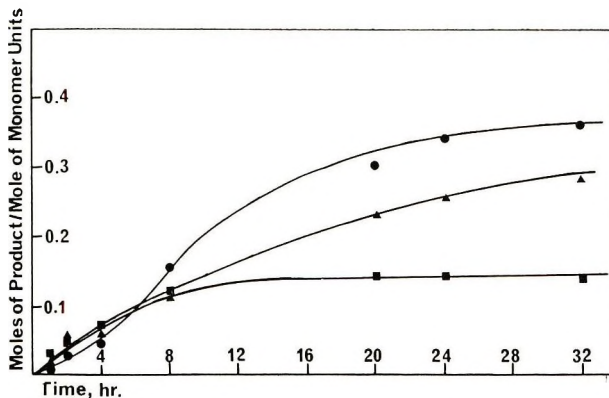


Fig. 3. Production of (▲) carbon dioxide, (■) 1-butene, and (●) *n*-butanol during degradation of poly(*n*-butyl acrylate).

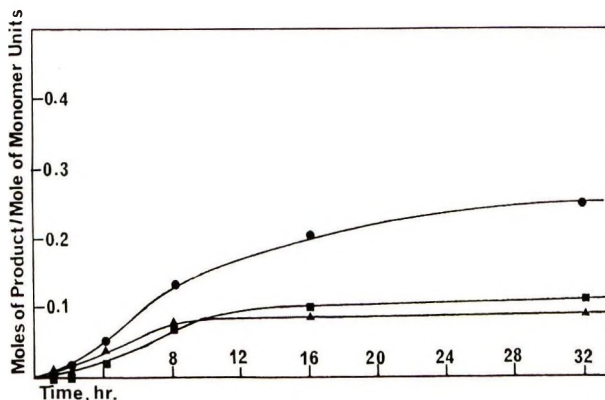


Fig. 4. Production of (▲) carbon dioxide (■) 2-ethyl-1-hexene, and (●) 2-ethyl-1-hexanol during degradation of poly(2-ethyl-hexyl acrylate).

The data are recorded in the mass-balance tables (Tables I–IV) and Figures 1–4 illustrate the course of the reaction in terms of the proportions of monomer units involved. The amounts of carbon dioxide produced from the ethyl, *n*-propyl and *n*-butyl esters are similar. Only about one third as much is liberated from the 2-ethylhexyl ester. The amounts of olefins produced seem to vary as the number of β -hydrogen atoms in the alkyl group. Thus most is produced from the ethyl ester and least from the 2-ethylhexyl ester, while the *n*-propyl and *n*-butyl esters behave similarly in this respect. From each polymer the molar ratio of olefin to carbon dioxide is of the order of unity over an appreciable part of the reaction.

TABLE I
Mass Balance Table for Degradation of Poly(Ethyl Acrylate) at 315°C
for Various Lengths of Time

	Products, wt-% of initial polymers					
	1 hr	2 hr	4 hr	8 hr	16 hr	32 hr
Residue	98.0	92.9	83.4	67.2	45.4	38.0
Insoluble	44.2	31.1	39.0	12.8	33.1	30.1
Soluble	49.8	60.8	45.6	50.8	7.2	5.1
Chain fragments	2.1	3.8	4.7	9.3	14.3	15.3
Total liquids	0.4	1.0	6.3	15.0	25.4	26.7
Alcohol	0.3	0.9	3.5	12.0	20.2	22.4
Monomer	0.00	0.02	0.18	0.19	0.26	0.32
Methacrylate	0.00	0.02	0.05	0.08	0.11	0.26
Remaining liquids	0.1	0.1	2.6	2.7	4.8	3.7
Condensable gases	1.9	4.5	10.3	15.0	16.1	18.5
Carbon dioxide	0.7	2.6	6.6	9.7	10.2	12.1
Ethylene	1.2	1.9	3.6	5.3	5.9	6.4
Noncondensables	0.1	0.1	0.2	0.3	0.9	0.9
Total volatiles	4.5	9.4	21.5	39.6	56.7	61.4
Total products	102.5	102.3	104.9	106.8	102.1	99.4

TABLE II
Mass Balance Table for Degradation of Poly(*n*-Propyl Acrylate) at 315°C
for Various Lengths of Time

	Products, wt-% of initial polymer					
	1 hr	2 hr	4 hr	8 hr	16 hr	32 hr
Residue	99.2	95.0	84.5	67.5	34.9	24.8
Insoluble	31.7	12.9	21.6	12.8	16.9	24.7
Soluble	66.3	73.7	58.9	56.5	20.0	0.0
Chain fragments	2.2	4.6	6.0	8.7	23.4	27.4
Total liquids	0.5	6.2	4.8	14.1	22.2	29.2
Alcohol	0.0	1.1	2.2	12.1	19.3	24.3
Monomer	0.00	0.00	0.02	0.08	0.18	0.23
Methacrylate	0.00	0.00	0.01	0.05	0.11	0.20
Remaining liquids	0.5	5.1	2.6	1.9	2.6	4.5
Condensable gases	3.5	4.8	7.4	11.7	15.7	17.3
Carbon dioxide	2.0	2.4	3.3	6.8	9.6	10.3
Propylene	1.5	2.4	4.1	4.9	6.1	7.0
Noncondensables	0.0	0.0	0.1	0.6	0.5	0.6
Total volatiles	6.2	15.6	18.3	35.1	61.8	74.5
Total products	105.4	110.6	102.7	102.6	96.7	99.3

TABLE III
Mass Balance Table for Degradation of Poly(*n*-Butyl Acrylate) at 315°C
for Various Lengths of Time

	Products, wt-% of initial polymer						
	1 hr	2 hr	4 hr	8 hr	20 hr	24 hr	32 hr
Residue	90.3	84.6	74.6	67.2	55.8	35.2	33.9
Insoluble	5.3	6.0	5.6	13.1	29.6	33.6	33.9
Soluble	85.0	78.6	69.0	54.1	26.2	1.6	0
Chain fragments	7.7	4.1	11.1	11.5	16.3	17.1	21.7
Total liquids	0.4	2.2	10.6	9.8	19.8	28.7	29.6
Alcohol	0.2	1.6	2.6	9.0	17.6	19.6	20.7
Monomer	0.00	0.04	0.08	0.10	0.16	0.20	0.20
Methacrylate	0.00	0.00	0.03	0.04	0.05	0.03	0.05
Remaining liquids	0.2	0.6	7.9	0.7	2.0	8.9	8.6
Condensable gases	1.8	4.0	5.1	9.4	14.8	15.4	15.5
Carbon dioxide	0.5	1.9	2.0	4.2	8.3	9.1	9.6
Butylene	1.3	2.1	3.1	5.2	6.5	6.3	5.9
Noncondensables	0.1	0.0	0.2	0.5	1.1	1.1	1.2
Total volatiles	10.0	10.3	27.0	31.2	52.0	62.3	68.0
Total products	100.3	94.9	101.6	98.4	107.8	97.5	101.9

Minor Gaseous Products

The gaseous products from the ethyl, *n*-propyl, and *n*-butyl esters were analyzed by gas chromatography on a silica gel column. The products from the *n*-butyl ester were also analyzed on a silver nitrate-benzyl cyanide column. Typical chromatograms are illustrated in Figure 5. Carbon dioxide and carbon monoxide are not detected by the flame ionization detector used.

TABLE IV
Mass Balance Table for Degradation of Poly(2-Ethyl Hexyl Acrylate)
at 315°C for Various Lengths of Time

	Products, wt-% of initial polymer					
	1 hr	2 hr	4 hr	8 hr	16 hr	32 hr
Residue (soluble)	84.0	78.1	69.4	57.2	41.1	15.8
Chain fragments	14.7	19.7	23.8	27.3	36.2	57.6
Total liquids	0.0	0.9	4.8	13.2	20.0	23.9
2-Ethyl-1-hexanol	0.0	0.9	3.6	9.1	14.3	17.3
2-Ethyl-1-hexene	0.0	0.0	1.2	4.1	5.7	6.6
Carbon dioxide	0.2	0.2	0.9	1.9	2.0	2.1
Noncondensables	0.0	0.1	0.0	0.3	0.8	1.0
Total volatiles	14.9	20.9	29.5	42.7	59.0	84.6
Total products	98.9	99.0	98.9	99.9	100.1	100.4

In each case the olefin peak was by far the largest. Next in size was that of the corresponding alkane. Assuming the areas of the peaks to be approximately proportional to the concentrations of these substances, the alkane-olefin ratio always lay in the range 10^{-2} - 10^{-3} . A small shoulder on the 1-butene peak in Figure 5B is attributed to *cis*-2-butene.

The amounts of gases volatile at -196°C were always very small and were only analyzed for the *n*-propyl ester at an advanced extent of degradation. The mass spectrum is shown in Figure 6. By far the largest peak was at mass number 28 and was attributed to carbon monoxide which has small subsidiary peaks at 16 and 12. The small peak at mass number 2 was attributed to hydrogen. It was deduced that carbon monoxide is the principal noncondensable product and that the molar ratio carbon monoxide-hydrogen is approximately 70.

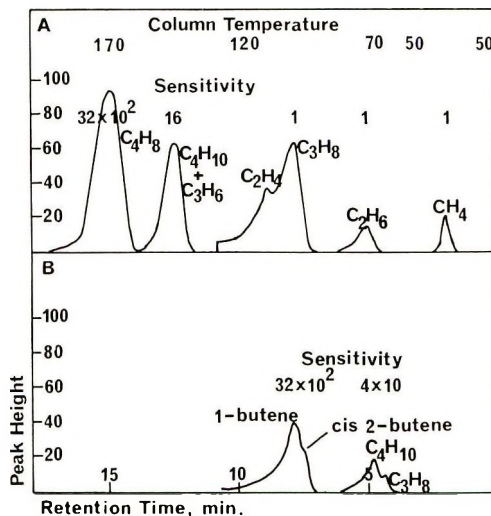


Fig. 5. GLC of the gaseous products of degradation of poly(*n*-butyl acrylate): (A) on a silica gel column; (B) on a silver nitrate-benzyl cyanide column.

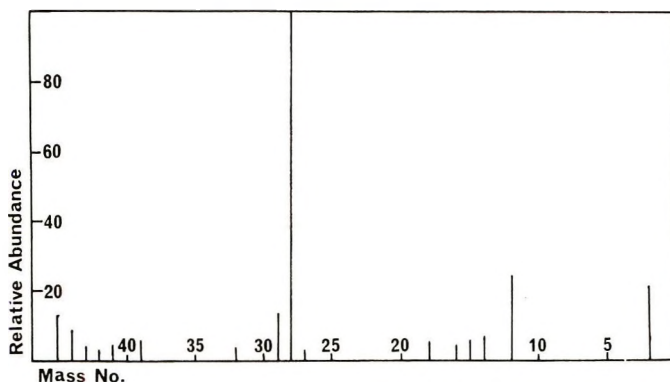


Fig. 6. Mass spectrum of the gases, noncondensable at 196°C, produced during degradation of poly(*n*-propyl acrylate). The peak at mass number 28 has a height of 1000 on the same scale.

Liquid Products from Ethyl, *n*-Propyl and *n*-Butyl Esters

The liquid products were subjected to quantitative GLC analysis. A chromatogram typical of all three polymers is illustrated in Figure 7, from which it is clear that alcohol is the major product with smaller amounts of the monomer and the corresponding methacrylate. It was confirmed for each polymer that the corresponding methacrylate is a genuine degradation product and was not present in the monomer used to prepare the polymers. Results are presented in Tables I–III.

Evolution of alcohol in terms of the proportion of monomer units involved is illustrated in Figures 1–3. Unlike olefin and carbon dioxide production, alcohol production exhibits induction or autocatalytic characteristics.

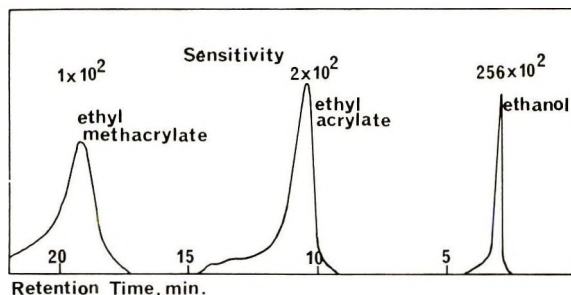


Fig. 7. GLC of the liquid products of degradation of poly(ethyl acrylate).

Liquid Products from Poly(2-Ethylhexyl Acrylate)

Two large peaks in the chromatogram of the liquid products from poly(2-ethylhexyl acrylate) were identified by their retention times as 2-ethyl-1-hexene and 2-ethyl-1-hexanol. The results of quantitative GLC analysis are presented in Table IV and Figure 4.

Chain Fragments

From the ethyl, *n*-propyl, and *n*-butyl esters this fraction was made up of all the material collected from the sealed tube except the residue, gases and those liquids which distilled under vacuum at ordinary temperature. In the case of the 2-ethylhexyl ester it also included the acrylate and methacrylate monomers which are of relatively low volatility.

Infrared spectra were run in carbon tetrachloride solution when the yield was sufficient. In every case the spectra are similar to those of the parent polymers with the following minor differences. The carbonyl peak and the

TABLE V
Molecular Weight of Chain Fragment Fraction

	Poly-(ethyl acrylate)	Poly-(<i>n</i> -propyl acrylate)	Poly-(<i>n</i> -butyl acrylate)	Poly-(2-ethylhexyl acrylate)
Molecular weight	317	379	470	1020
Chain length (monomer units)	3.2	3.3	3.6	5.6

peaks in the 1500–1000 cm^{-1} region show a general broadening which increases with time of degradation. Two shoulders at about 1760 cm^{-1} and 1715 cm^{-1} appear on the carbonyl peak at 1730 cm^{-1} , and the C—O single bond peak at 1160 cm^{-1} becomes more diffuse. Owing to the small amounts of material available the chain fragment fractions from all the degradations of each polymer were combined and the molecular weight determined using vapor pressure osmometry. Results are presented in Table V.

A chromatogram of chain fragments from the *n*-butyl ester is presented in Figure 8, which also includes a chromatogram of a mixture of *n*-alkanes for comparison,

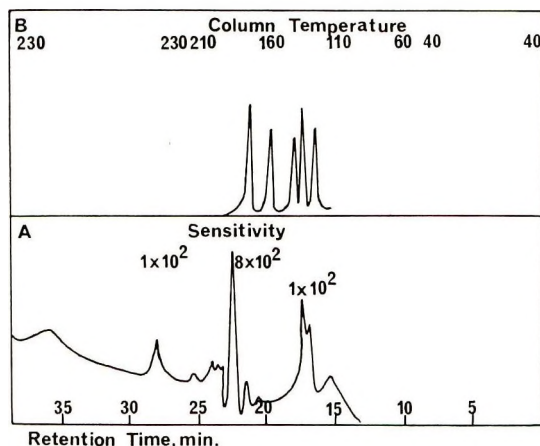


Fig. 8. GLC, of (A) chain fragments produced during degradation of poly(*n*-butyl acrylate) and (B) a mixture of C_{18} , C_{19} , C_{20} , C_{22} , and C_{24} *n*-alkanes for comparison,

comparison. This confirms the order of molecular weight measured directly.

The chain fragment fraction is usually yellow in color, the intensity increasing with time of degradation. However, all attempts to obtain significant ultraviolet or visible spectra were unsuccessful.

The amounts of this fraction produced from the various polymers during the course of the reactions are included in Tables I-IV.

Residue

The progress of volatilization in the four polymers is clear from the data in Tables I-IV. Insolubility develops in the residual polymer during degradation of the ethyl, *n*-propyl, and *n*-butyl esters. No insolubility was ever found in degraded poly(2-ethylhexyl acrylate).

Molecular weight data for the soluble residues from the four polymers are recorded in Table VI. Chain scission is clearly rapid in all cases.

TABLE VI
Molecular Weight of Soluble Residues

Degradation time, hr	Molecular weight $\times 10^{-3}$			
	Ethyl	<i>n</i> -Propyl	<i>n</i> -Butyl	2-Ethylhexyl
0	870	2300	1150	253
1	87.5	11.2	36.5	17.0
2	53.6	5.06	24.9	—
4	—	5.14	21.6	9.70
8	4.16	—	—	4.80
10	—	—	1.082	—
14	—	—	0.672	—
16	—	—	—	2.80
32	—	0.524	—	1.02

The insoluble part of the residue was found to be insoluble in all common organic solvents and in 0.1*M* sodium hydroxide even after prolonged treatment. Elemental analysis reveals that as degradation proceeds, the carbon content rises and the hydrogen and oxygen contents fall.

Since alcohol and olefin must be products of decomposition of the ester group, the data in Tables I-IV referring to alcohol and olefin formation and total volatilization would suggest that after 32 hr only a very small proportion of the ester groups in the residue is intact. One should therefore expect to observe quite significant changes in the infrared spectrum during degradation. The changes which occur in all four polymers are in fact qualitatively similar and are exemplified by the behavior of poly(*n*-butyl acrylate). Since the polymer develops insolubility the reaction was carried out between sodium chloride disks so that the sample could be transferred directly to the infrared spectrophotometer. Because of the different environment care

must be taken in comparing these results with the other data reported above. However, a comparison of the infrared spectra of poly(2-ethylhexyl acrylate), which remains soluble, degraded in both ways and measured in one case in chloroform solution and in the other as a solid between sodium chloride disks, shows no significant differences apart from the fact, as expected, that the peaks tend to be sharper and the maxima better defined in the solution than in the solid spectra.

The 900–1900 cm^{-1} regions of the infrared spectrum of undergraded and degraded poly(*n*-butyl acrylate) are compared in Figure 9. The principal

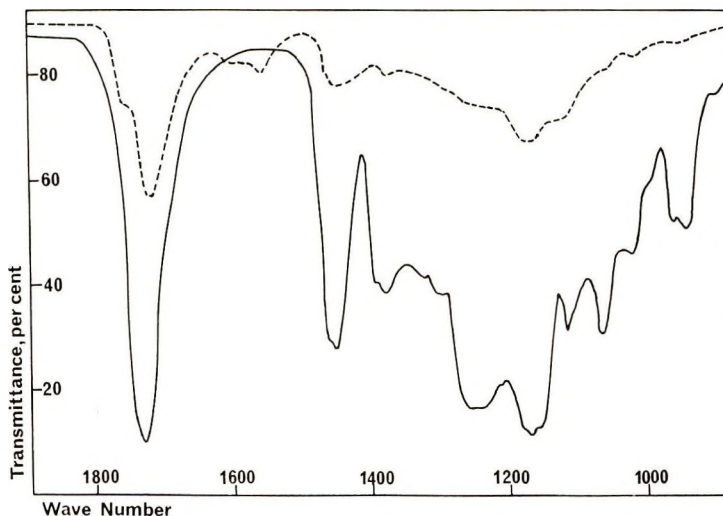


Fig. 9. The 900–1900 cm^{-1} region of the infrared spectra of (—) undergraded and (---) degraded poly(*n*-butyl acrylate).

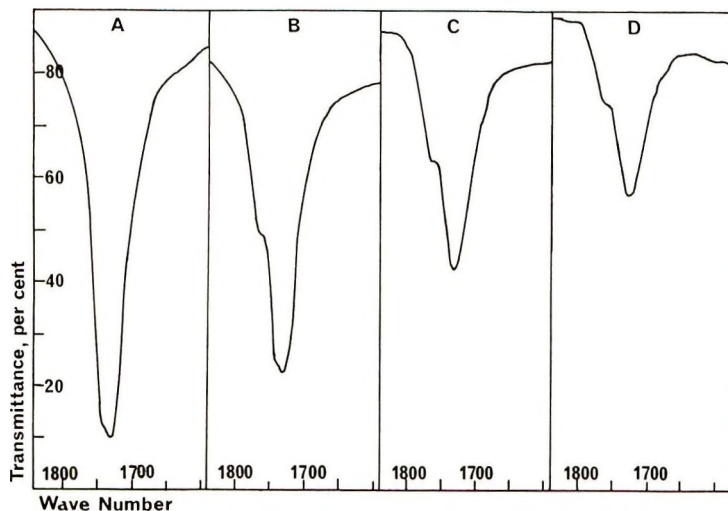


Fig. 10. Carbonyl region of the infrared spectrum of poly(*n*-butyl acrylate) during progressive degradation: (A) undergraded; (B) 4 hr; (C) 8 hr; (D) 16 hr.

changes are the development of a clear shoulder on the carbonyl peak at 1760 cm^{-1} , a general increase in absorption between 1650 and 1550 cm^{-1} and the appearance of a new peak at 1563 cm^{-1} . There is a shift in the carbonyl maximum from 1730 to 1720 cm^{-1} and in the C—O stretch region from 1165 to 1175 cm^{-1} . Outside the 1900 – 900 cm^{-1} region there are no significant changes. Changes in the carbonyl absorption during the course of degradation are illustrated in more detail in Figure 10.

Mass Balance

As the mass balance tables (Tables I–IV) show, all of the initial weights of the polymers are accounted for in the analyses described above. There remains the portion described as “remaining liquids” which is the difference between the total liquids and amounts of the individual materials estimated. The most likely substance to avoid detection and yet be weighed in the liquid fraction, is water. The yield of water remains uncertain since quantitative analyses were not carried out, but it should be expected to be less than the maximum values of 4.8%, 4.5%, and 8.9% found for the ethyl, *n*-propyl and *n*-butyl esters, respectively. There is, however, no smooth relationship between yield and time of degradation as in the other entries in these tables. A likely explanation is that at least part of this material is chain fragments. The amount of these which would find their way into the liquid fraction would depend upon such variables as temperature of distillation and the pressure in the system when distillation was carried out.

Preliminary Conclusions

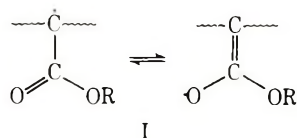
The characteristics of the production of olefin and alcohol are quite different, so that one may reasonably presume that they are formed in quite distinct ester decomposition processes. Olefin production almost inevitably implies the formation of carboxyl groups or carboxyl radicals whose decomposition could yield carbon dioxide. Thus carbon dioxide production should be expected to occur concurrently or subsequent to olefin production in a ratio carbon dioxide/olefin not greater than unity. However, since carbon dioxide production generally exceeds that of olefin, there is probably a third ester decomposition reaction operating. The characteristics of the formation of the other main product, chain fragments, are similar to those of olefin and carbon dioxide so it may be that the production of these materials is part of a complex series of radical processes with a common initiation step. The formation of hydrogen, carbon monoxide, the corresponding methacrylate monomer and the development of color must also be accounted for.

DISCUSSION

Madorsky⁴ has suggested that, because little monomer is formed, the mechanisms of the thermal degradation reactions which occur in poly-(methyl acrylate) do not involve free radicals. Indeed, small ester molecules do not normally undergo bond scission to give free radicals at tem-

peratures below 400°C.^{5,6} In a polymer environment, however, and particularly when a radical stabilized by resonance or inductive effects can be formed, there is overwhelming evidence that free-radical mechanisms may operate below 300°C. Indeed, at temperatures above 280°C degradation mechanisms not involving radicals are rare.

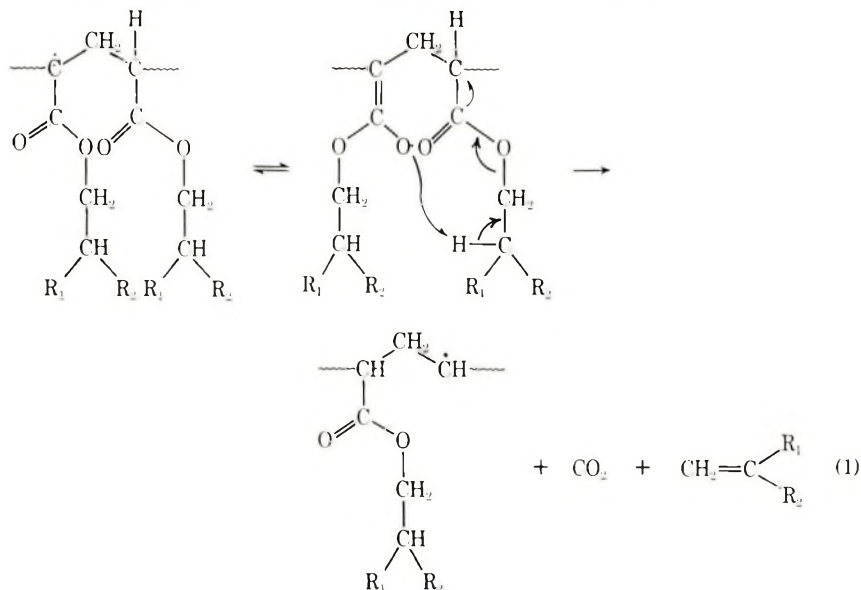
The initial step in the degradation of the primary polyacrylates is therefore likely to be scission at some unspecified point in the polymer molecule. Cameron and Kane⁷⁻⁹ suggest that these initially formed radicals would remove tertiary hydrogen atoms from the polymer backbone to give the relatively stable radical, I,



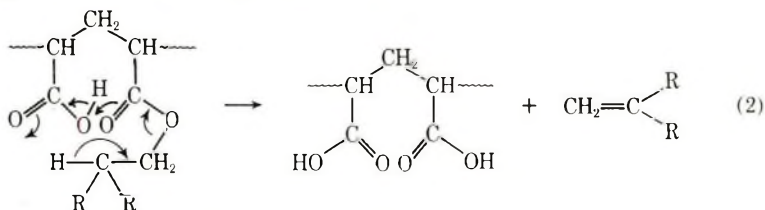
and that all the major decomposition reactions in poly(methyl acrylate) are initiated by this radical. Evidence that this theory may reasonably be extended to other poly(primary acrylates) is provided by their closely similar TVA thermograms (Figs. 1, 2, 3, 5, 6 in the previous paper¹) and the general comparabilities of their patterns of reaction products. It would be difficult to explain how such a variety of products could be formed in a one-stage process, as revealed by TVA, unless all the reactions have a common precursor.

Production of Olefin and Carbon Dioxide

Carbon dioxide and olefin are evolved from these polymers in a molar ratio close to unity, at least in the early stages of the reaction. It therefore seems probable that a reaction of the type (1) is operative.



There is no evidence for autocatalytic production of olefin so competition with reaction (1) by reaction (2), which was proposed by Grant and Grassie¹⁰ to account for the autocatalytic decomposition of poly(*tert*-butyl methacrylate), is assumed to be negligible.

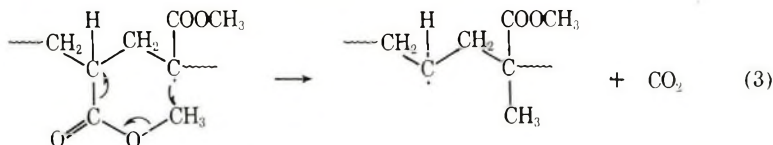


Although reaction (1) is represented as being catalyzed by a radical on a neighboring monomer unit, there is no reason why any available radical should not be the initiator.

Further evidence for reaction (1) is the fact that there appears to be a direct relationship between the production of olefin and the number of β -hydrogen atoms on the alkyl group. Thus the yield of olefin decreases in the order ethylene > propylene = 1-butene > 2-ethyl-1-hexene (Figs. 1-4) and the initial rates of production show a corresponding trend.

In the infrared spectrum of the residue from poly(2-ethyl-hexyl acrylate), a small peak is observed at 1810 cm^{-1} . This is indicative of anhydride structures so there may be some tendency for olefin elimination to occur unaccompanied by carbon dioxide production in this polymer. The carbonyl radical in reaction (1) may, for example, attack a neighboring ester unit to produce an anhydride ring and eliminate an alkoxy radical. This must be a minor reaction, however, and there is no evidence of anhydride formation from any of the other primary esters.

Carbon dioxide production exceeds that of olefin at longer reaction time. Reaction (3) represents a mechanism which may account for this. It was first suggested by Fox and his colleagues¹¹ and later used by Grassie and Torrance¹² and Cameron and Kane^{7,9} to explain the production of carbon dioxide in degradation systems involving methyl acrylate units.

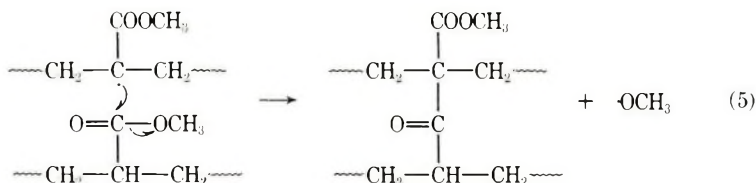
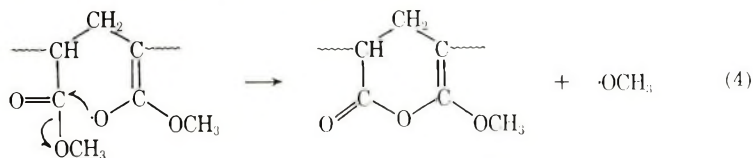


It is rather an unusual type of reaction, involving shift of an alkyl group, and it may therefore be thought to become less likely as the size of the alkyl group increases. This may explain why, in the present work, it is only observed at later stages of degradation and only in polymers which have developed insolubility. The restrictions on the movement of the side group which results from extensive crosslinking may tend to hold the alkyl group close to the polymer radical and hence encourage reaction. Previously,^{7,9,12} evidence for this reaction was provided by the existence of methyl meth-

acrylate monomer among the degradation products. In the present work, no corresponding α -substituted acrylate monomers were found although in each case a trace of the corresponding methacrylate was identified. It is believed that this may be due to reaction at chain terminal structures.

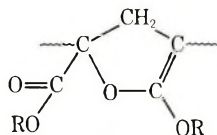
Production of Alcohol

Cameron and Kane⁷⁻⁹ have suggested four possible mechanisms for the production of a methoxyl radical from poly(methyl acrylate). Two of these are represented in reactions (4) and (5)



The other two involve formation of a ketene and of a vinyl ketone. The ketene-forming reaction was discounted in the present work because absorption was not detected at 2160 cm^{-1} in the infrared spectrum of the residual polymer. Similarly, only a very slight increase in absorption was observed in the $1695\text{--}1600\text{ cm}^{-1}$ region¹³ which is characteristic of the carbonyl of α,β -unsaturated ketones.

Reaction (4) produces a γ,δ -unsaturated δ -lactone ring system (intramolecular reaction) or an ester (intermolecular reaction) and reaction (5) produces a nonenolizable β -ketoester which can be in a six-membered ring (intramolecular reaction) or acyclic (intermolecular reaction). Although, at first sight, reaction (4) seems the less likely of the two, it receives strong support from infrared data. As shown in Figure 10, a shoulder develops at 1760 cm^{-1} which is at a higher frequency than most carbonyl absorptions and suggests the presence of a lactone. A β,γ -unsaturated γ -lactone (II) might be formed by radical coupling,



II

but this would absorb at rather higher frequency ($1805\text{--}1785\text{ cm}^{-1}$).¹³ The normal absorption for δ -lactones is $1750\text{--}1735\text{ cm}^{-1}$ but, with γ,δ -unsaturation in the ring, this would move to higher frequency so that the observed absorption at 1760 cm^{-1} agrees well with the product in reaction (4).

Carbon-carbon double bond absorption is normally much weaker than carbonyl absorption. However, in this case the polarity of the bond will be greater because of the presence of two carbon-oxygen bonds at one end and two carbon-carbon bonds at the other end. This should cause enhanced absorption in the carbon-carbon double bond region between 1680 and 1620 cm^{-1} . There is a general increase in absorption in this region as degradation proceeds but no clear peak can be distinguished. However, the carbonyl absorption overlaps into this zone at later stages of degradation so no firm conclusions about the structure can be drawn from absorption in this region.

The other route suggested for alcohol formation [reaction (5)] yields a saturated ketone which would absorb in the region 1720-1700 cm^{-1} . This is slightly lower than the absorption of ester carbonyl so that the presence of ketonic structures in the degradation residue may explain the shift in the carbonyl peak to lower frequency as degradation proceeds. This shift is observed in the residues from all the primary esters and is most marked in poly(ethyl acrylate) which would be expected to lose all of its ester groups at long times of degradation. Thus it may be concluded that there is strong infrared spectral evidence for lactone formation during degradation of poly(primary acrylates) while changes in infrared spectra are in accordance with, but do not prove, the formation of ketonic groups.

Shaw and Trotman-Dickenson¹⁴ found that methoxy radicals in the gas phase have a stability between that of a methyl radical and of a chlorine atom. In view of the known radical nature of many polymeric reactions, therefore, it seems not unreasonable that methoxyl radicals could be formed in a degrading polymer system at 315°C. It has also been shown¹⁵ that, in the gas phase, the alkoxy radicals have stabilities in the order $\text{CH}_3\text{O}\cdot > \text{CH}_3\text{CH}_2\text{O}\cdot > \text{CH}_3\text{CH}_2\text{CH}_2\text{CH}_2\text{O}\cdot > (\text{CH}_3)_2\text{CHCH}_2\text{O}\cdot$. Thus it may be expected that alcohol elimination reactions will be less likely to occur in polymers with fewer β -hydrogen atoms in the ester group, and this will account for the decreasing yield of alcohol in the primary acrylate polymers in the order ethyl $>$ *n*-propyl $>$ *n*-butyl $>$ 2-ethylhexyl (Figs. 1-4).

McBay and Tucker¹⁶ have shown that in solution, in the temperature range 110-155°C, the alkoxy radicals can react either by hydrogen abstraction from a solvent molecule to give alcohol or by disproportionation with another alkoxy radical to give equal yields of alcohol and aldehyde. Rust, Suebold, and Vaughan,¹⁵ studying the reaction of alkoxy radicals with cyclohexene in the gas phase at 195°C, showed that both hydrogen abstraction and disproportionation occur, and that the hydrogen abstraction/disproportionation ratio decreases in the order $\text{CH}_3\text{O}\cdot > \text{CH}_3\text{CH}_2\text{O}\cdot > \text{CH}_3\text{CH}_2\text{CH}_2\text{CH}_2\text{O}\cdot > (\text{CH}_3)_2\text{CHCH}_2\text{O}\cdot$. In the present work no aldehyde was recovered in spite of the fact that the tertiary hydrogen atoms in polyacrylates should be expected to be rather less reactive than the allylic hydrogens in cyclohexene. On the other hand, disproportionation of pairs of alkoxy radicals may be under strict diffusion control in the viscous polymer medium.

One striking feature of the production of alcohol is its apparent autocatalytic characteristics. The mechanisms proposed for alcohol production are all initiated by the same polymer radical (I) as are the other component parts of the overall reaction, and since no other part of the reaction is autocatalytic, there is no obvious direct chemical route by which the products of the alcohol elimination reaction might facilitate further production of alcohol. Alternatively, the answer may be associated with the changes in the physical nature of the polymer molecule brought about by elimination of alcohol. Both reactions (4) and (5) involve either the formation of a ring (when they occur intramolecularly) or of a crosslink (when they occur intermolecularly). These new structures would decrease the flexibility of the polymer molecules and this should be expected to encourage reactions involving six-membered rings such as those proposed for alcohol production [eqs. (4) and (5)], carbon dioxide production alone [eq. (3)] and intramolecular transfer, at the expense of reactions such as the production of olefin [eq. (2)] or the simultaneous production of olefin and carbon dioxide [eq. (1)] which involve ten-membered rings. This explanation of autocatalysis must be regarded as highly speculative, however, since no systematic investigation of the influence of chain flexibility, in isolation, on reactions in polymers has been reported.

Production of Short Chain Fragments and Chain Scission

The large amounts of chain fragments produced (Tables I-IV) and the rapid decrease in molecular weight (Table VI) indicate a considerable degree of chain transfer. Cameron and Kane^{7,8} suggested that intramolecular transfer predominates in the degradation of poly(methyl acrylate) since this favors the production of small chain fragments. They described as "unbuttoning" the process whereby a radical moves along the polymer chain eliminating small polymer molecules in contrast to "unzipping," in which monomer units are progressively eliminated as in the degradation of poly(methyl methacrylate). The main feature of interest in the "unbuttoning" reaction as it occurs in the present work is that it increases in importance, relative to the ester decomposition reactions, as the size of the alkyl group increases. There are probably two principal reasons for this.

Firstly, as the length of the alkyl group increases the polymer becomes less polar so that attractive forces between neighboring molecules, or segments of the same molecule, become smaller. Thus it is to be expected that with higher homologs, larger chain fragments will volatilize rather than be retained in the hot zone where further chain scission or ester decomposition may occur. That this factor is important is borne out by the data in Table V, which demonstrate that the molecular weight and even the chain length of the short chain fragment fraction increases with the length of the alkyl group.

Secondly, both the olefin and alcohol elimination reactions become less likely as the availability of the β -hydrogen atoms in the ester group de-

creases. This effect will increase the short chain fragment/ester decomposition product ratio as the number of β -hydrogen atoms decreases.

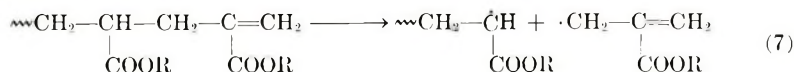
Crosslinking Reactions

Crosslinking certainly occurs in the ethyl, propyl, and butyl esters, which become insoluble, and may occur to some extent in the 2-ethylhexyl ester, although scission predominates since the polymer remains soluble. Crosslinking may be the result of radical coupling between adjacent chains or the intermolecular forms of the alcohol elimination reactions [eqs. (4) and (5)]. The residue is insoluble in alkali which would be expected to cause hydrolysis of the ester formed in reaction (4). On the basis of the experimental data available it is not possible to choose between the other two alternatives. Insolubility appears to develop faster in the lower homologs. This is probably a steric effect since the bulky ester groups should be expected to inhibit intermolecular reactions.

Minor Degradation Reactions

The residual polymer from all the poly(primary acrylates) becomes progressively more intensely colored as degradation proceeds. Unfortunately, all the good solvents for the polymer absorb in the ultraviolet region and no significant spectra could be found in the visible region. It is presumed, however, that the color is the result of conjugation involving principally carbon-carbon double bonds, but possibly also carbonyl groups. Carbon-carbon double bonds will be formed in the polymer as in reaction (4) or as a result of transfer. Once the first double bond is formed it will tend to weaken adjacent carbon-hydrogen bonds so that a reaction rather like the loss of hydrogen chloride from poly(vinyl chloride) will occur. Thus hydrogen will be liberated from sequences of adjacent acrylate units resulting in carbon-carbon conjugation in the polymer backbone. This kind of reaction has previously been discussed in some detail.¹² It certainly occurs in polyethylene¹⁷ polystyrene¹⁸ and methyl acrylate/methyl methacrylate copolymers¹² and it has been suggested that it may be a general reaction of ethylenic type addition polymers. These conjugated sequences do not appear to run to great length as there is no obvious bathochromic shift as degradation proceeds. Very little hydrogen is observed among the degradation products so that the reaction is comparatively unimportant.

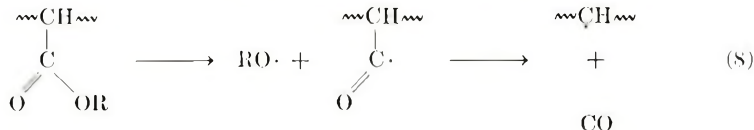
The presence of traces of the corresponding methacrylate monomer among the degradation products of each of the polymers cannot be accounted for in terms of the reaction suggested by Cameron and Kane⁹ to account for methyl methacrylate in the products of degradation of poly(methyl acrylate). A comparable reaction in poly(methyl acrylate), for example, would give methyl ethacrylate. It seems more likely that the methacrylates result from reactions at unsaturated chain ends [eq. (7)]



the bond β to the double bond being particularly vulnerable to attack.

From each polymer, acrylate is formed in rather greater amount than methacrylate and probably arises by depropagation from an acrylate terminated polymer radical although this is known to be only a very minor reaction in polyacrylates.

Carbon monoxide is another minor product from all the polyacrylates studied. It must obviously be derived from the ester group and the most likely source is through homolytic scission of the acyl-oxygen bond



The carbonyl radical is very unstable¹⁹ and will decompose immediately to give carbon monoxide.

One of the authors (J.G.S.) is grateful to the Science Research Council for a research scholarship.

References

1. N. Grassie and J. G. Speakman, *J. Polym. Sci. A-1*, **9**, 919 (1971) (Part I).
2. N. Grassie and D. R. Bain, *J. Polym. Sci., A-1*, **8**, 2653 (1970).
3. N. Grassie and D. R. Bain, *J. Polym. Sci., A-1*, **8**, 2665 (1970).
4. S. L. Madorsky, *Thermal Degradation of Organic Polymers*, Interscience, New York, 1964.
5. P. D. Ritchie, *Soc. Chem. Ind. Monograph*, "High Temperature Resistance and Thermal Degradation of Polymers," **13**, 107 (1961).
6. R. J. P. Allan, H. V. R. Iengar, and P. D. Ritchie, *J. Chem. Soc.*, **1957**, 2107.
7. G. G. Cameron and D. R. Kane, *J. Polym. Sci. B*, **2**, 693 (1964).
8. G. G. Cameron and D. R. Kane, *Makromol. Chem.*, **109**, 194 (1967).
9. G. G. Cameron and D. R. Kane, *Makromol. Chem.*, **113**, 75 (1968).
10. D. H. Grant and N. Grassie, *Polymer*, **1**, 445 (1960).
11. R. B. Fox, L. G. Isaacs, S. Stokes, and R. E. Kagarise, *J. Polym. Sci. A*, **2**, 2085 (1964).
12. N. Grassie and B. J. D. Torrance, *J. Polym. Sci. A-1*, **6**, 3303, 3315 (1968).
13. A. D. Cross, *Introduction to Practical Infrared Spectroscopy*, Butterworths, London, 1964.
14. R. Shaw and A. F. Trotman-Dickenson, *Proc. Chem. Soc.*, **1959**, 61.
15. F. E. Rust, F. H. Suebold, and W. E. Vaughan, *J. Amer. Chem. Soc.*, **72**, 338 (1950).
16. H. C. McBay and C. Tucker, *J. Org. Chem.*, **19**, 869, 1003 (1954).
17. S. Ohmishi, S. Sugimoto, and I. Nitta, *J. Polym. Sci. A*, **1**, 605 (1963).
18. N. Grassie and N. A. Weir, *J. Appl. Polym. Sci.*, **9**, 999 (1965).
19. H. W. Anderson and G. K. Rollefson, *J. Amer. Chem. Soc.*, **63**, 816 (1941).

Received September 1, 1970

Revised October 23, 1970

Thermal Degradation of Poly(alkyl Acrylates). III. A Secondary Ester: Isopropyl Acrylate

N. GRASSIE and J. G. SPEAKMAN,* *Department of Chemistry,
University of Glasgow, Glasgow W.2, Scotland*

Synopsis

A quantitative analysis of the products of the thermal degradation of poly(isopropyl acrylate) has been made principally by the application of GLC and mass and infrared spectrometry. The major products are carbon dioxide and propylene. The carbon dioxide/propylene ratio is very low in the initial stages but converges to approximately 0.6 late in the reaction. There is some tendency to autocatalysis in the production of propylene. Carbon monoxide and isopropanol are very minor products, and there is no chain fragment fraction as in the degradation products of the poly(primary acrylates). Changes in the infrared spectrum of the polymer during degradation are in accordance with the formation of these products and the products and reaction characteristics are accounted for mechanistically.

In the first paper of this series¹ it was demonstrated, principally by thermal analytical and spectroscopic methods, that there is a fundamental difference between the thermal degradation reactions which occur in a number of primary poly(alkyl acrylates) on the one hand and poly(isopropyl acrylate)—a secondary ester—on the other. The essentially identical nature of the reactions in all the primary esters was emphasized by the results described in the previous paper.² In the present paper a similar analysis of the products of reaction of the isopropyl ester is described and the mechanism of degradation discussed.

EXPERIMENTAL

The poly(isopropyl acrylate) was that described in the first paper of this series.¹ The degradation reaction was carried out at a standard temperature of 265°C, and the degradation and analytical techniques were exactly as described in the previous two papers.^{1,2}

RESULTS

Major Gaseous Products

Yields of carbon dioxide and propylene were measured as described in the previous paper. Results are presented in Table I. Figure 1 illustrates

* Present address: Department of Chemistry, University of Mainz, Mainz, West Germany.

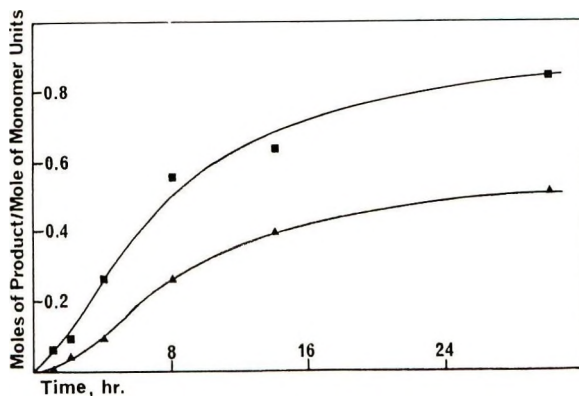


Fig. 1. Production of (▲) carbon dioxide and (■) propylene during degradation of poly(isopropyl acrylate).

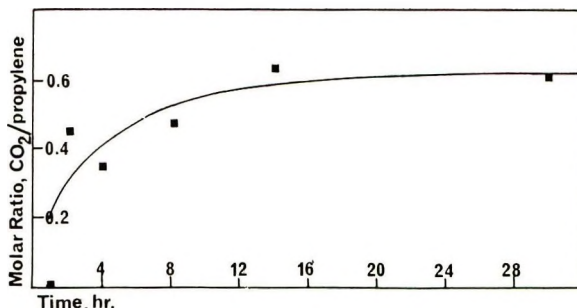


Fig. 2. Molar ratio carbon dioxide/propylene formed during degradation of poly(isopropyl acrylate).

the course of the reaction in terms of the proportions of monomer units involved. Figure 2 shows how the carbon dioxide/olefin ratio is very low in the initial stages of degradation and converges to approximately 0.6 later in the reaction. There is some tendency to autocatalysis in the production of propylene, but the effect is small compared with the same effect in poly(*tert*-butyl acrylate).^{3,4}

Minor Gaseous Products

A trace of material not condensable at -196°C was identified as carbon monoxide by the methods described in the previous paper.²

Liquid Degradation Products

A small amount of liquid product was recovered after long degradation times. Gas-liquid chromatographic (GLC) analysis on both dinonyl phthalate and Carbowax 20M columns gave a single peak with a retention time corresponding to isopropanol. Quantitative analysis demonstrates that there remains a substantial amount of liquid product not accounted for. This discrepancy is probably due to the presence of water.

TABLE I
Mass Balance Table for Degradation of Poly(isopropyl Acrylate) at 265°C
for Various Lengths of Time

	Products, wt-% of initial polymer					
	1 hr	2 hr	4 hr	8 hr	14 hr	30 hr
Residue	96.2	95.7	87.3	71.5	59.2	47.7
Insoluble	29.3	75.4	87.3	71.5	59.2	47.7
Soluble	66.7	20.3	0	0	0	0
Total liquids	0	0	0	1.4	1.6	1.6
Alcohol	0	0	0	0.3	0.3	0.3
Remaining liquids	0	0	0	1.1	1.3	1.3
Condensable gases	2.1	5.0	13.1	30.1	39.3	50.7
Carbon dioxide	0	1.5	3.6	10.0	15.6	19.7
Propylene	2.1	3.5	9.5	20.1	23.7	31.0
Noncondensables	0.1	0.1	0.1	0.2	0.3	0.4
Total volatiles	2.2	5.1	13.2	31.7	41.2	52.7
Total products	98.4	100.8	100.5	103.2	100.4	100.4

Residue

The polymer rapidly becomes insoluble and brittle during degradation and a yellow colouration develops. The amounts of soluble and insoluble residue at various degradation times are presented in Table I, and the weight loss can be almost completely accounted for by the amounts of carbon dioxide and propylene liberated. Infrared and NMR spectral measurements show that the soluble residue obtained at very short degradation times is not significantly different from the original polymer. Elemental analyses of the insoluble residue after 8 and 30 hr are presented in Table II. Yields of carbon dioxide and propylene suggest that after 30 hr degradation the residue should be essentially a terpolymer with a molar composition, isopropyl acrylate/acrylic acid/ethylene of 15.9/33.1/51.0. This ignores the possible formation of acrylic anhydride structures by elimination of water from pairs of acrylic acid units. The composition of the residue based on this estimate is also included in Table II.

TABLE II
Elemental Analysis of Poly(isopropyl Acrylate) Residues

Degradation time, hr	C, %	H, %	O, % (difference)
0	63.14	8.82	28.03
8	57.44	7.24	35.32
30 (measured)	64.60	6.01	29.39
30 (calculated)	63.3	8.8	27.9

With carbon dioxide and propylene evolved in the molar ratio $\text{CO}_2/\text{C}_3\text{H}_6 = 0.6$ the elemental composition of the residue should change very little, and, indeed, after 30 hr the composition of the residue is close to that of the original polymer. The lower ratio in the early stages of reaction is re-

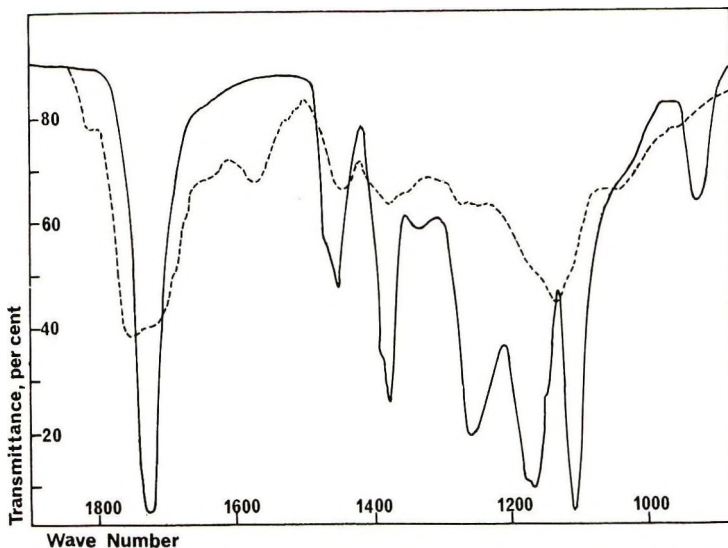


Fig. 3. The 900–1900 cm^{-1} region of the infrared spectra of (—) undegraded and (--) degraded poly(isopropyl acrylate).

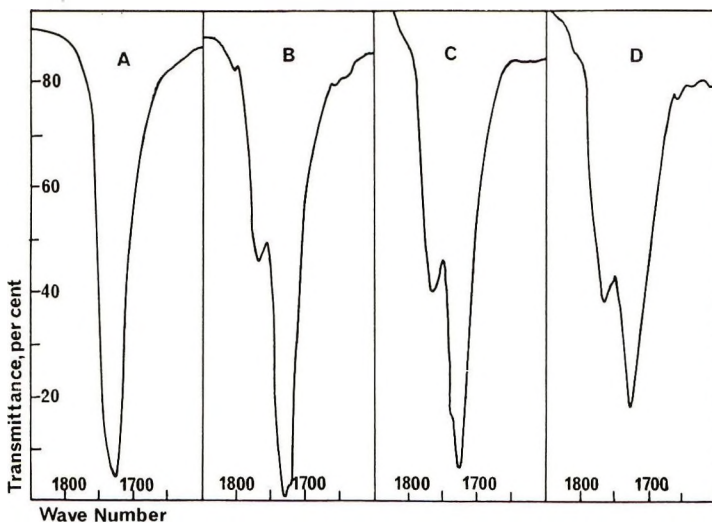


Fig. 4. Carbonyl region of the infrared spectrum of poly(isopropyl acrylate) during progressive degradation: (A) undegraded; (B) 4 hr; (C) 8 hr; (D) 14 hr.

flected in the higher carbon content after 8 hr. The low hydrogen content at long degradation times is surprising but may be related to the development of coloration.

A sample of the colored residue remaining after 30 hr was shaken with a mixture of benzene and 0.1M sodium hydroxide. The residue dissolved slowly in the aqueous layer, coloring it yellow.

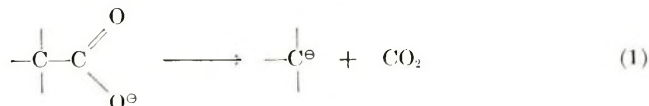
Infrared spectral changes during degradation are in accordance with ester group decomposition. Thus the absorption at 2980 cm^{-1} (C-H stretch in methyl groups) decreases faster than absorption at 2938 cm^{-1} (C-H stretch in methylene groups). The $1900\text{--}900\text{ cm}^{-1}$ region of the spectra of undegraded polymer and polymer degraded for 30 hr at 265°C are compared in Figure 3. Changes in the carbonyl region in the earlier stages of reaction are illustrated in Figure 4. A peak is seen to develop at 1762 cm^{-1} and a shoulder at 1810 cm^{-1} . Considerable changes also occur and a new peak develops at 1135 cm^{-1} in the C-O stretching region. After 14 hr a broad peak at 3400 cm^{-1} suggests the presence of water, and it is believed that the increased absorption between 1650 and 1550 cm^{-1} culminating in the appearance of a new peak at 1575 cm^{-1} after 30 hr is associated with the action of water on residual acid to produce carboxylate ion.

Preliminary Conclusions

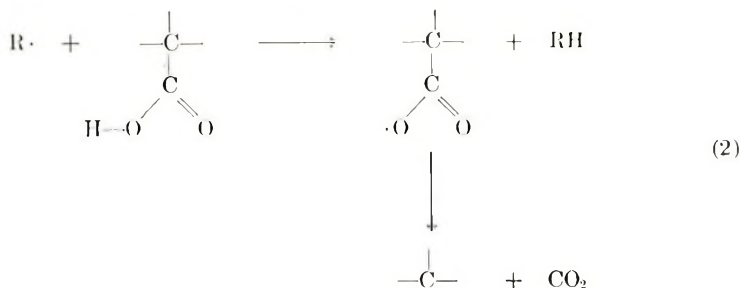
The products of degradation of poly(iso-propyl acrylate) at 265°C demonstrates that the principal reaction is ester decomposition which liberates propylene quantitatively and up to 60% of the theoretical yield of carbon dioxide. Cross-linking occurs simultaneously, resulting in rapid insolubilization of the residue. Comparatively, other reactions occur to a negligible extent in contrast to the behavior of the poly(primary acrylates).

DISCUSSION

The degradation characteristics of poly(iso-propyl acrylate) are quite different from these of the primary esters.² It degrades, for example, at a very much lower temperature and in a two-stage rather than a single-stage reaction.¹ The present paper is concerned primarily with the first stage. The major degradation product is the olefin and to this extent the reaction is similar to those of poly(*tert*-butyl acrylate)^{3,4} and poly(*tert*-butyl methacrylate).⁵ A non-radical molecular mechanism was proposed for ester decomposition in these two materials. On the other hand, Grassie and MacCallum⁶ proposed a radical mechanism for the ester decomposition reaction which occurs to some extent in poly(*n*-butyl methacrylate). No direct evidence is presented in this paper regarding the precise mechanism of the olefin elimination reaction but it may well be an example of a reaction in which the mechanism can vary, being molecular in absence of radicals but radical when radicals are available from accompanying reactions. Another example of this duality of mechanism which is relevant to the present discussion concerns the decarboxylation reaction. In small organic molecules in a polar medium, decarboxylation will usually occur by an ionic mechanism through the carboxylate ion,⁷



but in a nonpolar medium at higher temperatures a radical mechanism is considered more likely, as in reaction (2).



Although, as with poly(*tert*-butyl acrylate) and poly(*tert*-butyl methacrylate), quantitative yields of olefin are recovered and insolubility develops in the residue from poly(isopropyl acrylate), there are also considerable differences in behavior compared with the tertiary esters. Poly(isopropyl acrylate) decomposes only very slowly at 195°C, at which temperature the tertiary esters give high yields of iso-butene and water. Schaeffgen and Sarasohn⁴ found a molar ratio of isobutene to carbon dioxide of about 25/1 in the degradation products from poly(*tert*-butyl acrylate). Poly(iso-propyl acrylate) on the other hand, gives high yields of carbon dioxide. For example, after 30 hr at 265°C the molar ratio of propylene to carbon dioxide is 1.7/1, and by this time 84% of the alkyl groups have been eliminated as olefin and 51% of the carbonyl groups as carbon dioxide. The TGA thermogram¹ demonstrates that the rate of weight loss slows down after 59% volatilization. This corresponds closely to the loss of all the alkyl groups as olefin and 60% of the carbonyl groups as carbon dioxide. Water is also produced with a yield of about 8.0 mole-% after 30 hr, but this figure should be regarded as approximate since it was not estimated directly.

Grant and Grassie,⁵ Weir,³ and Schaeffgen and Sarasohn⁴ all observed autocatalytic behavior in the elimination of olefin from the tertiary butyl esters. They accounted for this by showing that the elimination of olefin is catalyzed by neighboring acid groups so that a chain reaction occurs in which sequences of adjacent ester groups decompose. They proposed the molecular mechanism shown in eq. (3).

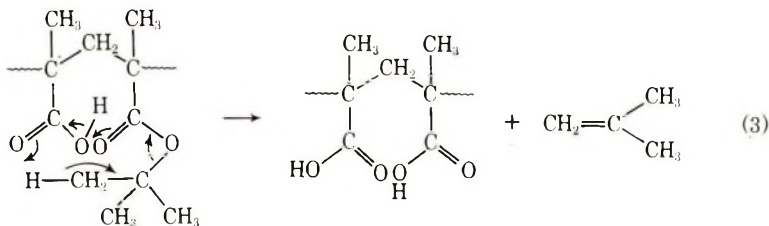
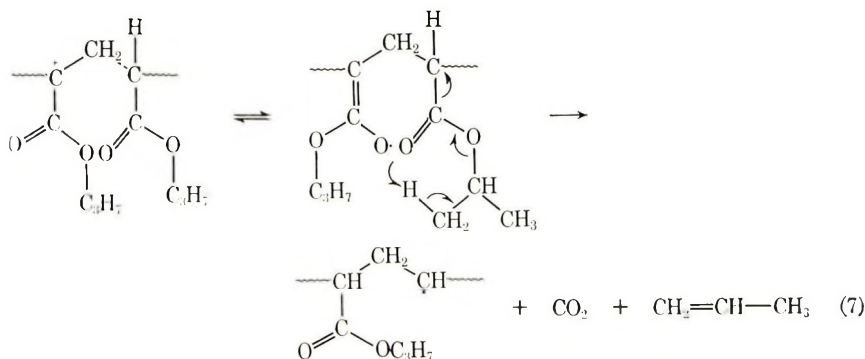


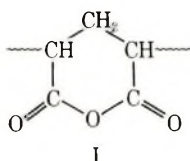
Figure 1 demonstrates similar behavior in poly(isopropyl acrylate), although it occurs to a very much smaller extent. This is not surprising,



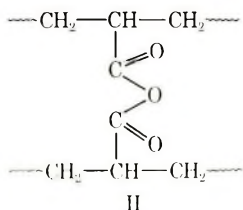
The acid groups formed in route 1 may remain unreacted in the residue, decompose to give carbon dioxide as in reaction (2) or couple with other acid groups on the same or another molecule to give anhydride structures, eliminating water and forming crosslinks.

The residue from poly(isopropyl acrylate) is insoluble in organic solvents, even polar solvents like dimethyl formamide (DMF), but soluble in sodium hydroxide solution. Uncrosslinked poly(methacrylic anhydride) is soluble in DMF.¹¹ It was therefore concluded that the development of insolubility in the isopropyl ester is probably due to crosslinking through anhydride groups. The data in Table I suggest that after 30 hr at 265°C the residual polymer has the following molar composition, isopropyl acrylate/2(acrylic anhydride)/acrylic acid/ethylene = 16/16/17/51. The factor of two associated with the acrylic anhydride units is due to the fact that one anhydride unit is derived from two original ester units.

The infrared spectrum (Fig. 3) is in good qualitative agreement with this estimate of composition. In association with their investigation of the degradation of poly(methacrylic acid) and the structure of the product anhydride, Grant and Grassie¹¹ studied the influence of anhydride structure on the position and magnitude of the twin carbonyl absorptions which are typical of all anhydrides. Using these two characteristics, they were able to distinguish in particular between succinic (five-membered ring), glutaric (six-membered ring) and butyric (acyclic) anhydrides. The carbonyl absorptions in Figure 3 occur at 1762 and 1810 cm^{-1} compared with those of glutaric anhydride at 1756 and 1802 cm^{-1} . In addition, the lower frequency absorption is more intense, an indication of cyclic rather than acyclic structures. Thus it is concluded that in the residue from poly(isopropyl acrylate) the anhydride structures are predominantly formed by reaction of adjacent units (I)

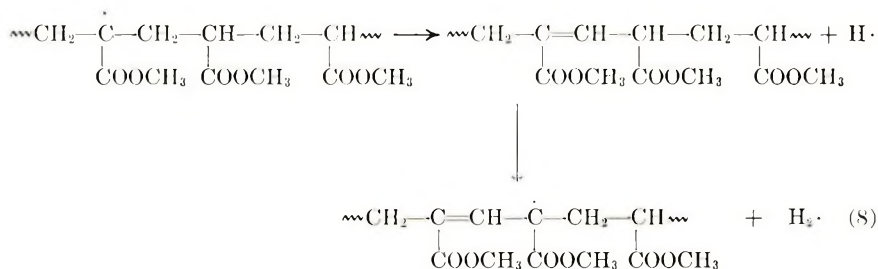


although it is necessary to assume a small proportion of intermolecular anhydride structures (II) to account for the development of insolubility.



Acid groups normally absorb in the carbonyl region at $1725\text{--}1700\text{ cm}^{-1}$.¹² The acrylic acid units remaining in the polymer could therefore account for the broadening towards lower frequency observed in the carbonyl absorption at 1730 cm^{-1} at long degradation times. The carboxyl ion peak at 1575 cm^{-1} is probably caused by ionization of acid groups by the sodium chloride disks or by hydrolysis of some anhydride or ester groups by traces of water.

In view of the rapid development of insolubility it was difficult to obtain satisfactory films for the measurement of ultraviolet or visible spectra for the investigation of the yellow coloration which develops during degradation. By comparison with the methyl methacrylate-methyl acrylate copolymer system coloration is believed to result from carbon-carbon conjugation in the polymer backbone as a result of the liberation of hydrogen in a radical chain process [eq. (8)].



It was previously suggested¹³ that this may be a general reaction in vinyl and acrylic polymers and may thus be used in the present instance as additional evidence for radical involvement in the reaction mechanism.

One of the authors (J.G.S.) is grateful to the Science Research Council for a research scholarship.

References

1. N. Grassie and J. G. Speakman, *J. Polym. Sci. A-1*, **9**, 919 (1971) (Part I).
2. N. Grassie, J. G. Speakman, and T. I. Davis, *J. Polym. Sci. A-1*, **9**, 931 (1971) (Part II).
3. N. Grassie and N. A. Weir, unpublished data.
4. J. R. Schaeffgen and I. M. Sarasohn, *J. Polym. Sci.*, **58**, 1049 (1962).
5. D. H. Grant and N. Grassie, *Polymer*, **1**, 445 (1960).
6. N. Grassie and J. R. MacCallum, *J. Polym. Sci. A*, **2**, 983 (1964).

7. E. S. Gould, *Mechanism and Structure in Organic Chemistry*. Holt, Rinehart and Winston, New York, 1965.
8. C. D. Hurd and F. H. Blunk, *J. Amer. Chem. Soc.*, **60**, 2419 (1938).
9. J. P. W. Houtman, J. van Steenis, and P. M. Heertjes, *Rec. Trav. Chim.*, **65**, 781 (1949).
10. A. MacColl, *J. Chem. Soc.*, **1958**, 3398.
11. D. H. Grant and N. Grassie, *Polymer*, **1**, 125 (1960).
12. A. D. Cross, *Introduction to Practical Infrared Spectroscopy*, Butterworths, London, 1964.
13. N. Grassie and B. J. D. Torrance, *J. Polym. Sci. A-1*, **6**, 3303,3315 (1968).

Received September 1, 1970

Revised October 23, 1970

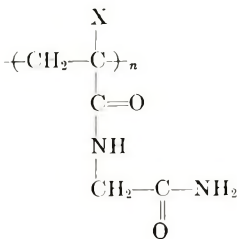
Synthetic Thermally Reversible Gel Systems. VII

HOWARD C. HAAS, RUBY L. MACDONALD, and
ALAN N. SCHULER, *Research Laboratories,*
Polaroid Corporation, Cambridge, Massachusetts 02139

Synopsis

Polymethacrylylglycinamides (PMG), like polyacrylylglycinamides (PAG), form thermally reversible aqueous gels, but higher molecular weights and/or concentrations are required and the melting points of the gels are lower. The heats of crosslinking for aqueous PMG gels fall in the range of -5 to -10 kcal/mole of crosslinks, the same as for aqueous PAG gels, implying that the crosslinks are chemically similar. PMG and PAG are incompatible with each other but both are individually compatible with some types of gelatin. The solubilities of PMG and PAG are similar. Various reagents, however, affect PMG and PAG gels in quite different manners. Aqueous PMG solutions, just outside conditions required for gelation, are rheopectic. Intrinsic viscosities $[\eta]$ of PMG in $2M$ NaCNS are about 2.5 times those in water. The Huggins' k' value for PMG in $2M$ NaCNS has a value of 0.39 – 0.40 , and both it and $[\eta]$ are essentially temperature-independent over the range 25 – 45°C . In water at 25°C for PMG, k' has an average value of about 1.4 . With increasing temperature, for H_2O , there is a considerable increase in $[\eta]$ which is accompanied by a decrease in the value of k' . Osmotic molecular weight measurements on unfractionated PMG in H_2O at 40°C yield π/c versus c plots having essentially zero slope, implying a value of close to zero for the second virial coefficient, a value of about 0.5 for the polymer-solvent interaction parameter, and a condition close to a θ condition. An approximate viscosity- \bar{M}_n relationship for polydisperse PMG is $[\eta]_{2M \text{ NaCNS}, 25^\circ\text{C}} = 1.7 \times 10^{-8} \bar{M}_n^{1.5}$. The low value of K and high value of the exponent do not result from large differences in polydispersity but rather from a stiff, rodlike configuration in solution. This steric hindrance to rotation also manifests itself in the extreme brittleness of PMG films and in a ΔH_p for homopolymerization of only -6 kcal/mole. The infrared spectra of MG monomer and PMG are recorded as well as the density and refractive index for PMG. PMG has a glass transition at 226°C by DTA and by TGA, thermal decomposition sets in at about 300°C . From copolymerization with acrylic acid, values of 1.66 and $+0.06$, respectively, were obtained for the resonance factor Q and the electrical factor e for MG monomer.

Previous papers in this series have been largely concerned with polyacrylylglycinamide¹ (PAG), where $X = \text{H}$ in the structural formula I,



I

Homopolymers, many copolymers and more complex interpolymers of acrylylglycinamide (AG) form thermally reversible aqueous gels. Similarly, polymethacrylylglycinamide (PMG), where $X = CH_3$, is also capable of forming thermally reversible gels in water. It is well known that an α -methyl group can greatly influence the polymerization behavior of a monomer and the properties of the resulting polymer. This paper describes a preliminary investigation of PMG with the ultimate aim of understanding the effect of α -methyl substitution on dilute solution properties and thermally reversible gel formation in this polymer class.

The preparation of PMG homopolymers is described and the infrared spectra of the monomer and polymer are given. Heats of polymerization of AG and MG have been measured. The density, refractive index, solubilities and results of DTA and TGA measurements on PMG are also reported. Copolymerization of MG with acrylic acid has been studied, and the r_1, r_2 values for this system and Q and e value for MG calculated. Dilute solution viscosity behaviors of PMG in H_2O and $2M$ NaCNS are compared, and an approximate molecular weight-viscosity relationship for polydisperse PMG was obtained by osmometry. By measuring the melting points T_m of aqueous thermally reversible PMG gels, a value was obtained for the heat of crosslinking, ΔH_c . The qualitative effects of various reagents on PMG gels are presented. Other observations are made on the compatibility of PMG with PAG and with gelatin and on the gelation behavior and rheological properties of PMG solutions.

Preparation of PMG Homopolymers

Methacrylylglycinamide (MG) was synthesized by reacting methacrylyl chloride with glycinamide.¹ Somewhat better yields are obtained if methacrylic anhydride is used, particularly when it is reacted with glycinamide which has been liberated from its hydrochloride with sodium methoxide in methanol at a low temperature. Pure MG, obtained by several recrystallizations from 10:1 acetone-methanol has a melting point of 139–140°C. Its infrared spectrum (KBr pellet) is given in Figure 1.

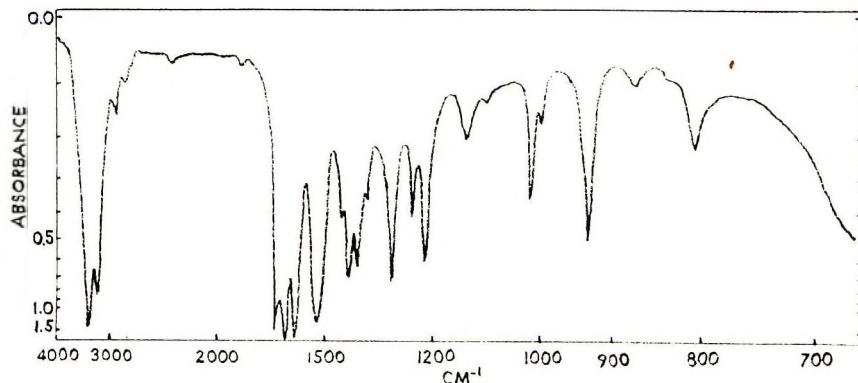


Fig. 1. Infrared spectrum of methacrylylglycinamide monomer (MG).

MG can be conveniently polymerized in aqueous solutions using the thermal decomposition of $K_2S_2O_8$ for initiation. Samples of PMG for this investigation were made using the conditions and amounts of reagents specified in Table I. All polymerizations were carried out in glass tubes which were frozen and then alternately evacuated and flushed with nitrogen three times before they were finally sealed off under vacuum. Various polymerization temperatures and amounts of isopropanol were used to obtain different molecular weight homopolymers.

TABLE I
Homopolymerization of MG Monomer

Sample	Mono- mer, g	Water, ml	Isopro- panol, g	Initiator, ml ^a	Polymerization temp, °C	Time, hr	Yield, g
1	10.0	40.0	20.0	10	75.0 ± 0.1	3 ³ / ₄	6.4
2	10.0	50.0	8.0	10	"	"	7.1
4	10.0	58.5	1.5	10	"	"	7.5
5	10.0	60.0	0	10	"	"	7.8
9	10.0	60.0	0	10	50.0 ± 0.1	21	7.5
10	10.0	60.0	0	10	25.0 ± 0.1	50	Insol.
11	10.0	60.0	0	10	60.0 ± 0.1	21	7.8

^a A solution of 0.100 g of $K_2S_2O_8$ in 100 ml H_2O .

After polymerization, the tubes were opened, if necessary the contents diluted with water, and the polymers isolated by precipitation into methanol. The PMG homopolymers were purified by reprecipitation from water into methanol followed by washing with warm methanol and drying under vacuum overnight at 35°C. Sample 10 swells but is insoluble in water and hot dimethylsulfoxide. In this respect, the behavior of MG is similar to that of AG, which often produces crosslinked polymers if polymerized in the absence of alcohol. The tendency for the formation of insoluble polymers is much greater with AG, however, as evidenced by the fact that PMG samples 5, 9, and 11 are water-soluble. Analysis of a typical sample of PMG gave: C, 50.43%; H, 7.12%; N, 18.84% (theory: C, 50.70%; H, 7.09%; N, 19.70%). As with PAG, nitrogen analyses below the theoretical value² are generally obtained. An infrared spectrum of PMG (cast from H_2O on an AgCl disk) is given in Figure 2.

By using the Model 900 duPont differential thermal analyzer and a heating rate of 20°C/min, the heat of polymerization ΔH_p of MG was found to be -5.5 ± 0.6 kcal/mole (20% MG in dimethylformamide containing 0.5% benzoyl peroxide based on monomer) and -6.1 ± 0.6 kcal/mole (20% MG in dimethyl sulfoxide containing 1% azobisisobutyronitrile based on monomer). Under similar conditions, values obtained for the homopolymerization of acrylylglycinamide are -17.7 ± 0.8 and -20.6 ± 1.2 kcal/mole. The low value of ΔH_p for MG is characteristic of a 1,1-disubstituted ethylene which yields a very sterically hindered polymer.

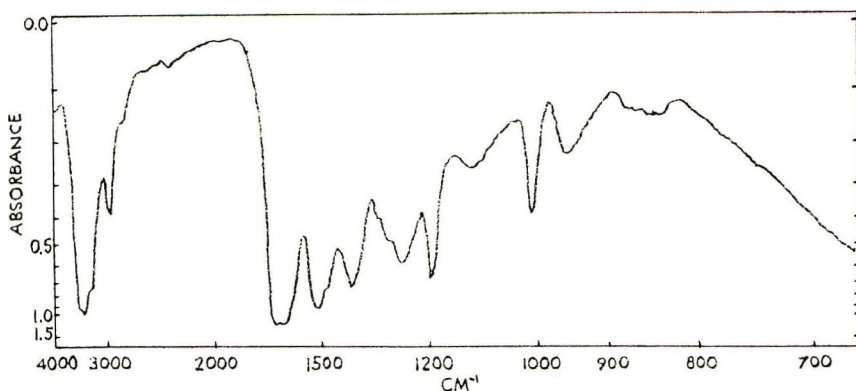


Fig. 2. Infrared spectrum of polymethacrylylglycinamide (PMG).

Properties of PMG Homopolymer

PMG is a colorless polymer very similar in appearance and solubility to PAG. It is soluble in H_2O , aqueous 2*M* NaCNS, hot dimethyl sulfoxide, and hot glacial acetic acid. It is considerably swollen by warm pyridine and *m*-cresol and is insoluble in the lower alcohols, acetone, dimethylformamide, and tetrahydrofuran.

Films of PMG cast from water on to glass or polyester are very brittle, considerably more so than those of PAG. A film of PMG cast on a mercury surface was used to determine the density at 25°C by a suspension method in carbon tetrachloride-hexane. The value obtained, 1.346 g/cc, is below that of PAG ($d = 1.378$ g/cc).³ The refractive index of PMG is 1.555, compared to $n_D^{25} = 1.542$ for PAG.²

By employing a Model 900 duPont differential thermal analyzer, identical DTA profiles were obtained on PMG samples 9 and 11 of Table I. The samples were measured as dry powders under a nitrogen atmosphere and with a heating rate of 10°C/min. A glass transition is found at 226°C. TGA indicates that a stepwise thermal decomposition begins at about 300°C. The T_g of PAG was found to be 182°C with thermal decomposition setting in at 260°C³ (cf. Fig. 3).

Some polymer-polymer compatibility experiments have yielded the following results. When a 10% aqueous solution of gelatin (Atlantic, bloom 225, pH = 4.6) is mixed with a 10% solution of PMG (sample 9), a hazy one-phase solution or gel (depending on the temperature) results. On drying, a film is obtained which, except for a slight haze, appears to be a compatible mixture of the two polymers. When 10% solutions of PMG and PAG are mixed there is considerable haze and accompanying phase separation and the appearance of the resulting dry film shows that the two polymers are distinctly incompatible.

An interesting property of some PMG samples deserves comment. It has been observed that when some viscous aqueous solutions of PMG (just outside conditions required for gelation) are stirred, they increase in vis-

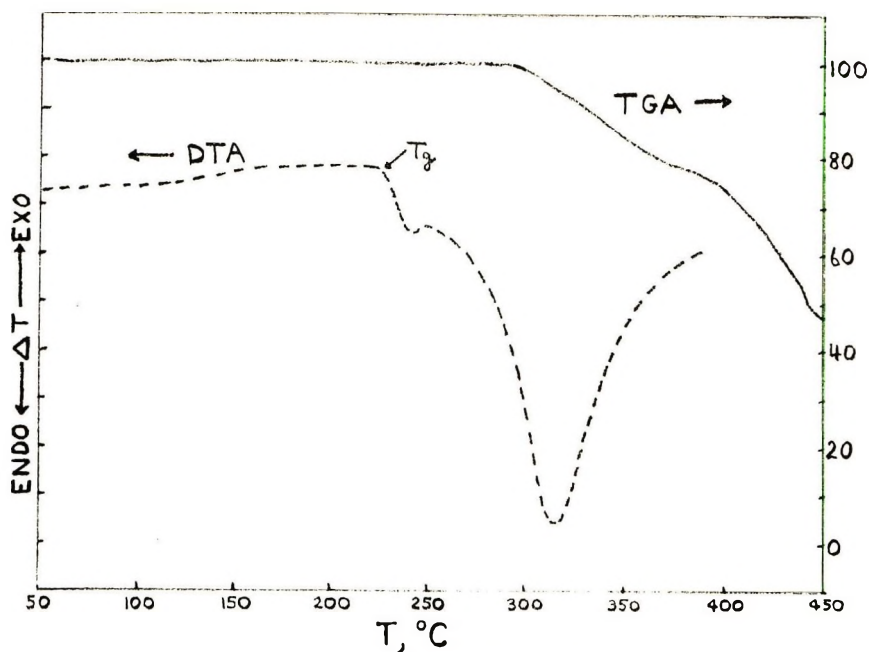


Fig. 3. Differential thermal and thermogravimetric analyses on PMG.

cosity and set to a gel. Gelation seems to be accompanied by an increase in haze. In qualitative experiments, the viscosity increase and subsequent gelation appear to occur at constant shear rate and a finite time is required for reversion. Following current terminology,⁴ the system is rheopectic. The PMG solutions have the stringiness which, according to Pryce-Jones,⁵ necessarily indicates dilatancy. Dilatancy, a somewhat similar phenomenon, an increase in viscosity with increasing rate of shear with no time dependency, has been explained⁶ as follows. During shear, the collision frequency between groups of different polymer molecules increases, causing the formation of local networks and ultimately a gel. It is believed that an increase in collision frequency as well as perhaps a change in molecular dimensions as a result of shear could also be invoked to explain rheopecty.

Aqueous Thermally Reversible PMG Gels

Depending on such factors as molecular weight, concentration, and temperature, aqueous solutions of PMG will form thermally reversible gels. PMG does not form gels as readily as PAG; in general, higher concentrations and/or molecular weights are required, and the melting points of the resulting gels are lower. When an attempt was made to use sample 4 to measure ΔH_c , very viscous hazy aqueous solutions resulted on cooling, rather than sharp-melting gels. Aqueous gels of PAG or PMG, like gelatin, can be clear or slightly hazy. This haze generally disappears with increasing temperature and when the temperature is lowered, the haze increases.

With decreasing temperature the order of development of haze is PMG \gg PAG $>$ gelatin. The presence of NaCNS in small quantities decreases the amount of haze in PAG and PMG gels.

To study the effect of various reagents on gelation, a 5% aqueous solution of PMG (sample 9) was prepared and allowed to gel at room temperature. The different reagents (in amounts specified in Table II) were stirred into 1.5 ml. of the gel and the effect observed at room temperature and after cooling to approximately 0°C.

TABLE II
Effect of Reagents on PMG Gels

Reagent added	Gelation state	
	At room temperature	After cooling to 0°C
H ₂ O (12 drops)	Gel dissolves	Gel re-forms
Acetic acid, glacial (12 drops)	Gel dissolves	Gel re-forms
Formic acid, glacial (12 drops)	Gel dissolves	Gel re-forms
Aqueous 10% NaOH (7 drops)	Gel dissolves	Gel re-forms
Hydroquinone solid		
Small amount	No effect	—
Large amount	Gel dissolves	Gel re-forms
NaCNS solid, small amount	Gel dissolves	Gel re-forms
Urea, solid	No effect	—
Phenol	Gel dissolves	Gel re-forms
MG monomer, solid	Gel dissolves	Gel re-forms
1M Hg(acetate) ₂ , several drops	Immediate ppt.	—
1M solutions of BaCl ₂ , ZnSO ₄ , AgNO ₃ , CrCl ₃ , CoCl ₂ , FeCl ₃ or NaCl (12 drops)	Gel dissolves	Gel re-forms
1M Al ₂ (SO ₄) ₃ (12 drops)	Gel contracts; syneresis	—

Some similarities and some interesting differences exist between the behaviors of PAG² and PMG gels toward different substances. In general, the tendency of a dissolved gel to re-form on cooling appear greater in the case of PMG, but since the experiments are qualitative and gel formation is so dependent on concentration, \bar{M}_w , etc., this cannot be said with certainty. A similarity is that addition of water, glacial acetic acid, formic acid, many aqueous salt solutions, and solid NaCNS cause both PAG and PMG gels to revert at room temperature to viscous liquids. Also with both gels, mercuric acetate causes immediate precipitation and Al₂(SO₄)₃ results in a stiffening of the gel accompanied by syneresis. Urea, which disrupted a PAG gel, has little effect on a PMG gel; phenolic reagents (phenol and hydroquinone), which dissolve a PMG gel, cause the formation of a precipitate with PAG. Aqueous alkali and MG monomer dissolve PMG gels, whereas AG and aqueous alkali result in PAG gels becoming more rigid. No attempt will be made here to explain these results, since each specific reagent-

polymer interaction would have to be studied and individually understood. Similarly, opposite effects have been observed between the homopolymers of acrylic (PAA) and methacrylic (PMA) acids when various reagents have been added to dilute solutions of these polymers.⁷ The observed changes in reduced specific viscosity are interpreted in terms of intramolecular bonding. Urea, for example, decreases the viscosity of PMA and increases that of PAA. In a way this parallels the effect that urea has on PMG and PAG gels. A recent paper⁸ discusses the zwitterion character of aqueous urea and how it mechanistically disrupts both hydrogen and hydrophobic bonding. The effect of various additives on the ability to form gels of alginic acid, acrylic acid-acrylic ester copolymers, and phthalated ethyl cellulose has been studied by Yudelsohn and Mack.⁹

The melting points of aqueous gels of sample 9 and of another sample of PMG prepared from monomer which was synthesized by the vinyl azlactone method¹⁰ were measured. The gels were conditioned in a refrigerator at 6°C for 18 hr prior to measurement, which was carried out as described previously.² The melting point data are given in Table III. PMG gels, when cooled to 6°C, become very hazy and some syneresis occurs; as a probable result there is some scatter in the data, particularly in that of sample 9. Heats of crosslinking were obtained from $\log c$ versus $1/T_m$ plots following the thermodynamic treatment of Eldridge and Ferry,¹¹ which predicts that for thermally reversible gels

$$\log c = (\Delta H_c / 2.303RT_m) + \text{constant} \quad (1)$$

TABLE III
Melting Points of Aqueous PMG Gels

Sample 9		PMG (azlactone method)	
Concn, g/l.	T_m , °C	Concn, g/l.	T_m , °C
40	24.7	40	10.6
60	26.3	60	21.8
80	35.5	80	29.3
100	40.1	100	34.6
$\Delta H_c = -6.1$ kcal/mole		$\Delta H_c = -9.2$ kcal/mole	

The values obtained for ΔH_c for aqueous PMG gels fall within the range of -5 to -12 kcal/mole of crosslinks obtained previously^{2,3} for aqueous PAG gels. It is probable, therefore, that the nature of the thermally reversible crosslinks in both gels are similar, and that like PAG, PMG gels are noncrystalline. A heat of crosslinking of -8 ± 0.4 kcal/mole crosslinks has been obtained for aqueous thermally reversible gels of phthalated ethyl cellulose and ethyl acrylate-acrylic acid copolymers.⁹ These amorphous polymers would also be expected to yield noncrystalline gels containing relatively noncomplex thermally reversible crosslinks.

Dilute Solution Behavior of PMG

Dilute solution viscosity measurements were made on the samples of Table I with water, aqueous 2*M* NaCNS, and dimethylsulfoxide (DMS) as solvents. The measurements were made at 25°C by employing a Cannon-Ostwald-Fenske viscometer. Solvent flow times were in excess of 100 sec. Intrinsic viscosities were obtained from η_{sp}/c plots by extrapolation to zero concentration and Huggins' k' values¹² were obtained from the slopes. These results are presented in Table IV and the water and thiocyanate data in Figures 4 and 5.

Intrinsic viscosities in 2*M* NaCNS are considerably higher than those in water. With PAG, this is true for low and medium \overline{DP} polymers but with very high \overline{DP} polymers, aggregation even in dilute solution results in higher values for $[\eta]$ in H₂O than in 2*M* NaCNS.¹³ Huggins' k' values for PMG in 2*M* NaCNS are characteristic of flexible polymers in a thermodynamically good solvent. Water is not a good solvent for either PMG or PAG, but for PAG, k' for water is close to zero whereas for PMG very high values

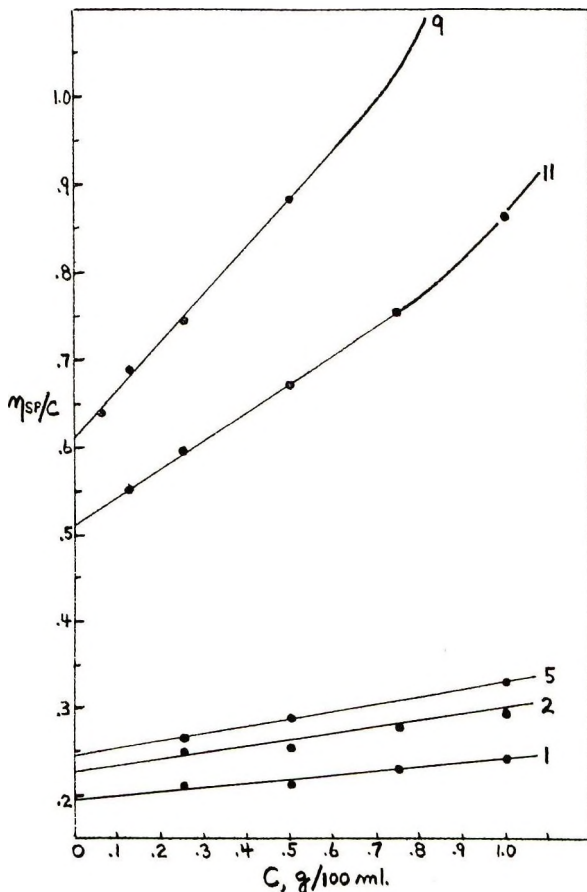


Fig. 4. Dilute solution viscosity behavior of PMG samples in H₂O, 25°C.

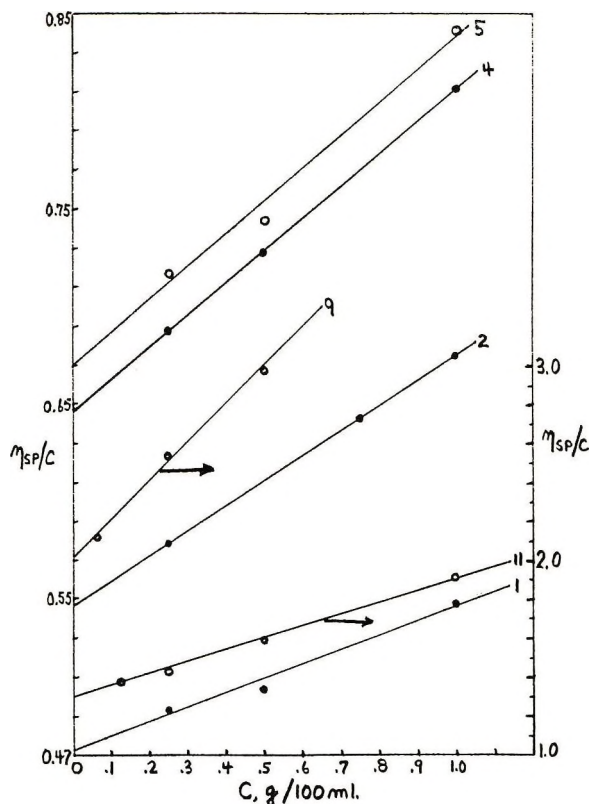


Fig. 5. Dilute solution viscosity behavior of PMG samples in 2M NaCNS, 25°C.

are obtained. This is another example where for polar polymers there is little correlation between k' and solvent power,¹⁴ particularly when large differences in rigidity can also be present. Intrinsic viscosities in dimethyl sulfoxide are somewhat higher than those in 2M NaCNS, and the k' values are comparable. What is surprising is that sample 11 has a value for $[\eta]$ of 3.4 in dichloroacetic acid, a solvent which effects the helix-coil transition in synthetic polypeptides.

TABLE IV
Dilute Solution Viscosity Behavior of PMG, 25°C

Sample	Water		2M NaCNS		DMS	
	$[\eta]$, dl/g	k'	$[\eta]$, dl/g	k'	$[\eta]$, dl/g	k'
1	0.196	1.22	0.473	0.335	0.67	0.356
2	0.228	1.38	0.547	0.431	—	—
4	—	—	0.646	0.397	—	—
5	0.248	1.40	0.670	0.374	0.91	0.435
11	0.512	1.22	1.30	0.361	1.62	0.339
9	0.612	1.50	2.02	0.486	—	—

Intrinsic viscosities of PMG (sample 9) have been measured in H₂O and 2*M* NaCNS at various temperatures. These data are given in Table V.

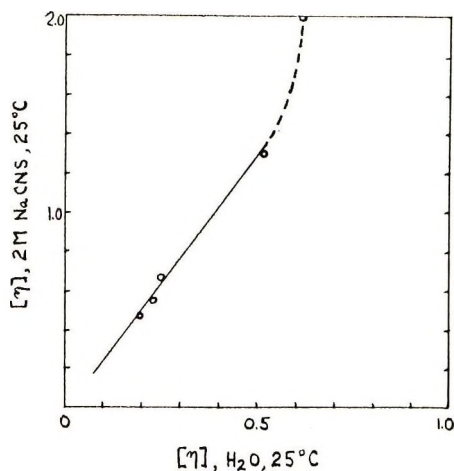
TABLE V
Temperature Dependence of Viscosity for PMG

Temp, °C	H ₂ O		2 <i>M</i> NaCNS	
	[η], dl/g	k'	[η], dl/g	k'
25	0.62	1.61	2.24	0.405
35	0.93	1.04	2.30	0.386
40	1.12	0.73	2.33	0.390
45	1.21	0.71	2.33	0.401

For water, the large increase in [η] with increasing temperature and the relative insensitivity of [η] in thiocyanate to temperature are additional evidence that water is a poor and thiocyanate a good solvent for PMG. PAG shows an increase in [η] in both solvents with the larger increase being found with water. The Huggins' k' value for PMG in 2*M* NaCNS is temperature-independent, which is the generally observed behavior. The very high value of k' for H₂O at 25°C and its large temperature dependence is usually found when aggregation is present. This would appear superficially contrary to the observation that much higher viscosities are found in 2*M* NaCNS, but Morawetz¹⁵ points out that the type of aggregate formed determines whether [η] decreases, increases, or remains unchanged. The very low value of k' in H₂O for PAG and its temperature independence as well as the temperature dependence of k' for PAG in 2*M* NaCNS are difficult to understand. If k' results are interpreted in the light of generally observed behavior¹⁶ regarding aggregation, one would expect PMG to form gels more readily than PAG, and this is opposite to the observed behavior. When [η]_{2*M* NaCNS} is plotted against [η]_{H₂O} for 25°C (Fig. 6), a reasonably linear relationship is obtained for the four lower \overline{DP} samples, with sample 9 falling off the plot. The intrinsic viscosities in 2*M* NaCNS at 25°C are 2.5 times those in H₂O.}}

Number-average molecular weights have been obtained on samples 1, 2, 5, and 11 by membrane osmometry.* Previous osmotic measurements on PAG³ with 2*M* NaCNS as the solvent involved so many difficulties, including pitting of the stainless steel parts of the osmometer, that we decided this time to use water. Triton X-100 (1%) was added to the water to improve wetting. A Schleicher and Schuell Co. B-19 membrane was employed. A temperature of 40°C was selected for the measurements, since at this temperature k' has essentially leveled off, and osmotic measurements on gelatin¹⁷ show it to be molecularly dispersed at 38°C. Low osmotic pressures coupled with somewhat unstable membrane dissymmetries in water have resulted in scatter in the π/c versus c plots (see Fig. 7), and the extrapolated data of Table VI are based on 3 out of 4 concentrations.

* Measurements by DeBell and Richardson, Inc., Hazardville, Conn. 06036.

Fig. 6. Plot of intrinsic viscosities in H_2O vs. $2M$ NaCNS, 25°C .TABLE VI
Osmotic Pressure Data and \bar{M}_n for PMG Homopolymers

Sample	$[\eta]$, dl/g		π/c ($c \rightarrow 0$), ml-atm/g	$\bar{M}_n \times 10^{-3}$
	H_2O , 25°C	$2M$ NaCNS, 25°C		
1	0.196	0.473	0.285	90.2
2	0.228	0.547	0.245	105.0
5	0.248	0.670	0.225	114.0
11	0.512	1.30	0.145	177.0

There is also some scatter among the slopes of the π/c versus c plots (Fig. 7) but the general flatness indicates that the second virial coefficient is very close to zero and the polymer solvent interaction parameter is about 0.5. Water at 40°C is close to being a θ solvent for PMG.

In Figure 8 the log-log plots of $[\eta]$ (H_2O , 25°C) and $[\eta]$ ($2M$ NaCNS, 25°C) versus \bar{M}_n are presented for PMG. A plot of $\log [\eta]$ ($2M$ NaCNS, 25°C) versus \bar{M}_n for PAG³ is included for comparison. Equations which relate $[\eta]$ and \bar{M}_n are:

For PMG:

$$[\eta]_{\text{H}_2\text{O}, 25^\circ\text{C}} = 0.68 \times 10^{-8} \bar{M}_n^{1.5} \quad (2)$$

$$[\eta]_{2M \text{ NaCNS}, 25^\circ\text{C}} = 1.7 \times 10^{-8} \bar{M}_n^{1.5} \quad (3)$$

For PAG:

$$[\eta]_{2M \text{ NaCNS}, 25^\circ\text{C}} = 1.30 \times 10^{-3} \bar{M}_n^{0.52} \quad (4)$$

There is some question as to whether PMG in H_2O at 25°C is molecularly dispersed, so the viscosity-molecular weight relationship for water should be taken with reservation. The high k' for PMG in water and its large tem-

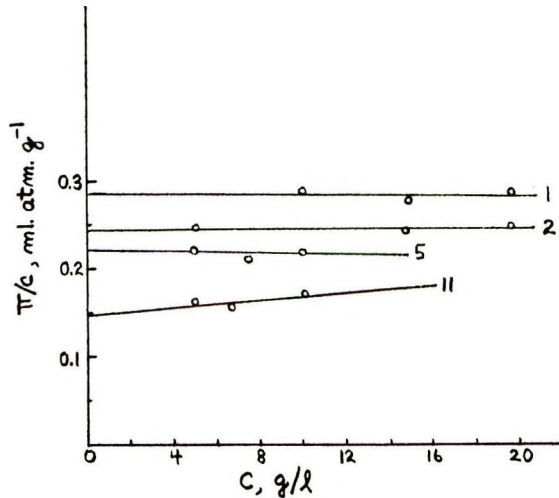


Fig. 7. Dilute solution osmotic pressure data for PMG samples, H₂O, 40°C.

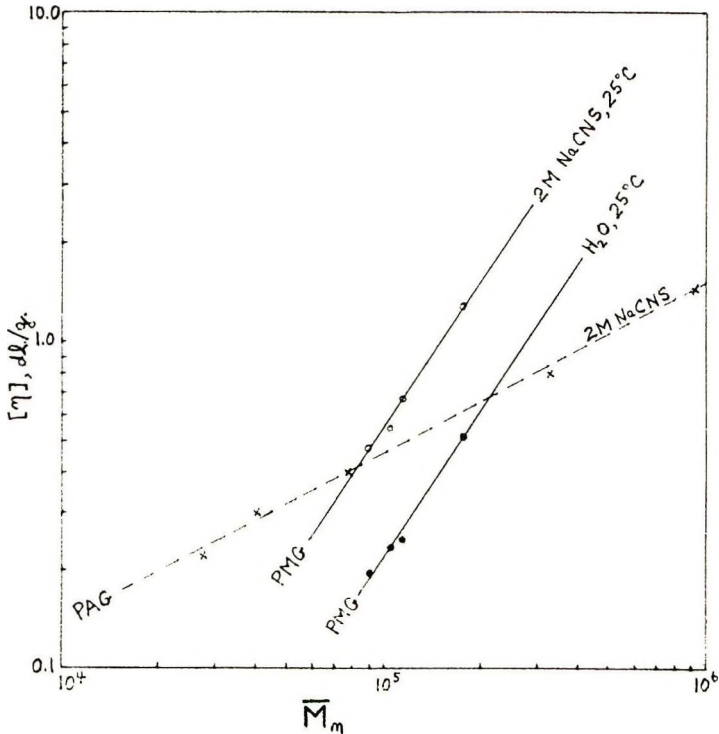


Fig. 8. Plots of $\log [\eta]$ vs. $\log \bar{M}_n$ for PAG and PMG.

perature dependence may indicate aggregation. On the other hand, the much larger intrinsic viscosities in 2M NaCNS, the increase in $[\eta]$ for water with temperature, and the reasonably good linearity of the plot of $\log [\eta]$ versus $\log \bar{M}_n$ plot for water argue against aggregation. The very high val-

ues for the exponents which almost approach those obtained for helices^{18,19} also require discussion. Equations (2)–(4) were obtained on unfractionated polymers and are therefore only approximate expressions. Accurate values for K and a can be obtained only if the molecular weight distributions for all of the samples are the same. If the distributions of higher molecular weight samples are broader than those of lower \overline{DP} and molecular weights are expressed as number averages, the value of a will be too high and that of K too low. This may contribute to some extent to the value of 1.5 which we have obtained, but we do not believe it to be the main cause for the high value of the exponent. All of the PMG samples were prepared in much the same manner so that we would not expect grossly different distributions. Furthermore, measurements on polydisperse PAG samples where chain transfer with monomer and/or polymer seems to be more prevalent and could lead to even broader distributions of molecular weight at high \overline{DP} gave an exponent of only 0.52 [cf. eq. (4)] and a very typical value for K . Values similar to those we observe for PMG are not unheard of. Values of 1.25–1.35 for a and 1.1 to 4.4×10^{-8} for K are reported for poly-*N-p*-carboxyphenylmethacrylamide).²⁰ It is not unreasonable that for PMG

the steric hindrance to rotation resulting from the α -methyl and $-\overset{\text{O}}{\parallel}{\text{C}}-\text{CH}_2-\text{CONH}_2$ groups could lead to a stiff, rodlike configuration in solution. This would account for the extreme observed brittleness of PMG in the solid state and for the low heat of homopolymerization. The larger excluded volume associated with a rodlike configuration compared to a more spherical configuration for a particle of the same molecular weight could result in fewer intermolecular interactions and other conditions being equivalent explain the decreased tendency of PMG to form gels when compared to PAG and also the lower melting points of the PMG gels.

If the $[\eta]-\overline{M}_n$ relationship for water is realistic, it is indeed unusual to have a situation where two different solvents yield the same value for a yet show vastly different intrinsic viscosities. It is probably fortuitous, but if it is assumed that two CNS⁻ anions are associated with each difunctional amide side chain of PMG and this new effective molecular weight substituted into eq. (2), the calculated $[\eta]$ for H₂O is almost identical with that measured in 2*M* NaCNS. This would not explain the much higher viscosities in DMS compared to water. Viscosity results for DMS lead to value of 1.27 for a . We do not discount entirely the possibility that PMG in solution exists in some partially helical conformation. We are now preparing polymethacrylyl-1-alaninamide to determine whether there might be some abrupt change in optical rotation as a result of a conformational helix-random coil change.

Copolymerization of MG

Copolymerization of MG (monomer 2) and acrylic acid (monomer 1) has been studied at 60°C. The data are presented in Table VII. All copoly-

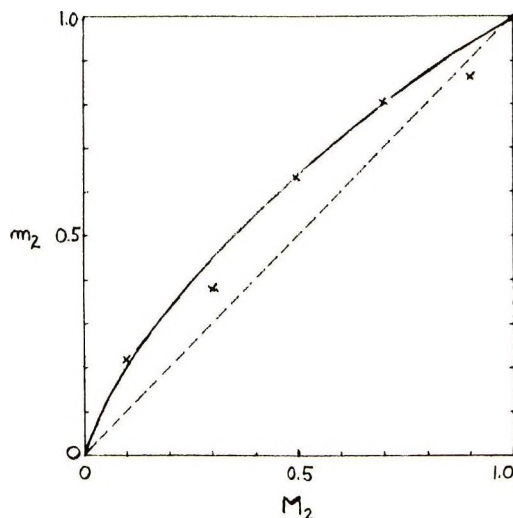


Fig. 9. Copolymerization curve for MG (monomer 2) with acrylic acid.

merization tubes contained, in addition to the monomers, 5 mg of azobisisobutyronitrile as the initiator, and 15 ml of 1:1 water-ethanol by volume.

TABLE VII
Copolymerization of *N*-Methacrylylglycinamide (M_2) and Acrylic Acid (M_1)

Monomer 2, g	Monomer 1, g	M_2^a	Time, min	Conversion, %	<i>N</i> , % ^b	m_2^a
0.475	2.109	0.102	21	4.17	6.83	0.212
1.427	1.685	0.300	20	12.85	10.92	0.387
2.380	1.201	0.501	13	4.05	15.23	0.633
3.329	0.720	0.701	13	4.12	17.52	0.803
4.282	0.239	0.901	6	3.24	18.25	0.865

^a M_2 is the mole fraction of monomer 2 in the monomer mixture and m_2 the mole fraction of monomer 2 in initial copolymer.

^b Analyses by Clark Microanalytical Laboratories, Urbana, Illinois.

If the best theoretical copolymerization curve is fitted to the data of Table VII (Fig. 9), values of $r_1 = 0.4$ and $r_2 = 1.5$ are obtained. The high conversion at a M_2 value of 0.3 has led to a copolymer too rich in acrylic acid, and hence this point falls below the curve. Similarly, inability to obtain theoretical values for nitrogen in PMG homopolymers interferes at high MG copolymer contents. By employing the Alfrey-Price^{21,22} scheme for monomer reactivity factors and values of $Q = 1.15$ and $e = 0.77$ for acrylic acid,²³ values for the resonance factor Q and the electrical factor e for MG are 1.66 and +0.06, respectively. For the AG (M_2)-acrylic acid (M_1) System,² $r_1 = 0.55$ and $r_2 = 0.40$, which yield $Q = 0.81$ and $e = -0.46$ for *N*-acrylylglycinamide. If methyl acrylate is compared with methyl methacrylate and acrylamide with methacrylamide,²³ it is seen that α -methyl

substitution raises the value of the resonance factor and makes e algebraically more negative. In the glycinamide series, α substitution raises the value of Q but the electron density of the double bond seems to be higher in AG than MG. This may be a consequence of choosing acrylic acid as the comonomer, where the possibility of partial protonation of the glycinamide monomers in aqueous solution exists, or may result from inherent inadequacies of the Alfrey-Price treatment.

References

1. H. C. Haas and N. W. Schuler, *J. Polym. Sci. B*, **2**, 1095 (1964).
2. H. C. Haas, R. D. Moreau, and N. W. Schuler, *J. Polym. Sci. A-2*, **5**, 915 (1967).
3. H. C. Haas, C. K. Chiklis, and R. D. Moreau, *J. Polym. Sci., A-1*, **8**, 1131 (1970).
4. W. H. Bauer and E. A. Collins, in *Rheology*, Vol. 4, F. R. Eirich, Ed., Academic Press, New York, 1967, Chap. 8.
5. J. Pryce-Jones, *J. Sci. Instr.*, **18**, 39 (1941).
6. J. Eliassaf, A. Silberberg, and A. Katchalsky, *Nature*, **176**, 119 (1955).
7. J. Eliassaf and A. Silberberg, *J. Polym. Sci.*, **41**, 33 (1959).
8. S. R. Erlander and R. Tobin, *J. Macromol. Sci.-Chem.*, **A2**, 1521 (1968).
9. J. S. Yudelson and R. E. Mack, *J. Polym. Sci. A*, **2**, 4683 (1964).
10. L. D. Taylor and T. E. Platt, *J. Polym. Sci. B*, **7**, 597 (1969).
11. J. E. Eldridge and J. D. Ferry, *J. Phys. Chem.*, **58**, 992 (1954).
12. M. L. Huggins, *J. Amer. Chem. Soc.*, **64**, 2716 (1942).
13. H. C. Haas, R. L. MacDonald, and A. N. Schuler, *J. Polym. Sci., A-1*, **8**, 3405 (1970).
14. W. R. Moore, J. Epstein, B. M. Tidswell, and A. M. Brown, *J. Polym. Sci.*, **23**, 23 (1957).
15. H. Morawetz, *Macromolecules in Solution*. Interscience, New York, 1965, pp. 368-369.
16. W. R. Moore, *Progr. Polym. Sci.*, **1**, 1 (1967).
17. J. Pouradier and A. M. Venet, *J. Chim. Phys.*, **47**, 11 (1950).
18. P. Doty, J. H. Bradbury, and A. M. Holtzer, *J. Amer. Chem. Soc.*, **78**, 947 (1956).
19. C. Tanford, *The Physical Chemistry of Macromolecules*, Wiley, New York, 1961, pp. 408-09.
20. G. M. Chetyrkina, V. G. Aldoshin, and S. Y. Frenkel, *Vysokomol. Soedin.*, **1**, 1133 (1959).
21. T. Alfrey, Jr., and C. C. Price, *J. Polym. Sci.*, **2**, 101 (1947).
22. C. C. Price, *J. Polym. Sci.*, **3**, 772 (1948).
23. J. Brandrup and E. H. Immergut, Eds., *Polymer Handbook*, Interscience, New York, 1966, p. II, 341.

Received May 27, 1970

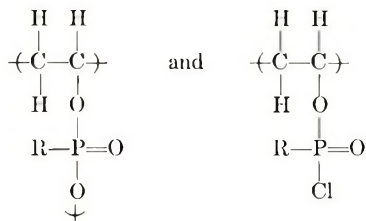
Revised October 29, 1970

Modification of Poly(vinyl Alcohol) Through Reaction with Phosphorus-Containing Reactants

CHARLES E. CARRAHER, JR.,* and LARRY TORRE,†
*Chemistry Department, University of South Dakota,
 Vermillion, South Dakota 57069*

Synopsis

Crosslinked products of the form:



have been formed from the interfacial condensation of phosphorus diacid halides with poly(vinyl alcohol). Product yield and amounts of phosphorus reactant included in the product increases as the amount of base increases. Product stability in aqueous systems decreases in the order neutral > base > acid.

Introduction

Modification of polymers has been accomplished by allowing portions of the chain to undergo chemical reactions.¹ Much work has been done with poly(vinyl alcohol) (PVA) via reaction at the hydroxide group. Much of the work has concerned itself with the melt and/or solution esterification,²⁻⁵ sulfonation,⁶⁻⁷ and phosphorylation¹⁰⁻¹⁴ of the hydroxide group.

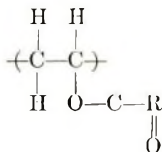
Volgina et al.¹¹ reacted PVA with phosphorus-containing halogen reactants such as trichloroethyl phosphate in dimethylformamide; subsequent heating to 200°C led to products which did not support combustion and smoldering and which were water- and rot-resistant. Brace¹² reported the formation of dialkyl poly(vinyl phosphate) flame-retardant textiles from the phosphorylation of PVA with a mono-acid chloride phosphate by the solution method. Motozato et al.^{13,14} reacted PVA with phosphorus oxychloride in an organic solvent. Hydrolysis of the products gave fibers with cation-exchange capacity.

* To whom correspondence should be directed.

† A project SEED operation "Catalysts" student supported during the 1970 summer.

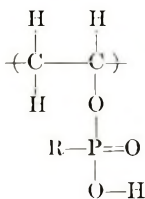
Much work has been reported on the synthesis of poly(phosphate esters) and poly(phosphonate esters) by the interfacial technique.¹⁵⁻¹⁸ This work excluded the use of polymers containing hydroxide groups.

Recently, work has been done by the interfacial technique to form polyesters of PVA of the form I.¹⁹⁻²⁴ This work has been restricted to the use of hydrocarbon acid chlorides. We report the extension

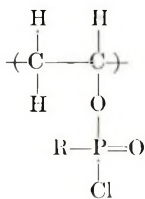


I

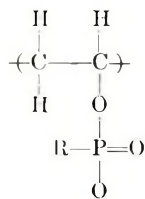
of the method to include the synthesis of phosphonate and phosphate esters through interfacial condensation with poly(vinyl alcohol) to produce products of forms II, III, and IV.



II



III



IV

In the interfacial method, two fast-reacting monomers are dissolved in a pair of immiscible liquids, one of which is generally water. Polymerization occurs at or near the liquid interface. It is a simple system, often producing high yields of products rapidly at or around room temperature. It offers a direct route to poly(phosphonate and phosphate esters) of forms II-IV by utilizing commercially available reactants.

Experimental

Poly(vinyl alcohol) was purchased from Matheson, Coleman, Bell (Norward, Ohio) and used without further purification. The acid chlorides were used as obtained from Aldrich Chemical Co. (Milwaukee, Wisconsin). Polymerizations were carried out in a 1-pt Kimax emulsifying jar placed on a Waring Blendor (Model 1001 or 1043). The jar was vented by placing a glass tube, inserted in a cork stopper, through a hole in the jar cap. A second hole in the cap contained a separatory funnel. The PVA in water, along with any added base, was initially added to the reaction jar. The cap was screwed on the jar. The organic phase containing the acid chloride and organic solvent was added to the separatory funnel. The blender was turned on and the funnel stopcock opened, the organic phase thus being allowed to fall freely into the reaction jar. Timing began when all the organic phase had entered the reaction vessel. After the desired period of time, the blender was turned off.

The aqueous phase was separated and filtered. The filtrate was washed with portions of water and then added to about 500 ml of distilled water. The mixture was stirred for about 1-3 days to dissolve any unreacted poly(vinyl alcohol) which may have precipitated from the reaction mixture along with the product.* The contents were filtered and the product collected as the filtrate and dried under vacuum (about 20 mm Hg).

The amount of phosphorus reactant included in the product was determined for some of the products (Table I). Given portions of the aqueous

TABLE I
Properties as a Function of Reactant^a

Phosphorus reactant	NaOH added, mole	Weight of product, g	PVA in product, %
POCl ₂ -C ₆ H ₅	0.0	0.06	75
POCl ₂ -C ₆ H ₅	0.023	0.06	
POCl ₂ -C ₆ H ₅ ^c	0.046	1.48	66
POCl ₂ -C ₆ H ₅	0.150	1.90	50
POCl ₂ -CH ₂ -Cl	0.0	0.01	
POCl ₂ -CH ₂ -Cl	0.023	0.02	
POCl ₂ -OC ₆ H ₅	0.0	0.01	
POCl ₂ -OC ₆ H ₅	0.023	0.06	
PSCl ₂ -C ₆ H ₅	0.0	0.18	70
PSCl ₂ -C ₆ H ₅	0.023	0.44	66
PSCl ₂ -C ₆ H ₅ ^d	0.046	0.83	56
PSCl ₂ -C ₂ H ₅	0.023	0.30	
POCl ₂ -C ₂ H ₅	0.0	0.18	
POCl ₂ -C ₂ H ₅	0.023	0.28	

^a Reaction conditions: 1.00 g (0.023 mole) of poly(vinyl alcohol) (limiting viscosity number of about 30 in water at 25°C) in 50 ml of water (plus added base) plus 0.023 mole phosphorus reactant in 50 ml of carbon tetrachloride at 25°C, 17,500 rpm no-load stirring rate for 2 min.

^b Calculated as described in Experimental section.

^c See Table II.

^d See Table II.

phase (combined with the wash and digestion water) were evaporated under vacuum.† Water was added to the solid; this dissolved the salt, unreacted NaOH, and hydrolyzed acid chloride but not the poly(vinyl alcohol), which takes about a day to go into solution. The mixture was filtered and the solid poly(vinyl alcohol) weighed. From knowledge of the unreacted poly(vinyl alcohol) the amount of poly(vinyl alcohol) incorporated in the product was calculated.

Softening ranges were measured by using a Fisher-Johns melting point apparatus at an approximate heating rate of 2°C/min. No softening point

* Repeating the reaction procedure but without the phosphorus reactant generally yielded portions of jelled poly(vinyl alcohol) which dissolved in water after several hours.

† The aqueous phases were found to turn brown and give inexact results if heat (>60°C) was employed to help evaporation, possibly due to the presence of hydrolyzed acid chlorides (which are soluble in water) and/or unreacted base.

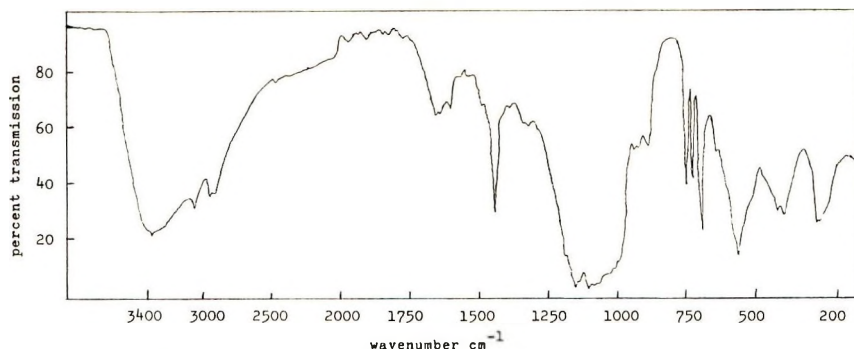


Fig. 1. Infrared spectrum of the product from condensation of poly(vinyl alcohol) with phenylphosphonic dichloride.

was observed for any of the products to a temperature of 300°C. The materials generally turned from white to cream to brown in color in the range of 140–260°C, indicating some degradation and/or change in structure.

Infrared spectra were obtained as KBr pellets for the solids and two KBr pellet-plates for liquids²⁵ by use of a Beckman IR-12 or a Perkin-Elmer 237B spectrophotometer. The spectra were consistent with inclusion of the phosphorus portion of the acid chlorides in the PVA chain. A representative spectrum appears in Figure 1.

The products were insoluble in all solvents, indicating crosslinking. This is expected, since the acid chlorides employed are difunctional.

Results and Discussion

Modification of poly(vinyl alcohol) by reaction with diacid chlorides containing phosphorus has been accomplished. The products can contain at least three types of linkages, structures II, III, and IV. Form III results from initial attack by the phosphorus reactant without subsequent reaction with the second halide. The presence of some P-Cl endgroups in the product results from the interfacial reaction between phenylphosphonic dichloride and hydroquinone.^{15–18} The P-Cl frequency is assigned the region 587–435 cm^{-1} .²⁶ Spectra of the products generally show a band in the region 560–570 cm^{-1} which is attributed to the presence of the P-Cl group. The products give a positive Beilstein test for halogen. Thus the presence of units of form III is believed to occur. Form III could result from either of the following reaction pathways: (1) diffusion away from the aqueous phase by the acid chloride after initial reaction of the first acid chloride; (2) entrapment of the acid chloride either through precipitation of the product and/or entanglement in the growing chain.

Form II could result from hydrolysis of the acid chloride either before or after the initial phosphonation or phosphorylation. The products generally exhibit weak or no bands in the infrared region assigned to the P-OH group (2700–2550 cm^{-1}).²⁷

The presence of units of form IV is indicated by the crosslinked nature of the products.

Several trends are apparent (Table I). As the amount of acid acceptor (NaOH) is increased, product yield and amount of phosphorus reactant included in the product increases. The yield trend is presumably a consequence of a greater efficiency of acceptance of the acid as the amount of base is increased. (Hydrogen chloride is formed as a condensation product and can protonate alcohol groups, thereby inactivating the alcohol functional

TABLE II
Stability of Products^a

Liquid	Poly(vinyl alcohol) product with phosphorus reactants	
	POCl ₂ -C ₆ H ₅ ^b	PSCl ₂ -C ₆ H ₅ ^c
Formic acid (98-100%)	-	-
Glacial acetic acid	+	+
<i>p</i> -Xylene	+	+
Acetonitrile	+	+
Triethylamine	-	-
Aqueous NaCl (sat.)	+	-
Methylene chloride	+	+
Benzene	+	+
Nitric acid (70%)	-	-
Distilled water	+	+
Sulfolane-W ^d	+	+
Isopropanol alcohol	+	+
Bromobenzene	+	+
Carbon tetrachloride	+	+
Tetrahydrofuran	+	+
2-Chloroethanol	-	+
Pentane	+	+
Acetophenone	+	+
Methanol	-	-
H ₂ SO ₄ (98%)	-	-
HCl (3 <i>M</i>)	-	-
H ₂ SO ₄ (3 <i>M</i>)	-	-
Acetone	+	+
Petroleum ether	+	+
Dimethyl sulfoxide	+	+
NaOH (0.1 <i>M</i>)	+	+
NaOH (1.0 <i>M</i>)	-	+
NaOH (3.0 <i>M</i>)	-	+
Ethyl acetate	+	+

^a The test samples were composed of about 0.02 g of product in 3 ml of liquid. The samples were shaken occasionally. Instability (-) was indicated by the disappearance of the solid in the given liquid; stability (+) was indicated by the absence of signs of degradation of the product.

^b Product properties given in Table I, see footnote c.

^c Product properties given in Table I, see footnote d.

^d A gift from the Stauffer Chemical Co., Dobbs Ferry, N. Y.

group to attack by the acid chloride. The reaction presumably occurs via a bimolecular pathway where the phosphorus is the site of nucleophilic attack by the alcohol.) The trend should only be accepted over the tested range, since an increase in base concentration should also increase the rate of acid chloride hydrolysis via attack by the hydroxide ion. Over the tested range the acid acceptor role of the base seemingly increases relative to its role as an acid chloride-hydrolyzing agent.

The amount of poly(vinyl alcohol) component (and thus the amount of phosphorus component) was calculated as indicated in the experimental section and appears in Table I. The increase in phosphorus component as amount of base increases is also indicated by an increase in infrared bands due to the phosphorus reactant relative to those attributed to the poly(vinyl alcohol) portion. Quantitative determination of the amounts of phosphorus-containing component was not made, since there was doubt as to the constancy of the baseline throughout the various spectra.

The trend can be explained by considering the requirements for crosslinking. There is a point for each given polymer beyond which insolubility in good solvents (and in fact, all solvents) occurs.* Insolubility presumably can occur with a small amount of crosslinking. The formation and precipitation of crosslinked material follows a tight reaction schedule. In low-base (or no-base) systems, HCl can more effectively protonate near-by alcohol groups, preventing the inclusion of greater amounts of the phosphorus reactants before precipitation occurs and ending the growth of the chain. In systems with more base, the base is more effective in deprotonating and/or acid-acceptor activity, permitting a higher amount of the phosphorus reactant to be included in the precipitating product.

The stability trend (Table II) of neutral > base > acid water solutions is somewhat different than that (neutral > acid > base) observed for linear poly(phosphonate esters) and poly(phosphate esters).²⁸ The reason for the difference in trend is not now known. Differences in wetting, permeability, etc. may be responsible.

Crosslinked products have been formed from the interfacial condensation of phosphorus diacid halides with poly(vinyl alcohol). Product yield and amount of phosphorus reactant included in the product increases as the amount of base increases over the tested range.

References

1. E. M. Fettes, Ed., *Chemical Reactions of Polymers*, Wiley, New York, 1964.
2. O. Wichterle, Ger. Pat. 1,065,621 (1959).
3. M. Dima, A. Carpoș, and S. Maxim, *Rev. Roum. Chim.*, **13**, 485 (1968).
4. M. Shiraiishi, Jap. Pat. 17,582 (1968).
5. G. Smirnov, I. Okhrimenko, and L. Mashlyakorski, *Zh. Prikl. Khim.*, **41**, 2304 (1968).
6. A. de Cat, J. Lemmerling, and A. van Paesschen, Brit. Pat. 976,392 (1964).
7. E. Korneva, O. Smirnov, and V. Urarova, *Zh. Prikl. Khim.*, **39**, 1876 (1966).

* Criteria other than insolubility can be used in considering crosslinking. Solubility is used since precipitation is believed to play an important part in the chain growth.

8. D. Reynolds and W. Kenyon, *J. Amer. Chem. Soc.*, **72**, 1584 (1950).
9. O. Klimova and V. Datsenko, *Zh. Prikl. Khim.*, **33**, 2582 (1960).
10. N. Kulikova, M. Androsova, and N. Orlov, *Zh. Prikl. Khim.*, **40**, 2318 (1967).
11. N. Volgina, I. Seregina, L. Volf, Y. Kirilenko, S. Borisov, E. Nifant'ev, N. Sviridova, and K. Tammik, *Zh. Prikl. Khim.*, **41**, 2563 (1968).
12. N. Brace, U.S. Pat. 2,733,229 (1956).
13. Y. Motozato, T. Tamura, and H. Egawa, Jap. Pat. 6,970 (1957).
14. Y. Motozato, H. Egawa, H. Maegaki, and K. Kunitate, *Kogyo Kagaku Zasshi*, **59**, 479 (1956).
15. F. Millich and C. Carraher, U.S. Pat. 3,491,061 (1970).
16. F. Millich and C. Carraher, *J. Polym. Sci. A-1*, **7**, 2669 (1969); and *ibid.*, **8**, 163 (1970).
17. F. Millich and C. Carraher, *Macromolecules*, **3**, 253 (1970).
18. C. Carraher, *Inorg. Macromol. Rev.*, in press.
19. V. Lavrishehev, Y. Bokov, and N. Vikulina, U.S.S.R. Pat. 194,310 (1967).
20. Y. Tsuda, Jap. Pat. 20,188 (1965).
21. T. Shermergorn and Y. Kamardin, *Vysokomol. Soedin.*, **7**, 2156 (1965).
22. Y. Kamardin, I. Shermergorn, and I. Magdeer, *Vysokomol. Soedin. B*, **9**, 419 (1967).
23. M. Tsuda, U.S. Pat. 3,329,664 (1967).
24. V. Lavrishehev, Y. Bokov, N. Vikulina, H. Larina, and N. Karantirov, U.S.S.R. Pat. 183,395 (1966).
25. C. Carraher, *J. Chem. Ed.*, **45**, 462 (1968).
26. C. Carraher and P. Billion, *Makromol. Chem.*, **128**, 143 (1969).
27. C. Rao, *Chemical Applications of Infrared Spectroscopy*, Academic Press, New York, 1963.
28. C. Carraher, Ph.D. thesis (68-9848).

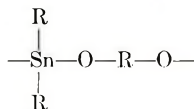
Received October 20, 1970

Production of Organometallic Polymers by the Interfacial Technique. XX. Synthesis of Polyoxystannyloxyalkylenes

CHARLES E. CARRAHER, JR.,* and GARY A. SCHERUBEL,
*University of South Dakota, Chemistry Department, Vermillion,
South Dakota 57069*

Synopsis

Polyoxystannyloxyalkylenes of low to intermediate molecular weight were synthesized in low to high yield by a modified nonaqueous interfacial technique.



At least some of the products possess Sn—Cl, Sn—OH, and R—OH endgroups. The aqueous stability of the products is in the order neutral \gg basic $>$ acidic.

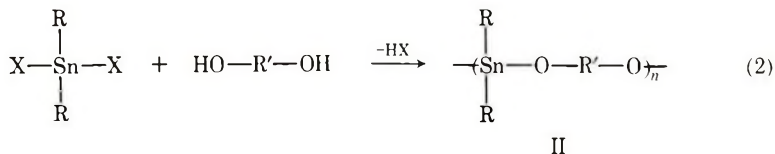
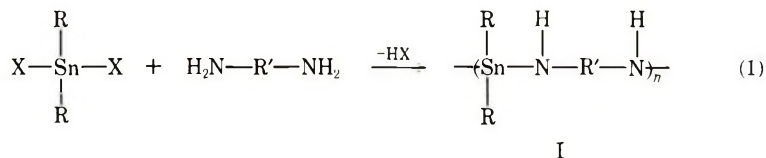
Introduction

We have been interested in the synthesis of organometallic polymers by means of the interfacial technique.¹⁻⁵ Synthesis can be accomplished at or below room temperature, which minimizes thermally induced side reactions and allows the use and/or synthesis of thermally unstable products. Modified, nonaqueous interfacial systems were devised for use with nucleophilic agents as diols and diamines because of preferential hydrolysis of the organometallic halide rather than the desired ammonolysis or alcoholysis.

We recently reported the interfacial synthesis of polystannylalkylene-(arylene)diamines (I) by using a modified interfacial system.⁶ We now wish to report the first synthesis by any method of polyoxystannyloxyalkylenes (II) by using another modified interfacial system. The modified system used in this study substitutes for the aqueous-phase liquid diol which acts as a reactant and forms an interface with the second stannane-containing phase. It has previously been successfully employed in the synthesis of polyalkyloxysilanes.^{7,8}

The interfacial technique offers a direct pathway to the synthesis of such products by use of commercially available reactants.

* To whom correspondence should be directed.



Experimental

Detailed description of the polymerization sequence is given elsewhere.⁷ Generally the organic phase,* containing a known amount of organostannane reactant, was added to stirred liquid diol containing triethylamine. The polymer separates from the liquid phases as a white tacky solid and was separated from the liquid phases by use of suction filtration. The salt, triethylamine hydrochloride, is washed from the product with water.

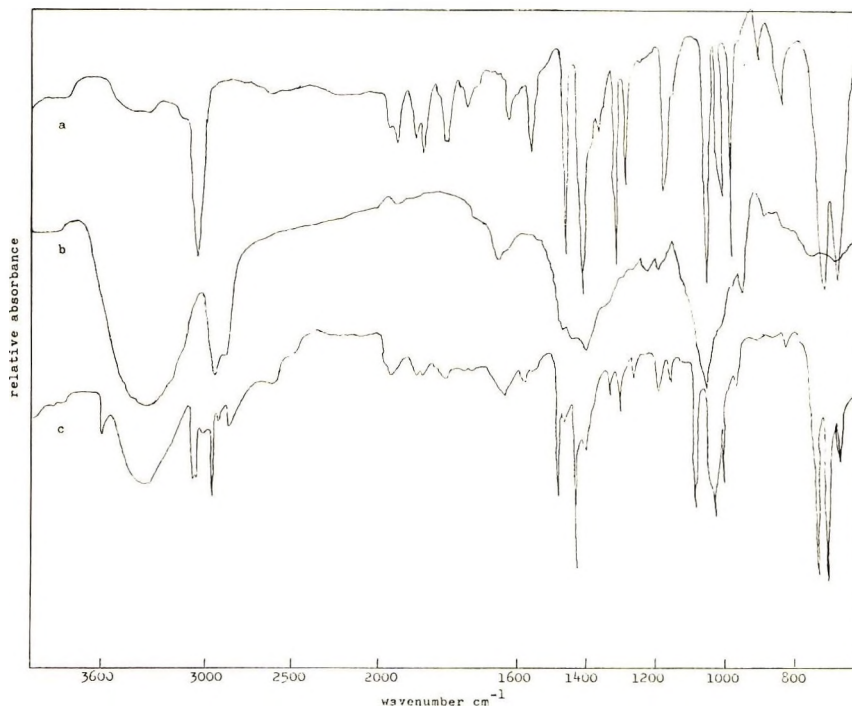


Fig. 1. Infrared spectra of (a) diphenyldichlorostannane, (b) 1,4-butanediol, and (c) polyoxy(diphenylstannylene)oxytetramethylene.

* The terms organic solvent or organic phase are used to describe the non-diol phase or solvent.

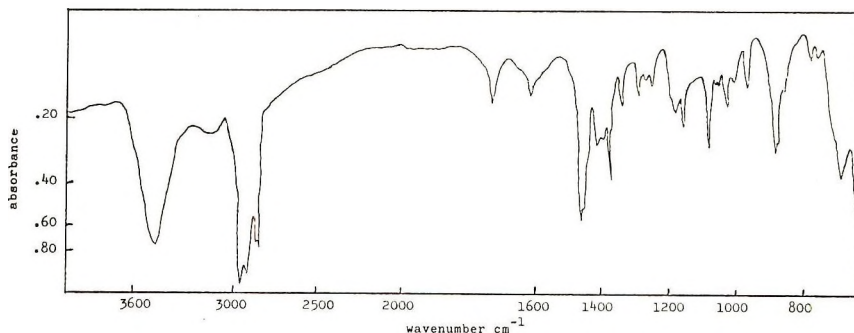


Fig. 2. Infrared spectrum of polyoxy(di-*n*-butylstannylene)oxytrimethylene.

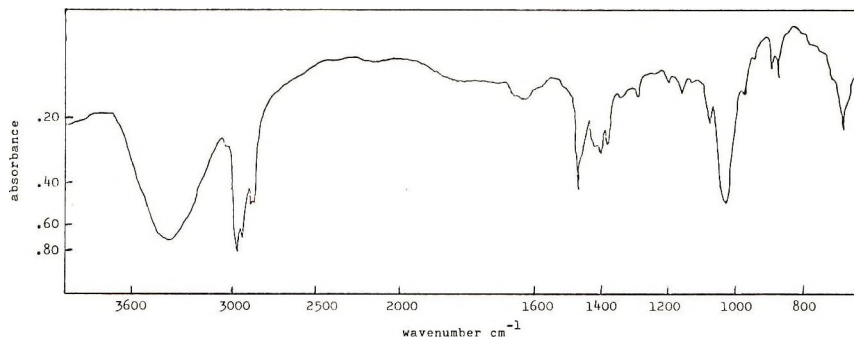


Fig. 3. Infrared spectrum of polyoxy(di-*n*-butylstannylene)oxy-2-butenylene.

Infrared spectra were obtained by using KBr pellets for solids and using two KBr pellets for liquids (the reactants) on Beckman IR-12 and Perkin-Elmer 237-B spectrophotometers. The spectra and elemental analysis were consistent with a repeating unit having the structure II. Representative spectra appear in Figures 1-3.

Viscometry was conducted in dioxane at 30°C by using a Cannon-Ubbelohde semimicro viscometer. Softening ranges were obtained by using a Fisher-Johns melting point apparatus at a heating rate of 5C°/min and are defined as the range between the beginning of melting and the point at which melting is complete.

Results and Discussion

Synthesis of polyoxystannoxyalkylenes by the modified technique is general for liquid diols (Table I). The products represent low to intermediate molecular weight chains (\overline{DP}_n in the range of 3-120⁹) and are obtained in low to high yields.

Reaction conditions are constant with regard to volume of diol rather than to molar amount of diol. The limiting reagent in each system is stannane, which is held constant from system to system. This was done for several reasons. If molar quantities of reactants are used and an

TABLE I
Polymer Properties as a Function of Reactant^a

Stannane	Diol	Diol content, mole	Reaction time, sec	Yield, %	η_{sp}/c , ml/g ^b	Softening range, °C
Diphenyldichlorostannane	2-Butenediol ^c	0.023	15	85	15	>300
Diphenyldichlorostannane	1,4-Butanediol	0.022	15	58	29	>300
Dibutyldichlorostannane	1,4-Butanediol	0.022	15	52	—	190-198
Dibutyldichlorostannane	2,2'-Oxydiethanol	0.021	30	2	—	220-227
Dibutyldichlorostannane	Ethylene glycol	0.037	30	90	3	198-205
Dibutyldichlorostannane	1,3-Propanediol	0.026	30	1	—	105-109

^a Reaction conditions: 0.0030 mole stannane in 50 ml hexane, 2 ml of diol, 0.0060 mole of triethylamine; 17,500 rpm stirring rate at 30°C.

^b Viscosity in dioxane, 1%.

^c A gift from GAF Corp., New York, N.Y., 10020.

attempt is made to hold the molar amount constant as diol is changed, the volume of the diol phase is varied. An analogous study¹⁰ showed that rate of polymer formation with silanes was consistent with the rate expression (3):

$$\text{Rate} = k[\text{ethylene glycol}]^{2/3}[\text{silane}] \quad (3)$$

Equation (4) is derived if one assumes a model consisting of spheres of diol reactant in a "sea" of organic solvent. (Other necessary assumptions are given in ref. 10.) This is consistent with

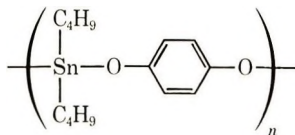
$$\text{Rate} = k(\text{spherical area of ethylene glycol})[\text{silane}] \quad (4)$$

the rate expression given in eq. (3), since spherical area is proportional to (concentration)^{2/3}. Thus volume of the diol phase may be critical in determining reaction parameters. In addition, the nature of the diol may be critical in determining product trends. This is difficult to assess in such systems, since not only would diol volume vary but also the surface tension, viscosity, solubility, etc. of the diol phase would vary as the diol reactant varied. Work is in progress to determine the effect of varying the nature of the stannane on the reaction parameters.

A soluble base (triethylamine) was the acid acceptor. It has been shown in studies involving the nature of the acid acceptor in the production of polyalkyl(aryl)oxysilanes, that systems with soluble bases are superior to systems with no added base or solid insoluble added base with respect to acid-acceptor properties. This is demonstrated by an increase in product yield and molecular weight in systems^{11,12} with soluble base.

Many polymers containing Group IV elements are hydrolytically unstable. Degradation is often catalyzed by the presence of acid or base; e.g., 1 g of polyoxy-1,4-phenyleneoxy(di-*n*-butylstannylene) (III, LVN in dioxane of 7 ml/g) undergoes complete hydrolysis in less than 1 min stirring (17,500 rpm) in 50 ml 1*N* HCl. In 1*N* NaOH hydrolysis is

slower, about 10 min being required for partial hydrolysis of the product. This observed difference in rate of hydrolysis can be explained by considering that the site of attack by the hydroxide ion is at the more sterically encumbered tin whereas attack by the proton occurs at the more open oxygen.



III

The products exhibit relatively good hydrolytic stability in neutral water if "unwetted."

Both yield and molecular weight remain approximately constant over short stirring times but decrease at long stirring times (Table II). A similar study was made in the synthesis of polyoxyethyleneoxy(diphenylsilyle).⁷ Yield increased with molecular weight, remaining constant as stirring time increased. The two systems are the same except the silane system employed an insoluble base (NaOH) as the acid acceptor whereas the present systems employed a soluble acid acceptor (triethylamine). As noted above, the tin products undergo acid- or base-catalyzed degradation. In the silane systems the insoluble base was (presumably) not effective in promoting degradation. In the stannane systems it is possible that degradation of the tin polymer, catalyzed by the soluble base, occurs more rapidly than does polymer formation, resulting in the observed trend.* (It must be noted that such base-catalyzed degradation should also be promoted by the reactant base diol.)

TABLE II
Polymer Properties as a Function of Reaction Time^a

Reaction time, sec	Yield, %	η_{sp}/c , ml/g
15	85	15
30	90	16
120	78	16
300	69	10

^a Reaction conditions: 0.0030 mole of diphenyldichlorostannane in 50 ml hexane, 2 ml (0.023 mole) of 2-butene-1,4-diol, 0.0060 mole triethylamine; 17,500 rpm stirring rate at 30°C. Softening ranges of all products greater than 300°C.

^b Viscosity in dioxane, 1%.

The tin products are generally soluble in dioxane, *p*-cumene, and methyl ethyl ketone but insoluble in such solvents as dimethyl sulfoxide, dimethyl-

* The relative decrease observed between decreases in yield compared with molecular weight may indicate a pathway of degradation but the system has not been widely enough studied to make such speculation profitable.

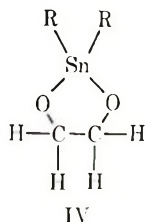
formamide, carbon tetrachloride, benzene, acetone, toluene, and chloroform. The analogous silicon products exhibit a wider range of solubility. Thus the general order of solubility range is $\text{Si} > \text{Sn}$, which is consistent with the order $\text{Si} > \text{Ge} > \text{Sn}$ observed for other Group IV condensation polymers.⁹

There are four possible endgroups. They are $\text{Sn}-\text{Cl}$, $\text{Sn}-\text{OH}$ (resulting from hydrolysis of $\text{Sn}-\text{Cl}$ endgroups in the isolation procedure), $\text{R}-\text{OH}$, and $\text{Sn}-\text{NEt}$, or similar species resulting from attack of the triethylamine on the tin halide ending chain growth. The presence of triethylamine groups is generally indicated by the presence of characteristic bands in the 2770–2700 and 1320–1240 cm^{-1} regions.^{2,12} Spectra of products obtained in the present study (Figs. 1–3) do not exhibit infrared-detectable inclusion of triethylamine groups.

Spectra were obtained in the 200–800 cm^{-1} region by using the Beckman IR-12 spectrophotometer. The $\text{Sn}-\text{Cl}$ stretching region is in the 320–350 cm^{-1} range.^{13,14} Spectra of the products generally exhibit bands in the 325–335 cm^{-1} region. They also generally give positive Beilstein tests for halide. The presence of at least portions of $\text{Sn}-\text{Cl}$ endgroups is established.

It is difficult to distinguish between the presence of $\text{Sn}-\text{OH}$ and $\text{R}-\text{OH}$ groups since their characteristic absorption ranges overlap (3400–3500 cm^{-1} for $\text{Sn}-\text{OH}$ ¹⁴ and 3100–3400 cm^{-1} for $\text{R}-\text{OH}$). Some of the products exhibit two bands which indicated the presence of both groups. Other products exhibit broad spectral bands which may result from the presence of both groups. It is tentatively concluded that at least some products have both $\text{Sn}-\text{OH}$ and $\text{R}-\text{OH}$ endgroups.

The low molecular weight found for the product with ethylene glycol (Table I) may be due to the formation of cyclic material having the structure IV. This is not totally true, since the product exhibits infrared detectable $\text{R}-\text{OH}$ (and possibly $\text{Sn}-\text{OH}$) endgroups.



Low to intermediate molecular weight polyoxystannyleneoxyalkylenes were synthesized by the interfacial technique. The system is limited to the use of only those diols which are liquid at or near room temperature.

This work was supported in part by an American Chemical Society Petroleum Research Foundation Grant, 1338,G3.

This paper was abstracted in part from the thesis submitted by G. A. Scherubel to the University of South Dakota.

References

1. C. E. Carraher, *Macromolecules*, **2**, 306 (1969).
2. C. E. Carraher and J. Greene, *Makromol. Chem.*, **131**, 259 (1970).
3. C. E. Carraher and G. Klimiuk, *J. Polym. Sci. A-1*, **8**, 973 (1970).
4. C. E. Carraher and R. Dammeier, *Makromol. Chem.*, **135**, 107 (1970).
5. C. E. Carraher and G. Klimiuk, *Makromol. Chem.*, **183**, 211 (1970).
6. C. E. Carraher and D. Winter, *Makromol. Chem.* **141**, 237 (1971).
7. C. E. Carraher, *J. Polym. Sci. A-1*, **7**, 2351 (1969).
8. C. E. Carraher, paper presented at American Chemical Society Meeting, 1969; *Polym. Preprints*, **10**, 418 (1969).
9. C. E. Carraher, *Inorg. Macromol. Rev.*, **8**, 305 (1970).
10. C. E. Carraher, *J. Polym. Sci. A-1*, **7**, 2359 (1969).
11. C. E. Carraher, *J. Polym. Sci. A-1*, **8**, 3051 (1970).
12. C. E. Carraher and J. Greene, paper presented at American Chemical Society Meeting, 1970; *Polym. Preprints*, **11**, 66 (1970).
13. E. Ebsworth, in *The Bond to Carbon*, Vol. 1, Part 1, A. MacDiarmid, Ed., Dekker, New York, 1968.
14. C. E. Carraher and R. Dammeier, *J. Polym. Sci. A-1*, **8**, 3367 (1970).

Received October 20, 1970

Revised November 19, 1970

Preparation and Structure of Chlorinated Poly(vinyl Flouride)*

R. BACSKAI, L. P. LINDEMAN, and J. Q. ADAMS, *Chevron Research Company, Richmond, California 94802*

Synopsis

The low-temperature chlorination of poly(vinyl fluoride) (PVF) proceeds readily in CCl_4 suspension. The rate of chlorination is high initially, but the reaction slows down considerably when the chlorine content of the polymer reaches 40-50%. At long reaction times, polymers containing 62% chlorine (1.88 chlorine atoms per monomer unit) can be obtained. As the degree of chlorination increases, the solubility of PVF in organic solvents increases. Polymer crystallinity and polymer softening point decrease with chlorination. Polymers containing 40% chlorine appear to be completely amorphous by x-ray analysis. In this respect, PVF differs from poly(vinyl chloride) (PVC), where chlorination increases the softening point, and it resembles polyethylene where both crystallinity and softening point decrease with chlorination. ^{19}F NMR analysis of the polymers indicates that up to a degree of chlorination of 1 chlorine atom per monomer unit, 50% of the substitution occurs on the α -carbon of the PVF molecule. This result is very different from the predominant β -chlorination of PVC reported by several workers. The chemical selectivity observed in the chlorination of PVF is in qualitative agreement with the results of free-radical chlorination of organic compounds and can be rationalized by considering the size and the electronic properties of the fluorine atom. The results of ^1H NMR analysis are also in support of a polymer structure where the chlorine atoms are distributed between α - and β -carbons. Based on a comparison of the ^{19}F and ^1H NMR data, the average composition of chlorinated PVF at the 1 chlorine atom per monomer unit level can be represented as: $\text{C}_{200}\text{H}_{200}\text{F}_{100}\text{Cl}_{100} = (\text{CH}_2)_{63}(\text{CHF})_{30}(\text{CHCl})_{24}(\text{CClF})_{30}(\text{CCl}_2)_{13}$.

INTRODUCTION

There are numerous reports in the literature dealing with the halogenation of high molecular weight polymers.¹ Much of the work has been aimed toward the modification of some physical property of the base polymer, such as solubility,² stiffness,^{1a} shape retention at elevated temperature,^{3,4} etc. Other investigations explored the possibility of introducing reactive sites by halogenation in order to prepare crosslinkable products.^{1b} The chlorination of poly(vinyl chloride) (PVC) has attracted particular attention, mainly because of the higher solubility² and the increased softening point^{3,4} of the product. Both of these features are

* Presented in part at the International Symposium on Macromolecular Chemistry of the IUPAC, Toronto, Canada, September 1968, and at the Fourth Western Regional Meeting of the American Chemical Society, San Francisco, California, November 1968.

important from the practical point of view. The structure of chlorinated PVC was also studied in great detail,⁵⁻¹³ but there is considerable disagreement among the various investigators with regard to the distribution of chlorine atoms in the polymer chain.

The chlorination of poly(vinyl fluoride) (PVF), a reaction not investigated previously, provides an interesting opportunity to prepare and study a polymer having both fluorine and chlorine substituents in its main chain. Although there are many reports on the physical properties of chlorinated polymers, it is difficult to predict how the properties of PVF will be affected by chlorination. The fact that chlorination reduces the softening point of polyethylene¹⁰ but increases that of PVC^{3,4} serves to illustrate this point. In this work, the synthesis of chlorinated PVF and some physical properties of the products is described. An analysis of the distribution of chlorine atoms in the polymer, based on ¹H and ¹⁹F NMR studies, is also discussed in detail.

EXPERIMENTAL

Materials

The PVF used in this investigation was obtained from the Diamond Alkali Company, and it was designated Dalvor 720 fluorocarbon resin. This polymer, a fine, white powder, is soluble in *N,N*-dimethylformamide, *N,N*-dimethylacetamide, and dimethyl sulfoxide at 110°C.

ANAL. Calcd for (CH₂-CHF)_n: C, 52.17%; H, 6.56%; F, 41.27%. Found: C, 51.66, 51.80%; H, 6.43, 6.60%; F, 39.3%.

The infrared spectrum of the polymer between 600 and 1400 cm⁻¹, obtained on a film cast from *N,N*-dimethylformamide solution onto a sodium chloride plate, was identical to that reported by Koenig and Mannion.¹⁴

PVC (Geon 103 EP), was obtained from the B. G. Goodrich Chemical Company. Analysis showed 56.6% Cl [calculated for (CH₂-CHCl)_n, 56.75% Cl].

Polymer Characterization

The degree of chlorination Φ of PVF, defined in this work as the number of chlorine atoms in 100 monomer units, was determined from the elemental analysis of the polymers. The two independent equations [eqs. (1) and (2)] were used in the calculations.

$$\Phi = \frac{46.04\text{Cl}\%}{35.45 - 0.344\text{Cl}\%} \quad (1)$$

$$\Phi = \frac{240,000 - 4,604\text{C}\%}{34.44\text{C}\%} \quad (2)$$

Typical calculations are summarized in Table I.

TABLE I
Calculation of the Degree of Chlorination Φ in Chlorinated PVF

Sample	Elemental analysis		Φ^a		Mean
	Cl, %	C, %	From % Cl	From % C	
PVF		51.73	—	—	—
1	1.53	51.45	2.0	1.9	2.0
2	6.03	49.11	8.3	8.3	8.3
3	10.04	47.27	14.5	13.9	14.2
4	14.7	44.87	22.3	21.8	22.1
5	30.05	37.68	55.1	51.4	53.3
6	40.0	31.96	84.9	84.5	84.7
7	60.1	22.92	187.2	170.6	178.9
8	61.75	22.58	200.7	175.2	188.0

^a Number of chlorine atoms in 100 monomer units.

In the case of chlorinated PVC, used for comparison, the degree of chlorination was calculated from eq. (3).

$$\Phi = \frac{62.5\text{Cl}\% - 3.550}{35.5 - 0.345\text{Cl}\%} \quad (3)$$

For chlorinated PVC, Φ measures the number of additional chlorine atoms in 100 monomer units.

Reduced specific viscosities were measured in *N,N*-dimethylacetamide at 110°C and 0.1 g/100 ml polymer concentration.

¹H NMR spectra were obtained on a Varian HA-100 spectrometer. The polymers were dissolved in hexadeuterodimethylsulfoxide (approximately 11 wt-%), and the measurements were carried out at 110°C; 5% benzene was added for internal lock signal. The chemical shifts (reported in ppm) are all downfield relative to TMS, the dimethyl sulfoxide solvent impurity being used as a standard ($\delta = 2.50$ ppm). Relative proton counts were calculated from the electronic integral.

¹⁹F NMR spectra were obtained on a conventional Varian wide-line NMR spectrometer at 40 MHz to avoid bothersome side bands which were present in the 100 MHz high-resolution spectra. The polymers were dissolved in *N,N*-dimethylformamide (approximately 18 wt-%), and the measurements were carried out at 40–60°C. Chemical shifts were measured by conventional audio side banding of the 40 MHz transmitter. Chemical shifts are reported in ppm, upfield relative to internal CF₃COOH standard. The areas under the absorption curves were obtained by computer integration of the experimental first-derivative spectra. An indefinite integration was performed twice, the first giving the absorption curve; the second giving the area under the absorption curve.

Preparation of Chlorinated PVF

The chlorination apparatus, consisting of a three-necked, 500-ml Pyrex flask equipped with stirrer, condenser, thermometer, and gas inlet tube

was charged with 10 g PVF and 150 ml CCl_4 . The stirrer was started, and nitrogen gas was bubbled through the polymer suspension. After 10 min the nitrogen was shut off, and chlorine gas was introduced at a rate of 170 ml/min. At the same time the reaction mixture was illuminated with a 275-W General Electric sunlamp placed at a distance of 5 cm from the flask. The introduction of chlorine was continued for 20 min, and during that time the temperature inside the flask rose from 21°C to 49°C. Following that, the flask was purged with nitrogen, and the polymer suspension was poured into 500 ml of methanol. The precipitate was filtered, washed on the filter with methanol, and dried at 50°C in a vacuum oven. The polymer yield was 10.38 g ($\text{Cl} = 6.03\%$, $\eta_{sp}/c = 1.06$ dl/g).

RESULTS AND DISCUSSION

Polymer Preparation

The chlorination of PVF in CCl_4 suspension proceeds readily under the conditions described in the experimental part. Chlorine replaces hydrogen in the polymer, and HCl is evolved. The results, summarized in Figure 1, indicate that initially the reaction is fast, but it becomes considerably slower at higher conversions. A similar decrease in the rate of chlorination was previously observed by Fuchs and Louis⁷ in a study of the chlorination of PVC. Although we have found that the initial rates of chlorination of PVF and PVC are about the same, it is interesting to note that more than one chlorine atom per monomer unit can be incorporated relatively easily into PVF. With PVC this takes place only under drastic conditions⁷ or, according to other reports, not at all.⁹ It is known that PVC is chlorinated preferentially on the methylene group, and after the incorporation of one chlorine atom per monomer unit the polymer consists mainly of 1,2-dichloroethylene repeating units.⁷⁻¹³ Further chlorination of PVC would lead to the formation of CCl_2 groups, which is probably prevented by the bulky chlorine substituents. Since PVF is chlorinated about equally readily both on the CH_2 and CH groups (this will be discussed later), substitution of one chlorine atom per monomer unit will still leave about 50% of the CH_2 and CHF groups of the starting polymer unchanged. Thus, further substitution may occur without the formation of CCl_2 groups.

As the degree of chlorination of PVF increases, the reduced specific viscosity of the polymer decreases. This behavior is again similar to that of PVC. Whether this decrease in the reduced specific viscosity results from chain scission cannot be ascertained at present, since the molecular weight-solution viscosity relationship is not known.

The suspension chlorination of PVF can also be carried out at higher temperature or in reaction media other than CCl_4 . Such experiments are summarized in Table II. The data show that the degree of chlorination is increasing at higher temperature. If part of the CCl_4 is replaced with concentrated aqueous HCl , the reaction becomes faster; the chlorination

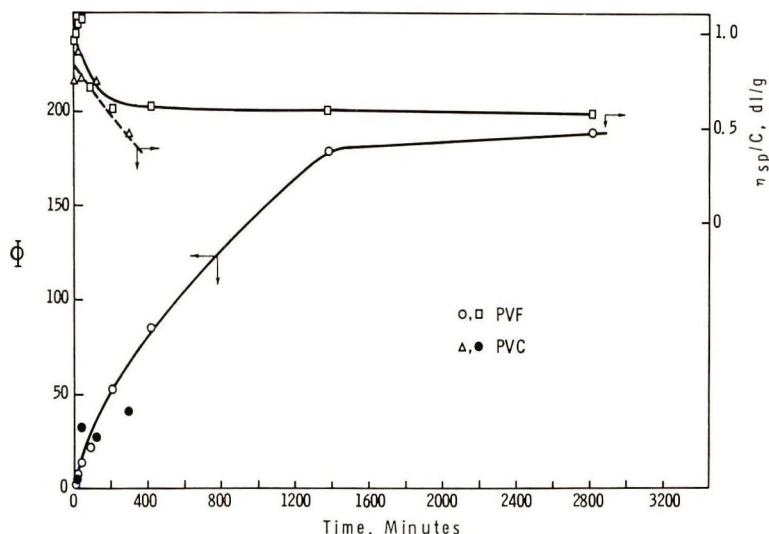


Fig. 1. Suspension chlorination of PVF and PVC in CCl_4 . Polymer, 10 g; CCl_4 , 150 ml; $21\text{--}51^\circ\text{C}$; 170 ml Cl_2 /min.

proceeds also readily in benzene. In CS_2 , the chlorination is extremely slow. This is probably caused by the reduced reactivity of Cl_2 complexed with CS_2 .¹⁵

TABLE II
Suspension Chlorination of PVF in Different Reaction Media^a

Sample	Reaction medium	Time of chlorination, min	Temperature of chlorination, $^\circ\text{C}$	Cl_2 , wt-%	η_{sp}/c , dl/g	Φ , $\text{Cl}_2/100$ monomer units
4	CCl_4	90	21–40	14.7	0.73	22
9	CCl_4	60	77	16.27	0.82	25
10	Benzene	240	80	42.9	0.76	95
11	CS_2	1440	46	4.16		5
12	CCl_4 -conc. HCl^b	30	21–46	9.2	0.85	13
13	CCl_4 -conc. HCl^b	60	25–43	20.09	0.91	32

^a Reaction conditions: 10 g PVF, 150 ml reaction medium, 170 ml Cl_2 /min.

^b 100 ml CCl_4 + 50 ml concentrated aqueous HCl (37–38% HCl).

Polymer Properties

Solubility. PVF is soluble only in strongly polar solvents such as *N,N*-dimethylacetamide or dimethyl sulfoxide at elevated temperatures, usually above 100°C . Chlorination increases the solubility of PVF, and polymers containing 30% or more chlorine are soluble in *N,N*-dimethylformamide at room temperature. At even higher degrees of chlorination (60% Cl), the product becomes soluble in the reaction medium, CCl_4 , as well. The in-

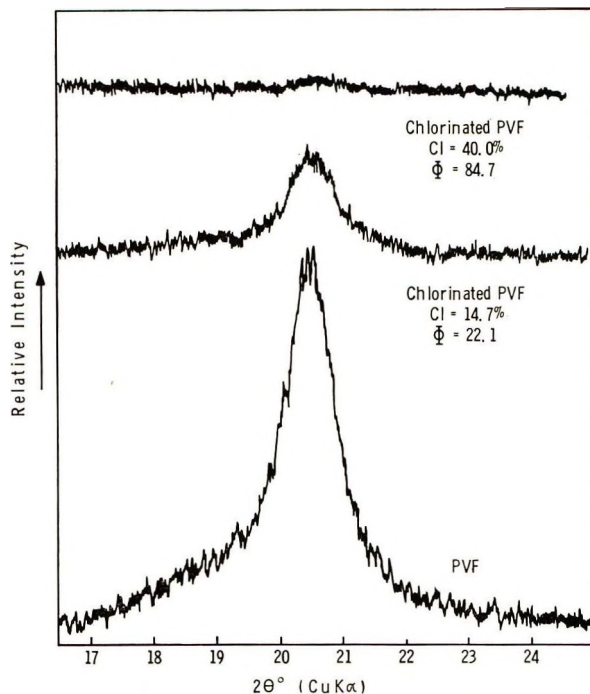


Fig. 2. X-ray diffraction spectra of PVF and chlorinated PVF.

creased solubility of the polymer allows the casting of films from organic solvents at room temperature.

Crystallinity, Softening Point. The investigations of Natta and co-workers¹⁶ have shown that PVF is crystalline in spite of being essentially atactic. We have found that as the degree of chlorination increases, the crystallinity of the products decreases. The powder x-ray diffraction spectra of representative chlorinated PVF's are shown in Figure 2. It can be seen that the sample with 40.0% chlorine shows no crystallinity, indicating that the polymer is completely amorphous. The decrease in the crystallinity of the chlorinated products is probably caused by randomly distributed chlorine atoms along the chain having different steric requirements than the hydrogens they replace.

A probable consequence of the reduced crystallinity is the lower softening point of chlorinated PVF compared to PVF; this allows the melt processing of chlorinated PVF at a lower temperature. Softening point data on compression-molded sheets are summarized in Figure 3. The results show that as the degree of chlorination increases, the softening point of the products decreases.

In this connection it is interesting to note that a similar decrease of the softening point has been reported in a study of polyethylene chlorination.¹⁶ On the other hand, chlorination increases the softening point of PVC^{3,4} as shown in Figure 3. Therefore, it appears that crystallinity, present

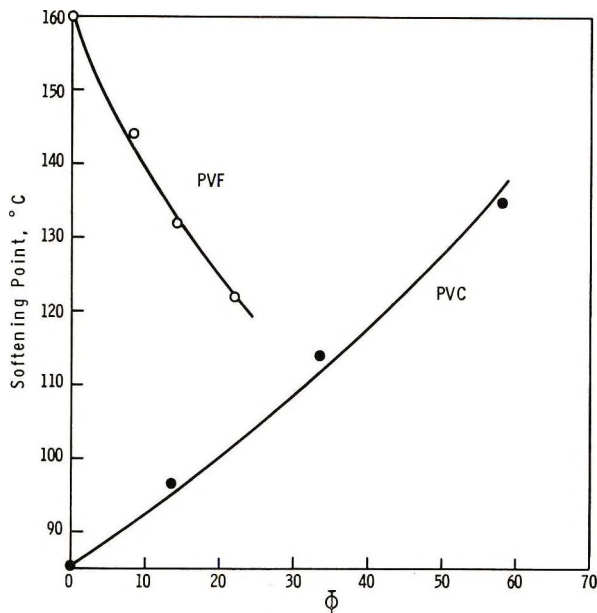
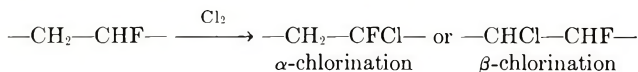


Fig. 3. Effect of chlorination on the softening point of PVF and PVC. Softening point by Vicat method (ASTM D1525-58T). PVF stabilized with 2% Ferro 203 (a cadmium octoate solution with organic inhibitor) and compression-molded at 182°C. PVC data from Bier.⁴

both in PVF and polyethylene, and not chemical similarity, such as found in PVF and PVC, determines the polymer softening point after chlorination.

Structure of Chlorinated PVF

When PVF reacts with chlorine, substitution may take place on either of the two carbon atoms of the polymer repeating unit. The nomenclature to be followed in this discussion distinguishes the incorporated chlorine atoms on the basis of their relative position with respect to the fluorine atom of PVF. Thus, substitution of the CHF or CH₂ groups will be referred to as α - or β -chlorination, respectively.



The principal goal of the structure analysis to be presented here is to determine the relative frequencies of α - and β -chlorinations and to describe the average composition of the chlorinated PVF chain. Others have made similar attempts with the analogous PVC which yielded contradictory results. Thus, on the basis of infrared analysis in the CH₂ and CH stretching vibration region, it was reported that PVC is exclusively β -chlorinated.⁹ (In this case, α - or β -chlorination refers to the position of the added chlorine atom with respect to the chlorine atom of PVC.) The other extreme possibility, 100% α -chlorination, has been claimed as the result of x-ray

diffraction measurements^{5,6} and the chemical reactivity of chlorinated PVC.^{17,18} There are also several reports, representing the intermediary opinion, that PVC is chlorinated in both α - and β -positions with β -chlorination predominating. This conclusion, which appears the most probable, is based on infrared investigations in the CH_2 bending vibration region^{7,8,11} and on proton magnetic resonance measurements.^{12,13}

¹⁹F NMR Analysis

The analytical method employed in this work to determine the relative amounts of α - and β -substituted chlorine atoms in chlorinated PVF is based on the qualitative and quantitative evaluation of the ¹⁹F NMR spectra of these polymers. As it is expected, the ¹⁹F resonance in chlorinated PVF, depending on the molecular environment, occurs at different magnetic fields. The first derivative of the ¹⁹F NMR absorption curve of PVF and that of a typical chlorinated PVF is presented in Figures 4a and 4b. By integrating the derivative curve, one can obtain the more familiar absorption curve. This is shown for chlorinated PVF in Figure 4c.

The resonance in the PVF spectrum at 100.0 ppm is in good agreement with that reported earlier,¹⁹ and it is assigned to structure I. The same structure, represented by the high field resonance at 94.8 ppm, is present in chlorinated PVF as well. The slight downfield shift of this resonance, compared to PVF, is probably caused by the β -chlorine substitution. A similar downfield shift of the ¹⁹F resonance, due to β -chlorine substituents, can be observed by comparing the NMR spectra of polytrifluoroethylene and polytrifluorochloroethylene.¹⁹



Based on comparison with model compounds, the additional downfield resonance in the spectrum of chlorinated PVF can be assigned to the α -chlorinated structure II. This assignment is reasonable because the shift of ¹⁹F resonance to lower magnetic field, due to substitution of an α -hydrogen with a more electronegative halogen atom, has been observed previously.^{19,20} Although in chlorinated PVF and in polytrifluorochloroethylene²¹ the resonance corresponding to structure II occurs at 26.8 ppm and 50.2 ppm, respectively, this difference is probably caused by the fact that β -fluorine substituents shift the ¹⁹F resonance to higher magnetic field.^{19,20}

In Figure 4c the areas under the absorption curve at high and low magnetic field are proportional to structures I and II, respectively. Therefore, by determining these areas, the relative amounts of I and II can be calculated. A summary of such calculations on a series of chlorinated PVF's is presented in Table III. The data show that the α -chlorinated structure II (low field ¹⁹F resonance) increases with the degree of chlorina-

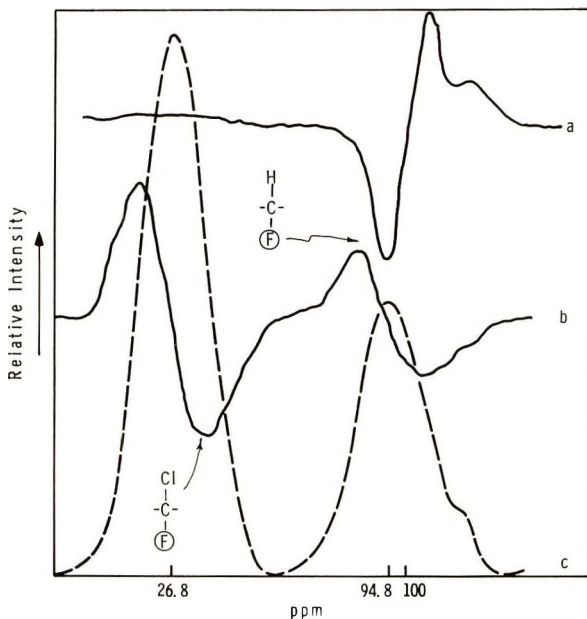


Fig. 4. 40 MHz ^{19}F NMR spectra of PVF and chlorinated PVF: (a) PVF first derivative curve, 83°C ; (b) chlorinated PVF (60.1% Cl, $\Phi = 178.9$), first derivative curve, 55°C ; (c) chlorinated PVF (60.1% Cl, $\Phi = 178.9$), calculated absorption curve.

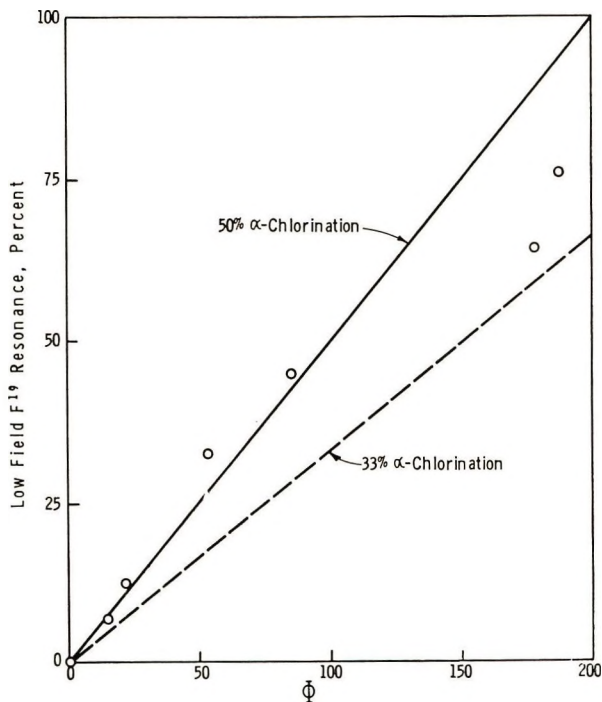


Fig. 5. Change of low-field ^{19}F resonance with degree of chlorination.

tion. If the results are plotted, as shown in Figure 5, the data points, up to a degree of chlorination of one chlorine atom per monomer unit, lie fairly close to the solid straight line drawn with a slope of 45° . From Figure 5 one can see that, if the degree of chlorination is 100, the amount of low field ^{19}F resonance (structure II) is approximately 50%. Since at this composition there is one chlorine atom for each fluorine atom in the polymer, the above result indicates that 50% of the chlorination occurs in α -position and, consequently, 50% in β -position.

TABLE III
Quantitative ^{19}F NMR Analysis of Chlorinated PVF

Sample	Φ , Cl/100 Monomer units	^{19}F resonance	
		High field, % ^a	Low field, % ^a
PVF	0	100	0
3	14.2	93.2	6.8
4	22.1	87.4	12.6
5	53.3	66.7	33.3
6	84.7	54.5	45.5
7	178.9	35.2	64.8
8	188.0	22.8	77.2

^a Per cent of total ^{19}F resonance.

Selectivity of Chlorination

The fact that the ratio of α - to β -chlorination in PVF is close to one points to considerable chemical selectivity operating in this system. In the absence of directive forces, and considering only the number of hydrogen atoms available for substitution, the expected α - to β -chlorination ratio would be 1:2. The ^{19}F NMR analysis corresponding to this "statistical" chlorination is represented by the broken straight line in Figure 5. Although at higher degrees of chlorination less than 50% of the chlorine atoms is substituted in the α -position, even in those cases the α -substitution is higher than it would be expected in a "statistical" chlorination.

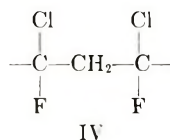
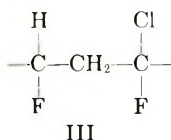
The selectivity favoring α -chlorination in PVI is actually in good agreement with results of free-radical chlorination of organic compounds. Thus, comparing the chlorination of aliphatic compounds, Fredricks and Tedder²² reported relative reactivities of 0.92 and 0.54 at the CHF (α -carbon) and CH_2 (β -carbon) groups of 2-fluorobutane, respectively. These values are lower than the relative reactivity of 1, determined at the CH_2 group of *n*-butane. To explain these results, the British workers suggest that in free-radical chlorination the chlorine atom is electrophilic; and, although fluorine deactivates by electron withdrawal in both α - and β -positions, it also stabilizes the incipient radical by conjugation in the α -position. This will result in an increase of the relative reactivity of the α -position. These arguments are also applicable to the chlorination of PVF, where the β -position is relatively more deactivated than in 2-fluorobutane, due to the presence of two adjacent CHF groups.

The selectivity, favoring α -chlorination, appears to be even slightly higher for a reaction carried out in benzene (sample 10 in Table II; low field ^{19}F resonance = 59.5%). This is probably caused by the reduced reactivity of Cl_2 complexed with benzene.¹⁵

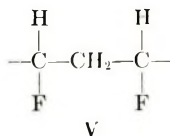
On comparing the chlorination of PVF with PVC, it is interesting to point out that the latter reacts predominantly in the β -position.⁷⁻¹³ Apparently, in the case of PVC, steric interference from the bulky chlorine atoms effectively hinders the reaction in the α -position. Since fluorine atoms are much smaller than chlorine atoms, steric effects in the chlorination of PVF probably play an unimportant role in determining the polymer structure.

^1H NMR Analysis

Additional information regarding the structure of chlorinated PVF can be obtained from the study of the high resolution ^1H NMR spectra. The ^1H NMR spectra of PVF and typical representatives of chlorinated PVF are presented in Figure 6. For our purpose, the sharp peaks at 2.5 and approximately 3.3 ppm can be disregarded; they are caused by solvent impurities. The spectrum of PVF consisting of CH_2 and CH protons centered at 2.1 and 4.9 ppm, respectively, is identical to that reported previously by Bovey and co-workers.²³ In the chlorinated PVF's an additional resonance centered around 3.5 ppm appears. On the basis of comparison with model compounds, we assign this resonance to CH_2 groups represented by structures III and IV.



In these structures the CH_2 group, compared to PVF, is flanked by additional halogen atoms which cause the proton resonance to appear at lower magnetic field due to deshielding. This effect can clearly be seen also in PVC,¹³ poly(vinylidene fluoride)¹⁹ (CH_2 resonance at 2.92 ppm), and in halogenated cyclobutane derivatives^{24,25} (CH_2 resonance in cyclobutane at 1.96 ppm, in 1-chloro-2,3,3-trifluorocyclobutane at 2.82 ppm, and in 1,1,2-trichloro-2,3,3-trifluorocyclobutane at 3.36 ppm). It is significant, however, that even in highly chlorinated PVF there remains a resonance at 2.1 ppm, indicating the presence of CH_2 groups with structure V.



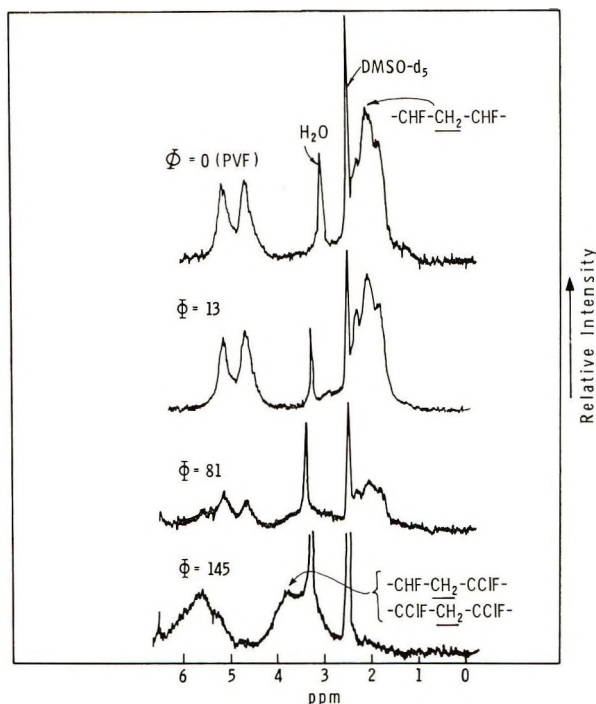


Fig. 6. 100 MHz ^1H NMR spectra of PVF and chlorinated PVF.

The resonance at 4.9 ppm in chlorinated PVF is assigned to CHF and CHCl groups; this becomes broad and shifts to lower magnetic field in the highly chlorinated samples.

A quantitative evaluation of the H^1 -NMR spectra is summarized in Table IV. The data show that the amount of high field CH_2 , characteristic of structure V, decreases, and the amount of low field CH_2 , characteristic for structures III and IV, increases with the degree of chlorination. All these changes are in the expected direction. If these data are plotted as shown in Figure 7, the amount of various protons in chlorinated PVF with a degree of chlorination 100 can be estimated. These estimates are also included in Table IV.

TABLE IV
Quantitative ^1H NMR Analysis of Chlorinated PVF

Sample	Φ , Cl/100 monomer units	H^1 resonance		
		High field CH_2 , % ^a	Low field CH_2 , % ^a	CH, % ^a
PVF	0	65.8	0	34.2
4	22.1	53.7	10.8	35.5
6	84.7	38.4	24.3	37.5
7	178.9	10.2	50.8	39.0
Estimated	100	35	28	37

^a Per cent of total ^1H resonance (resonance due to solvent impurities subtracted).

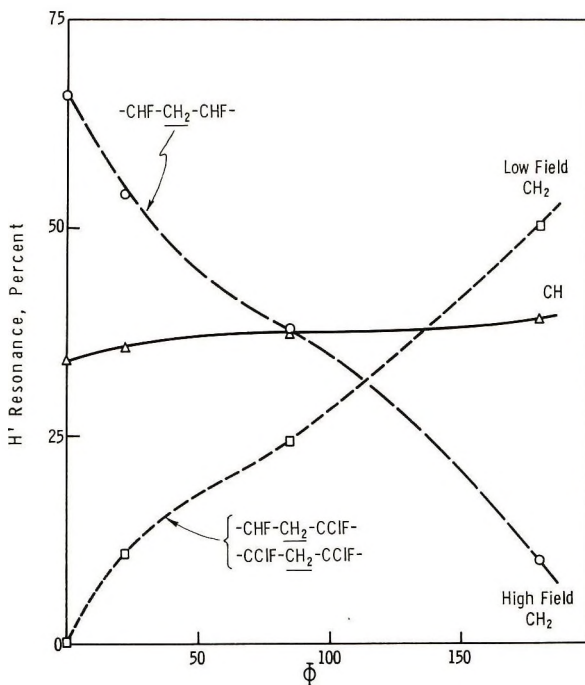
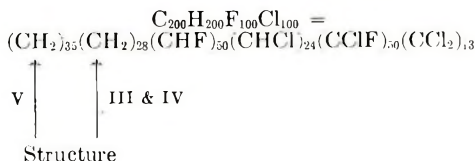


Fig. 7. Change of ¹H resonance with degree of chlorination.

Average Composition of the Polymer

Taking into account the results of the quantitative ¹H and ¹⁹F NMR analyses, one can give now a more detailed description of the chlorinated PVF chain. For the discussion, let us consider a polymer molecule containing 100 monomer units chlorinated to a degree of 100. The formula of this polymer can be given as C₂₀₀H₂₀₀F₁₀₀Cl₁₀₀. From ¹H NMR measurements we know that this polymer has 63 CH₂ groups (35 corresponding to structure V and 28 to structures III and IV) and 74 CH groups. The number of CH groups is equal to the sum of CHF and CHCl groups. Since from ¹⁹F NMR measurements we know that the polymer contains 50 CClF and 50 CHF groups, the number of CHCl groups is 74 - 50 = 24. Until now we have accounted for 74 chlorine atoms, and we postulate that the remaining 26 are part of 13 CCl₂ groups. Thus, the average composition of chlorinated PVF is the following:



Although the analytical method discussed here determines only the number of chemically different groups without giving information about their sequence in the polymer chain, a qualitative assessment of the homogeneity of the chlorination reaction is still possible. Considering

again a degree of chlorination of 100, it is evident that each α -chlorination involves the change of two adjacent CH_2 groups from the structure V to structure III. According to the above discussion, this results in a shift of the ^1H NMR resonance to lower magnetic field. From the ^{19}F NMR data it is known that there are 50 α -chlorine atoms in 100 monomer units; therefore, if these α -chlorine atoms were distributed randomly in the polymer chain, practically no high-field CH_2 resonance could be observed in the ^1H NMR spectrum.

The fact that there are 33 CH_2 groups with structure V in 100 monomer units indicates the presence of long polymer segments which are not α -chlorinated at all. Since certain segments of the polymer are not chlorinated in the more reactive α -position, these portions are apparently not chlorinated in the less reactive β -position either. From this conclusion, it is also obvious that other segments of the polymer must consist of monomer units containing more than one chlorine atom. This heterogeneity of chlorinated PVF probably results from the nonhomogeneous chlorination conditions.

References

1. G. D. Jones, in *Chemical Reactions of Polymers*, E. M. Fettes, Ed., Interscience, New York, 1964, (a) p. 259; (b) p. 262; (c) p. 258.
2. W. Trautvetter, *Kunststoffe Plastics*, **13**, 54 (1966).
3. W. Trautvetter, *Makromol. Chem.*, **101**, 214 (1967).
4. G. Bier, *Kunststoffe*, **55**, 694 (1965).
5. O. Seipold, *Chem. Techn.*, **1**, 107 (1949).
6. O. Seipold, *Chem. Techn.*, **5**, 467 (1953).
7. W. Fuchs and D. Louis, *Makromol. Chem.*, **22**, 1 (1957).
8. H. Germar, *Makromol. Chem.*, **86**, 89 (1965).
9. H. Kaltwasser and W. Klose, *Plaste Kautschuk*, **13**, 515 (1966).
10. H. Kaltwasser and W. Klose, *Plaste Kautschuk*, **13**, 583 (1966).
11. O. Fredriksen and J. A. Crowo, *Makromol. Chem.*, **100**, 231 (1967).
12. J. Petersen and B. Ranby, *Makromol. Chem.*, **102**, 83 (1967).
13. S. Sobajima, N. Takagi, and H. Watase, *J. Polym. Sci. A-2*, **6**, 223 (1968).
14. J. L. Koenig and J. J. Mannion, *J. Polym. Sci. A-2*, **4**, 401 (1966).
15. G. A. Russell, *J. Amer. Chem. Soc.*, **80**, 4987 (1958).
16. G. Natta, G. Allegra, I. W. Bassi, D. Sianesi, G. Caporiccio, and E. Torti, *J. Polym. Sci. A*, **3**, 4263 (1965).
17. H. Ohé, *J. Soc. Chem. Ind. Japan*, **46**, 1109 (1943); *ibid.*, **45**, 67, 824 (1942).
18. W. Fuchs and D. Louis, *Makromol. Chem.*, **22**, 1 (1957).
19. C. W. Wilson III and E. R. Santee, Jr., in *Analysis and Fractionation of Polymers* (*J. Polym. Sci. C*, **8**), J. Mitchell, Jr., and F. W. Billmeyer, Eds., Interscience, New York, 1965, p. 97.
20. R. E. Naylor, Jr., and S. W. Lasoski, Jr., *J. Polym. Sci.*, **44**, 1 (1960).
21. F. A. Bovey and G. V. D. Tiers, *Fortschr. Hochpolym. Forsch.*, **3**, 171 (1964).
22. P. S. Fredricks and J. M. Tedder, *J. Chem. Soc.*, **1961**, 3520.
23. F. A. Bovey, E. W. Anderson, and D. C. Douglass, *J. Chem. Phys.*, **39**, 1199 (1963).
24. J. H. Adams, Thesis, University of Colorado, Boulder, Colorado, 1965, p. 52.
25. J. D. Park, J. R. Dick, and J. H. Adams, *J. Org. Chem.*, **30**, 400 (1965).

Received April 20, 1970

Revised October 8, 1970

Studies in Some New Initiator Systems for Vinyl Polymerization. IV. Amino Acids as the Reducing Component

DINABANDHU PRAMANICK* and SANTI R. PALIT, *Department of Physical Chemistry, Indian Association for the Cultivation of Science, Jadarpur, Calcutta 32, India*

Synopsis

Amino acids have been found to form good redox initiator systems with halogens (Cl_2 and Br_2), KBrO_3 , KMnO_4 , and $\text{Fe}(\text{NH}_4)(\text{SO}_4)_2$. The three systems, viz., glycine- Cl_2 , taurine- Cl_2 , and sulfamic acid- Cl_2 incorporate amine, carboxy (or sulfoxy), chlorine, and hydroxy endgroups in the resulting polymers, the monomer investigated being mainly methyl methacrylate. On the basis of endgroup results it is suggested that initiation through amino acid radical, chlorine radical and also through some hydroxyl radicals takes place. The probable termination mechanism is discussed.

INTRODUCTION

In the course of our search for new redox initiator systems with halogens as one of the components (Parts I, II, and III of this series¹⁻³), we have found amino acids to be very efficient as reductants; some results are reported here.

EXPERIMENTAL

Materials

The amino acids used, e.g., glycine, alanine, sulfamic acid, etc. were all analytical reagent grade E. Merck products. Aqueous solutions of Cl_2 , Br_2 , and I_2 were prepared as described elsewhere.¹⁻³ Other oxidants used were either B.D.H. or E. Merck analytical reagents. Monomers were purified before use through usual procedures.

Polymerization Procedure

Aqueous polymerization of purified methyl methacrylate (MMA) and other monomers was carried out at ambient temperature ($\approx 30^\circ\text{C}$) under nitrogen atmosphere in conical Pyrex flasks in the dark. Poly-

* Present address: Department of Chemistry, Kalyani University, Kalyani, West Bengal, India.

merization proceeded through sol to a coagulated phase, and the polymers (after filtration, washing, and drying in an air oven at 45°C) were purified by the usual methods.⁴

Intrinsic Viscosity and Molecular Weight Determination

Intrinsic viscosity $[\eta]$ of the polymers was determined by an Ostwald viscometer. Number-average molecular weight \bar{M}_n for poly(methyl methacrylate) (PMMA) in benzene at $35 \pm 0.1^\circ\text{C}$ was calculated from the following equation:⁵

$$\bar{M}_n = 2.81 \times 10^5 [\eta]^{1.32}$$

Endgroup Analysis

The purified PMMA'S were subjected to dye techniques^{6,7} developed in our laboratory for the detection and estimation of the expected amine,⁸ carboxyl⁴ or sulfoxyl,⁹ halogen,¹⁰ and hydroxyl¹¹ end groups. The amount of halogen endgroup was calculated from the excess color after quaternization^{2,3} when both halogen and amine endgroups were present in the same polymer.

RESULTS

Glycine-Oxidant Systems

Of the large number of oxidants used, halogens (Cl_2 and Br_2), chloramine-T, BrO_3^- , Fe^{+3} , $\text{S}_2\text{O}_8^{2-}$, and MnO_4^- form good redox initiators in combination with glycine (Table I). However, chlorine has been used as the oxidant in further study.

Amino Acid-Halogen Systems

The activating effect of different amino acids (Table II) decreases in the order glycine > β -alanine > γ -valine, while α -leucine is nearly as effective as glycine. Sulfamic acid and taurine initiate better than glycine and β -alanine, respectively, indicating that the sulfoxy amino acid is more efficient than a carboxy amino acid. With sulfamic acid initiator the polymerization proceeds in the precipitated phase from the very beginning, and the polymers obtained have rather low $[\eta]$.

Among the halogens, Cl_2 is most potent. Br_2 also initiates, but with less efficiency, whereas I_2 does not initiate at all with any of the amino acids, though iodine is known sometimes to form an efficient redox component.^{1,3}

Monomer Selectivity

The glycine- Cl_2 initiator system initiates the polymerization of MMA, ethyl methacrylate, ethyl acrylate, and methyl acrylate after some induction period (IP) as shown in Table III. It also initiates the polymerization of acrylonitrile with a comparatively higher induction period,

TABLE I
Initiator Systems Involving Glycine as Reductant for the Aqueous
Polymerization of MMA^a

Oxidant	Induction period (IP), min	$[\eta]$	Maximum yield, %	Remarks
Cl ₂	32	1.08	42	Rate is faster with Cl ₂ than with Br ₂
Br ₂	55	0.66	31	
I ₂	—	—	No initiation	Lower concentrations of I ₂ were also tried unsuccessfully
Chloramine-T	210	1.68	39	Rate is very slow; polymerization continued for more than 24 hr
KBrO ₃ (acidified)	50	0.28	40	Polymerization continued for more than 24 hr; no initiation with neutral bromate
KClO ₄ (acidified and neutral)	—	—	No initiation	Probably reduction through non-radical path
KMnO ₄ (acidified and neutral)	5	1.13	62	MnO ₂ separates out immediately; rate faster when acidified than when neutral
K ₂ Cr ₂ O ₇ (acidified and neutral)	—	—	No initiation	Slow reduction takes place
[Co(NH ₃) ₅ Cl] ⁺⁺ Cl ₂	—	—	"	Pink color remained unchanged; probably no reduction
H ₂ O ₂	—	—	"	—
K ₂ S ₂ O ₈	66	0.85	37	Activation was observed by comparing with a blank
Fe(NH ₄)(SO ₄) ₂	7	1.41	53	Rate is fairly fast

^a Conditions: N₂ atmosphere, 30°C, [MMA] = $9.4 \times 10^{-2}M$, [glycine] = $1 \times 10^{-2}M$, [oxidant] = $1 \times 10^{-2}M$.

the yield being very low ($\approx 6\%$). Styrene (biphasic system) also polymerizes with a prolonged induction period and with a small conversion ($\approx 8\%$). Acrylamide gives a very low yield, whereas acrylic acid and vinyl acetate do not polymerize at all.

Endgroup Analysis

Glycine, taurine, and sulfamic acid each with Cl₂ were used as initiators for detailed endgroup study. The initial pH of the polymerizing mixture due to hydrolytic acidity of Cl₂ was between 4.8 and 5.3.

With glycine (Table IV), the polymer incorporated both amine and carboxyl endgroups to the extent of 0.36–0.53 and 0.28–0.61 endgroups per chain, respectively, the ratio of carboxyl to amine being 0.77–1.15. Some Cl endgroups (0.16–0.28) and some OH endgroups (0.31–0.62) per polymer chain were also found. The sum of the amine, Cl, and OH endgroups considered as the effective total endgroup (reasons to be apparent later) comes to slightly greater than 1.0 for this system.

TABLE II
 Amino Acid-Halogen Systems for Aqueous Redox Polymerization of MMA^a

Amino acid	Halogen	IP, min	Rate	[η]	Maximum yield, %
Glycine	Cl ₂	34	Moderate	0.99	43
H ₂ N—CH ₂ —CO ₂ H	Br ₂	58	"	0.62	32
β -Alanine	Cl ₂	50	"	0.92	36
H ₂ N(CH ₂) ₂ CO ₂ H	Br ₂	82	"	0.54	25
γ -Valine	Cl ₂	69	Slow	0.95	28
H ₂ N(CH ₂) ₃ CO ₂ H	Br ₂	102	"	0.53	16
α -Leucine	Cl ₂	40	Moderate	1.10	48
CH ₃ (CH ₂) ₃ CH—CO ₂ H					
NH ₂	Br ₂	61	"	0.71	35
Aspartic acid	Cl ₂	183	Slow	1.22	14
H ₂ N—CH—CO ₂ H	Br ₂	310	Very slow	0.87	8
CH ₂ —CO ₂ H					
Taurine	Cl ₂	62	Fast	1.05	40
H ₂ N(CH ₂) ₂ SO ₃ H	Br ₂	91	"	0.87	31
Sulfamic acid	Cl ₂	52	Fast	0.25	51
H ₂ N—SO ₃ H	Br ₂	76	"	0.17	32

^a Conditions: N₂ atmosphere, 30°C, [MMA] = $9.4 \times 10^{-2}M$, [halogen] = $1.30 \times 10^{-3}M$, [amino acid] = $1 \times 10^{-3}M$.

With taurine (Table V), the polymers contain both amine and sulfonate endgroups to the extent of 0.36–0.60 and 0.39–0.74 per chain, respectively. The sulfonate to amine ratio is 1.07–1.23. A small proportion of Cl endgroups (0.11–0.32 Cl per chain) and OH endgroups (0.08 to 0.26 per chain) is also present. The effective total endgroup as defined above is about one per chain.

 TABLE III
 Aqueous Polymerization of Different Vinyl Monomers by Glycine-Cl₂ Redox Initiators^a

Monomer	IP, min	Rate	[η]	Yield, %
Methyl methacrylate	30	Moderate	1.13	46
Ethyl methacrylate	25	"	1.08	48
Ethyl acrylate	42	"	1.25	16
Methyl acrylate	37	"	0.92	13
Acrylic acid	—	—	—	No initiation
Acrylonitrile	60	Slow	0.63	6
Acrylamide	—	—	—	Practically nil
Styrene ^b	180	Very slow	1.37	8

^a Conditions: N₂ atmosphere, 30°C, [monomer] = 1 vol-%, [Cl₂] = $1.30 \times 10^{-3}M$, [glycine] = $1 \times 10^{-3}M$.

^b 1 g in 100 cc water.

TABLE IV
Endgroup Results on PMMA Obtained by Initiation with Glycine-Cl₂ System in Aqueous Medium^a

[Glycine], <i>M</i> × 10 ⁵	[Cl ₂], <i>M</i> × 10 ⁴	[η]	Endgroups per chain				Total (effective)	Car- boxyl/ amine
			Amine	Carboxyl	Cl	OH		
1.00	1.37	3.02	0.36	0.28	0.23	0.62	1.21	0.77
10.00	1.37	2.17	0.48	0.42	0.16	0.49	1.13	0.88
100.00	1.37	1.57	0.52	0.54	0.18	0.45	1.15	1.03
500.00	1.37	1.21	0.53	0.61	0.19	0.31	1.03	1.15
100.00	6.85	1.18	0.49	0.51	0.26	0.38	1.13	1.04
100.00	13.70	0.99	0.46	0.45	0.28	0.51	1.25	0.98

^a Conditions: N₂ atmosphere, 30°C., [MMA] = 9.4 × 10⁻²*M*.

With sulfamic acid (Table VI), both amine and sulfonate endgroups have been incorporated to the extent of 0.21–0.33 and 0.29–0.43 per chain, respectively, the sulfonate:amine ratio being 1.26–1.52. Some Cl endgroups (0.13–0.22) and some OH endgroups (0.25–0.38) per chain are also present. The effective total endgroup is slightly less than one.

DISCUSSION

Of the oxidants used (Table I), Cl₂, Br₂, chloramine-T, KBrO₃ and Fe-(NH₄)(SO₄)₂ have no initiating power by themselves, but the other two (KMnO₄ and K₂S₂O₈) do themselves initiate, though after some induction period. Definite proof of activation by glycine in the case of the last two oxidants has been observed by comparison with a control.

Table II indicates that activating efficiency of the amino acid increases with the proximity of the amino and acidic groups, the stronger sulfonic group providing higher initiating power than the weaker carboxyl group (compare β-alanine and taurine). Sulfamic acid, in which the amino and acidic groups are closest, is the most efficient among the amino acids used,

TABLE V
Endgroup Results of PMMA Obtained by Initiation with Taurine-Cl₂ System in Aqueous Medium^a

[Taurine], <i>M</i> × 10 ⁵	[Cl ₂], <i>M</i> × 10 ⁴	[η]	Endgroups per chain				Total (effective)	Car- boxyl/ amine
			Amine	Sulfo- nate	Cl	OH		
1.00	6.40	3.93	0.36	0.39	0.11	0.26	0.83	1.08
10.00	6.40	1.97	0.58	0.62	0.32	0.08	0.98	1.07
100.00	6.40	0.77	0.59	0.72	0.30	0.12	1.01	1.22
1000.00	12.80	0.64	0.60	0.74	0.25	0.17	1.02	1.23
100.00	1.28	1.02	0.52	0.59	0.23	0.13	0.98	1.13

^a Conditions: N₂ atmosphere, 30°C., [MMA] = 9.4 × 10⁻²*M*.

TABLE VI
Endgroup Results of PMMA obtained by Initiation with Sulfamic Acid-Cl₂
System in Aqueous Medium^a

[Sulfamic acid] × 10 ⁴	[Cl ₂], × 10 ³	[η]	Endgroups per chain				Total (effective)	Sulfonate/amine
			Amine	Sulfonate	Cl	OH		
1.00	1.12	0.38	0.21	0.32	0.22	0.38	0.81	1.52
2.50	1.12	0.31	0.22	0.29	0.18	0.31	0.71	1.32
5.00	1.12	0.27	0.31	0.43	0.17	0.34	0.82	1.37
7.50	1.12	0.22	0.30	0.39	0.13	0.29	0.72	1.30
10.00	1.12	0.17	0.33	0.41	0.21	0.25	0.79	1.26

^a Conditions: N₂ atmosphere, 30°C, [MMA] = 9.4 × 10⁻²M.

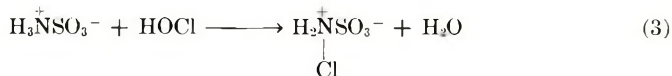
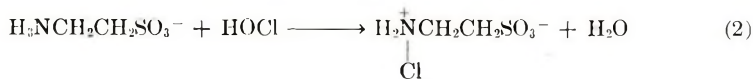
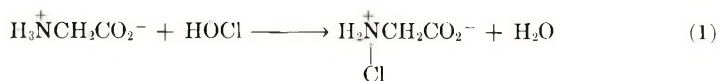
the low [η] of the polymers being probably due to too fast generation of radicals and rapid coagulation.

The interesting monomer selectivity of glycine-Cl₂ initiator probably arises from the interference due to Cl₂ addition to the different monomers similar to the addition of bisulfite compounds to monosubstituted monomers suggested earlier by Bacon¹² and others.^{13,14} Here disubstituted monomers (CH₂=CXY) like MMA and ethyl methacrylate sterically hinder the addition of Cl₂ and favor the initiation process leading to efficient polymerization. With other monomers (monosubstituted) which would allow free addition of Cl₂, either polymerization is very inefficient or no initiation takes place at all, depending upon the bulk and polarity of the substituent.

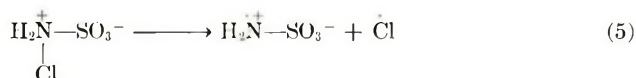
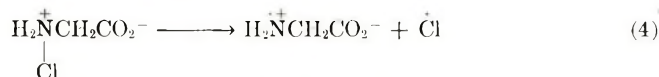
The endgroup results with all the three systems, viz., glycine-Cl₂, taurine-Cl₂ and sulfamic acid-Cl₂, show that carboxyl (or sulfonate) endgroups increase with increase of amine endgroup and decrease with a decrease of the latter. Moreover, the amount of acid endgroup is approximately the same as amine endgroup in all the glycine-Cl₂-initiated polymers, though with taurine and particularly with sulfamic acid the acid to amine ratio is somewhat greater than unity (to be clarified later).

Amino acids exist in aqueous solution as zwitterions and are known¹⁶ to react with aqueous Cl₂ or better with NaOCl to produce an unstable *N*-chloro derivative. Our experimental findings that chloroamine-T, which reacts slowly with water to generate HOCl, initiates polymerization in the presence of glycine to yield polymers with comparable conversion indicates that in aqueous solution the potential oxidant is HOCl and not Cl₂. This is further supported by the fact that an attempt to initiate the polymerization of MMA by glycine-Cl₂ initiator in nonaqueous media like formamide and methylformamide where formation of HOCl is not possible has proved unsuccessful.

Formation of the *N*-chloro derivative through a nucleophilic displacement on the Cl₂ by the amine as in the case of amine-chlorine reaction³ is precluded, since in the zwitterion the lone pair of electrons on the N atom is already donated to H⁺ ion. The *N*-chloro derivatives are probably formed as shown in eqs. (1)–(3).



The intermediate *N*-chloroamino acid derivatives are expected to undergo homolytic cleavage at room temperature to produce chlorine and aminium radicals [eqs. (4) and (5)].



Decomposition of similar compounds, *N*-haloammonium salts, to generate the same type of radicals has recently been reported^{16,17} in the literature. In fact, this reaction has proved a potential synthetic path¹⁸ for preparing halogenated amines from substituted olefins. A further example of quaternary nitrogen compounds generating $\overset{+}{\text{N}}\text{R}_3$ ion radicals on decomposition is to be found in the quaternary hydroxylamine derivative, the postulated intermediate, for example, in the reaction of benzoyl peroxide and dimethylaniline.¹⁹

The results of endgroup analysis discussed earlier and consideration of the mechanism of initiation by amine-halogen initiators³ suggest that the entire amino acid radical bearing both amino and acidic groups (carboxy or sulfoxy) is one of the initiating species making the amounts of amine and acid endgroups equal.

Slightly higher results of sulfonate endgroup compared with amine endgroup in case of taurine and particularly in case of sulfamic acid is probably due to a limitation of the dye-partition method. This arises from the fact shown²⁰ by independent experiments that when a polymer with an $\text{SC}(=\overset{+}{\text{N}}\text{H}_2)\text{NH}_2$ endgroup and another with a SO_3H group are present in solution in equivalent amounts, the response for amine was much less and the response for SO_3H was slightly less than when they are present separately. This probably arises from the stronger association of these oppositely charged endgroups compared with their respective association with the oppositely charged dye ions in the dye-partition tests. Consequently, the results of amine and sulfonate endgroups obtained by the dye-partition technique may be somewhat lower than the actual amount present in such systems.

It has been found that Cl incorporation is always very small, the amino acid radical being the major incorporated species. Besides, all the polymer

samples contain some OH endgroup, in contrast to our previous results^{2,3} with other ammonia compounds containing initiators where the OH endgroup was totally absent. These results indicate that some of the Cl radicals probably react with water to produce OH radicals which appear as polymer endgroups.



This also suggests that while ammonia² or amines³ are very strong scavengers for OH radicals, aminoacids in zwitterionic forms are either non-scavengers or very feeble scavengers for them.

The effective total endgroup incorporated per polymer molecule is about one. The mode of termination appears, therefore, to be disproportionation between the macroradicals, which is usually definitely the case for PMMA radicals.²¹⁻²³ However, some terminations by primary or small radicals²⁴ in the particle-phase polymerization of MMA in an aqueous medium can not be ruled out, since our total endgroup results may be somewhat lower than the actual value, as discussed earlier.

Thanks are due to C.S.I.R. for financial assistance to D. P.

References

1. M. K. Saha, M. Sen, and D. Pramanick, *J. Polym. Sci. A-1*, **4**, 2137 (1966).
2. D. Pramanick and S. R. Palit, *J. Polym. Sci. A-1*, **6**, 2179 (1968).
3. D. Pramanick and S. R. Palit, *J. Polym. Sci. A-1*, **7**, 47 (1969).
4. S. R. Palit and P. Ghosh, *J. Polym. Sci.*, **58**, 1225 (1962).
5. J. H. Baxendale, S. Bywater, and M. G. Evans, *J. Polym. Sci.*, **1**, 237 (1946).
6. S. R. Palit, *Makromol. Chem.*, **36**, 89 (1959).
7. S. R. Palit, *Chem. Ind. (London)*, **1960**, 1531.
8. S. Maiti and M. K. Saha, *J. Polym. Sci. A-1*, **5**, 151 (1967).
9. P. Ghosh, S. C. Chadha, A. R. Mukherjee, and S. R. Palit, *J. Polym. Sci. A*, **2**, 4433 (1964).
10. M. K. Saha, P. Ghosh, and S. R. Palit, *J. Polym. Sci. A*, **2**, 1365 (1964).
11. P. Ghosh, P. K. Sengupta, and A. Pramanick, *J. Polym. Sci. A*, **3**, 1725 (1965).
12. R. G. R. Bacon, *Trans. Faraday Soc.*, **42**, 140 (1946).
13. F. H. Firsching and I. Rosen, *J. Polym. Sci.*, **36**, 305 (1959).
14. C. Walling, *Free Radicals in Solution*, Wiley, New York, 1957.
15. J. P. Greenstein and M. Winitz, *Chemistry of Amino Acids*, Vol. 1, Wiley, New York, 1961.
16. M. E. Wolff, *Chem. Revs.*, **63**, 55 (1963).
17. R. S. Neale and R. L. Hinman, *J. Amer. Chem. Soc.*, **85**, 2666 (1963).
18. R. S. Neale, *Tetrahedron Letters*, **1966**, 483.
19. C. Walling and N. Indictor, *J. Amer. Chem. Soc.*, **80**, 5814 (1958).
20. B. Mandal, and S. R. Palit, *Rev. Macromol. Chem.*, **3**, 225 (1968).
21. C. H. Bamford and A. D. Jenkins, *Nature*, **176**, 78 (1955).
22. C. H. Bamford, A. D. Jenkins, and R. Johnston, *Trans. Faraday Soc.*, **55**, 179 (1959).
23. J. C. Bevington, H. W. Melville, and R. P. Taylor, *J. Polym. Sci.*, **12**, 449 (1954); *ibid.*, **14**, 463 (1954).
24. M. Durup and M. Magat, *J. Polym. Sci.*, **18**, 586 (1955).

Received April 28, 1970

Revised November 11, 1970

Radiation-Induced Crosslinking of Cellulose with Acrolein*

M. M. ISHANOV, U. A. AZIZOV, M. S. NIGMANKHODZHAYEVA,
and Kh. U. USMANOV,
*Research Institute for Cotton Cellulose Chemistry and Technology,
Tashkent GSP, Tashkent, USSR*

Synopsis

The process of radiation-induced crosslinking of cellulose is found to be highly influenced by radiation dosage and dose as well as by the solvents used and their concentration. The best crease resistance has been obtained in cases when cellulose is crosslinked with acrolein in the vapor phase. Moreover, the process is entirely radiation-induced and practically no homopolymer is formed. Chemical analysis and investigations of infrared spectra indicate that crosslinking proceeds on vinyl as well as on aldehyde groups of acrolein.

Modification of cellulose properties by means of chemical crosslinking with bifunctional compounds, aimed at developing improved crease- and wrinkle-resistance, has been discussed earlier; however, the process of radiation-induced crosslinking has not been studied previously. The crosslinking of cellulose with compounds possessing two and more double bonds by means of radiation is not believed to give the desired results; for this reason some authors suggest combining it with chemical crosslinking.^{1,2}

The present work is an attempt to investigate the effect of dose rate, radiation dose, various solvents, and many other factors on the radiation-induced crosslinking of cellulose with acrolein and to illustrate some properties of the crosslinked cellulosic derivatives.

The problem of obtaining crease resistance in cotton fabric by means of chemical crosslinking of cellulose macromolecules and acrolein as well as investigations of the mechanism of the process have been earlier discussed in number of publications.³⁻⁵ It is shown that in the course of chemical interaction of acrolein with cellulose, depending on the reaction conditions, the process of grafting of polyacrolein appears to be simultaneous with crosslinking of cellulose macromolecules. This makes the cellulosic products shrink- and crease-proof. The main drawback of the method of crosslinking lies in the increasing homopolymer content at reduced strength values (50%), which is highly undesirable for textile applications.

* Paper presented at IUPAC meeting in Macromolecular Chemistry, Budapest, August 26, 1969.

We used two methods of crosslinking in cellulose: samples of cellulose have been irradiated (1) in acrolein solutions and (2) irradiated in acrolein vapors. Standard methods and samples of purified cotton fibers and fabric (coarse calico) at 5–6% RH were used in our investigations.⁶ Acrolein was previously distilled at 49–51°C/750 mm Hg (lit. bp. 52–53°C/760 mm Hg); its refractive index n_D^{20} was 1.4020.

Crosslinking of Cellulose in Acrolein Solutions

Water, ethyl alcohol, acetone, diethyl ether, and benzene were used as solvents for acrolein at 0.6–20% monomer concentration and 1:3 bath modulus, which is quantitative ratio of cellulose and acrolein solution. Samples of cellulose were put into glass vessels, filled with acrolein solution, sealed, and then exposed to γ -rays from a ⁶⁰Co source at 40–43°C. A quantity of homopolymer was removed from the irradiated samples by extraction with heated *p*-cresol until constant weight was obtained. Table I pre-

TABLE I
Effect of Acrolein Concentration and Solvents on Radiation-Chemical Yield and Some
Physicomechanical Properties of Modified Cotton Fabric (Coarse Calico)
(Dose 1 Mrad, Dose Rate 9 rad/sec)

Solvent	Acrolein concn, %	Weight gain, %		G, mole/100 eV	Warp strength, kg	Axial elonga- tion, mm	Crease recovery angles (W + F), degrees
		Before irradiation	After extraction				
Water	None	—	—	—	21	5	107
	2.5	3.6	—	—	—	—	—
	5.0	5.2	—	—	—	—	—
	10.0	10.0	0.8	164	21	4	116
Ethyl alcohol	20.0	25.0	5.6	1148	21	4	126
	2.5	1.6	—	—	—	—	—
	5.0	2.5	—	—	—	—	—
	10.0	6.0	1.5	30	21	4	124
Acetone	20.0	18.0	8.0	1640	18	4	147
	0.62	1.2	0.9	104	19	5	118
	1.25	1.9	1.1	225	19	5	120
	2.5	3.3	2.1	430	19	5	138
	5.0	4.3	2.8	574	18	4	148
Diethyl ether	10.0	7.4	6.4	1312	18	4	156
	0.62	2.4	1.4	287	19	5	130
	2.5	4.7	3.1	635	18	5	145
	5.0	6.0	5.0	1025	18	4	154
	10.0	11.8	8.2	1681	17	4	189
Benzene	20.0	15.2	8.4	1722	16	4	191
	1.25	0.3	0.3	61	19	4	120
	2.5	0.8	0.7	146	19	4	125
	5.0	1.5	1.4	297	19	4	130
	10.0	3.2	2.2	453	18	4	141
	20.0	6.7	4.1	840	17	3	157

TABLE II
Effect of Dosage and Radiation Dose Rate on Yield and some Physicomechanical Properties of Cotton Fabric (Coarse Calico) in Crosslinking of Cellulose with Acrolein Solutions at 20% Monomer Concentration

Radiation dose rate, rad/sec	Dosage, Mrad	Acetone as solvent						Diethyl ether as solvent					
		Weight gain, %			Strength, kg	Elongation, mm	G, mole/100 eV	Weight gain, %			Strength, kg	Elongation, mm	G, mole/100 eV
		Before extraction	After extraction	After extraction									
70	0.25	5.0	4.3	21	4	3550	6.5	4.9	19	3	4000	19	3
	0.5	8.5	6.5	21	4	2650	9.0	6.9	19	3	2840	19	3
	1.0	15.9	8.5	19	3	1740	16.0	8.9	18	3	1830	18	3
	1.5	19.5	9.4	19	3	1280	22.0	10.2	18	3	1400	18	3
	0.1	3.4	2.7	23	4	5550	3.5	3.0	21	4	6150	21	4
	0.25	4.8	4.1	22	4	3380	6.1	4.9	20	4	4000	20	4
265	0.5	8.8	5.8	21	3	2380	8.6	6.3	20	3	2600	20	3
	1.0	12.6	7.9	20	3	1620	14.0	8.7	19	3	1780	19	3
	1.5	18.0	8.7	19	3	1190	19.0	9.6	19	3	1315	19	3
	0.1	2.2	1.7	22	4	3500	2.7	2.5	22	4	5150	22	4
	0.5	6.9	3.7	20	3	1520	6.9	4.6	20	4	1900	20	4
	1.0	8.0	5.3	20	3	1095	8.4	5.7	20	3	1170	20	3
1.5	11.0	7.0	20	3	960	12.5	7.2	20	3	985	20	3	

sents data showing the effect of monomer concentration in different solvents on the radiation-induced crosslinking of cellulose with acrolein.

As shown in Table I, an increase in the monomer concentration increases the overall conversion of acrolein itself, radiation-chemical yield (G), and weight gain after extraction for all solvents investigated. The overall conversion which comprises the amount of acrolein needed for the interaction with cellulose and for homopolymerization, reaches a maximum when water and diethyl ether are used as acrolein solvents. When water is used as solvent for acrolein, the process is usually accompanied by increased homopolymer formation. This might be attributed to the increased total free radical content, which, as a rule, is the result of radiolysis of water.

It should be noted, that in this case a weight gain is followed by some decrease in breaking strength and elongation and rising values of crease recovery angles. The best crease resistance has been achieved when diethyl ether was used as the solvent for acrolein, which might be attributed to inactivity of aldehyde groups towards ethers. Also, the estimated effects of radiation dose and dose rate show that increasing doses cause marked weight gain at a decreased radiation-chemical yield (G), accompanied by low breaking strength and small elongation. The increased dose, though, applied at an equal integral dose, causes a decrease in weight gain, which is attributed to the radiation-chemical processes proceeding on radicals as well as on chains (Table II).

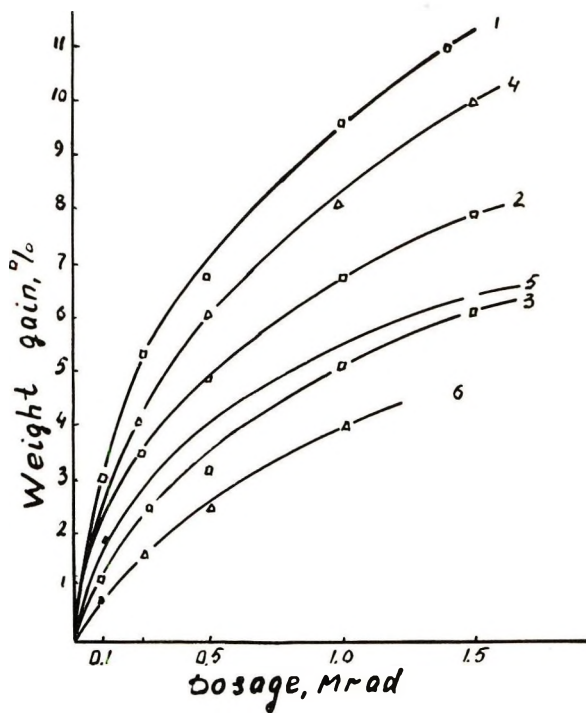
Thus, the irradiation of cellulose in various acrolein solutions makes possible an increase in the values of crease recovery angles at negligible losses in the initial breaking strength and elongation. The presence of a comparatively high content of homopolymer makes the process economically ineffective, however.

Radiation-Induced Crosslinking of Cellulose with Acrolein in Vapor Phase

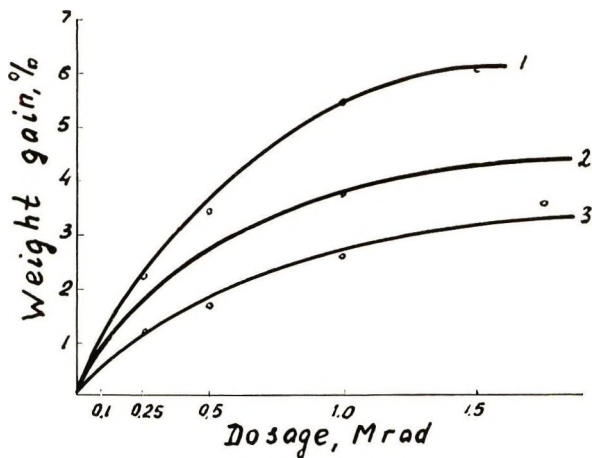
This process is performed in special vessels,⁶ with continuous feed of acrolein vapor. Hydroquinone serves as an inhibitor. The process is carried out at 10^{-3} mm Hg pressure in the presence of dry monomer; systems saturated with water, ethyl alcohol, diethyl ether, or acetone vapor or air have been used. It is found, that all polyacrolein bonds to the crosslinked cellulose. The irradiated samples were washed with water and dried in air in order to remove the adsorbed acrolein.

In all cases we studied the effect of radiation dose and dose rate on the kinetics of the process and some properties in the modified fabric.

Results given in Table III and in Figure 1 show that for a higher radiation dose at a given dose rate the weight gain increases, while the radiation-chemical yield (G) and the rate of the process (V) generally fall (Fig. 2), beginning from an initial high. This might be attributed to the fact that cellulose can adsorb molecules of the monomer initially. At a later time, the process becomes dependent upon the rate of acrolein diffusion into cellulose. Figure 1 shows that the increase in dose rate at a given integral radia-



(a)



(b)

Fig. 1. Effect of radiation dose and dose rate on the yield of cellulose crosslinked with acrolein vapor: Weight gain obtained in systems (a) with dry acrolein vapor (curves 1-3) and in water-saturated systems (curves 4-6) and (b) with acrolein vapor in air: (1, 4) 70 rad/sec; (2, 5) 110 rad/sec; (3, 6) 300 rad/sec.

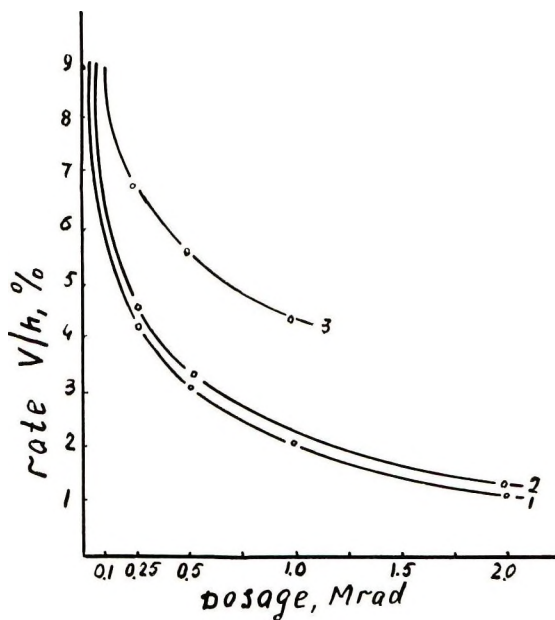


Fig. 2. Changes in the rate V of radiation-induced crosslinking of cellulose with acrolein vapor at various dose rates: (1) 70 rad/sec; (2) 110 rad/sec; (3) 300 rad/sec.

TABLE III
Physicomechanical Properties of Cotton Fabric (Coarse Calico) Crosslinked with Acrolein from Vapor Phase at Various Radiation Doses

Radiation dose rate, rad/sec	Weight gain, %	G , mole/100 eV	Aldehyde groups, %		Warp strength, kg	Elongation, mm	Crease recovery angle (W + F) degrees
			Bound	Free			
—	Initial	—	—	—	22	5	107
70	0.4	8200	—	—	20	4	134
	0.7	5710	—	—	19	4	144
	2.5	5125	64.0	36.0	19	4	154
	4.1	3370	69.4	30.6	19	4	174
	6.0	2460	77.9	22.1	19	4	199
	8.0	1640	79.5	20.5	18	3	221
	10.0	1373	83.4	16.6	17	3	242
110	13.0	1332	89.4	10.6	15	3	248
	1.9	3895	59.0	41.0	22	5	142
	3.5	2950	66.3	33.7	21	4	152
	4.0	1602	72.0	28.0	20	4	168
	4.9	1004	72.6	27.4	18	3	178
300	7.5	768	78.6	21.4	17	3	221
	0.8	1640	44.0	56.0	22	5	122
	1.8	1480	50.0	50.0	22	4	136
	2.9	1190	54.0	46.0	22	4	160
	4.0	820	70.7	29.3	18	4	165

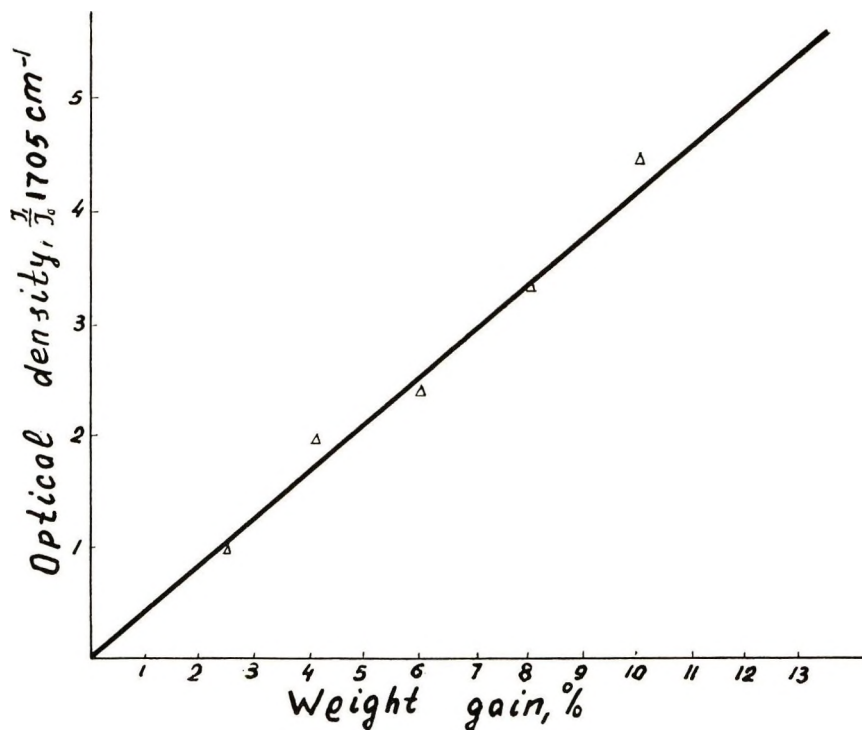
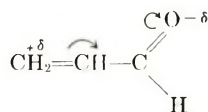


Fig. 3. Changes in free aldehyde group content, as shown by change in optical density vs. weight gain.

tion dose lowers radiation-chemical yield (G) and weight gain in all studied systems and samples. This is characteristic of all radiation-chemical and radical-chain processes. It must be noted, though, that the increase in weight gain causes low breaking strength and small elongation and markedly improves crease resistance. For example, an 0.8% weight gain instead of 0.4% can be obtained at an increased radiation dose as compared to that previously used (0.01 Mrad) at 70 rad/sec dose rate. The breaking strength falls from 20 to 18 kg at 8 mm elongation, with crease recovery angles ($W + F$) rising from 134° to 221° . Such an improvement in crease resistance on one hand and lowered breaking strength at small elongation on the other characterize the crosslinked cellulosic derivatives.

The conjugated molecule of acrolein itself presents certain interesting aspects.



Due to the presence of the electron-accepting oxygen atom, the average electron density shifts towards oxygen; this is the reason the vinyl group becomes more reactive than the aldehyde. Investigations of changes in both

TABLE IV
Radiation-Induced Crosslinking of Cellulose with Acrolein Vapor
at 70 rad/sec Dose Rate

Ambient atmosphere	Weight gain, %	G, mole/100 eV	Reaction rate, V, %/hr	Warp strength, kg	Elongation, mm	Crease recovery angles (W + F), degrees	
Water vapor	3.0	6150	7.5	20	4	140	
	(saturated)	5.3	4350	5.3	20	—	
	no air	6.7	2750	3.4	20	4	187
		9.6	1970	2.4	18	3	—
		11.0	1500	1.8	18	3	206
Diethyl ether	2.2	4530	5.62	19	4	126	
	(saturated)	3.0	2470	3.0	19	136	
	no air	4.0	1640	2.0	18	4	145
		5.5	1125	1.4	17	3	181
		6.2	850	1.0	16	3	183
8.1		515	0.7	15	3	183	
Air	1.3	2665	3.27	20	4	117	
	2.2	1804	2.2	20	4	130	
	3.4	1594	1.8	20	4	146	
	5.5	1125	1.4	19	4	160	
	6.1	943	1.2	16	3	177	
	8.1	833	1.0	16	3	201	
	11.0	615	0.7	15	3	206	
Acetone vapor,	2.5	5150	6.5	19	4	139	
	3.8	3110	3.8	19	4	147	
	no air	5.9	2420	2.9	18	3	177
		7.1	1455	1.8	17	3	—
		8.8	1185	1.1	17	3	185

vinyl and aldehyde groups are of interest, especially when various radiation doses and dose rates are used. Application of either integral or differential methods in the studies of infrared spectra show that no absorption band characteristic of the vinyl group is observed in the cellulose preparations subjected to crosslinking with acrolein in the vapor phase, whereas there is a carbonyl group band in the 1705 cm^{-1} region. Moreover, the intensity of this band depends linearly on the increase in weight gain (Fig. 3). The hypiodide method of determination of aldehyde groups⁷ shows that the increase in radiation dose lowers the content of free aldehyde groups while the number of bound aldehyde groups rises. This shows, that aldehyde groups also take part in the crosslinking of cellulose macromolecules by means of hemiacetal bonds. As the data of Table III show, crease resistance in cotton fabric depends on content of bound aldehyde groups as well as on the weight gain. For example, 70% aldehyde groups content and crease recovery angles up to 170° can be obtained at 4% weight gain, regardless of the radiation dose and dose rate. Peculiarities of this kind are observed in cases when cellulose is subjected to radiation-induced crosslinking with acrolein performed either in the presence of water and diethyl ether or in the presence of acetone or air. The results are given in Table IV and

in Figure 1. As Table IV and Figure 1 show, a higher weight gain can be obtained in systems saturated with water vapor than in systems with irradiation of cellulose in dry acrolein vapor under otherwise similar experimental conditions. This is believed to be due to changes in the structure of cellulose on swelling, when diffusion of acrolein into cellulose pores reaches a maximum.

We found low weight gains in systems saturated with acetone or diethyl ether vapor and in air, as compared to the cases, when cellulose was irradiated in pure acrolein vapor. The lowest weight gains were on irradiation in air. A 6% gain can be obtained with the use of dry acrolein at 0.5 Mrad and 70 rad/sec, when the system contains 6.7% water vapor, or 5.9% acetone, or 4.2% ethyl alcohol, or 4% diethyl ether, or 3.4% air. In all cases, except the first two, the decrease in weight gain is attributed to inhibiting of the process and, probably, to a decrease in activity of acrolein molecules.

Results given in Tables III and V reveal a marked decrease in percentage of aldehyde group content (10% less) at an increased dosage for a constant weight gain. In preparations in which the cellulose was previously irradiated in dry acrolein vapor, there is a high aldehyde group content. For example, 30% free aldehyde groups content gives 4.0% weight gain after cel-

TABLE V
Chemicommechanical Properties of Cotton Fabric (Coarse Calico) after Radiation-Induced Crosslinking of Cellulose with Acrolein from a Vapor Phase Saturated with Ethyl Alcohol Vapors^a

Dose rate, rad/sec	Weight gain, %	G, mole/100 eV	Aldehyde groups, %		Warp strength, kg	Warp elongation, mm	Crease recovery angle (W + F), degrees
			Bound	Free			
—	Initial	—	—	—	22	5	105
70	0.3	6765	7.5	92.5	22	4	138
	1.6	3280	69.8	30.2	22	4	153
	2.7	2217	73.0	27.0	21	4	162
	4.2	1722	78.7	21.3	19	3	174
	6.8	1394	85.8	14.2	18	3	184
	8.0	1095	88.0	12.0	17	3	196
110	0.2	4100	13.5	86.5	22	5	129
	0.8	1640	36.0	64.0	20	4	137
	2.0	1540	66.6	33.4	20	4	140
	3.5	1435	77.0	23.0	19	4	147
	4.1	840	80.0	20.0	18	4	161
	6.0	820	85.7	14.3	18	4	188
300	0.7	1435	54.0	46.0	21	5	123
	1.7	1394	63.7	36.3	21	4	133
	2.7	1230	68.8	31.2	21	4	155
	3.9	799	78.8	21.2	20	4	157

^a Weight gain was controlled by varying the total irradiation dose from 0.01 to 1.5 Mrad.

lulose has been irradiated in dry acrolein vapors; this value is reduced to 2.0% for the system saturated with ethyl alcohol vapors. This is attributed to the fact, that some aldehyde groups take part in the formation of by-products.

Moreover, estimation of various physico-mechanical properties of fibers undergoing radiation-induced crosslinking of cellulose with acrolein vapor leads to the conclusion, that the fiber properties are influenced by the radiation-induced crosslinking (Table VI). For example, the metric number (meters of thread per gram), breaking strength, and average elongation all decrease with increasing polymer weight gain. The per cent irreversible recovery of elongation also decreases with increasing polymer add-on. The higher the weight gain, the lower is the metric number and the higher the values of delayed and immediate elastic recovery at a decreased index of

TABLE VI
Properties of Cotton Fabric after Irradiation-Induced Crosslinking of Cellulose with Acrolein Vapor at 70 rad/sec

Sam- ple	Weight gain, %	Metric number, m/g ^a	Single fiber strength, g	Average elonga- tion, %	Deformation component in elongation recovery		
					Delayed, %	Immedi- ate, %	Irrevers- ible, %
Initial	—	6120	4.88	7.8	33.2	12.5	54.3
1	3.7	5141	4.60	7.2	45.1	19.8	35.1
2	6.1	4770	4.08	6.2	49.0	20.5	30.5
3	7.5	4576	3.81	5.3	51.1	21.5	27.4

^a The thickness of textile threads is characterized by metric number, which equals the linear quantity (meters) of thread per gram and can be defined by the formula, $N = L/g$, where L is the length of fiber in meters and g its weight in grams.

elastic deformation. This is a sign that the cellulosic material is becoming brittle due to the fixation of its macromolecules due to crosslinking, and is characteristic for all cellulose derivatives.⁸

Electron microscopic investigations show, that in dispersed preparations there are distinct signs of structural changes⁹ at weight gains of 8% and more, which is typical for cellulosic fibers containing the same number of crosslinks. The changes are expressed shown by abrupt thickening of the fragments and in the formation of specific cogged edges across the microfibril axis; moreover, there are forms numerous small lengthened particles. These are probably the result of crosslinking between various structural elements, which causes unequal distribution of breaking strength in the process of mechanical destruction of the fiber and its increasing brittleness as estimated by the comparison of physico-mechanical properties of the fibers. Moreover, investigations of sorption of water vapor on radiation-induced crosslinking in cellulose show, that weight increases as sorbed water

vapor decreases (Fig. 4). For example, for the control sample, the sorption was 2.6% at 65% RH, while at an average 13% weight gain it was only 4.3%.

Estimation of changes in free aldehyde group content, definition of crease recovery angles, and evaluation of breaking strength in samples of fabric after heat treatment yield very interesting results (Table VII). It is found that cellulose crosslinked with acrolein does not have improved thermostability as compared to the samples which have been subjected to 24 hr heating at 160°C. However a certain increase in the crease recovery

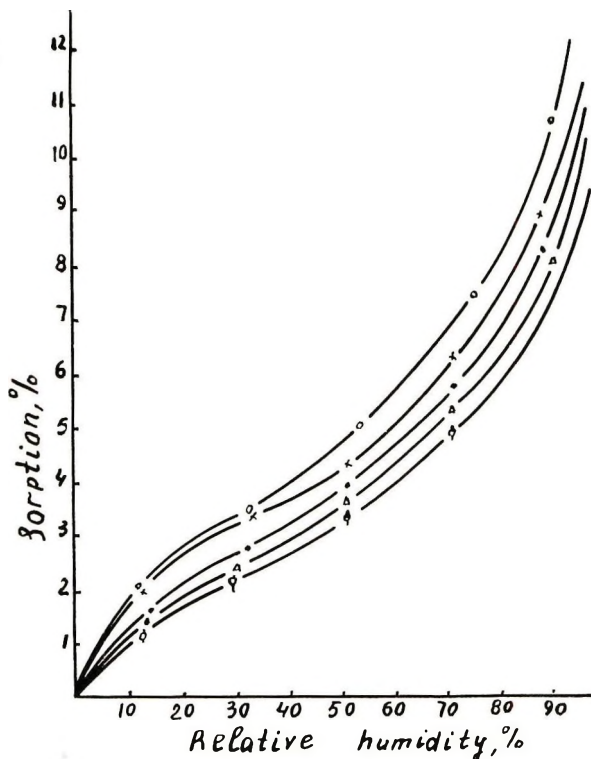


Fig. 4. Isotherms of water vapor sorption in the radiation-induced crosslinking of cellulose with acrolein: (O) initial sample; (X) 2.5% weight gain; (●) 6% weight gain; (Δ) 8% weight gain; (∅) 13% weight gain.

angles (nearly 10%) was noted at a reduced free aldehyde group content, which may indicate additional crosslinking of cellulose macromolecules.

Moreover, cellulosic materials which have been subjected to crosslinking, show increased rot resistance; this can be visually estimated by means of a conditional five-ball system. The results are given in Table VIII.

Thus, for the first time we suggest the possibility of modification, and improving of properties of cotton fabric by the method of radiation-induced crosslinking of cellulose macromolecules.

TABLE VII
Effect of Heat Treatment at 160°C on Radiation-Induced Crosslinking of Cellulose with Acrolein Vapor (Cotton Fabric, 5.6% Weight Gain)

Heating time at 160°C, hr	Aldehyde groups, %		Warp strength, kg		Elongation, mm		Crease recovery angle, degrees
	Bound	Free	Initial	Cross-linked	Initial	Cross-linked	
0 ^a	—	—	22	—	5.0	—	107
0 ^b	80.2	19.8	22	18.7	5.0	3.0	204
3	82.9	17.1	16.3	13.4	4.0	2.0	206
6	83.7	16.3	13.6	10.6	3.0	2.0	212
9	84.5	15.5	9.9	10.4	2.0	2.0	217
12	85.4	14.6	7.1	8.1	2.0	1.0	220
24	86.1	13.9	6.4	6.8	2.0	1.0	225

^a Initial uncrosslinked sample.

^b Crosslinked sample, not heated.

TABLE VIII
Influence of Cell-Destroying Fungus on Properties of Cotton Cloth^a

Fungus	Degree of destruction (5-ball system)			Weight loss, %		
	Initial sample	Acrolein add-on		Initial sample	Acrolein add-on	
		4%	10%		4%	10%
<i>Aspergillus terreus</i>	5	0	0	58	2	0
<i>Penicillium asperulum</i>	5	0	0	48	1	0
<i>Penicillium cherisogenium</i>	5	0	0	41	0	0
<i>Penicillium notatum</i>	4	0	0	25	0	0
<i>Penicillium soppi</i>	4	0	0	24	0	0

^a Samples subjected to radiation-induced crosslinking with acrolein vapor and then buried 30 days at 30°C.

CONCLUSIONS

The effect of dose and dose rate as well as of solvents and their concentration on the process of radiation-induced crosslinking of cellulose with acrolein in solutions or in vapor phase has been investigated. No acrolein homopolymer is formed in the vapor systems.

It is found, that vinyl as well as aldehyde groups of acrolein take part in the process of radiation-induced crosslinking of cellulose macromolecules. Being highly reactive, all of the vinyl groups participate in the reaction, while the content of free aldehyde groups depends on the radiation conditions.

Radiation-induced crosslinking of cellulose with acrolein at increasing dose rates is shown to increase the values of crease recovery angles and

causes changes in the deformation, although the breaking strength of the samples becomes lower; this is characteristic of all the crosslinked cellulosic derivatives. The best crease resistance was found in cotton cloth which has been irradiated in pure acrolein vapor at 1 Mrad and 70 rad/sec. The radiation-induced crosslinking in such conditions is shown to be better for obtaining improved crease resistance at high breaking strength than the chemical method of crosslinking.

It is shown, that cellulosic materials subjected to radiation-induced crosslinking with acrolein become fungus- and rot-proof.

References

1. W. K. Walsh, C. R. Jin, and A. A. Armstrong, Jr., *Text. Res. J.*, **35**, 648 (1965).
2. A. A. Armstrong, Jr. and H. A. Rutherford, *Text. Res. J.*, **33**, 264 (1963).
3. Kh. U. Usmanov, T. G. Gafurov, and Kh. Dustmukhamedov, *Uzbek. Khim. Zh.*, **1962**, No. 6, 31.
4. S. Howorth and J. R. Holker, *J. Soc. Dyers & Colourists*, **81**, 212 (1965).
5. U. Einsele, *Textil Praxis*, **22**, 866 (1967).
6. Kh. U. Usmanov, U. A. Azizov, and M. U. Sadykov, *Radiatsionnaya Khimiya Polimerov*, Izdatelstvo AN SSSR, Moscow, 1966, pp. 153-57.
7. Kh. U. Usmanov, and R. V. Perlina, *Uzbek. Khim. Zh.*, **1961**, No. 4, 22.
8. M. S. Nigmankhodzhayeva, Kh. U. Usmanov, T. G. Gafurov, and M. Allimbekova, *Struktura i Modifikatsiya Khlopkovoy Tsellyulozy*, Izdatelstvo Fan, Tashkent, 1966, p. 144.
9. G. V. Nikonovich, S. A. Leontyeva, V. P. Shatkina, A. A. Adylov, Y. T. Tashpulatov, and Kh. U. Usmanov, *Vysokomol. Soedin.*, **7**, 2131 (1965).

Received July 22, 1969

Revised October 8, 1970

Synthesis and Investigation of Polybenzimidazoles Containing Alkyl Substituents in Aromatic Nuclei

V. V. KORSHAK, M. M. TEPLYAKOV, and R. D. FEDOROVA,
*Institute of Elemento-Organic Compounds, Academy of Sciences and
D. I. Mendeleev Institute of Chemical Technology, Moscow, USSR*

Synopsis

Polybenzimidazoles have been synthesized from 3,3'-diamino-5,5'-dimethylbenzidine, 3,3',4,4'-tetraamino-5,5'-dimethyldiphenylmethane, bis(3-amino-4-methylamino)phenylmethane, bis(3-amino-4-methylamino-5-methyl)phenylmethane, and diphenyl esters of adipic, sebacic, isophthalic, and terephthalic acids and 4,4'-dicarboxydiphenyl oxide by solid-phase polyheterocyclization. Properties of the polybenzimidazoles have been studied. The polymers have high thermal stability. They are soluble in a number of organic solvents and give strong, elastic films. Solubility and thermal stability of polybenzimidazoles is determined by the methyl group position in the polymeric chain. The influence of other alkyl substituents on properties of polybenzimidazoles have been investigated. The polymer structure has been studied by infrared and PMR spectroscopy and elemental analysis.

INTRODUCTION

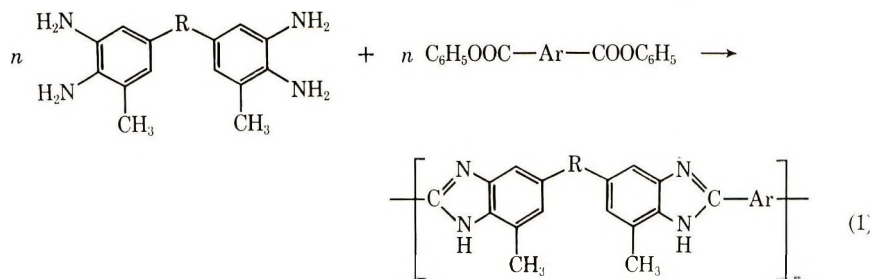
Among polybenzimidazoles reported,^{1,2} fully aromatic polymers³ are most thermally stable, but the limited solubility of these polymers in available organic solvents generated a need for the introduction of bridged groups into polymer chain, for instance, oxygen,^{4,5} methylsiloxane,^{7,8} silane,⁹ and sulfo groups,⁶ as well as for the formation of mixed polybenzimidazoles, where a part of the aromatic acid is substituted for the aliphatic.^{10,11} In most cases, an increase in polybenzimidazole solubility is accompanied by an decrease in their heat and thermal stability.

Therefore, it seemed to be of interest to investigate the possibility of chemical modification of polybenzimidazoles by introduction of side substituents. The formation of polybenzimidazoles containing methyl and other alkyl groups in the macromolecule was chosen as the main way of chemical modification, our belief being that the introduction of alkyl groups in the polymer macromolecule would have a negligible effect on thermal and heat stability. The possible synthesis of aromatic polybenzimidazoles with methyl substituents in the imidazole ring had been reported,¹² but the data given did not allow one to draw a conclusion on changes in polymer properties.

RESULTS AND DISCUSSION

Synthesis of Polybenzimidazoles Containing Methyl Groups in the Benzene Ring

Polybenzimidazoles containing methyl groups in the benzene ring were obtained from 3,3'-diaminotolidine, 3,3',4,4'-tetraamino-5,5'-dimethyldiphenylmethane, and diphenyl esters of some dicarboxylic acids by the method of Vogel and Marvel³ according to the scheme shown in eq. (1).



The structure and properties of polymers are given in Table I.

The structure of the polybenzimidazoles obtained was confirmed by infrared spectroscopy and elemental analysis data. Figure 1 shows the spectrum of *m*-phenylenedibenzimidazolyl-2,2' obtained as a model compound

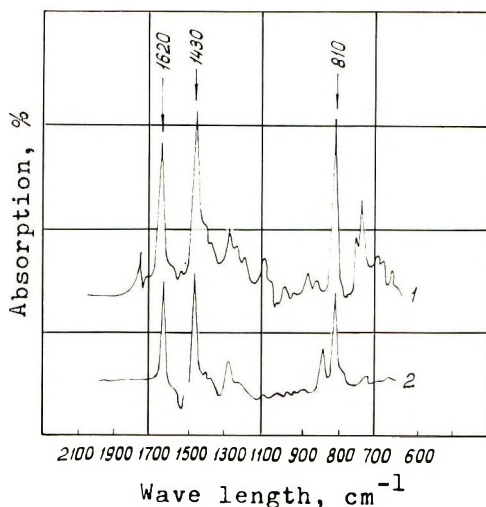


Fig. 1. Infrared spectra of (1) *m*-phenylenedibenzimidazolyl-2,2' and (2) polybenzimidazole based on 3,3',4,4'-tetraamino-5,5'-diphenylmethane and isophthalic acid.

and that of poly-2,2'-(*m*-phenylene)-4,4'-dimethyl-6,6'-dibenzimidazolylmethane. As seen from Figure 1, the polymer spectrum is in good agreement with that of the model compound. The benzimidazole ring¹³ is characterized by the absorption bands at 1430, 1600, and 1620 cm^{-1} .

Synthesis of Polybenzimidazoles Containing Methyl Groups in the Azole Ring

To obtain *N*-substituted polybenzimidazoles, the following tetraamines and the reaction (2) were used: bis(3-amino-4-methyl-amino)phenylmeth-

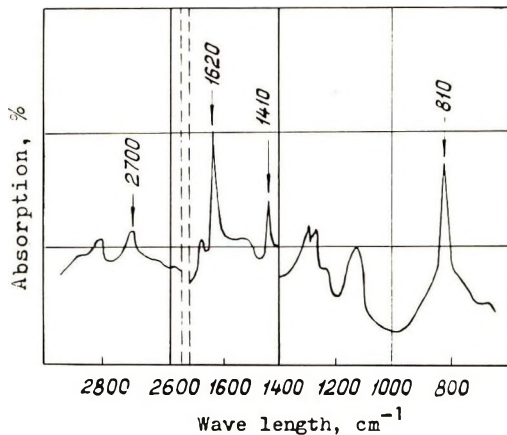


Fig. 2. Infrared spectrum of poly-1,1'-dimethyl-2,2'-(*p*-phenylene)-6,6'-dibenzimidazolylmethane.

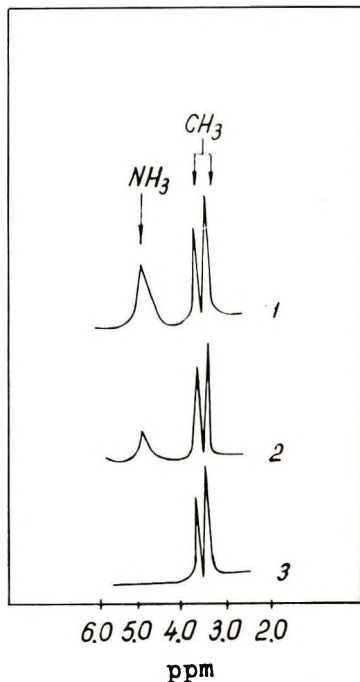
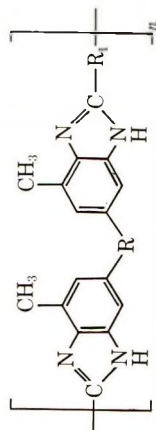
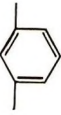

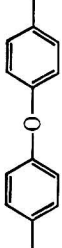
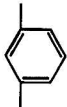

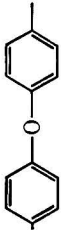


Fig. 3. PMR spectra of *N*-substituted polybenzimidazoles obtained under various conditions: (1) 270°C, 5 hr; (2) 270°C, 5 hr, 10^{-3} mm Hg; (3) 300°C, 5 hr, 10^{-3} mm Hg.

TABLE I
Properties of Polybenzimidazoles of General Formula



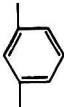

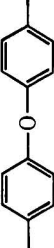
No.	R	R ₁	Intrinsic viscosity (DMSO), dl/g	Softening temperature, °C	Elemental analysis		Solubility ^a					
					Found, %	Calcd, %	DMA	DMF	Pyridine	Benzyl alcohol	Cyclohexanone	
1	None	—(CH ₂) ₄ —	0.82					++	++	+	++	+
2	"	—(CH ₂) ₈ —	0.95					++	++	++	++	++
3	"		0.4 ^b 0.86	480	C	78.75	78.82	++	++	++	++	+
4	"		0.80	490	H	5.03	4.98	++	+	+	+	+
					N	16.60	16.71					
					C	78.77	78.82	++	++	—	+	+
					H	5.09	4.98					
					N	16.80	16.71					

5	"		1.0	470	C 81.85 H 4.52 N 13.26	81.98 4.64 13.31	++ ++ ++	++ ++ ++	++ ++ ++	++ ++ ++
6	$\text{---CH}_2\text{---}$	$\text{---(CH}_2)_4\text{---}$	0.80							
7	$\text{---CH}_2\text{---}$	$\text{---(CH}_2)_8\text{---}$	1.05							
8	"		0.47 ^b 0.95	470	C 73.41 H 3.71 N 15.89	73.10 3.89 16.02	++ ++ ++	++ ++ ++	++ ++ ++	++ ++ ++
9	"		0.86	490	C 73.52 H 3.81 N 16.12	73.10 3.89 16.02	++ ++ ++	++ ++ ++	++ ++ ++	++ ++ ++
10	"		0.95	470	C 82.07 H 4.90 N 3.15	81.98 4.94 3.18	++ ++ ++	++ ++ ++	++ ++ ++	++ ++ ++

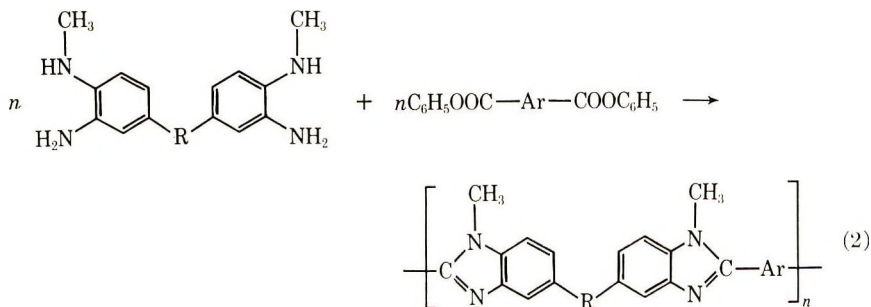
^a Code: ++, polymer solubility > 33 g/l; +, polymer solubility < 33 g/l; -, polymer is insoluble.

^b Reduced viscosity was measured in formic acid.

TABLE II
Properties of Polybenzimidazoles of General Formula

No.	R ₁	R ₂	R ₃	Intrinsic viscosity (DMSO), dl/g	Softening temperature, °C	Solubility				
						DMF	Pyridine	Benzyl alcohol	Cyclohexanone	Tricresol
1	—CH ₂ —	H—	—(CH ₂) ₇ —	0.98	230	++	++	++	++	++
2	"	"	—(CH ₂) ₈ —	1.52	220	++	++	++	++	++
3	"	"		0.88	350	++	++	+	++	+
4	"	"		0.85	380	++	+	+	+	+
5	"	"		0.86	350	++	++	++	++	++

ane, di(3-amino-4-methyl-amino)-5-methylphenyl, bis(3-amino-4-methyl-amino-5-methyl)-phenylmethane.



The structure of polybenzimidazoles synthesized was confirmed by infrared and PMR data. Besides the infrared absorption bands at 1430, 1600, and 1620 cm^{-1} assigned to the benzimidazole ring, a characteristic absorption band at 2700 cm^{-1} corresponding to the methyl group at the nitrogen is also observed (Fig. 2).

Figure 3 shows the PMR spectra of polybenzimidazoles obtained from bis(3-*N*-methylamino-4-aminophenyl)methane and isophthalic acid under various synthesis conditions. During full cyclization, the maximum characteristic of the amide hydrogen must disappear in the spectrum of *N*-substituted polybenzimidazoles. It is seen from Figure 3 that the qualitative polybenzimidazole polycyclization takes place on prolonged heating under high vacuum at a temperature not below 300°C.

Properties of Polybenzimidazoles Containing Methyl Substituents

Solubility. The introduction of a methyl group into the benzene ring of polybenzimidazoles (Table I) leads to formation of polymers, most of which are soluble in dimethylformamide, benzyl alcohol, pyridine, polymers with a viscosity of 0.4–0.5 being better soluble than similar polymers with a viscosity of 0.8–0.9 dl/g.

As seen from Table II, polybenzimidazoles with methyl groups in the azole ring are easily soluble in benzyl alcohol, pyridine, cyclohexanone, and tricresol. *N*-Methyl-substituted polybenzimidazoles are capable of formation of more concentrated solutions compared with polybenzimidazoles containing no methyl groups in the azole ring (Table III).

Thermal and Heat Stability. Polybenzimidazoles based on aromatic acids have high thermal stability, starting to decompose in air at above 400°C (Figs. 4 and 5). As would be expected, polybenzimidazoles based on terephthalic acid are most thermally stable, but less soluble in organic solvents (Tables I and II). Polybenzimidazoles based on isophthalic acid and diphenyl oxide dicarboxylic acid have an optimum combination of high thermal stability and good solubility.

Isothermal thermogravimetric analysis of polybenzimidazoles at 450°C (Fig. 6) showed that polymers containing methyl groups in the benzene ring

TABLE III
Properties of Polybenzimidazoles with Different Structures

No.	Structural unit	Reduced viscosity (H ₂ SO ₄), dl/g	Softening temperature, °C	Solubility in DMF, g/l	Specific impact strength, kg-cm/ cm ²	Properties of unoriented films	
						σ , kg/cm ²	ϵ , %
1		2.50	490	45	2.5		Brittle film
2		1.54	470	180	10.5	650-900	28
3		1.22	350	250	6.0	600-750	35

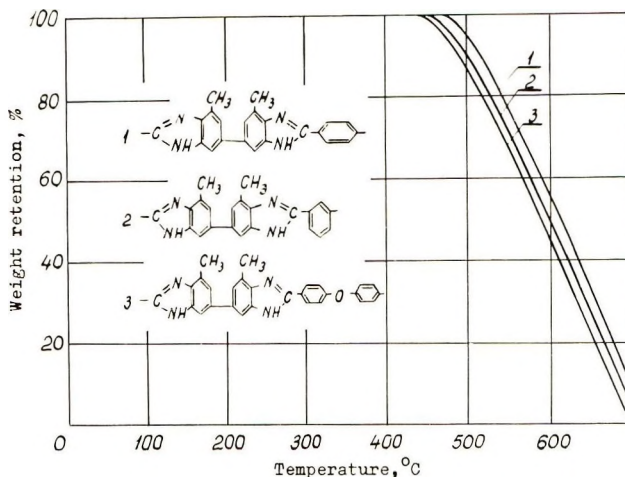


Fig. 4. Thermogravimetric curves of polybenzimidazoles.

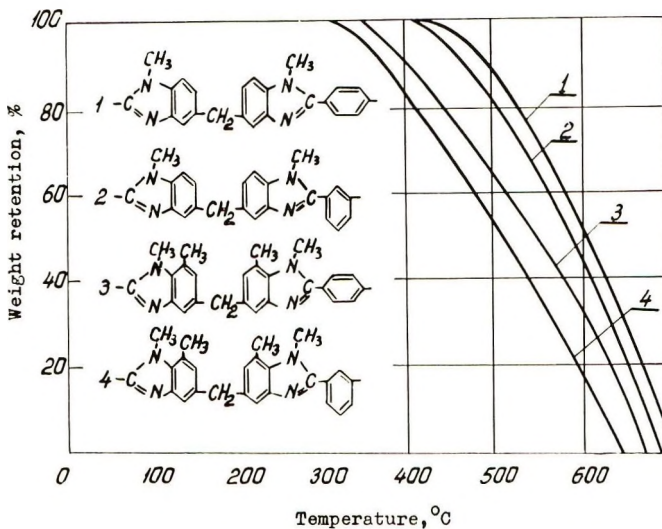


Fig. 5. Thermogravimetric curves of polybenzimidazoles.

proved to be more stable on a prolonged exposure to high temperatures, their thermal stability being close to that of the polybenzimidazole based on 3,3',4,4'-tetraaminodiphenylmethane. Maximum 15–20% weight loss of the polymers occurs at 450°C, followed by stabilization. The weight loss stabilization is explained by crosslinking processes at these temperatures, since polybenzimidazoles become insoluble after heating at 450°C for 90 min. There is no weight loss on conducting the isothermal thermogravimetric analysis at 300°C. As evidenced by data of Table III, the melting point of polybenzimidazoles depends on the position of the methyl group in the macromolecule. Substitution of imidazole hydrogen for a methyl

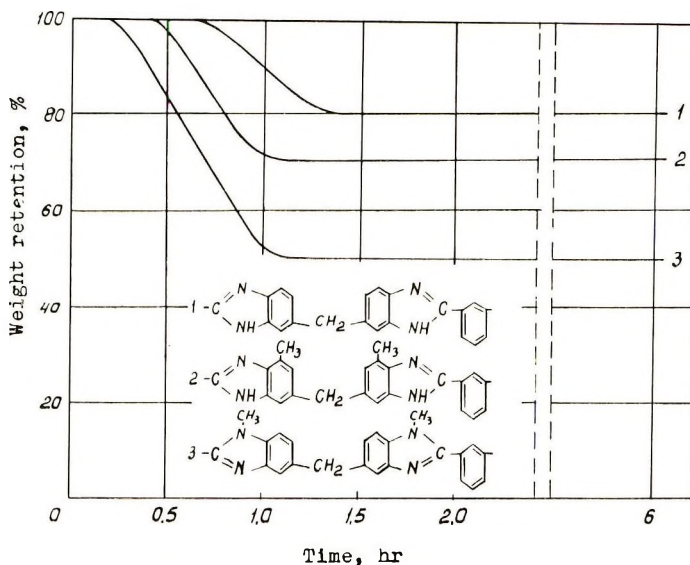


Fig. 6. Isothermal thermogravimetric analysis of polybenzimidazoles.

group is more effective, which may be attributed to the disappearance of hydrogen bonds in the polymer.

Mechanical Properties. The presence of a methyl group in the polybenzimidazole macromolecule together with methylene bridges between rings leads to fairly strong and elastic polybenzimidazoles. For instance, poly-

TABLE IV
Chemical Resistance of Polybenzimidazoles to the Action
of Various Reagents at 100°C for 5 Hours

No.	Polymer	Reduced viscosity in H ₂ SO ₄ (η_{sp}/c), dl/g	Reagent	Reduced viscosity in H ₂ SO ₄ after chemical treatment (η_{sp}/c), dl/g
1	No. 1, Table III	1.25	40% KOH	1.25
			35% HCl	1.22
			10% H ₂ SO ₄	1.20
			10% HNO ₃	1.00
			40% KOH	1.04
2	No. 8, Table I	1.04	35% HCl	1.04
			10% H ₂ SO ₄	1.03
			10% HNO ₃	1.02
			40% KOH	1.15
			35% HCl	0.95
3	No. 3, Table II	1.20	10% H ₂ SO ₄	0.90
			10% HNO ₃	0.62

2,2'(*m*-phenylene)-4,4'-dimethyl-6,6'-dibenzimidazolymethane (polymer 8, Table I) yields transparent films with tensile strength σ of 1000 kg/cm² and 25% elongation (ϵ).

Table III shows that polybenzimidazoles with methyl groups in the benzene cycle form films with a higher tensile strength, than those with methyl groups in theazole ring. The films from *N*-substituted polybenzimidazoles are more elastic.

Chemical Resistance. Hydrolysis resistance data for polybenzimidazoles are given in Table IV. It is seen that the polymers synthesized are resistant to acid and base hydrolysis. The introduction of the methyl group in the benzene cycle of polybenzimidazole (polymer 2, Table IV) resulted in a slight increase in chemical resistance, which may be explained by screening effect of the methyl group.

Mixed Polybenzimidazoles Containing Methyl Groups in the Benzene Ring

Homopolybenzimidazoles based on 3,3'-diaminotolidine and aromatic acids form brittle films unlike polybenzimidazoles containing methylene bridges between benzimidazole cycles (polymer 2, Table V).

It has been shown previously that the formation of mixed polybenzimidazoles could improve physicomechanical properties of the polymers. For this purpose, a series of mixed polybenzimidazoles was obtained from 3,3'-diaminotolidine; their properties are given in Table V.

It is seen from the data given that copolymers containing 0.3 mole of isophthalic acid are most capable of film formation. The strength of the resulting films is 600–800 kg/cm². But copolymers containing 0.7 mole of isophthalic acid are most readily soluble, which agrees with common ten-

TABLE V
Mixed Polybenzimidazoles Obtained from 3,3'-Diamino-5,5'-dimethylbenzidine and Diphenyl Esters of Dicarboxylic Acids

No.	Diphenyl ester of			Reduced viscosity in DMF (η_{sp}/c), dl/g	Softening temperature, °C.	Solubility in DMF, g/l	Properties of unoriented films	
	Iso-phthalic acid, mole	Ter-ephthalic acid, mole	Diphenyl-oxydicarboxylic acid, mole				σ , kg/cm ²	ϵ , %
1	0.0		1.0	1.0 ^a	470	80	Brittle film	
2	0.3		0.7	1.15	420	120	800	20
3	0.5		0.5	1.36	415	250	Brittle film	
4	0.7		0.3	1.20	410	320	"	
5	1.0		0.0	0.86 ^a	480	30	"	
6	0.0	1.0		0.80 ^a	490	20	"	
7	0.3	0.7		1.17	450	90	600	15
8	0.5	0.5		1.35	440	220	Brittle film	
9	0.7	0.3		1.12	435	290	"	

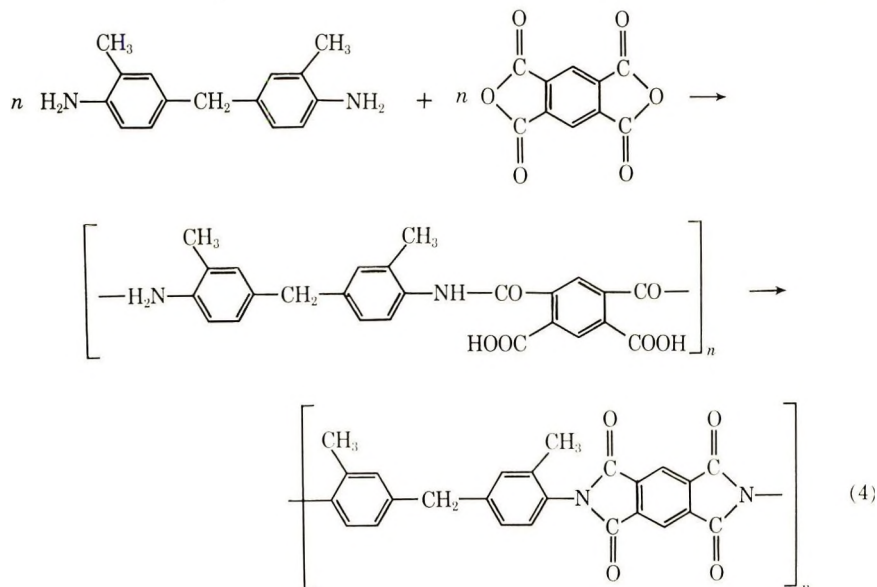
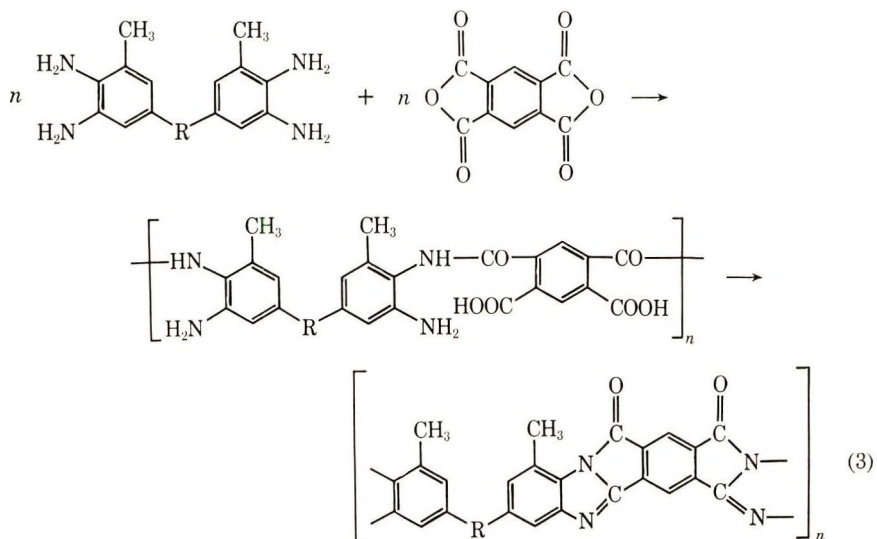
^a Intrinsic viscosity.

dencies observed previously with polybenzimidazoles containing no substituents.¹⁴

The synthesized copolybenzimidazoles have high thermal stability. The heat stability depends on the composition (Table V, polymer 1, 3, 4, 6).

Polybenzimidazopyrrolones and Polyimides Containing Methyl Groups

To clarify the general character of the effect of the methyl groups on solubility of polyheteroarylenes, we have also obtained the corresponding polybenzimidazopyrrolones and polyimide.



Polybenzimidazopyrrolones were obtained by polyheterocyclization of 3,3',4,4'-tetraamino-5,5'-dimethyldiphenylmethane with pyromellitic acid dichloride according to the scheme (3).

In the case of polybenzimidazopyrrolones, however, the introduction of methyl groups in the macromolecule did not result in an increase in solubility. Polybenzimidazopyrrolones containing methyl groups proved to be insoluble in organic solvents but swelled in concentrated sulfuric acid.

The initial decomposition temperature of these polymers is about 360°C. The weight loss is 30% on heating up to 500°C.

A methyl-containing polypyromellitimide has been obtained by the two-stage polycyclization of 3,3'-dimethyl-4,4'-diaminodiphenylmethane with pyromellitic acid dianhydride according to the scheme (4).

Studies on polymer properties showed that the synthesized polypyromellitic imide was insoluble in DMA, DMSO, and formic acid.

Thus, the effect produced by introduction of methyl groups in the polybenzimidazole macromolecule is not regular for other polyheteroarylenes.

Polybenzimidazoles Containing Alkyl Groups in the Azole Ring

It was found that more than 50% of methyl groups of the tetraamine were replaced by ethyl, isopropyl, and benzyl radicals, respectively (Fig. 7), on boiling the tetraamines containing methyl groups at the hydrogen atom in ethyl, isopropyl, and benzyl alcohol in the presence of catalysts. The reaction provided a means for obtaining polybenzimidazoles with various alkyl substituents in macromolecule.

TABLE VI
Properties of Polybenzimidazoles of General Formula

No.	R	Intrinsic viscosity (DMSO), dl/g	Soft- en- ing point, °C.	Solubility					
				DMA	DMF ^a	Pyri- dine	Ben- zyl al- co- hol	Cyclo- hexa- none	Tri- cre- sol
1	CH ₃ —	0.88	350	++	++	++	+	+	+
2	C ₂ H ₅ , CH ₃ —	0.80	350	++	++	++	++	+	++
3	 CH—, CH ₃ —	0.70	340	++	++	++	++	++	++
4	 —CH ₂ —, CH ₃ —	0.80	320	++	++	++	++	++	++

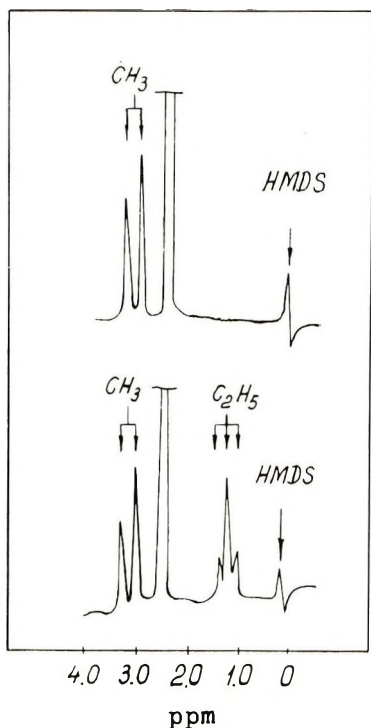


Fig. 7. PMR spectra of bis(3-amino-4-methylaminophenyl)methane (a) before and (b) after realkylation reaction in ethyl alcohol.

It is seen from the data of Table VI that these polymers are readily soluble in organic solvents, showing no sharp difference from polybenzimidazoles containing methyl groups in heterocycle.

Introduction of bulky substituents decreases the polymer chain packing density and leads to the lowering of thermal stability. These polybenzimidazoles are thermally stable to 400–450°C.

Polybenzimidazoles with various alkyl groups yield elastic films with tensile strength of 400–600 kg/cm².

EXPERIMENTAL

Synthesis of Starting Compounds

The starting bisnitroamines were obtained by nitration of the corresponding diamines by the Meyer-Rohmer¹⁵ and Marvel³ methods or by the Fischer-Busch method.¹⁶ The subsequent reduction was accomplished as previously detailed.¹⁷ The melting point was 138.5–139.5°C for 3,3,4,4-tetraaminodiphenylmethane, 150–151°C for 3,3-diamino-5,5-dimethylbenzidine, 165–166°C for 3,3',4,4' - tetraamino-5,5' - dimethyldiphenylmethane, 125–126°C for bis(3-amino-4-methyl-amino)phenylmethane, 133–135°C for di(3-amino-4-methyl-amino-5-methyl)phenyl, 143–144°C for

bis(3-amino-4-amino-4-methylamino-5-methyl)phenylmethane. 3,3'-Dimethyl-4,4'-diaminodiphenylmethane was obtained by the method described by Eberhardt and Welter,¹⁸ mp 156–157°C.

Diphenyl esters of isophthalic and terephthalic acids and 4,4'-dicarboxy-diphenyl oxide were obtained by reacting the dichlorides of the corresponding acids with phenols. Their melting points agreed with those reported.^{5,19}

The dianhydride of pyromellitic acid was twice sublimed *in vacuo*, mp 284–286°C.

Synthesis of Model Compounds

m-Phenylenedibenzimidazolyl-2,2' was obtained by reacting 0.01 mole of diphenyl ester of isophthalic acid with 0.02 mole of *o*-phenylenediamine at 180–260°C for 2 hr. The resulting dibenzimidazole was washed with water and alcohol and recrystallized from dimethylformamide, mp 285–287°C.

ANAL. Calcd for C₂₀H₁₄N₄: C, 77.42%; H, 3.55%; N, 18.07%. Found: C, 78.02%; H, 4.10%; N, 18.21%.

Synthesis of the Polymers

Polybenzimidazoles were obtained by polyheterocyclization of the starting materials in the solid phase by the method of Vogel and Marvel.³ To achieve more complete cyclization the final stage was carried out under a vacuum of 10⁻³–10⁻⁶ mm Hg at 270–300°C. Polybenzimidazoles synthesized were purified by reprecipitation from dimethyl sulfoxide into water, followed by careful washing from the solvent.

Polybenzimidazopyrrolones were synthesized by low-temperature polycondensation in amide solvents followed by thermal cyclization. Starting component concentration was 0.09 g/ml, reaction temperature 20°C, reaction time, 1 hr. The polymer was precipitated with acetone cooled to -20°C; the cyclization took place under vacuum of 10⁻³ mm Hg at 300°C for 4 hr. Polypyromellitic imide was synthesized at -20°C in dimethylacetamide. The reduced viscosity of the poly(amido acid) in DMF at 25°C was 0.94 dl/g. The poly(amido acid) was precipitated with acetone and dried under vacuum. The cyclization took place at 200–300°C.

Studies on Polymer Properties

Thermal stability of the polymers was determined by dynamic^{20,21} and isothermal thermogravimetric analysis. The temperature increase rate of the derivatograph was 4.5°C/min. Isothermal analysis was carried out under vacuum of 10⁻³ mm Hg. The viscosity of the polymers was measured in 0.5% dimethyl sulfoxide solution at 20°C.

To determine the polymer stability in various solvents, 0.1 g of ground polymer was heated in the glass tube with a solvent at 100°C for 30 min.

PMR spectra were obtained on a Perkin-Elmer spectrometer in 15% dimethyl sulfoxide solution at a frequency of 60 Mcps, hexamethyldisiloxane being used as a reference material.

Heat stability of the polymers was determined by means of thermomechanical curves taken on a Tsetlin apparatus²² for pellets of powder-like polymers.

References

1. A. A. Izyneev, M. M. Teplyakov, V. G. Samsonova, and A. D. Maksimov, *Uspekhi Khim.*, **36**, 2086 (1967).
2. J. I. Jones, *J. Macromol. Sci.*, **C2**, 303 (1968).
3. H. Vogel and C. S. Marvel, *J. Polym. Sci.*, **50**, 511 (1961).
4. V. V. Korshak, T. M. Frunze, and M. A. Surikova, SSSR Pat. 176398 (1965); *Bull. Izobret.*, No. **22**, 58 (1965).
5. R. T. Foster and C. S. Marvel, *J. Polym. Sci. A*, **3**, 417 (1965).
6. T. V. L. Narayan and C. S. Marvel, *J. Polym. Sci. A-1*, **5**, 1113 (1967).
7. I. E. Mulvaney and C. S. Marvel, *J. Polym. Sci.*, **50**, 541 (1961).
8. T. Makajata and C. S. Marvel, *J. Polym. Sci. A-1*, **7**, 1295 (1969).
9. H. N. Kovacs, A. D. Delman, and B. B. Simms, *J. Polym. Sci. A-1*, **6**, 2103 (1968).
10. V. V. Korshak, T. M. Frunze, V. V. Kurashev, and G. P. Lopatina, *Vysokomol. Soedin.*, **6**, 1251 (1964).
11. V. V. Korshak, I. F. Manucharova, T. M. Frunze, and V. V. Kurashev, *Vysokomol. Soedin.*, **6**, 1394 (1964).
12. K. Mituhashi and C. S. Marvel, *J. Polym. Sci. A*, **3**, 1661 (1965).
13. A. R. Katritskii, Ed., (*Physical Methods in Chemistry of Heterocyclic Compounds*), Izdadelstvo Khimiya, Moscow, 1966, p. 540.
14. G. L. Berestneva, V. V. Korshak, M. M. Teplyakov, and R. D. Fedorova, *Vysokomol. Soedin. A*, **11**, 2260 (1969).
15. J. Meyer and M. Rohmer, *Ber.*, **33**, 250 (1900).
16. O. Fischer and M. Busch, *Ber.*, **24**, 2682 (1891).
17. V. V. Korshak, M. M. Teplyakov, and R. D. Fedorova, SSSR Pat. No. 218898; *Bull. Izobret.*, No. **30**, 188 (1968).
18. C. Eberhardt and A. Welter, *Ber.*, **27**, 1807 (1894).
19. L. Sheder, *Ber.*, **7**, 707 (1874).
20. J. Paulik, M. Macskasy, F. Paulik, and L. Erdey, *Plaste Kautschuk*, **8**, 588 (1961).
21. F. Paulik, J. Paulik, and L. Erdey, *Z. Anal. Chem.*, **160**, 241 (1959).
22. B. L. Tsetlin, V. A. Gavrilov, K. A. Velikovskaya, and V. V. Kochkin, *Zavodskaya Lab.*, **3**, 352 (1956).

Received June 9, 1970

Polyimidazopyrrolones and Related Polymers. I. Dianhydrides and *o*-Acetamidodiamines

L. W. FROST and G. M. BOWER, *Polymer Chemistry,
Research and Development Center, Westinghouse Electric Corporation,
Pittsburgh, Pennsylvania 15235*

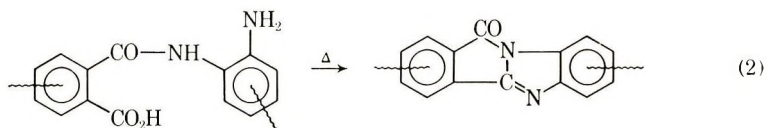
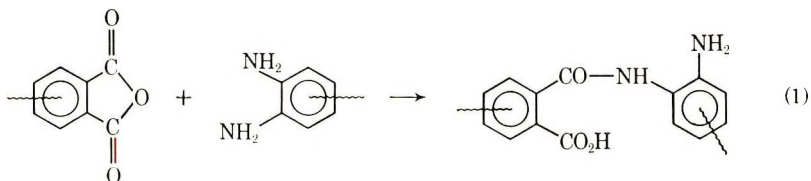
Synopsis

Solutions of polyimidazopyrrolone precursors prepared by reaction of tetraamines and dianhydrides in polar solvents tend to crosslink and gel very easily. Substitution of *o*-acetamidodiamines for the tetraamines gives stable solutions. A study of cure mechanisms by TGA, infrared, and pyrolysis experiments with polymers and model compounds indicates that the acetylated materials are converted cleanly to imides at 150°C. At temperatures above 350°C, structural changes and further polymerization occur, with little imidazopyrrolone formation. Polymers derived from tetraamines cure by multiple mechanisms but finally yield the imidazopyrrolone structure. The acetylated polymers and copolymers give acceptable laminates but poor films.

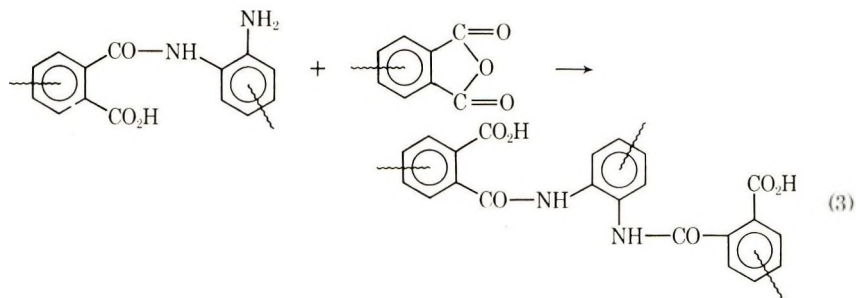
INTRODUCTION

The preparation and properties of polymers containing the imidazopyrrolone (pyrrone) linkage have been described by several authors.¹⁻⁶ The usual method of synthesis has been the reaction of a dianhydride with an aromatic *o,o*-tetraamine in a polar aprotic solvent. In this procedure, a solution of the dianhydride is added slowly to a rapidly stirred solution of the tetraamine. A soluble poly(amino acid amide) is produced, which is converted to the pyrrone by heating.

Ideally, the polymerization and cure reactions proceed as shown in eqs. (1) and (2).



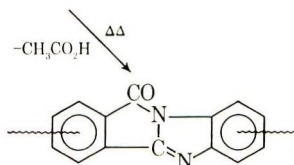
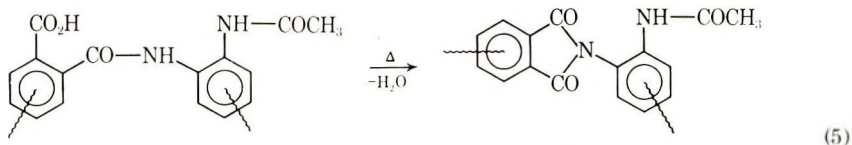
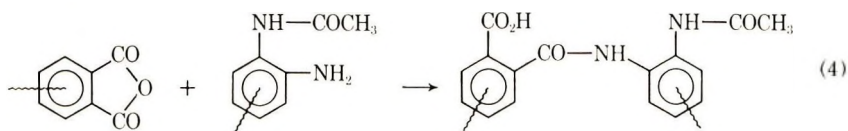
One shortcoming of this procedure is that a slight local excess of dianhydride results in gelation. This behavior is presumably caused by reaction of the dianhydride with the free amino group *ortho* to the acylamide group in the linear polymer with resulting crosslinking, as in eq. (3).



This reaction becomes more important when reaction (1) nears completion, and the concentration of *ortho* diamino structure becomes small relative to that of the amino group *ortho* to the acylamido group.

The procedure^{3,5} for avoiding gelation has been to use dilute solutions (10% or less) and to add the last portions of the dianhydride very slowly with good stirring.

The gelation and high viscosity resulting from crosslinked structures can be reduced or eliminated by blocking one of the amine groups in each of the *ortho* pairs. Since we are now dealing with the reaction of a diamine and a dianhydride, behavior typical of normal polyamide acids can be expected. For example, if one of the groups is acetylated the reaction sequence (4)–(5) is expected.



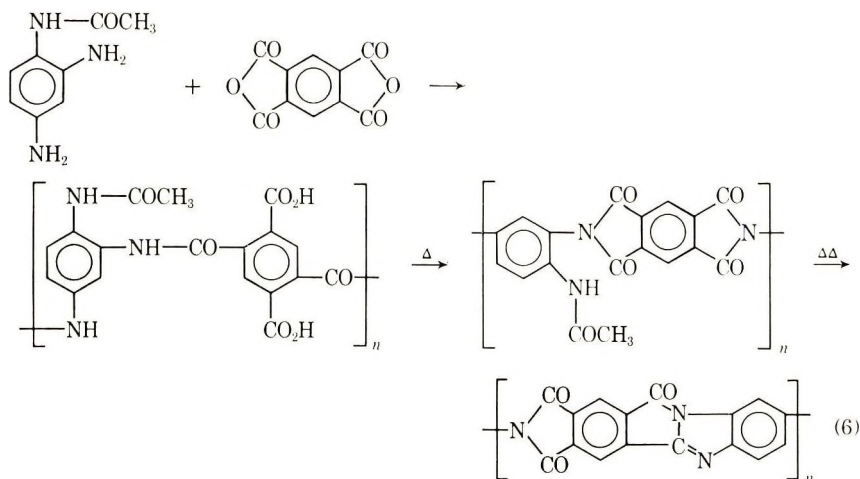
The acetamido group will not react with anhydrides at room temperature to give crosslinking as in eq. (3). Therefore the polymerization reaction [eq. (4)] will proceed without gelation, at concentrations higher than can be used in the usual reaction [eq. (1)].

This paper reports the preparation, properties, cure mechanism, and degradation of polymers from dianhydrides and *o*-acetamidodiamines. Other methods of preventing gelation in pyrrone precursor solutions will be discussed in succeeding papers.

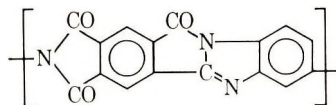
POLYMER PREPARATION AND PROPERTIES

Polymers from 2,4-Diaminoacetanilide (DAA)

The most readily available diamine containing the desired *o*-acetamidoamine structure is 2,4-diaminoacetanilide (DAA). Equation (6) shows the reactions expected with pyromellitic dianhydride (PMDA).



Two isomers are possible in the product of the first reaction, only one of which is shown. The cured product, which contains equal numbers of imide and pyrrone groups, is expected to be the same as the polymer previously prepared from 1,2,4-triaminobenzene (TRAB) and PMDA by Bell¹⁰ and by Dunnivant,¹¹ except that the latter contains the additional isomeric configuration I in the trisubstituted benzene ring.



I

polymers, in addition to the structures shown, some of the tetrasubstituted benzene rings will be linked to two imide groups, with an equal number linked to two pyrrone groups. The latter structure occurs in two geometric isomers. The DAA polymers were studied primarily to compare the reactivity of an isolated amino group with that of an *o*-acetamidoamine and to study the elimination of acetic acid to form a pyrrone linkage in the final step.

When PMDA was added in portions to a stirred solution of DAA in *N,N*-dimethylacetamide (DMAC) the viscosity behavior was similar to that observed previously for simple diamines,⁷ with a sharp viscosity peak at equivalence as the final increments of PMDA were added. Apparently, both amino groups were of similar reactivity. Maximum viscosity was obtained with about a 1% excess of PMDA, and further addition gave a viscosity decline. The inherent viscosity of the polymer solution 28 hours after preparation was 0.69 dl/g. Attempts to cast films from the solution gave only brittle materials. Similar results were obtained when 3,4,3',4'-benzophenonetetracarboxylic dianhydride (BTDA) was substituted for PMDA.

Polymers from 4,4'-Diacetamido-3,3'-oxydianiline (DATADPO)

Polymer Solution Preparation. Polymer preparation from DATADPO proceeded smoothly with either PMDA or BTDA in DMAC, dimethylformamide (DMF), dimethyl sulfoxide (DMSO), *N*-methylpyrrolidone (NMP), or DMAC-xylene. Polymer solutions prepared in DMSO had the highest viscosity at 20–25% solids, although they did not have higher inherent viscosities. Table I summarizes viscosity data for several solvent systems. Although this polymer was expected to be relatively flexible, and the inherent viscosities are in the range expected to give good films, all efforts to cast films from DATADPO–BTDA failed to give a flexible cured product. Uncured films, plasticized with solvent, were tough and flexible, but as the cure progressed they became extremely fragile. Final cure at 300–325°C gave a somewhat tougher product, but we did not succeed in getting a film of reasonable size past the fragile stage without fragmentation.

Laminates. Glass cloth laminates were made by methods similar to those used for laminates from polyimides prepared in aprotic solvents.¹² The system was not studied extensively, but the values given in Table II are at least as high as those of the polyimides. No aging studies were made.

Precipitated Polymer. DATADPO reacted smoothly with PMDA in refluxing THF to give a precipitated powder. Infrared spectra, elemental analysis, and inherent viscosity indicate that this product was a low molecu-

TABLE I
Viscosities of DATADPO–BTDA Polymers

Solids, %	Solvent	Viscosity		
		Gardner	cP	Inherent (35°C), dl/g
23	DMSO	Z-6	14,800	0.62
25	DMF	V+	900	—
24	DMAC-xylene (2:1)	X-Y	1,500	—
25	NMP	X-Y	1,500	0.48
16	DMSO	W	1,070	—
26	DMAC-xylene (3:2)	W	1,070	—
25	DMAC	S	500	0.62

TABLE II
Laminates from DATADPO-BTDA on 181 E Glass Cloth (A1100 Soft Finish)^a

No. plies	Precure		Resin, %		Thickness, in.	Flexural strength, psi ^c		Flexural modulus, psi ^c
	Time, min	Temperature, °C ^b	Prepreg	Laminate		25°C	316°C (600°F)	
12	30	180	36.8	17	0.085	50,100	56,100	3.79 × 10 ⁶
12	30	210	44.8	20	0.101	71,300	67,400	3.87 × 10 ⁶
16	10	210	45.0	25	0.143	64,000	59,000	3.2 × 10 ⁶

^a Initial press temperature 200°C. Temperature and pressure raised gradually to 300°C and 500 psi. Held for 30 min.

^b Warmed from 25°C to indicated temperature in 30 min. Held at temperature as shown.

^c Average of three determinations.

lar weight polymer, largely in the form of the amide acid. Infrared spectra showed that on heating for 2 hr at 150°C it was largely converted to the imide.

Polymers from 3,3'-Diamino-*N,N'*-diacetylbenzidine (DADAB)

DADAB and BTDA. Although DADAB has a very low solubility in DMAC, a slurry of the two reacted with BTDA to give a clear solution, inherent viscosity 0.28 dl/g. A film cast from the solution was very brittle.

DADAB and PMDA. Two products were obtained from the reaction of PMDA and DADAB. One was quite soluble in DMAC and similar solvents. The other was insoluble in any organic solvent tested. When an equimolar mixture of DADAB and PMDA was added to stirred DMAC or DMSO, a clear solution was obtained, from which the insoluble product gradually precipitated.

Some additional experiments were run to clarify the solubility behavior of this polymer. Several preparations were filtered, and the precipitates were washed and dried. It was found that the amount of material dissolved was a fairly constant fraction of the total solids and almost independent of the ratio of solids to solvent.

The soluble and insoluble fractions had nearly identical analyses (Table VII) and infrared spectra, which are consistent with the expected amide acid structure. However, in spite of these similarities, the insoluble fraction was found to have a solubility of less than 0.1% in DMAC, DMF, DMSO or NMP, while the soluble fraction, after precipitation and drying, could be redissolved in DMAC to give a 40% solution. The only solvent found for the insoluble fraction was concentrated sulfuric acid.

Inherent viscosities, measured on fresh solutions before precipitation occurred, ranged from 0.56 dl/g in DMSO to 0.32 dl/g in DMAC. Films cast from the solutions were brittle.

Polymer from 1,3-Diamino-4,6-diacetamidobenzene (DATAB)

Polymers from 1,3-diamino-4,6-diacetamidobenzene (DATAB) and PMDA are of particular interest because they would form complete ladders when fully cyclized. DATAB was synthesized from 4,6-dinitro-1,3-phenylenediamine by acetylation followed by reduction. It turned out to be so insoluble and high-melting that purification was very difficult. A small amount of polymer prepared from crude DATAB and BTDA gave very poor films.

Copolymers with Simple Diamines

Evidence is presented in the section on curing reactions suggesting that polymers derived from diacetyl tetraamines do not cure smoothly to pyrrones, but undergo other reactions leading to crosslinking. Therefore, copolymers obtained by the reaction of dianhydrides with mixtures of diamines and diacetyl tetraamines, when fully cured, are expected to con-

TABLE III
Laminates from Acetamidoimide Copolymers

	DADAB ₂ -MPD ₃ -BTDA ₁₀ ^a		DATADPO-MPD ₂ -BTDA ₃			
	A	B	C	D	E	F
Precure						
Time, min	20	20	20	20	110	110
Temperature, °C	150	150	150	150	250	250
Press conditions						
Time, min	15	30	60	60	60	60
Temperature, °C	470	400	350	350	325	340
Pressure, psi	1000	1000	1000	1000	500	500
Resin content, %	—	—	—	—	38	38
Prepreg						
Laminate	24	22	27	27	36	33.5
Flexural strength, kpsi^b						
At 25°C, initial	35	36.4	33.6	11.8		
At 316°C, initial		27.1		7.6	30.0 ^c , 40.7 ^d	41.3, ^e 45.0 ^d
At 316°C, aged (24 hr, 316°C)		22.2		8.5		
At 316°C, aged (48 hr, 316°C)						
At 316°C, aged (100 hr, 316°C)	9.4	19.1	26.1			
At 316°C, aged (250 hr, 316°C)		14.3				
Flexural modulus, Mpsi^b						
At 25°C, initial	3.4	3.4	2.7	2.2		
At 316°C, initial		2.8		1.7	2.5 ^c , 2.6 ^d	2.6 ^c , 2.6 ^d
At 316°C, aged (24 hr, 316°C)		2.7		2.0		
At 316°C, aged (48 hr, 316°C)						
At 316°C, aged (100 hr, 316°C)	2.5	2.4	2.3			
At 316°C, aged (250 hr, 316°C)		2.5				

^a MPD refers to *m*-phenylenediamine, subscripts to mole ratios.

^b Average of three specimens.

^c Not post-cured.

^d Post-cured 30 min at 325°C.

sist of some kind of crosslinked structure containing imide, pyrrone, and other linkages. Crosslinked polyimides derived from somewhat similar structures have been reported by Bower et al.¹⁴

We have evaluated two polymers of this type. Compositions and laminate data are given in Table III. Although initial strength and modulus values are low compared with pyrrones made by the ester method,⁴ retention of properties appears better and is comparable to values reported for polyimides.^{12,14}

CURING REACTIONS

We have studied the mechanism of cure and the nature of cured and pyrolyzed products for these polymers and related model compounds. The chief methods used were thermogravimetry and infrared analysis.

TABLE IV
Infrared Correlations

Wave number, cm ⁻¹	Probable assignment ^a		
	Polyimide	Polybenzimidazole ^b	Pyrrone
1780	$\begin{array}{c} \\ -\text{C}=\text{O} \end{array}$		
1760			$\begin{array}{c} \\ -\text{C}=\text{O} \end{array}$
1738 ^c			$\begin{array}{c} \\ -\text{C}=\text{O} \end{array}$
1720	$\begin{array}{c} \\ -\text{C}=\text{O} \end{array}$		
1620		$\begin{array}{c} \\ -\text{C}=\text{N}- \\ \left[\begin{array}{c} \text{O} \\ \\ -\text{C}=\text{O} \end{array} \right]^- \text{ if present} \end{array}$	$\begin{array}{c} \\ -\text{C}=\text{N}- \end{array}$
1590			Pyrrone ring (?)
1560			
1460 ± 20		$\begin{array}{c} \quad \\ -\text{N}-\text{C}=\text{N}-^d \end{array}$	$\begin{array}{c} \quad \\ -\text{N}-\text{C}=\text{N}- \end{array}$
1430			$\begin{array}{c} \quad \\ -\text{N}-\text{C}=\text{N}- \end{array}$
1380		$\begin{array}{c} \text{O} \\ \\ \left[-\text{C}=\text{O} \right]^- \text{ if present} \end{array}$	
1370	$\begin{array}{c} \text{O} \\ \\ -\text{C}-\text{N}- \end{array}$		$\begin{array}{c} \text{O} \\ \\ -\text{C}-\text{N}- \end{array}$
930 (multiplet)			Pyrrone ring (?)
830-880	Imide ring (?)		Imide ring (?)
720	Imide ring		Imide ring

^a Identification and assignment of absorption bands based upon data of Young.¹⁵

^b Data of Iwakura et al.¹⁶ and Vogel and Marvel.¹⁷

^c Present in 1,2-benzoylenebenzimidazole but not in model compounds containing two pyrrone groups. It reappears in many pyrrone polymers. We have no explanation for this behavior.

^d Often a doublet.

A consideration of published and unpublished spectra of various polymers and model compounds has led to the tentative infrared absorption correlations shown in Table IV.

Figure 1 shows successive spectra of a film of DAA-PMDA as it was cured. Curve 3 (2 hr, 150°C) is a typical polyimide spectrum, with characteristic bands at 1780, 1725, 1370, and 720 cm^{-1} . After further heating,

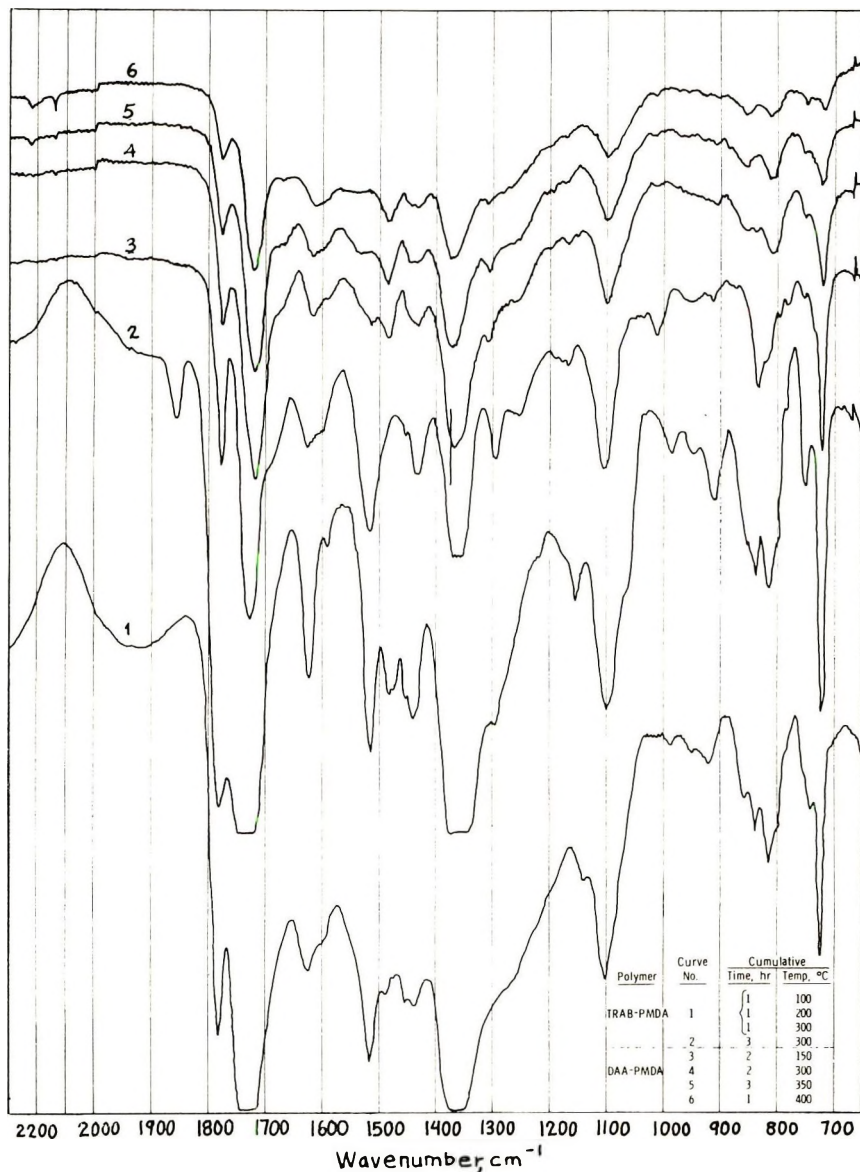


Fig. 1. Infrared spectra of DAA-PMDA and TRAB-PMDA as a function of cure. DAA-PMDA film cast on CsI plate; TRAB-PMDA free film. Cure times are cumulative.

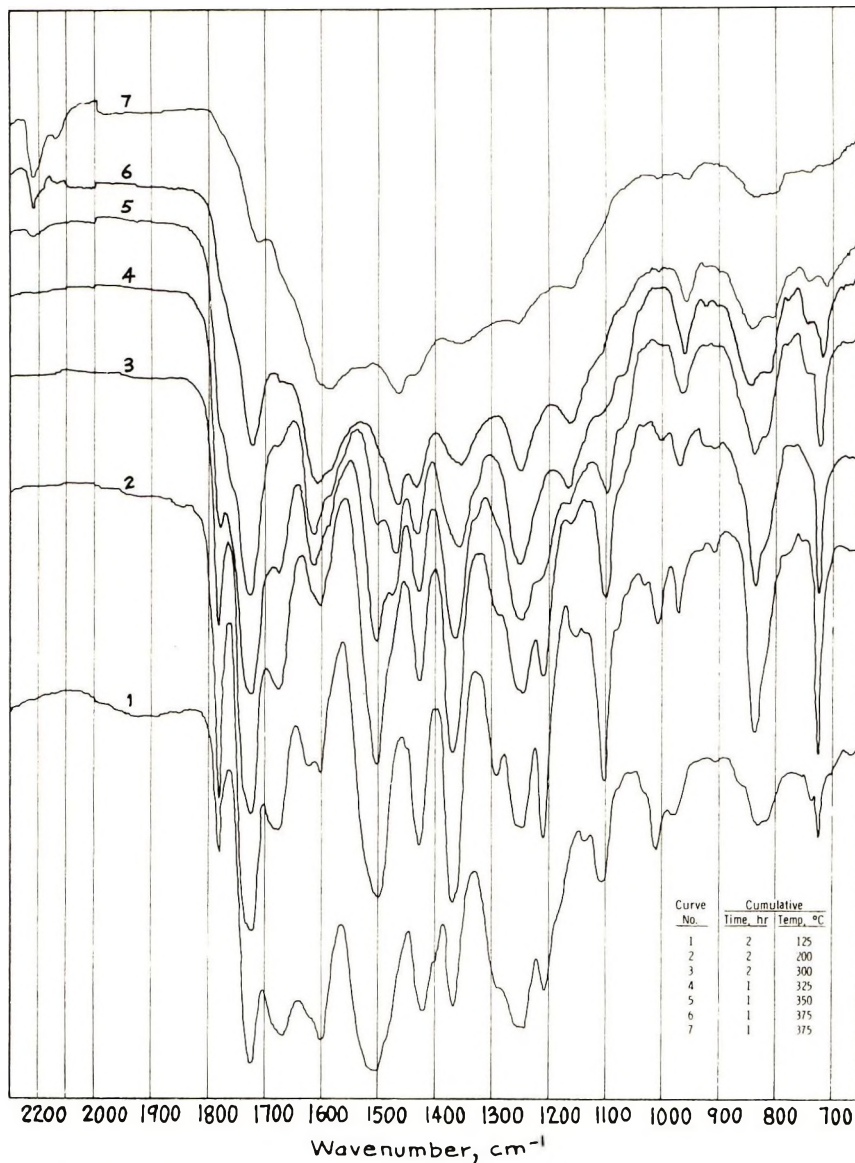


Fig. 2. Infrared spectra of DATAIPO-PMDA as a function of cure. Film cast on CsI plate. Cure times are cumulative.

these bands remained, although the 720 cm^{-1} band appeared to weaken relative to the others. Bands at 1515 , 1290 , 1010 , and 840 cm^{-1} weakened or disappeared. An increase in relative intensity was found at the pyrrone frequencies of 1480 , 860 and 810 cm^{-1} . For comparison, spectra of a film of cured TRAB-PMDA (obtained from Dr. V. L. Bell, NASA-Langley) are included (curves 1 and 2). The spectra are considerably heavier than those derived from DAA-PMDA, but correspond very closely to curves

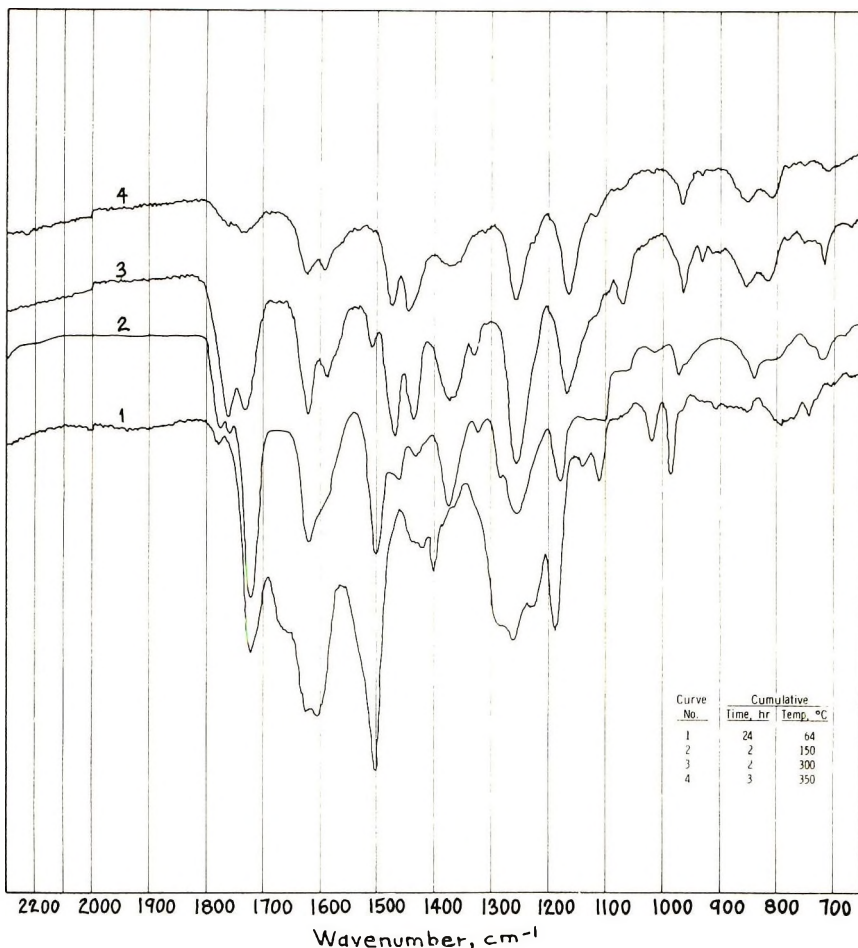


Fig. 3. Infrared spectra of TADPO-PMDA as a function of cure. Film cast on CsI plate. Cure times are cumulative.

4 and 5. When the TRAB-PMDA film was heated for 3 hr at 300°C, an additional band appeared at 1855 cm^{-1} , probably due to anhydride produced by cyclodehydration of terminal carboxyl groups.

Although some of the spectral changes shown in Figure 1 are consistent with pyrrone formation, absence of the strong pyrrone band at 1760 cm^{-1} suggests that very little pyrrone was formed from either TRAB or DAA polymers. Similar results were obtained in an infrared study of the cure of DAA-BTDA polymer.

Figures 2 and 3 present a comparison of the spectra of DATADPO-PMDA and TADPO-PMDA during cure. A typical polyimide spectrum was obtained in the former case after 2 hr at 200°C. Further heating caused gradual elimination of one imide carbonyl at 1780 cm^{-1} , the amide carbonyl at 1680 cm^{-1} , the ring vibration at 1505 cm^{-1} , and bands at 1290,

1210, 1100, 1010 and 840 cm^{-1} . A relative increase was observed at the pyrrone frequencies of 1620, 1470, 960, 850, and 820 cm^{-1} . At the higher temperatures, a band at 2220 cm^{-1} appeared, which has been identified tentatively as nitrile. In the case of TADPO-PMDA, the reaction apparently

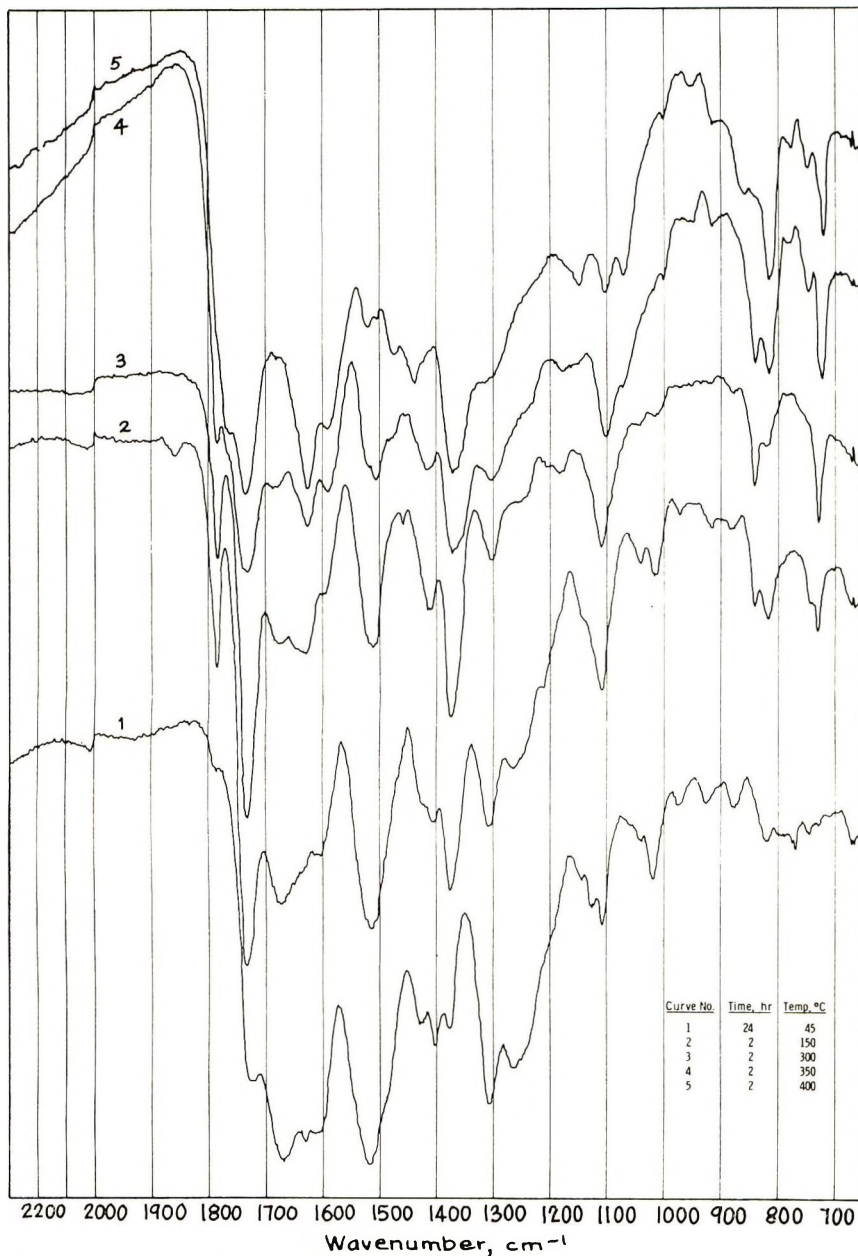


Fig. 4. Infrared spectra of DADAB-PMDA (DMAC-soluble fract.) as a function of cure. Powder in KBr disk. Cure times are not cumulative.

followed a somewhat different course. The polyimide spectrum in curve 2 is not very well defined. The 1780 and 720 cm^{-1} bands are weak, while pyrrolic or benzimidazole bands have begun to appear. The spectrum of the cured polymer corresponds closely to that reported by Bell and Pezdirtz.¹ Essentially the same bands appeared on curing both the TADPO and DATADPO polymers (Fig. 2, curve 5 vs. Fig. 3, curve 3), but the intensities were different. For example, the bands at 1760, 1330, and 1070 cm^{-1} in the TADPO-PMDA polymer were present only as shoulders in the

TABLE V
Pyrolysis Products from DADAB-PMDA

Fraction	Treatments, successive		Weight loss, %	Volatile products	Acid, % of calcu- lated
	Time, hr	Tem- pera- ture, °C			
Insoluble fraction (D92-143-1)					
	14	150	13.0	CO_2 , H_2O , THF ^a	1.18
	2	300	7.4	CO_2 , H_2O ^b	2.88
	2	350	1.9	CO_2 , H_2O , HOAc, Ac_2O ^b	6.28
	18	350	2.9	CO_2 , H_2O , HOAc, Ac_2O	6.66
Total			25.2		17.00
(Calculated 35%)					
Soluble fraction (D93-1-7)					
	2	105	7.8	H_2O , DMAC	
	2	150	5.0	H_2O , DMAC	
	2	300	8.8	H_2O , CO_2 ^c	
	2	350	5.6	H_2O , HOAc, Ac_2O ^d	
Total			27.2		
(Calculated 42%)					

^a Tetrahydrofuran used to wash sample was not completely removed. Probably aliphatic ester or ketone also (1735, 1460, 1370 cm^{-1}).

^b Probably triple bond also (2160, 3070 cm^{-1}).

^c Bleached indicator paper. NMR showed no aromatic protons. Odor of cooked cabbage.

^d Vapor absorbed also at 1135, 1100 cm^{-1} ; liquid at 1370, 1133 cm^{-1} .

DATADPO polymer. Substantial absence of the strong 1760 cm^{-1} pyrrolic band from the spectra of DATADPO polymers indicates a low degree of pyrrolic formation.

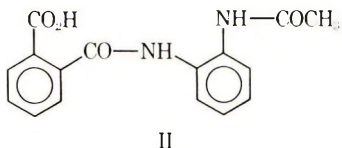
In Figure 4 the infrared spectra of the soluble fraction of DADAB-PMDA polymer after several temperature exposures are presented. Almost identical spectra were observed from the insoluble fraction with the same treatment. The changes on heating were similar to those noted for DATADPO-PMDA although the band at 1470 cm^{-1} did not develop as strongly. The spectrum of the fully cured material resembles that reported by Dawans and Marvel² for DAB-PMDA. However, none of these

spectra show a degree of pyrrone formation approaching that of TADPO-PMDA.

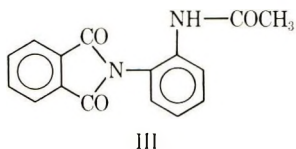
Uncured DATADPO-PMDA and DATADPO-BTDA polymers gave programmed TGA curves with poorly defined steps at 200, 400, and 550°C, probably corresponding roughly to loss of water, loss of acetic acid, and degradation, respectively. Since the observed weight losses were higher than the calculated values for loss of water and acetic acid, it appears that the reactions occurred in an overlapping sequence.

Additional information on the cure mechanisms of DADAB-PMDA was provided by vacuum pyrolysis experiments in which the volatile products were trapped and analyzed. A sample of the polymer under test was sealed in a glass apparatus which was evacuated to about 10^{-6} torr. The sample was then heated while volatiles were trapped in a liquid nitrogen trap. After a heating period, the trap was removed and its contents analyzed by infrared spectroscopy. The trap was cleaned and replaced, and the cycle repeated. Several successive heating cycles were applied to each polymer sample, using various times and temperatures. For the insoluble fraction, the condensates were also titrated to obtain a quantitative measure of the acetic acid produced. Results from the two samples are summarized in Table V. The observation that the acetyl group begins to be eliminated at about 350°C agrees with the infrared spectra data and the TGA results. CO_2 elimination suggests that decarboxylation was a side reaction. If some of the linkages were converted to benzimidazole groups through reaction with the acetamido group in the initial ring closure, an isolated carboxyl group would be left, which could easily lose CO_2 . There was some indication of the formation of a volatile nitrile, isonitrile, or substituted acetylene.

A considerable amount of work was done with model compounds in an effort to understand the reactions occurring in the cure of polymers derived from diacetyl tetramines. The compound II was held at 200°C for 30 min

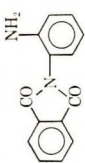
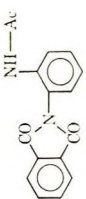
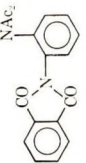

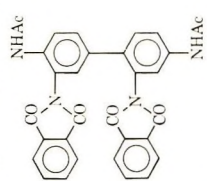


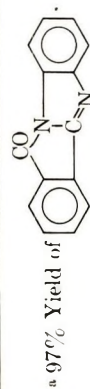
in a slow stream of nitrogen. The weight loss was 90% of that calculated for simple dehydration, and the residue gave a 92% yield of III.



Programmed TGA of this product gave complete sublimation without pyrolysis.

TABLE VI
Pyrolysis of Model Compounds at 400°C in N₂

Code Name	Structure	Sample wt, g	Residue		Sublimate	
			g	% of sample wt	g	% of sample wt
OPD-PA		1.7757	0.0008	0.5	1.5849	89.3 ^a
OAA-PA		0.6553	0.0248	3.78	0.4598	70.2
DAOPD-PA		1.0118	0.1684	16.64	0.3537	34.96
(OAA) ₂ -PMIDA		3.3058	1.90	57.5	0.65	19.7
DADAB-(PA) ₂		0.65	0.44	68.0	0.07	11.0



When the less volatile DADAB-(PA)₂ (imide) (see Table VI for structure and abbreviations for model compounds) was subjected to programmed TGA (2.5°C/min) in flowing nitrogen, a curve was obtained with a well-defined step at 430°C, which is about the temperature at which acetic acid was expected to be eliminated. Under the same conditions, (OAA)₂-PMDA (amide acid) gave steps at 200 and 420°C, which correspond to loss of water and acetic acid, respectively. However, since some sublimation also occurred in both cases, observed weight losses were higher than the calculated values. Weight loss of both materials was very slow above 500°C, and a residue of about 35% remained at 1000°C.

With isothermal TGA at 400°C, the weight loss of (OAA)₂-PMDA (imide) in flowing nitrogen was 40% in less than 2 min; 45.5% in 1 hr. No additional loss occurred in the next 2 hr. Apparently both sublimation and reaction occurred during the initial rapid loss, and a nonvolatile polymeric residue remained. Similar results were obtained with DADAB-(PA)₂ except that the weight loss occurred over a period of several hours.

The second step in the cure was also studied by pyrolyzing several imidized model compounds for 3 hr at 400°C in a slow stream of nitrogen and examining the products. A horizontal glass tube was used, 25 mm in diameter, with a 30 cm hot zone. The sample was contained in a porcelain boat near the inlet end of the hot zone, to provide for pyrolysis of vapors as well as residues. Results with five model imides of interest are summarized in Table VI.

OPD-PA was converted almost quantitatively to the pyrrone, which sublimed. In the case of OAA-PA, the infrared spectrum of the sublimate was almost identical to that of the starting material. Apparently, most of the compound sublimed without change. The spectrum of the residue contained bands at 1720 (similar to pyrolyzed DADAB-PMDA polymer), 1680 (amide), 1620 (pyrrone or benzimidazole), 1450 (pyrrone or benzimidazole), and 730 cm⁻¹ (imide or pyrrone).

The compound DAOPD-PA incorporates a blocking structure that was not evaluated in polymers. It was studied briefly here to determine its suitability. The spectra of both sublimate and residue were essentially identical to the corresponding fractions from OAA-PA. Apparently, the second acetyl group is lost easily to give the monoacetyl compound.

Pyrolysis of (OAA)₂-PMDA gave sublimate and residue fractions having essentially identical spectra, similar to Figure 4, curve *δ*, but differing in intensity ratios. Strong absorption bands at 1730, 1620, 1450, 1370, and 740 cm⁻¹ suggest a pyrrone structure. However, the strong 1760 cm⁻¹ pyrrone band was present only as a shoulder.

In the case of DADAB-(PA)₂, both sublimate and residue gave typical pyrrone spectra, almost identical to that of benzoylenebenzimidazole. Attempts to isolate pure compounds from pyrolysis products by crystallization and chromatography failed for all compounds except OPD-PA.

The results of cure and pyrolysis experiments are not entirely free from ambiguities, but the following statements are reasonably consistent with observations.

Polymers derived from tetraamines and dianhydrides cure by more than one mechanism. The amino-carboxamide linkages in the uncured polymer are converted to both carboxybenzimidazole and aminoimide groups in the initial stage of curing. Further heating converts the latter structure almost completely to pyrrole. Conversion of carboxybenzimidazole groups to pyrrole is less complete, and some decarboxylation occurs. Other linkages present in the uncured polymer lead to branching and the formation of imide, benzimidazole, and other groups in the fully cured polymer.

Polymers derived from diacetyl tetraamines and dianhydrides are converted almost quantitatively to linear acetamido imide intermediates. A high temperature (350°C) is required for further cure. Both acetic acid and carbon dioxide are eliminated in the latter stages, with the formation of small amounts of pyrrole, together with benzimidazole and other structures, and some crosslinking.

Details of structure play an important part in determining cure mechanism and final products. For example, DADAB-(PA)₂ cures readily to a pyrrole, whereas (OAA)₂-PMDA does not, and the *o*-diamino grouping in TRAB is not as cleanly converted to pyrrole as the corresponding structures in tetraamines.

EXPERIMENTAL

DTA-TGA Determinations

Differential thermal and thermogravimetric analyses were performed on a duPont 900-950 Thermal Analyzer. Melting points were determined with the same apparatus at a heating rate of 15°C/min. In some cases the melting point was observed visually, but usually it is reported as the minimum point in the DTA curve.

DAA Polymers

Purification. DAA (Gallard-Schlesinger) was purified by recrystallization from water containing a trace of sodium hydrosulfite. Colorless prisms were obtained, mp 163°C.

Polymers Prepared in DMAC. A solution of 16.520 g (0.1 mole) of purified DAA in 217 ml of DMAC (dried over 5 Å Molecular Sieve) was stirred in flame-dried apparatus under dry nitrogen while 21.813 g (0.1 mole) of PMDA was added rapidly. Complete solution occurred exothermically in a few minutes. The solution was stirred for about 3 hours to be sure reaction was complete. A solution of PMDA in DMAC (0.100 g/ml) was then added in 1.00 ml increments to the stirred polymer solution. Viscosity was measured by drawing the solution up into a 7 mm tube and measuring the flow time between two marks about 10 cm apart, at a head of about 25 cm. After each addition the flow time was checked periodically until it became essentially constant. At this point, another increment was added and the process repeated until no further increase occurred. The

final addition of PMDA gave a decline in viscosity. Apparently, the optimum amount of PMDA was about 1% more than the calculated quantity. The final solution was light amber, and had an inherent viscosity (0.5% in DMAC, 25°C) of 0.69 dl/g 28 hr after the initial PMDA addition.

A 20% solution of DAA-BTDA was prepared by adding solid BTDA to an equimolar quantity of DAA in DMAC. It had a viscosity of about 630 cS. Films were very brittle.

DATADPO Polymers

Preparation of DATADPO. 3,3'-Dinitro-4,4'-diacetamidodiphenyl ether was prepared by a modification of the procedure of Foster and Marvel¹⁸ and was recrystallized from acetic acid. A 15-g portion of this compound in 200 ml of methanol was hydrogenated in a Parr shaker at 50–70°C and 50 psi by using 0.2 g of 5% Pd-on-C catalyst. The product was recrystallized from methanol to give 8.5 g (68% yield) of DATADPO, mp 230°C.

ANAL. Calcd. for $C_{16}H_{18}N_4O_3$: C, 61.13%; H, 5.77%; N, 17.82%. Found: C, 61.05, 61.28%; H, 5.81, 5.86%; N, 17.75, 17.99%.

Infrared and NMR spectra were consistent with the desired structure and showed that essentially no cyclization to benzimidazole had occurred. Preparation of DATADPO by hydrazine reduction has been reported by Korshak et al.¹⁹

DATADPO and BTDA. A solution of 6.28 g (0.020 mole) of DATADPO in 36 g of DMAC was stirred while 5.0 g of BTDA was added. When solution was complete, additional BTDA was added in small increments until a total of 6.7 g (0.021 mole) has been added. The viscosity rose after each addition, and the final solution had a viscosity of about 500 cS at 25% solids.

Similar preparations in other solvents gave the viscosities shown in Table I.

DATADPO and PMDA. This polymer was prepared by the preceding procedure.

Film Casting Attempts. Fully cured films cast on aluminum dishes, glass, and copper foil adhered very strongly to the substrate. In only one example was a creasable film obtained. This was a small sample cast on an aluminum dish and removed by soaking in water. The film could not be removed from the glass except in shreds. The samples on copper foil blistered in spite of a very cautious cure cycle. When the copper was removed by dissolving in ferric chloride the film was in shreds.

Uncured films were cast by spreading the solution on aluminum plates and air-drying at room temperature for 24 hr. These films were easily peeled from the substrate. They were clear, pale yellow and very flexible but became extremely brittle when attempts were made to cure them further by baking (100°C in vacuum) or by treatment with acetic anhydride-pyridine at room temperature.

DADAB Polymers

Preparation of DADAB. 3,3'-Dinitro-*N,N'*-diacetylbenzidine (American Aniline) was recrystallized from DMF. A 301-g sample of the product was hydrogenated in 16 batches, using about 20 g per batch, together with 200 ml of DMF and 2 g of 5% Pd-on-C catalyst. A pressure of 40–50 psi and a temperature of 50–70°C were used. The product in each case was filtered while warm and the filtrate mixed with 250 ml of water. After standing overnight in a refrigerator, the mixture was filtered and the solid product washed with water followed by acetone, and dried at 100°C under vacuum. The combined hydrogenated product weighed 206.5 g (83% yield).

A solution of 205 g of this material in 800 g of DMSO was allowed to flow through a 1³/₄ × 22 in. column of adsorption alumina (activated by heating overnight at 325°C). Additional DMSO was added immediately thereafter and the column was kept filled with liquid as long as product was being collected. The first 1800 ml of solution to come through was diluted with 3600 ml of water and allowed to stand overnight in the refrigerator. The resulting precipitate was filtered off, washed with water and with acetone, and dried at 100°C under vacuum to give 175 g of pale yellow powder (sharp DTA endotherms at 263 and 348°C).

ANAL. Calcd. for C₁₆H₁₈O₂N₄: C, 64.41%; H, 6.08%; N, 18.78%. Found: C, 64.19, 64.40%; H, 6.06, 6.18%; N, 18.79, 18.55%.

DADAB and BTDA. A slurry was made of 0.5454 g (1.828 mmole) of DADAB and 4.54 g of dry DMAC, in which it is only slightly soluble at room temperature. BTDA (recrystallized from acetone) was added in portions, with stirring, until 0.5888 g (1.828 mmole) had been added. A clear yellow solution of 20% solids was obtained. Inherent viscosity in DMAC (0.5% solution, 25°C) was 0.28 dl/g. Films cast from the solution were very brittle.

DADAB and PMDA. A mixture of 29.835 g (0.1 mole) of DADAB and 207 ml of dry DMAC was stirred under dry nitrogen while 21.813 g (0.1 mole) of PMDA was added in about 10 min. A somewhat exothermic reaction occurred, and a very cloudy orange fluid was formed, weighing 239.8 g (21.54% solids). It was found necessary to dilute a sample of the product with DMAC to 1% or less in order to get a clear solution. The inherent viscosity (0.5%, 26°C) in DMAC was 0.32 dl/g.

When the preparation was repeated in DMSO, a clear solution was obtained, inherent viscosity 0.56 dl/g. It became cloudy on standing overnight, and was converted to a non-fluid grease in a few days.

A series of 20% solutions was made by adding portions of a dry mixture of equimolar quantities of DADAB and PMDA to DMF, DMAC, DMSO, and mixtures of them. The only solution that remained reasonably clear for 18 hr was the one made in DMAC. Several preparations of this type were filtered after aging. The precipitates were washed several times with the solvent used in the preparation and several times with THF and were dried under vacuum at 45°C. The amount of polymer left in solution

TABLE VII
Partial Precipitation of DADAB-PMDA Solutions

Run no.	Solvent	Solids, %	Aging, hr	Total, g ^a	Polymer solids			
					Insoluble ^b		Soluble ^c	
					g	%	g	
D92-141-3	DMAc	3	265	0.75	0	Trace	0.75	100
D92-141-4	DMAc	6	265	1.50	<7.0	<0.1	>1.4	>93
D92-141-5	DMAc	12	265	3.00	7.7	0.23	2.77	92.3
D92-141-6	DMAc	24	265	6.00	11.5	0.69	5.31	88.5
D92-141-7	DMAc	30	267	7.70	9.5	0.73	6.97	90.5
D92-139-11	DMAc	25	220	2.00	15.0	0.30	1.70	85.0
D92-123-5	DMAc	21.5	1370	—	15.5	6.65	36.4 ^d	84.5
D92-141-8	DMF + 3 DMAc	11	480	51.6	2.55	2.55	39.8 ^e	85.7
D92-126-1	DMSO	18.8	1320	—	8.00	8.00	49.0	95.1
							31.7 ^d	79.9

^a Total weight of PMDA + DADAB used. Corresponds to weight of amic acid form of polymer. In two cases an unknown portion of the original solution was used, so this value was not known.

^b Precipitate washed with THF, dried at 45°C under vacuum.

^c By difference, except as noted below.

^d Calculated for amic acid form from TGA data (to 400°C at 10°/minute), assuming TGA residue to be imide.

^e Precipitated with acetone, washed with acetone, dried at 45°C under vacuum.

was calculated from TGA data on the filtrate (per cent residue after heating to 400°C at 10°C/min), by difference, or by precipitation with acetone and weighing. Results are summarized in Table VII.

Batches D92-141-3 to 7 were prepared at the same time, from the same batch of dry-mixed reactants. A clear solution was obtained in each case. The 24 and 30% solutions precipitated about 2 hr after preparation. Fifteen hours after preparation, the other three clear solutions were seeded with a trace of solid from the first two. Precipitation occurred slowly over a period of several hours. The amount of precipitate in the 6% solution was not measured, but estimated visually to be considerably less than half that of the 12% solution.

A 51.3 g sample of the clear solution obtained by filtration of the product from D92-123-5 was added, with stirring, to 500 ml of acetone. The mixture was allowed to stand for 2 hr and filtered. The precipitated polymer was washed with acetone and dried for 24 hr at 45°C under vacuum to give 11.5 g of pale yellow powder.

Analyses of various DADAB-PMDA precipitates were made, with the results shown in Table VIII.

TABLE VIII
Analysis of DADAB-PMDA Polymer Precipitates

Run no.	Analysis of precipitate ^a				
	C, %	H, %	N, %	O, %	S, %
D92-141-5	59.66	4.57	9.17	26.48	—
D92-141-6	57.92	4.81	9.82	27.77	—
D92-139-11	56.92	4.28	9.88	—	—
D92-141-8	57.88	4.78	9.68	27.41	—
D92-123-5 (soluble fraction)	58.12	4.87	11.31	25.81	—
D92-123-5 (insoluble fraction)	59.10	4.74	9.85	26.21	—
D92-126-1	54.56	4.65	8.44	24.70	7.56
Calculated for ^b					
DADAB-PMDA · 1.5 DMSO	55.00	4.62	8.84	24.00	7.58
DADAB-PMDA · DMAC · H ₂ O	58.00	5.03	11.27	25.75	—
DADAB-PMDA	60.50	3.91	10.85	24.80	—

^a Average of two determinations.

^b Amide acid form of polymer.

The soluble and insoluble fractions from D92-123-5 were studied further. Separate samples of each were heated for 2 hr at 150, 300, 350, and 400°C (not successively). The 150 and 300°C bakes were in ovens in air. The 350 and 400°C samples were heated in nitrogen in a TGA apparatus from 25°C to temperature at 10°C/min and then held at temperature for 2 hr. Observed weight losses are shown in Table IX.

TABLE IX

Fraction	Weight loss, %	
	350°C	400°C
Soluble fraction	32	37
Insoluble fraction	23	31

Another sample was heated in nitrogen at 10°C/min to 755°C with a weight loss of 51%.

DATA B Polymer

A mixture of 10 g of 1,3-diamino-4,6-dinitrobenzene (Burdick and Jackson) and 50 ml of acetic anhydride was stirred while three drops of concentrated sulfuric acid was added. The mixture became clear and warm. It was heated to 135°C, held for 15 min, and cooled. A precipitate formed, which was filtered off, washed and dried to give 9.8 g (69% yield) of 1,3-diacetamido-4,6-dinitrobenzene, mp 197°C.

ANAL. Calcd. for $C_{10}H_{10}N_4O_6$: C, 42.56%; H, 3.57%; N, 19.86%. Found: C, 43.00, 42.90%; H, 3.59, 3.63%; N, 19.89, 19.92%.

A mixture of 10 g of 1,3-diacetamido-4,6-dinitrobenzene, 0.2 g of 5% Pd-on-C, 50 ml of DMAC, and 150 ml of methanol was hydrogenated at 55 psi and 65°C. The mixture was cooled and filtered. The solid material was washed and dried to give 6.4 g of a mixture of catalyst and crude DATA B, which gave DTA endotherms at 260 and 467°C, with an exotherm at 277°. Infrared and NMR spectra were consistent with the expected structure. Because of low solubility and the hazard of conversion to benzimidazole on heating, the product was not purified further.

A polymer was prepared from 25 g of DMAC, 4.44 g (0.02 mole) of the mixture of catalyst and DATA B and 6.44 g (0.02 mole) of BTDA. A moderately viscous solution was obtained. It was diluted with 12 g of DMAC and filtered to remove hydrogenation catalyst. Samples baked out in aluminum dishes gave very poor films.

Copolymers

A suspension of 5.97 g (0.02 mole) of DADAB in 140.5 g DMAC was stirred while 6.44 g (0.02 mole) of BTDA was added. A clear solution was obtained, in which was dissolved 8.65 g (0.08 mole) of MPD. To this solution was added 25.78 g (0.08 mole) of BTDA, with stirring. A clear amber solution was obtained, viscosity X (Gardner). Additional batches of polymer prepared on a larger scale by the same procedure gave solutions with viscosities of S-X (Gardner) at 23–24% solids.

A 6 × 6 in. 10-ply laminate was made with 181 A-1100 E-glass cloth. The coated cloth was air-dried for 45 min and then precured for 20 min at 150°C. The laminate was pressed at 1000 psi and a temperature that rose

from 300 to 490°C in 30 min and was held at 450–490°C for 15 min. A smooth black board was obtained, 0.09 in. thick, containing 24% resin. A 12-ply 12 × 12 in. laminate was made from the same prepreg, at 1000 psi and 400°C for 30 min. The pressure was released momentarily to release volatiles (bumped) in the early part of the pressing, and some resin blew out of the board at that time. The final laminate was 0.106 in. thick, contained 22% resin, and did not appear as uniform as the small board.

Table III includes test results for these and other similar laminates.

Model Compound Syntheses

2'-Nitrophthalanil. A mixture of 27.63 g (0.2 mole) of *o*-nitroaniline, 29.62 g (0.2 mole) of sublimed PA, 150 ml of DMAC, and 50 ml of xylene was refluxed with stirring under a Dean-Stark trap. During an 18-hr period 5.9 ml of aqueous layer collected in the trap, after which no additional material was obtained. The cooled product was mixed with 200 ml of water, stirred for 2 hr, and filtered. The resulting precipitate was filtered off, washed with water, and dried at 140°C under vacuum to give 36.5 g (68% yield) of crude 2'-nitrophthalanil. Recrystallization from 350 ml of glacial acetic acid gave 34.1 g of yellow needles, mp 203°C.

ANAL. Calcd. for $C_{14}H_8N_2O_4$: C, 62.75%; H, 3.01%; N, 10.45%; O, 23.87%. Found: C, 62.60, 62.71%; H, 3.07, 2.93%; N, 10.34, 10.50%; O, 24.05; 23.81%.

2'-Aminophthalanil. A mixture of 34.0 g of 2'-nitrophthalanil, 1700 ml of ethanol, and 2 g of 5% Pd-on-C catalyst was hydrogenated at 150 psi and 75–95°C. The product was filtered hot. The filtrate was cooled, and the resulting yellow crystals were filtered off and dried to give 19.0 g (63% yield) of 2'-aminophthalanil, mp 193°C. A second recrystallization from ethanol raised the mp to 194°C (lit. mp 194–195°C).³

2'-Acetamidophthalanilic Acid. A mixture of 136 g (0.92 mole) of sublimed PA, 136 g (0.91 mole) of OAA, and 1050 ml of chloroform was refluxed with stirring for 2 hr and allowed to cool. The precipitate was filtered off and dried at 50°C under vacuum to give 260 g (96% yield) of 2'-acetamidophthalanilic acid as a white powder, mp 164°C. Recrystallization from ethanol gave white needles, mp 168°C.

ANAL. Calcd. for $C_{16}H_{14}N_2O_4$: C, 64.42%; H, 4.73%; N, 9.39%; O, 21.45%. Found: C, 64.37, 64.41%; H, 4.70, 4.69%; N, 9.31, 9.29%; O, 21.51, 21.66%.

2'-Acetamidophthalanil, 2'-(Diacylamino)phthalanil, and $C_{16}H_{10}N_2O_2$. A mixture of 29.6 g (0.2 mole) of PA (sublimed), 29.9 g (0.2 mole) of OAA, and 225 ml of chloroform was refluxed with stirring for 3 hr. Acetic anhydride (200 ml) was added, and solvent was distilled until a vapor temperature of 130°C was reached. The residual clear yellow solution (212 g) was evaporated nearly to dryness at room temperature in a stream of nitrogen. The resulting moist solid was recrystallized twice from methanol to give 22.1 g of white crystals (D93-15-4). An additional 6.2 g was recovered from the filtrate from the second crystallization.

Evaporation of the filtrate from the first crystallization, followed by drying for 4 days at 135°C under vacuum, gave 20.9 g of a yellow-brown solid. Extraction of this material with 200 ml of boiling methanol gave a solution and a yellow solid. The latter was filtered off and dried to give 2.2 g of tan powder. A 0.5 g sample of this residue was recrystallized twice from 50 ml of DMSO to give 0.3 g of fine yellow crystals.

ANAL. Calcd. for $C_{16}H_{10}N_2O_2$: C, 73.27%; H, 3.85%; N, 10.69%; O, 12.20%. Found: C, 72.42, 72.19%; H, 3.82, 3.78%; N, 10.56, 10.36%; O, 13.29, 13.40%.

The DTA curve gave only poorly defined endotherms, the major one being at about 440°C. The infrared spectrum showed no absorption bands in the imide carbonyl region, but absorbed strongly at 3200 (broad), 1620, 1590, 1570, 1470, 1410, 1370, 1350, 1340, 1280, 1190, 1150, 740, 530, and 480 cm^{-1} . The mass spectrum showed the presence of two compounds, MW 262 (corresponding to analysis $C_{16}H_{10}N_2O_2$) and 276. The former lost two units of $m/e = 28$ in steps, giving 234⁺ and 206⁺ (206⁺⁺ and 206⁺⁺⁺ also observed). The latter also lost a 28 unit to give 248⁺. The NMR spectrum was inconclusive because of partial solubility problems. The structure of this by-product has not been established.

D93-15-4 was recrystallized several times from methanol and from chloroform. Two major fractions were obtained. The first, mp 205°C, was identified as 2'-acetamidophthalanil.

ANAL. Calcd. for $C_{16}H_{12}N_2O_3$: C, 68.56%; H, 4.32%; N, 10.00%; O, 17.12%. Found: C, 68.45, 68.70%; H, 4.46, 4.46%; N, 9.85, 10.06%; O, 17.30, 17.20%.

The second fraction, mp 182°C, was identified as 2'-(diacetylamino)-phthalanil.

ANAL. Calcd. for $C_{18}H_{14}N_2O_4$: C, 67.07%; H, 4.38%; N, 8.69%; O, 19.86%. Found: C, 66.87, 67.10%; H, 4.30, 4.37%; N, 8.89, 8.69%; O, 20.06, 19.90%.

2'-Acetamidophthalanil was also synthesized from 2'-aminophthalanil. A mixture of 0.50 g of the latter and 2.5 ml of acetic anhydride was heated to boiling to give a clear solution. On cooling, a granular solid separated. An equal volume of water was added to the mixture, which was warmed for a few minutes and filtered. The solid was washed with water and dried to give 0.49 g of a tan granular solid product mp 203°C.

ANAL. Calcd. for $C_{16}H_{12}N_2O_3$: C, 68.56%; H, 4.32%; N, 10.00%; O, 17.12%. Found: C, 67.66, 67.87%; H, 4.16, 4.26%; N, 9.64, 9.80%; O, 18.33, 18.45%.

The infrared spectrum contained the features expected for 2'-acetamidophthalanil.

Pyromellitic Diacid Bis(*o*-acetamidoanilide). A solution of 21.8 g (0.1 mole) of sublimed PMDA in 225 ml of THF was added to a warm stirred mixture of 30.0 g (0.2 mole) of OAA and 150 ml of THF. A brick red color appeared where the solutions first mixed, but faded rapidly. A heavy white precipitate formed. The mixture was refluxed gently for 30 min, cooled and filtered. The solid product was dried at 65°C under vacuum to give

52.0 g (100% yield) of pyromellitic diacid bis(*o*-acetamidoanilide), probably a mixture of the two expected isomers.

ANAL. Calcd. for $C_{26}H_{22}N_4O_8$: C, 60.23%; H, 4.28%; N, 10.80%; O, 24.69%. Found: C, 60.20, 60.05%; H, 4.83, 4.74%; N, 10.03, 9.92%; O, 24.95, 25.12%.

DTA gave a rather broad endotherm at 187°C (mp and dehydration of amide acid) and a sharp one at 384°C (mp of imide).

Pyromellitic Bis(*o*-acetamidoanil). A mixture of 25.9 g (0.05 mole) of the preceding product and 100 ml of xylene was refluxed with stirring, using a Dean-Stark trap to remove water. After 7 hr of reflux, 1.7 ml (calculated 1.8 ml) of water had collected. The solid product was filtered off and dried at 130°C under vacuum to give 23.8 g (99% yield) of crude product. A 10 g sample was recrystallized from 250 ml of DMF to give 4.1 g of purified pyromellitic bis(*o*-acetamidoanil), mp 390°C.

ANAL. Calcd. for $C_{26}H_{18}N_4O_6$: C, 64.73%; H, 3.76%; N, 11.61%; O, 19.90%. Found: C, 64.79, 64.88%; H, 3.90, 3.77%; N, 11.50, 11.53%; O, 19.82, 19.99%.

***N,N'*-Diacetyl-3,3'-bis(*N''*,*N'''*-phthalimido)benzidine.** A mixture of 14.9 g (0.05 mole) of DADAB, 14.8 g (0.10 mole) of sublimed PA, and 50 ml of DMSO (dried over Molecular Sieve) was heated slowly. A clear solution was obtained at 70°C. The solution was held at 80°C for 2 hr and at 115–120°C for 1 hr. During the latter period a heavy precipitate slowly formed. The mixture was cooled and filtered. The solid product was washed with acetone and dried at 130°C under vacuum to give 12.0 g of pale yellow powder. An additional 7.4 g of product was recovered by diluting the filtrate with water (70% total yield). A 10 g sample of the first crop was recrystallized from NMP to give 8.8 g of purified *N,N'*-diacetyl-3,3'-bis(*N''*,*N'''*-phthalimido)benzidine, mp 415°C.

ANAL. Calcd. for $C_{32}H_{22}N_4O_6$: C, 68.81%; H, 3.97%; N, 10.04%; O, 17.19%. Found: C, 68.05, 68.19%; H, 4.08, 4.11%; N, 10.07, 10.09%; O, 17.99, 17.85%.

The authors are indebted to Mr. R. M. Skena and Mr. J. Gasper for synthesis, fabrication, and evaluation of polymers and to Dr. D. H. Lemmon and Mr. J. R. Ray for infrared and NMR spectra.

Financial support of this research by the National Aeronautics and Space Administration is gratefully acknowledged (Contract NAS1-7354).

References

1. V. L. Bell and G. F. Pezdirtz, *J. Polym. Sci. B*, **3**, 977 (1965).
2. F. Dawans and C. S. Marvel, *J. Polym. Sci. A*, **3**, 3549 (1965).
3. J. G. Colson, R. H. Michel, and R. M. Paufler, *J. Polym. Sci. A-1*, **4**, 59 (1966).
4. L. E. Karre, L. B. Keller, and L. J. Miller, NASA CR-1310 (1969).
5. V. L. Bell and R. A. Jewell, *J. Polym. Sci. A-1*, **5**, 3043 (1967).
6. V. L. Bell, *J. Polym. Sci. B*, **5**, 941 (1967).
7. L. W. Frost and G. M. Bower, *J. Polym. Sci. A*, **1**, 3135 (1963).
8. C. E. Sroog, A. L. Endrey, S. V. Ambromo, C. E. Berr, W. M. Edwards, and K. L. Olivier, *J. Polym. Sci. A*, **3**, 1373 (1965).
9. L. W. Frost and I. Keese, *J. Appl. Polym. Sci.*, **8**, 1039 (1964).

10. V. L. Bell, paper presented at SPE RETEC, Washington, D.C., September 1967.
11. W. R. Dunnivant, *J. Polym. Sci. B*, **6**, 49 (1968).
12. J. H. Freeman, L. W. Frost, G. M. Bower, E. J. Traynor, H. A. Burgman, and C. R. Ruffing, *Polymer Eng. Sci.*, **9**, 56 (1969).
13. R. A. Jewell, *J. Appl. Polym. Sci.*, **12**, 1137 (1968).
14. G. M. Bower, J. H. Freeman, E. J. Traynor, L. W. Frost, H. A. Burgman, and C. R. Ruffing, *J. Polym. Sci. A-1*, **6**, 877 (1968).
15. P. R. Young, Langley Research Center, NASA, unpublished data.
16. Y. Iwakura, K. Uno, and J. Imai, *J. Polym. Sci. A*, **2**, 2605 (1964); *Makromol. Chem.*, **77**, 33 (1964).
17. H. Vogel and C. S. Marvel, *J. Polym. Sci.*, **50**, 511 (1961).
18. R. T. Foster and C. S. Marvel, *J. Polym. Sci. A*, **3**, 417 (1965).
19. V. V. Korshak, V. V. Rode, G. M. Tseitlin, G. M. Cherkasova, and N. A. Berezina, *Polym. Sci. USSR*, **11**, 36 (1969).

Received November 23, 1970

Icosahedral Carboranes. XVI. Preparation of Linear Poly-*m*-carboranylenesiloxanes

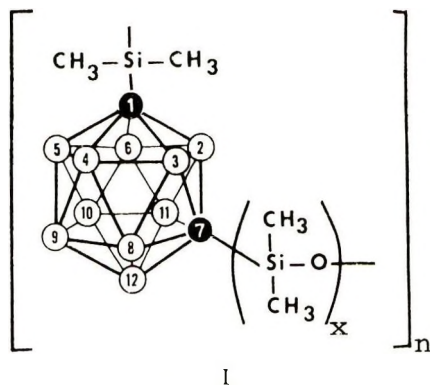
KARL O. KNOLLMUELLER, ROBERT N. SCOTT,
HERBERT KWASNIK, and JOHN F. SIECKHAUS,
Olin Research Center, Chemicals Group, New Haven, Connecticut 06504

Synopsis

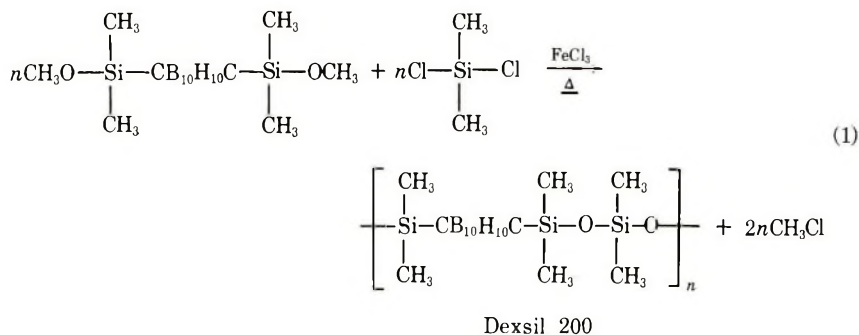
The first members of the series of poly-*m*-carboranylenesiloxanes were synthesized by the ferric chloride-catalyzed condensation of methoxy- and chloro-terminated monomers and generally obtained as insoluble crosslinked gums. It has now been discovered that long-chain, linear polymers can be prepared by simple hydrolytic condensation of $m\text{-B}_{10}\text{H}_{10}\text{C}_2(\text{SiMe}_2\text{OSiMe}_2\text{Cl})_2$ and $m\text{-B}_{10}\text{H}_{10}\text{C}_2(\text{SiMe}_2\text{OSiMe}_2\text{OSiMe}_2\text{Cl})_2$ at ice bath temperature, as well as by acid-catalyzed condensation of the corresponding silanols. In addition, phenyl-substituted copolymers have been obtained which show outstanding thermo-oxidative stability at elevated temperature. These linear polymers are soluble waxes and liquids with molecular weights between 16,000 and 30,000; they are potentially useful as high-temperature liquids and coatings and can be cured at room temperature to form elastomers.

INTRODUCTION

The seventh paper in this series¹ describes the synthesis of the first members of a family of polysiloxanes characterized by *m*-carborane units incorporated in the polymer backbone. These materials have the general formula I:



and are prepared by the ferric chloride-catalyzed copolymerization of chloro- and methoxy-terminated monomers as shown in eq. (1) for the case where $x = 2$.



Except for the species where $x = 1$ (a soluble crystalline material), these carborane siloxanes are rubberlike polymers which swell in organic solvents. In a recent study, Dietrich et al.² have found that the final stage of reaction (1) involves a crosslinking step and, consequently, a network polymer is obtained instead of the expected linear species.

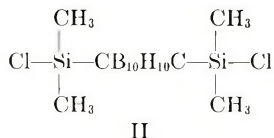
All of these polycarboranylenesiloxanes have excellent high-temperature properties, and Dexsil 200,* in particular has shown great promise as a thermoresistant elastomer.^{3,4}

We now wish to report the preparation of a system of linear polycarboranylenesiloxanes obtained by condensation of chloro and hydroxy terminated monomers.

RESULTS

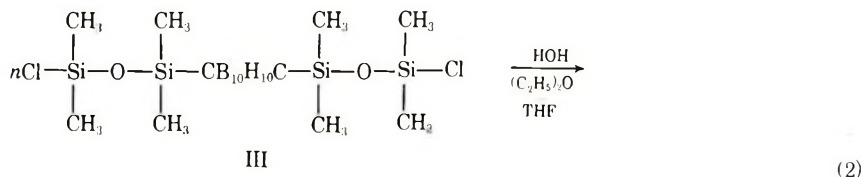
Condensation of Chloro-Terminated Monomers

It was recently discovered that while the silicon atom attached directly to the carborane cage in II is particularly reluctant to form

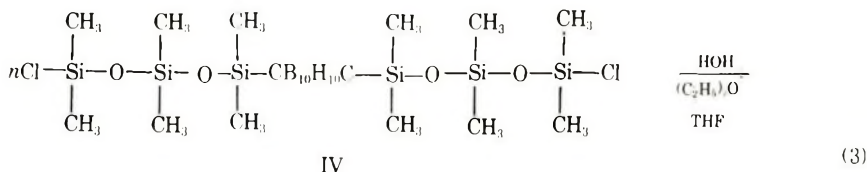
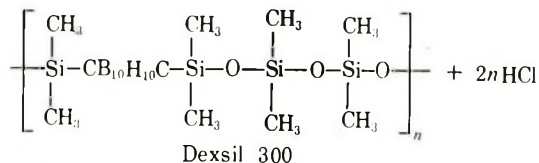


siloxane linkages in simple hydrolytic condensation reactions (the silanol is quite stable), carborane-based siloxanes like III¹ and IV⁵ can be hydrolyzed at room temperature to form long chain, linear polymers. (For the sake of simplicity these polymers will be referred to by their tradenames as Dexsil 300 and Dexsil 500, respectively.)

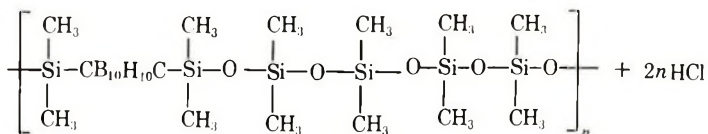
* The correct chemical name of this compound is poly-1-dimethylsilyl-7-(bisdimethylsiloxy)-1,7-dicarbasododecaborane. For sake of brevity, the name SiB polymers had been coined and a digit was used to indicate the number of dimethylsiloxy groups in the repeating unit, in this case 2. When Olin introduced these polymers in an exploratory marketing program in 1967, the trade name Dexsil was adopted. In the numbers then employed such as 200, 201, 402, etc., the first digit represents the number of siloxy groups in the recurring unit; the remaining digits identify the individual polymer species within a specific "hundred" series.



(2)



(3)



Dexsil 500

In contrast to the high temperatures required in the ferric chloride-catalyzed reaction (1), these condensations occur at ice-bath temperature and can be controlled to produce polymers with specific molecular weight ranges. This is illustrated in Figure 1, which shows the effect of the water/monomer ratio on the molecular weight distribution of Dexsil 300 polymer, the highest molecular weight products (16,000–20,000) being obtained with a ratio of 1.2–1.4/1.0.

The water/monomer ratio has a similar effect on the molecular weight of Dexsil 500, and a gel-permeation chromatogram of the highest molecular weight material (20,000–30,000) is shown in Figure 2.

Both of these polymers are truly linear species, as attested by the fact that they are low-melting (30–50°C) waxes (Dexsil 300) or viscous liquids (Dexsil 500), and are extremely soluble in common organic solvents. Evidence for their regular structure was obtained from an analysis of the NMR spectra (Table I).

Proton spectra of Dexsil 300 polymers contain only two distinct CH_3 -Si resonances in an exact 1/1 ratio, corresponding to the methyl protons on the two different types of silicon atoms in the polymer structure. In the Dexsil 500 case, three resonance lines corresponding to methyl groups a, b, and c would be expected, but only two are observed. The intensity ratio of these signals is 2/1, however, and it is assumed that line broadening (due to the

TABLE I
Proton Magnetic Resonance Spectra of Carborane Siloxanes in CDCl_3

Compound	Chemical shifts of Methyl Silicon Protons ^a		
	a	b	c
III	15.2	27.1	
Dexsil 300	11.7	5.2	
VI	12.3	6.8	
VII	9.3	4.8	
XII ^b	12.1	8.2	
IV	13.0	8.2	26.6
Dexsil 500	11.8	4.9	4.9
V	10.3	6.4	5.3
XI	8.0(4) ^c	11.3(2)	22.6(1)
		4.8(2)	
XIII ^b	12.2	8.1	6.1

^a Relative to tetramethylsilane. Assignments are based on spectra of model compounds described in Paper XV of this series;^b a refers to $(\text{CH}_3)_2\text{Si}$ moiety immediately adjacent to carborane; similarly, b is $(\text{CH}_3)_2\text{Si}$ group next removed, etc.

^b Chemical shift assignments are tentative.

^c Relative intensity.

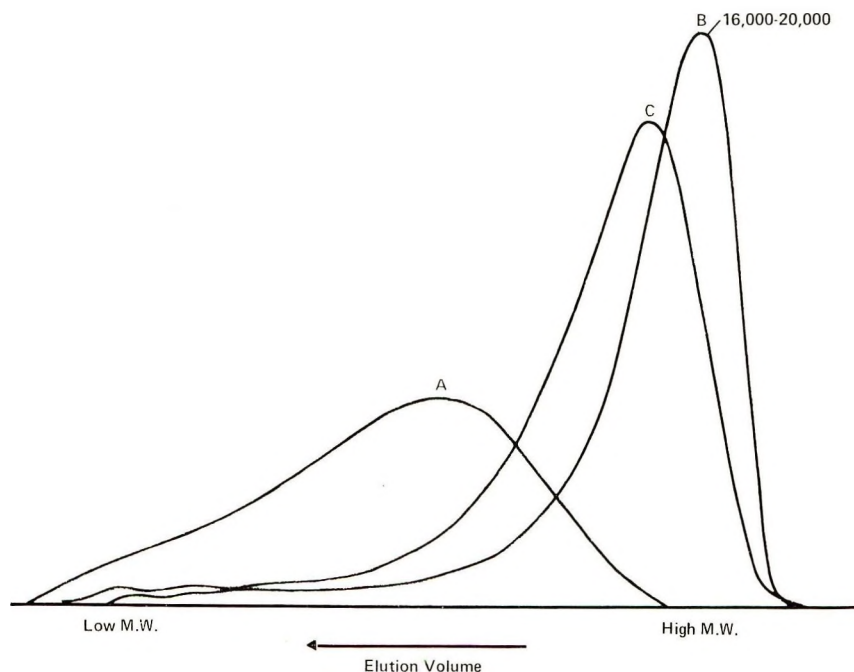
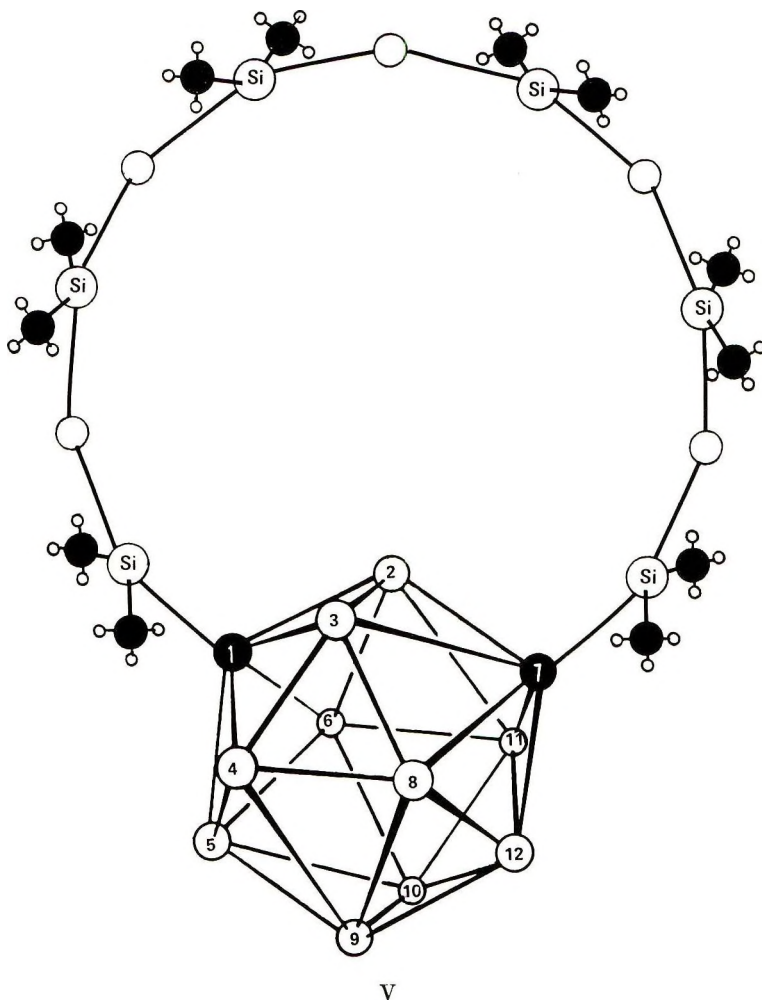
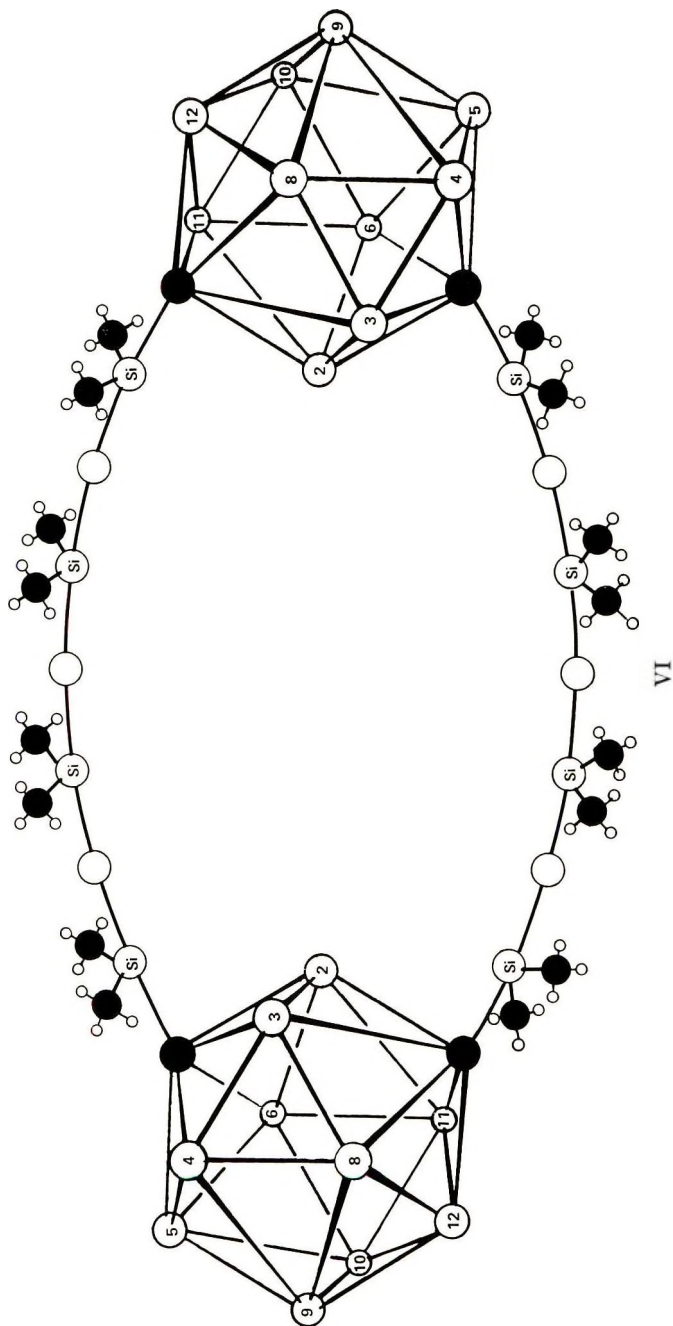


Fig. 1. Effect of water/monomer ratio on molecular weight distribution of Dexsil 300 (gel-permeation chromatography): (A) water/monomer = 1.0/1.0; (B) 1.2-1.4/1.0; (C) 1.6/1.0.



molecular weight, and infrared spectrum (no Si-OH absorptions) of this monomeric species are in complete agreement with structure V, and the proton magnetic resonance spectrum (Table I) contains the expected three $\text{CH}_3\text{-Si}$ signals, all clearly resolved and of equal intensity.

The methanol-soluble material obtained by fractional precipitation of Dexsil 300 contains a broad distribution of oligomer and polymeric species (Fig. 3). Two major components appear at molecular weights corresponding to dimer and trimer and the former was isolated by extraction with acetone. This material was purified by recrystallization from petroleum ether and is presumed to have structure VI. The molecular weight of this cyclic carborane siloxane was found to be 851 (calcd, 844); the NMR spectrum (Table I) contains only two C-H resonances (equally intense), and, again, no Si-OH absorption is observed in the infrared spectrum.



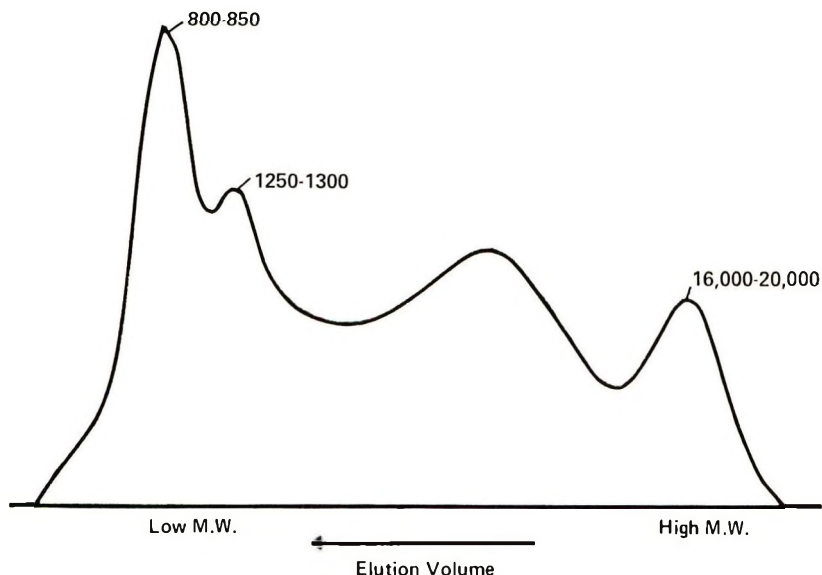
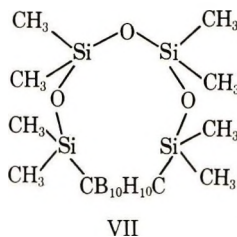


Fig. 3. Gel-permeation chromatogram of methanol-soluble Dexsil 300 fraction.

The trimeric species has not been isolated to date, but a few milligrams of a crystalline material tentatively identified as VII were obtained by vacuum

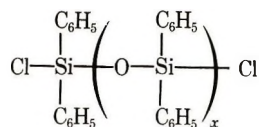


distillation of the methanol-soluble phase. The mass spectrum of this species contains a major molecular ion at 407 mass units (attributed to the parent compound minus a methyl group), and the NMR spectrum shows only two equally intense methyl proton resonances (Table I). (These signals have quite different chemical shifts from those of VI.)

Copolymers with Phenylsilanes

Since some evidence had been obtained from previous studies^{1,4} that phenyl substituents on silicon atoms have a beneficial effect upon the thermoxidative stability of carborane-based siloxanes, a series of copolymerization reactions was conducted between III and the phenylsilanes VIII-X

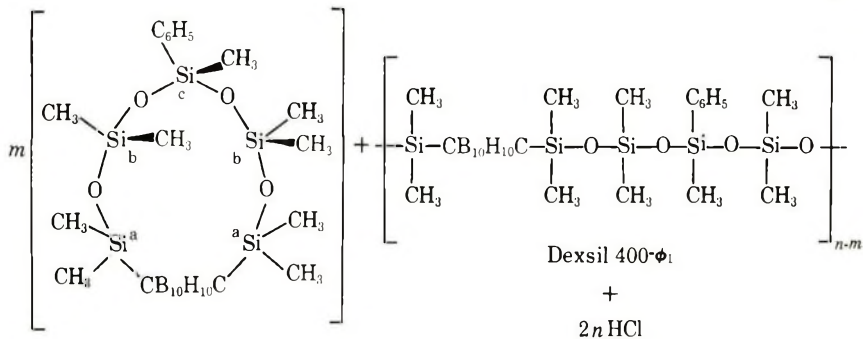
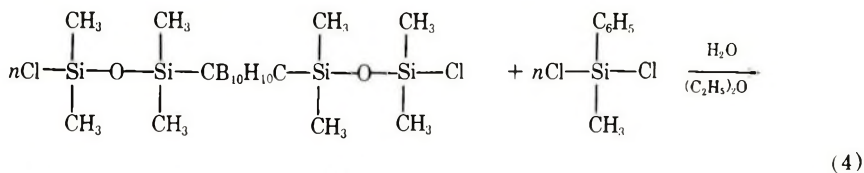
Cohydrolysis of III and VIII proceeds in uniform fashion with the formation of cyclic compound XI (~15%) and the linear polymer, Dexsil 400- ϕ_1


 VIII $x = 0$

 IX $x = 1$

 X $x = 2$

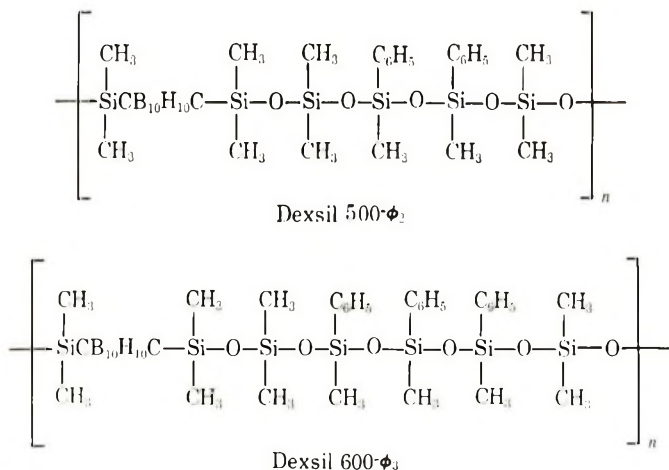
[eq. (4)]. XI was separated from the liquid polymer (mol. wt. 15,000–17,000) by fractional precipitation and purified by distillation.



XI

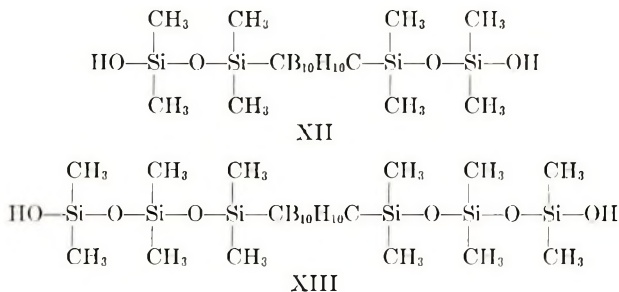
The proton magnetic resonance spectrum of this apparent cyclic species is quite interesting in that it exhibits two b-methyl signals (Table I) which arise, presumably, as a result of stereochemical interaction between the phenyl group and methyl substituents on adjacent silicon atoms (b). A spectrum of the polymer, on the other hand, is not as easily interpreted since six methyl proton resonances are observed. It is reasonable to assume, though, that this material has a random structure and this would certainly cause the appearance of additional methyl signals. The $\text{CH}_3/\text{C}_6\text{H}_5$ ratio (as calculated by integration of the areas under all methyl and phenyl signals) agrees exactly with the theoretical value based on the initial stoichiometry.

Dexsil 500- ϕ_2 and 600- ϕ_3 polymers are obtained by condensation of III with IX and X and have molecular weights comparable to Dexsil 400- ϕ_1 . These are liquid species and presumably also have random structures, since seven and eight methyl proton signals (respectively) are observed in their NMR spectra.



Condensation of Hydroxy-Terminated Monomers

Another approach to the synthesis of high molecular weight, linear carborane-siloxane polymers that has proved successful has been the acid-catalyzed* condensation of hydroxy-terminated monomers, XII and XIII.



These silanols are obtained in quantitative yield by treatment of III and IV with NaHCO_3 in moist ether. Sulfuric acid has proved to be the best of the catalysts tested, but it has not led to the production of Dexsil 300 and 500 species with molecular weights greater than those of the polymers obtained via hydrolytic condensation of III and IV.

Thermal Stability

Since the poly-*m*-carboranylenesiloxanes obtained as crosslinked gums in ferric chloride-catalyzed condensations [such as (1)] have outstanding stabilities at elevated temperature,¹ it was of great interest to observe the thermal behavior of these linear polymeric waxes and liquids.

Thermal gravimetric analysis (TGA) was employed as the principal tool in this study, and Figure 4 contains comparative weight loss profiles in argon of polydimethylsiloxanes (PDMS) and various linear Dexsil polymers.

* Basic catalysts as weak as CaO effect cleavage of the carborane-silicon bond.

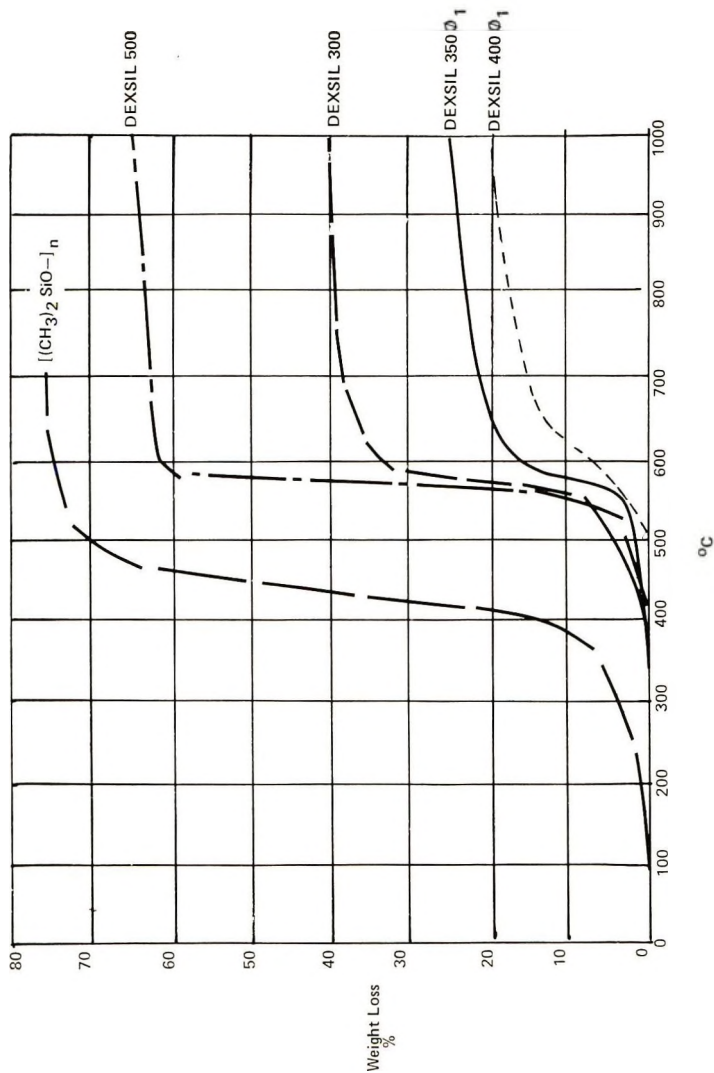


Fig. 4. TGA of linear Dexsil polymers in argon. Heating rate, 2.5°C/min.

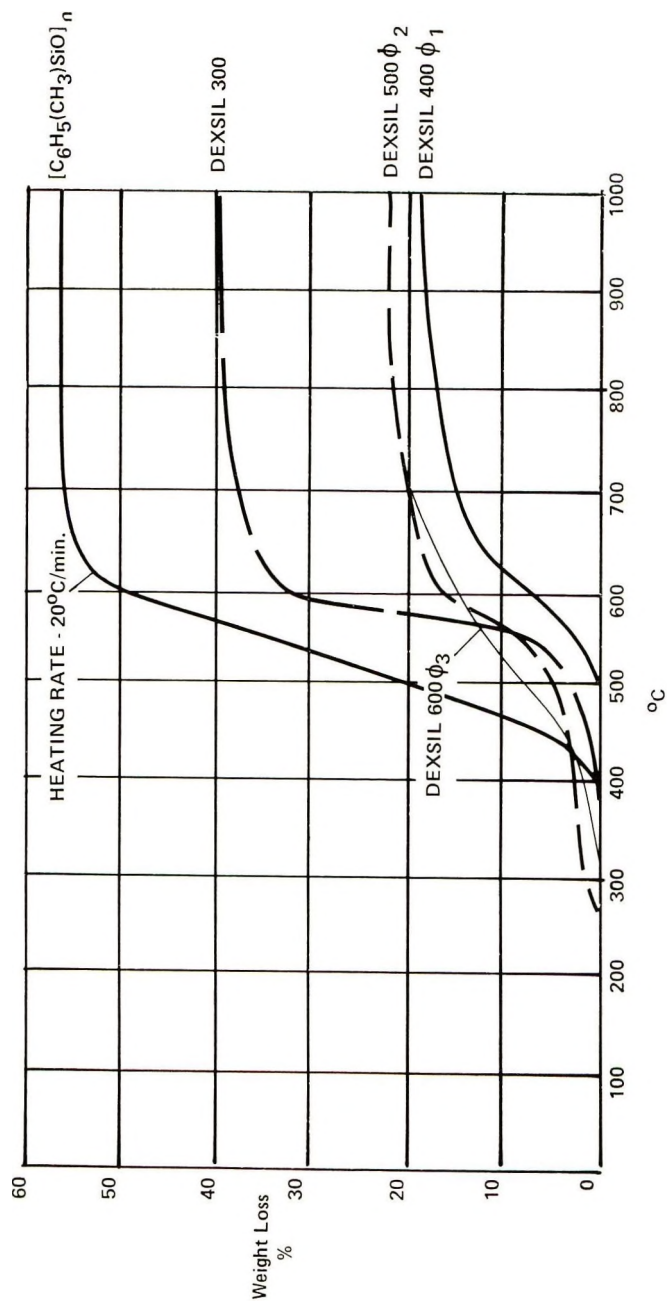


Fig. 5. TGA of phenylated Dexsil copolymers, Dexsil 300, and polydimethylsiloxane in argon. Heating rate, 2.5°C/min.

[Dexsil 350- ϕ_1 is a copolymer prepared from a 2/1 molar ratio of II and $C_6H_5(CH_3)SiCl_2$.] Weight loss increases quite markedly with the concentration of $(CH_3)_2SiO$ groups in the series Dexsil 300 < Dexsil 500 < PDMS, and the temperature interval of maximum weight loss is some 100–200°C lower for PDMS (400–500°C) than for the carborane-based siloxanes (550–650°C).

In the case of Dexsil polymers 350- ϕ_1 and 400- ϕ_1 , a dramatic improvement in stability (over Dexsil 300) is brought about by incorporation of small concentrations of phenyl substituents (~ 5 and 10 mole-%, respectively), despite the fact that the chain length between carborane moieties has been increased. Isothermal gravimetric analyses (Table II) provide additional evidence of this enhanced stability, as an appreciable difference is observed in the rates of weight loss of Dexsils 300 and 400- ϕ_1 when heated at 500°C. Furthermore, weight loss of the partially phenylated polymer had ceased during the last half hour of heating whereas the rate of weight loss of the methylated species did not change significantly during the course of the measurement.

TABLE II
Isothermal Gravimetric Analysis of Dexsil Polymers

Polymer	Temperature, °C	Time, hr	Rate of weight loss, %/hr
Dexsil 300	300	5	—
	400	2 ² / ₃	1.8
	500	3	11.1
Dexsil 400- ϕ_1	400	3	1.0
	500	2 ¹ / ₃	2.4

Figure 5 contains thermograms of copolymers with varying concentrations of phenyl substituents and proportionately long siloxane chains between carborane moieties. All of these phenylated materials experience smaller weight losses than their methylated analogs, but the 500- ϕ_2 and 600- ϕ_3 species suffer most of this weight loss at temperatures 50–100°C lower than Dexsil 400- ϕ_1 . The opposing effects of enhanced stabilization due to higher phenyl group concentration and destabilization caused by greater intercarborane chain length apparently combine in this latter species to produce the maximum thermal stability. In the former two polymers, the effect of a higher percentage of phenyl substituents is more than offset by the longer siloxane chain and the net result is a slight destabilization (relative to Dexsil 400- ϕ_1). The TGA of polyphenylmethylsiloxanes is given in this figure also to demonstrate the ultimate effect of increasing the phenyl group concentration to 50% and eliminating carborane moieties from the polymer backbone.

TGAs of linear Dexsil polymers in air show a pattern of stabilities quite similar to that in argon but the overall weight losses are much less (Fig. 6). All of these species presumably undergo oxidative cross-linking between 300

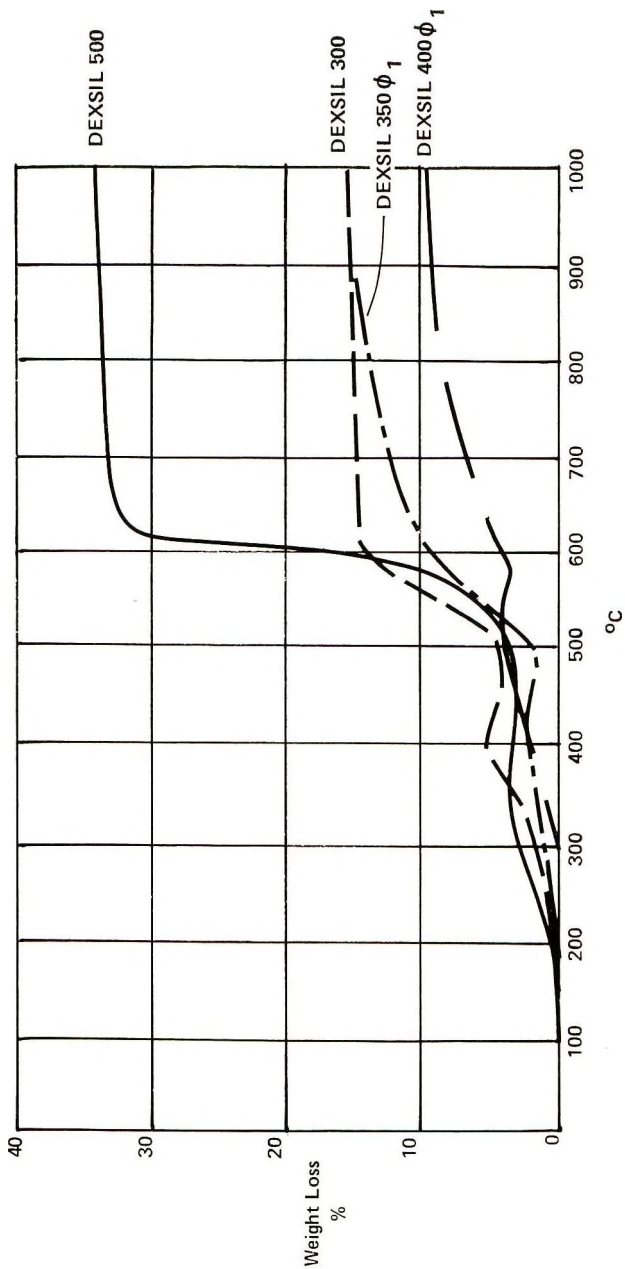


Fig. 6. TGA of linear DEXSIL polymers in air. Heating rate, 2.5°C/min.

and 500°C, resulting in network structures that are somewhat more stable toward depolymerization and volatilization. (Normal methyl and phenyl silicones suffer weight losses of 60–80% when heated under these conditions.) Dexsil polymers 500- ϕ_2 and 600- ϕ_3 have weight loss profiles quite comparable to that of Dexsil 400- ϕ_1 .

The unusual properties of these linear Dexsil species have led to their use in a number of applications. They have demonstrated potential as high temperature fluids and coatings, and can be cured at room temperature to form elastomers. Details of this work will be reported subsequently.

EXPERIMENTAL

Monomers

Compounds III and IV were prepared as described in papers VII¹ and XV² of this series.

Dexsil 300 Polymer

All operations were conducted under nitrogen. A 5-l, three-necked flask equipped with a truebore stirrer, dropping funnel, and thermometer was charged with 502.6 g (1.052 mole) of III and 2100 ml diethyl ether. The flask was cooled with an ice bath, and 26.527 g (1.473 mole) H₂O in 400 ml THF was added over a period of 30 min. Stirring was continued for an additional 30 min, and no significant temperature change was noted. The flask was warmed to 25°C and, after continued stirring for 2½ hr, the solvents were stripped under reduced pressure. Last traces of solvent were removed from the viscous liquid product by continuous pumping at 0.5 mm Hg and 30–35°C for 24 hr and then at room temperature for 3 days. After 30 hr at room temperature, the liquid turned to a wax (mp 30–40°C), yield 422 g (95%). The Dexsil 300 polymer thus obtained had a number-average molecular weight of 10,000 (by VPO) with a GPC peak maximum at 16,000–20,000 (Fig. 1). When a water/monomer ratio of 1.2/1.0 is employed in this reaction, waxy polymer with a similar molecular weight distribution is obtained. With ratios of 1.0/1.0 and 1.6/1.0, however, products with GPC peak maxima at 5000–6000 and 12,000–16,000, respectively, are produced.

ANAL. Calcd for C₁₀H₃₄B₁₀O₃Si₄: C, 28.41%; H, 8.11%; B, 25.57%; Si, 26.56%. Found: C, 28.38%; H, 7.66%; B, 25.58%; Si, 25.95%.

Compound VI

A 420 g sample of Dexsil 300 polymer (prepared with a 1.4/1.0 water/monomer ratio) was dissolved in 600 ml diethyl ether, and 1500 ml of methanol was added slowly with stirring over a 2-hr period. Stirring was then stopped and the precipitated polymer allowed to settle. The slightly turbid methanol phase was decanted and set aside. The procedure was repeated and the combined methanol phases were concentrated *in vacuo*, giving an oily material which contained the desired product as well as a mixture of oligomeric Dexsil 300 species (Fig. 3). The oil was pumped on overnight

at 0.5 mm Hg to remove traces of solvent, and 35 ml of acetone was added. After shaking for 10 min and allowing the mixture to stand in a refrigerator for ~ 4 hr, a crystalline material formed and was filtered. The cyclic dimer was recrystallized from high-boiling petroleum ether, mp 149.4°C; yield 1.85 g; molecular weight in benzene (VPO) 851 (calcd, 844).

ANAL. Calcd for $C_{26}H_{68}B_{20}O_6Si_6$: C, 28.41%; H, 8.11%; B, 25.57%. Found: C, 28.60%; H, 8.58%; B, 25.67%.

Compound VII

The filtrate from above was concentrated *in vacuo* and the small amount of VI that formed was removed by pressure filtration. Distillation of the oily filtrate (~ 3 ml) then gave a fraction (~ 0.5 ml) boiling up to 153°C at 0.01 mm Hg which was allowed to stand for 48 hr. The crystals which slowly formed in the oil were filtered and recrystallized twice from petroleum ether (bp 30–60°C); yield 58 mg (0.01%); mp 158.3–158.6°C.

Dexsil 500 Polymer

The procedure is essentially that described for Dexsil 300. A 500 ml flask was charged with 62.87 g (0.1 mole) of IV in 350 ml diethyl ether and 2.53 g (0.14 mole) of H_2O in 35 ml THF was added over a 20-min period. After stirring for 1 hr at 0°C and 2.5 hr at 25°C, the solvents were removed at reduced pressure and pumping of the residue for 4 days *in vacuo* over NaOH produced a viscous liquid product with the molecular weight distribution shown in Figure 2. The high molecular weight fraction was isolated by dissolving this material in 150 ml ether and slowly adding 300 ml methanol. The precipitate was allowed to settle and the supernatant liquid was decanted. The procedure was repeated, and the precipitate was dried at 40°C *in vacuo*. The Dexsil 500 polymer thus obtained had a number-average molecular weight of 21,000 (VPO).

ANAL. Calcd for $C_{14}H_{46}B_{10}O_5Si_6$: C, 29.44%; H, 8.12%; B, 18.94%. Found: C, 29.53%; H, 8.03%; B, 19.14%.

Compound V

The combined methanol phases from the Dexsil 500 polymer fractionation were evaporated *in vacuo* and the residual oil was pumped on over NaOH for 2 days (0.5 mm Hg). Distillation of this material then gave a clear, viscous liquid, bp $135 \pm 3^\circ C/0.01$ mm Hg, which solidified on standing; mp 37°C.

ANAL. Calcd for $C_{14}H_{46}B_{10}O_5Si_6$: C, 29.44%; H, 8.12%; B, 18.94%; Si, 29.50%. Found: C, 29.56%; H, 8.07%; B, 18.86%; Si, 29.07%.

Copolymers of III with VIII, IX, and X

The procedure used in the synthesis of Dexsils 400- ϕ_1 , 500- ϕ_2 , and 630- ϕ_3 was a slightly modified version of that described for Dexsil 300. In a typical experiment, a 2-l flask was charged with 100 g (0.209 mole) of III, 40.95

g (0.214 mole) of methylphenyldichlorosilane (VIII) and 675 ml diethyl ether. After addition of 10.7 g (0.593 mole) of H_2O in 70 ml THF over a 45-min period, the solution was stirred for 2.5 hr at 25°C. The solvents were then removed at reduced pressure and the residual viscous liquid was stored over KOH *in vacuo* (continuous pumping) for 5 days. The gel-permeation chromatogram of this material exhibited a small peak at 500–600 molecular weight in addition to the major peak at 15,000–17,000. The high molecular weight product was precipitated from diethyl ether with methanol, and the resulting viscous liquid polymer was dried *in vacuo* at 25°C. Composition was verified by NMR analysis.

Dexsil polymers 350- ϕ_1 , 500- ϕ_2 , and 600- ϕ_3 were prepared in similar fashion, and the liquid polymeric products thus obtained had molecular weights of \sim 13,000–17,000.

Compound XI

The methanol-soluble phase from the fractionation of Dexsil 400- ϕ_1 was stripped of solvent and distilled *in vacuo* to give a pale yellow liquid, bp 183°C/0.25mm Hg.

ANAL. Calcd for $C_{17}H_{42}B_{10}O_4Si_5$ (559 g/mole): C, 36.54%; H, 7.57%; B, 19.34%. Found: C, 36.95%; H, 7.71%; B, 18.72%; mol wt. (VPO), 576.

Compound XII

A solution of 450 g of II in 450 ml diethyl ether was added rapidly (\sim 25 min) to a suspension of 600 g sodium bicarbonate in 2.7 l. of ether containing 4.5 ml H_2O . Stirring was continued for 2 hr, at which time the evolution of CO_2 had ceased. The salts were then filtered off, and the filtrate was concentrated *in vacuo*. The last traces of solvent were removed at reduced pressure and the product crystallized on standing, mp 48–51°C; yield 413 g (99.5%). Vacuum distillation then gave the monomer in 98% yield; bp 138°C/0.01 mm Hg.

ANAL. Calcd for $C_{16}H_{36}B_{10}O_4Si_4$: C, 27.24%; H, 8.23%; B, 24.54%; Si, 25.48%. Found: C, 27.38%; H, 8.22%; B, 24.30%; Si, 25.53%.

Compound XIII

This liquid monomer was obtained from IV in the same manner as that described for XII; yield 94%; bp 156°C/0.01 mm Hg.

ANAL. Calcd for $C_{14}H_{36}B_{10}O_6Si_6$: C, 28.54%; H, 8.21%; B, 18.36%; Si, 28.60%. Found: C, 28.67%; H, 8.20%; B, 18.09%; Si, 27.88%.

Condensation of XII with H_2SO_4

XII was heated *in vacuo* with a catalytic quantity of H_2SO_4 (\sim 0.6 wt-%) for 20 min at 200°C and 4 hr at 170°C. The product was then dissolved in diethyl ether and treated with $NaHCO_3$ and activated carbon to neutralize the acid and remove a slight discoloration. After filtration and removal of the solvent at reduced pressure, a Dexsil 300 polymer was obtained with a molecular weight distribution quite comparable to B in Figure 1.

The authors are indebted to Drs. H. A. Schroeder and S. I. Trotz for stimulating discussions, and to Mr. H. Hoberecht and Dr. T. Groom for the mass spectral and NMR analyses, respectively. This work was supported by the Office of Naval Research.

References

1. S. Papetti, B. B. Schaeffer, A. P. Gray, and T. L. Heying, *J. Polym. Sci. A-1*, **4**, 1623 (1966).
2. H. J. Dietrich, R. P. Alexander, H. Kwasnik, C. O. Obenland and H. A. Schroeder, *J. Polym. Sci.*, in press.
3. H. A. Schroeder, O. G. Schaffling, T. B. Larchar, F. F. Frulla, and T. L. Heying, *Rubber Chem. Technol.*, **39**, 1184 (1966).
4. H. A. Schroeder, *Rubber Age*, **58**, 101 (Feb. 1969).
5. R. N. Scott and H. A. Schroeder, *Inorg. Chem.*, **9**, 2597 (1970).

Received March 27, 1970

Revised July 29, 1970

Stereospecific Polymerization of Isobutyl Vinyl Ether. III. Polymerization with $VCl_3 \cdot LiCl$ *

YASUSHI JOH,[†] KOICHI HARADA,[‡] HEIMEI YUKI, and SHUNSUKE MURAHASHI, *Department of Polymer Science, Faculty of Science, Osaka University, Toyonaka, Osaka 560, Japan*

Synopsis

The polymerization of isobutyl vinyl ether by vanadium trichloride in *n*-heptane was studied. $VCl_3 \cdot LiCl$ was prepared by the reduction of VCl_4 with stoichiometric amounts of BuLi. This type of catalyst induces stereospecific polymerization of isobutyl vinyl ether without the action of trialkyl aluminum to an isotactic polymer when a rise in temperature during the polymerization was depressed by cooling. It is suggested that the cause of the stereospecific polymerization might be due to the catalyst structure in which LiCl coexists with VCl_3 , namely, $VCl_3 \cdot LiCl$ or $VCl_2 \cdot 2LiCl$ as a solid solution in the crystalline lattice, since VCl_3 prepared by thermal decomposition of VCl_4 and a commercial VCl_3 did not produce the crystalline polymer and soluble catalysts such as VCl_4 in heptane and $VCl_3 \cdot LiCl$ in ether solution did not yield the stereospecific polymer. It was found that some additives, such as tetrahydrofuran or ethylene glycol diphenyl ether, to the catalyst increased the stereospecific polymerization activity of the catalysts. Influence of the polymerization conditions such as temperature, time, monomer and catalyst concentrations, and the kind of solvent on the formed polymer was also examined.

INTRODUCTION

In previous papers^{1,2} we reported the stereospecific polymerization of isobutyl vinyl ether with the trialkylaluminum-vanadium chlorides system in which vanadium trichloride is effective at AlR_3/VCl_n ratio higher than 6, and found that a crystalline poly(isobutyl vinyl ether) was obtained even at room temperatures. Catalytic species in this system are substantially different from VCl_n ($n = 2, 3, 4$) which acts as a cationic polymerization catalyst.

On the other hand, $VCl_3 \cdot LiCl$ and $VCl_2 \cdot 2LiCl$ without any trialkylaluminum induce the stereospecific polymerization of isobutyl vinyl ether to a crystalline polymer when a rise of temperature during polymerization was depressed by cooling. Recently, several studies on the cationic polymeriza-

* Presented at 12th Annual Meeting of the Society of Polymer Science, Tokyo, Japan, 1963.

[†] Present address: Research Laboratory, Mitsubishi Rayon Co., Ltd., Otake, Hiroshima, Japan.

[‡] Present address: Research Department, Sumitomo Chem. Co., Ltd., Niihama, Ehime, Japan.

tion with heterogeneous catalysts have been reported. Typical examples of these catalysts are LiClO_4 ,³ CrO_3 ,⁴ and an $\text{Al}_2(\text{SO}_4)_3 \cdot \text{H}_2\text{SO}_4$ complex.⁵⁻⁷ $\text{VCl}_3 \cdot \text{LiCl}$ and $\text{VCl}_2 \cdot 2\text{LiCl}$ are of interest as heterogeneous cationic polymerization catalysts; therefore, the polymerization of isobutyl vinyl ether with $\text{VCl}_3 \cdot \text{LiCl}$ was studied in considerable detail.⁸ The optimum polymerization temperature for this polymerization was around 20–30°C, which is considered to be one of the characteristics of the polymerization with heterogeneous cationic polymerization catalysts.⁵⁻⁷ Some of the additives to the catalyst, such as tetrahydrofuran or ethylene glycol diphenyl ether, increased the stereospecificity of polymerization. The influence of polymerization conditions on the polymerization was carefully studied by using $\text{VCl}_3 \cdot \text{LiCl}$ catalyst.

EXPERIMENTAL

Materials

Isobutyl vinyl ether, *n*-heptane, vanadium tetrachloride, and *n*-butyllithium were the same as those described in a previous paper.¹ Ethers such as diethyl ether, dibutyl ether, diphenyl ether, anisole, ethylene glycol dimethyl ether, ethylene glycol diphenyl ether, and tetrahydrofuran were refluxed over metallic sodium under nitrogen and then distilled once. The distillates were again refluxed over lithium aluminum hydride, then fractionally distilled under nitrogen immediately before use. TiCl_3 (types AA, HA, and H) were obtained from Wako Chemical Drug Co. A commercial VCl_3 was obtained from Mitsuwa Chemical Co.

Polymerization Catalyst

A VCl_4 solution (0.5 mole/l. in *n*-heptane) and *n*-BuLi solution (0.5 mole/l. in *n*-heptane) were prepared and stored in special catalyst solution vessels. The Schlenk-type polymerization reactor was thoroughly dried by flaming while it was being flushed with a dry nitrogen gas. To this, *n*-heptane was first added, followed by a given amount of the VCl_4 solution by means of a hypodermic syringe. The color of VCl_4 solution was light yellow. To the mixture, an equimolar amount of *n*-butyllithium was added dropwise under vigorous stirring. A simultaneous appearance of a purple dispersion was observed, and the yellow color of the supernatant liquid caused by the presence of VCl_4 disappeared just as the addition of an equimolar amount of *n*-butyllithium was completed. The reaction mixture was heated to 90°C in order to complete the reaction, then the mixture was aged for 1 hr at room temperature. Thus $\text{VCl}_3 \cdot \text{LiCl}$ catalyst was obtained.

Addition of Ethers to $\text{VCl}_3 \cdot \text{LiCl}$

To the dispersion of $\text{VCl}_3 \cdot \text{LiCl}$ in heptane, an ether was added under stirring and the mixture was aged for 2 hr at room temperature. Ethers used were previously diluted by *n*-heptane to a concentration of 0.5 mole/l.

Polymerizations

After the catalyst was prepared in the Schlenk polymerization vessel by the procedure mentioned above, the vessel was placed in a water bath which was kept at a constant temperature.

The polymerization was started by injecting the monomer with a syringe through a self-sealing rubber cap. A positive nitrogen pressure was maintained during the polymerization. After an appropriate time, a small amount of triethylamine-methanol mixture was added to stop the polymerization. The reaction mixture was then poured into 500 ml of methanol containing a small amount of phenyl- β -naphthylamine. The polymer mass obtained was dried for 48 hr under vacuum in a desiccator.

Solubility Index

The crude polymer which had previously been chopped into small pieces (approximately 1 mm³) was placed in a vessel and acetone (100 ml/g polymer) was introduced. This was refluxed for 5 hr; an insoluble material was isolated. The percentage of the insoluble fraction was used as the solubility index. It was previously confirmed that the index was independent of the amount of acetone used when the volume of acetone was more than 50 times that of the polymer. The index is based on a simple extraction with a refluxing solvent such as acetone which selectively dissolves the amorphous polymer. It should be noted that the index means percentage of insoluble material and does not directly correspond to stereoregularity of the polymer; however, the index is useful in studying a large number of catalysts and their stereospecific activity.

Viscosity Measurements

The intrinsic viscosity and the reduced viscosity ($c = 1.0$) were determined at 30°C in benzene solution in an Ostwald or Ubbelohde viscometer.

RESULTS AND DISCUSSION

Influence of Polymerization Temperature

The influence of temperature on the polymerization of isobutyl vinyl ether by $VCl_3 \cdot LiCl$ is shown in Figures 1 and 2. The $VCl_3 \cdot LiCl$ has no catalytic activity at low temperatures ($-78^\circ C$). The conversion, the solubility index, and the molecular weight of the polymer reached maxima at about 20°C and then decreased with further rise in polymerization temperature. Similar behavior was observed in the polymerization by $Al_2(SO_4)_3 \cdot H_2SO_4$ complex catalyst.⁵

At temperatures lower than 10°C, both the acetone-soluble fraction and the acetone-insoluble fraction decreased with decreasing polymerization temperature. This may be due to low activities of both catalytic species yielding the crystalline and the amorphous polymer at low temperatures. At temperatures higher than 20°C, the acetone-insoluble fraction decreased

with increasing polymerization temperature, while the acetone-soluble fraction remained approximately constant. Therefore, the solubility index decreased with increasing polymerization temperature at temperatures above 20°C. There was no appreciable change in molecular weight of the

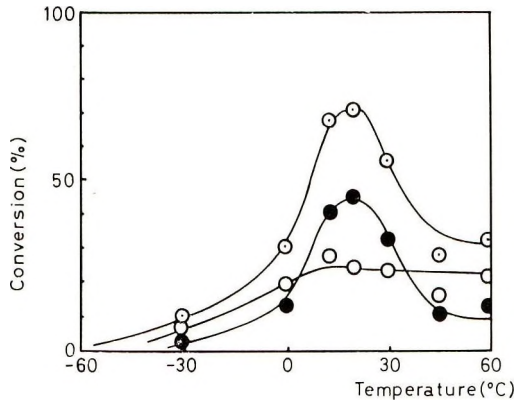


Fig. 1. Influence of polymerization temperature on the polymerization of isobutyl vinyl ether by $VCl_3 \cdot LiCl$: (○) total conversion; (●) acetone-insoluble; (○) acetone-soluble. Polymerization conditions: $VCl_3 \cdot LiCl$, 0.0005 mole; *n*-heptane, 30 ml; monomer, 3 g; polymerization time, 30 min. Temperature rises observed were 2, 4.5, 6, 5.5, 1.5 and 1.5°C when polymerizations were performed at 0, 13, 20, 30, 45, and 50°C, respectively.

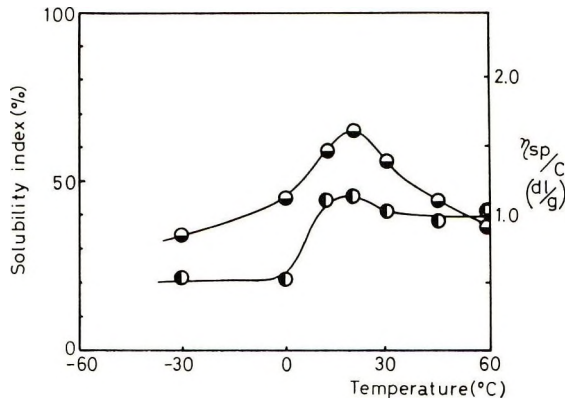


Fig. 2. Influence of polymerization temperature on the polymerization of isobutyl vinyl ether by $VCl_3 \cdot LiCl$: (○) solubility index, (●) η_{sp}/c ($c = 1.0$) measured for the acetone-insoluble fraction. The polymerization conditions are as in Fig. 1.

acetone-insoluble fraction obtained at temperatures higher than 20°C. These data suggest that number of the active centers which induces the stereospecific polymerization decreased with increasing temperature above 20°C.

Influence of Polymerization Time

Figures 3 and 4 show the influence of polymerization time on the polymerization of isobutyl vinyl ether with $VCl_3 \cdot LiCl$ catalyst at $20^\circ C$. Temperature elevations which ranged from 6 to $8^\circ C$ were observed after the addition of monomer. However, within 4 min the temperature of reaction

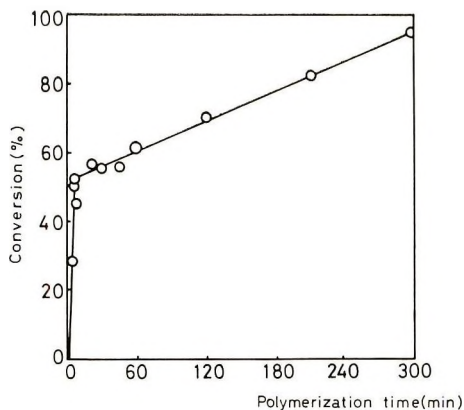


Fig. 3. Influence of polymerization time on total conversion in the polymerization of isobutyl vinyl ether by $VCl_3 \cdot LiCl$. Polymerization conditions: $VCl_3 \cdot LiCl$, 0.0005 mole; *n*-heptane, 30 ml; monomer, 3 g; polymerization temperature, $20^\circ C$.

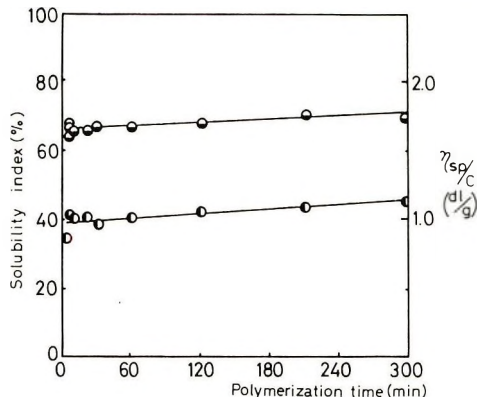


Fig. 4. Influence of polymerization time on the polymerization of isobutyl vinyl ether by $VCl_3 \cdot LiCl$: (○) solubility index; (●) η_{sp}/c ($c = 1.0$) measured for the acetone-insoluble fractions. The polymerization conditions are as in Fig. 3.

medium fell to the prescribed temperature ($20^\circ C$). Thus there was no appreciable temperature increase during the polymerization except during the initial period of monomer addition. The polymerization proceeds very rapidly to about 50% conversion within 3 min, and then it proceeds slowly at a constant rate probably by the action of the complexes formed by the coordination of monomer to the catalyst.

The solubility index and the molecular weight of the acetone-insoluble polymer increased slightly with increasing polymerization time, as shown in Figure 4.

Influence of Monomer Concentration

The influence of monomer concentration on the polymerization was studied. Figure 5 shows that the acetone-soluble fraction decreased as monomer concentration increased, while the acetone-insoluble polymer increased with increasing monomer concentration until it reaches 3×10^{-1} mole/l then it became approximately constant. Consequently, the solu-

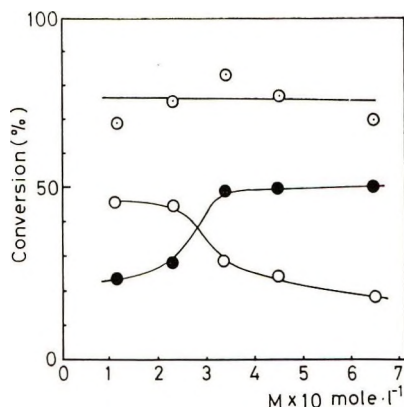


Fig. 5. Influence of monomer concentration on the polymerization of isobutyl vinyl ether by $VCl_3 \cdot LiCl$: (○) total conversion; (●) acetone-insoluble; (○) acetone-soluble. Polymerization conditions: $VCl_3 \cdot LiCl$, 0.0001 mole; *n*-heptane, 60 ml; polymerization temperature, 20°C; polymerization time, 30 min. Temperature rise was observed in the range of 4–10°C, increasing with increasing monomer concentration.

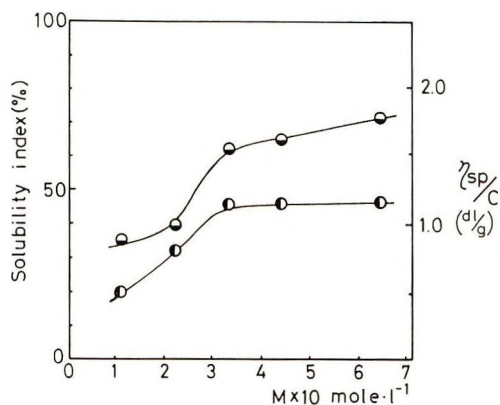


Fig. 6. Influence of monomer concentration on the polymerization of isobutyl vinyl ether by $VCl_3 \cdot LiCl$: (○) solubility index; (●) η_{sp}/c ($C = 1.0$) measured for the acetone-insoluble fractions. Polymerization conditions are as in Fig. 5.

bility index increased rapidly until monomer concentration reached $[M] = 3 \times 10^{-1}$ mole/l., then it increased gradually as monomer concentration further increased as shown in Figure 6.

The molecular weight of polymer was approximately constant in the range of $[M] \geq 3 \times 10^{-1}$ mole/l. This suggests by that termination of propagating chains by chain transfer to monomer might predominate at monomer concentrations higher than 3×10^{-1} mole/l.

On the contrary, the molecular weight decreased with decreasing monomer concentration when the monomer concentration $[M]$ is lower than 3×10^{-1} mole/l. It is speculated that other termination reactions besides the chain transfer to monomer might occur rather predominantly in case of lower monomer concentration.

Influence of Catalyst Concentration

The influence of catalyst concentration on the polymerization was studied and the results are shown in Figures 7 and 8. The conversion increased approximately in proportion to catalyst concentration until it reached 1.25×10^{-4} mole/l., then it became constant mainly because the conversions

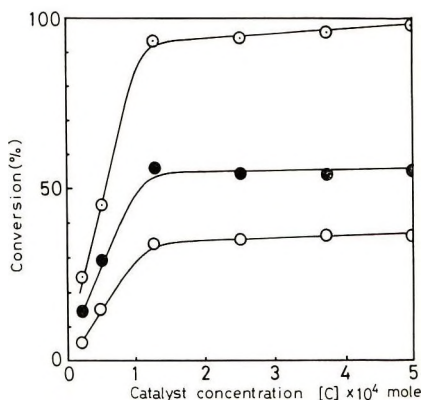


Fig. 7. Influence of catalyst concentration on the polymerization: (○) total conversion; (●) acetone-insoluble; (○) acetone-soluble. Polymerization conditions: *n*-heptane, 30 ml; monomer, 3 g; polymerization temperature, 20°C; polymerization time, 30 min. Temperature rises observed were 1, 7, 15, 20, 25, and 27°C as the catalyst concentration increased from 0.25×10^{-4} to 5×10^{-4} mole/l. in this figure.

have already reached 90% at catalyst concentrations higher than 1.25×10^{-4} mole/l.

The slight decrease in the solubility index shown in Figure 8 at higher catalyst concentrations is probably due to the temperature elevation of polymerization medium which was rather violent at high catalyst concentration. The molecular weight of polymer was approximately constant regardless of catalyst concentration.

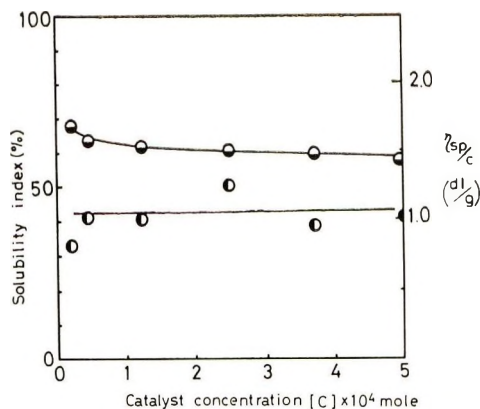


Fig. 8. Influence of catalyst concentration on the polymerization: (●) solubility index; (○) η_{sp}/c ($C = 1.0$) for the acetone-insoluble fractions. Polymerization conditions are as in Fig. 7.

Polymerization in Ether Solvents

The polymerizations of isobutyl vinyl ether by $VCl_3 \cdot LiCl$ were performed in several ethers instead of *n*-heptane as solvent. The results are shown in Table I. The $VCl_3 \cdot LiCl$ catalyst exhibits polymerization activity only

TABLE I
Effect of Ether Solvent on the Polymerization of Isobutyl Vinyl Ether by $VCl_3 \cdot LiCl$ Catalyst^a

Solvent	Color on VCl_3 addition	Solubility of $VCl_3 \cdot LiCl$	Conversion, %	Solubility index, %	η_{sp}/c , dl/g ^b
Diethyl ether	Red-brown	Soluble	Trace	—	—
Diphenyl ether	Dark brown	Soluble	73.1	0	0.12 ^c
Dibutyl ether	Dark brown	Soluble	79.1	2.98	0.19
Anisole	Black	Soluble	Trace	—	—
Tetrahydrofuran	Green-yellow	Soluble	0	—	—
<i>n</i> -Heptane	Yellow	Violet precipitate	93.7	45.0	0.61

^a Polymerization conditions: solvent, 30 ml; monomer, 3 g; polymerization temperature, 0°C; polymerization time, 60 min; catalyst 0.0005 mole.

^b Measured for the acetone-insoluble fraction.

^c Measured for the acetone-soluble fraction.

when dibutyl ether and diphenyl ether were used as solvents. The molecular weight and solubility index of these polymers were markedly lower than those of the polymer obtained in *n*-heptane solvent. The $VCl_3 \cdot LiCl$ is a purple dispersion insoluble in heptane, while it easily dissolves in ethers to form homogeneous transparent solutions.

Effect of Addition of Ethers on $VCl_3 \cdot LiCl$

As already mentioned above, $VCl_3 \cdot LiCl$ has high catalytic activity in the polymerization of isobutyl vinyl ether, and the optimum polymerization temperature is around 20°C.

On considering that proper depression of the catalytic activity of $VCl_3 \cdot LiCl$ by combination with a suitable Lewis base would be advantageous for the stereospecific polymerization, the polymerizations were performed in the presence of ethers as Lewis base. The results are summarized in Table II. The conversions in the polymerizations decreased in the order,



A rapid decrease in polymerization activity in case of THF addition is probably ascribed to the depression of cationic nature of the catalyst by the high basicity of THF.

TABLE II
Effect of the Addition of Ethers to the $VCl_3 \cdot LiCl$ Catalyst

Ethers	Temperature rise on monomer addition, °C	Conversion, %	Acetone-insol, %	Solubility index, %	η_{sp}/c , dl/g
Diethyl ether	24	95.6	48.9	51.3	0.78
Dibutyl ether	22	95.4	49.2	46.3	0.67
Diphenyl ether	22	91.3	21.8	23.9	0.51
Anisole	23	93.6	34.4	36.8	0.57
Tetrahydrofuran ^b	0	43.8	39.6	90.5	1.39
Tetrahydrofuran	0	32.0	26.2	81.8	1.07
EGDME	0	2.2	—	—	—
EGDPhE	17	93.0	73.6	79.1	1.16
Blank ^a	25	93.1	60.3	64.7	0.73
Blank	24	94.1	42.3	45.0	0.64

^a Polymerization conditions: catalyst, $VCl_3 \cdot LiCl$ -ether (1:1), 0.0005 mole; *n*-heptane, 30 ml; polymerization temperature, 30°C; polymerization time, 60 min.

^b Polymerization temperature, 0°C.

When the effect of ethylene glycol dimethyl ether (EGDME) is compared with that of ethylene glycol diphenyl ether (EGDPhE), the polymerization activity decreased sharply in the former case, which may be accounted for by the smooth and strong co-ordination of the former to vanadium mainly because of its small steric hindrance and its higher basicity.

Among the ethers examined, tetrahydrofuran and ethylene glycol diphenyl ether are particularly interesting. When THF was used as the additive, the acetone-soluble fraction decreased significantly; accordingly, the solubility index increased. On the other hand, in the case of ethylene

glycol diphenyl ether, the acetone-insoluble fraction increased considerably, while the acetone-soluble fraction decreased. The reason for this effect is not well clarified at present.

Effect of Molar Ratio of THF/VCl₃·LiCl

The influence of the amount of additive THF to VCl₃·LiCl on the polymerization was examined. The results are shown in Figures 9 and 10. The acetone-soluble fraction is approximately constant, while the acetone-insoluble fraction decreased gradually with increasing THF/VCl₃·LiCl ratio. Figure 10 shows the maxima in solubility index and the molecular weight of the polymer when THF/VCl₃·LiCl ratio was around 0.75–1.0.

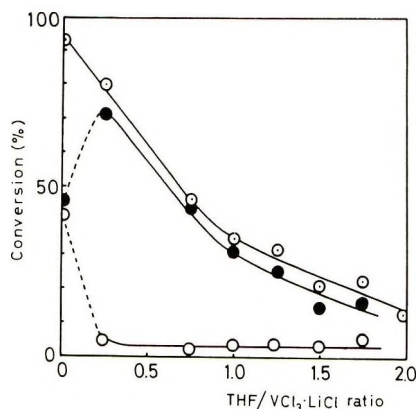


Fig. 9. Influence of THF/VCl₃·LiCl ratio on the polymerization: (○) total conversion; (●) acetone-insoluble; (○) acetone-soluble. Polymerization conditions: VCl₃·LiCl, 0.0005 mole; *n*-heptane, 30 ml; monomer, 3 g; polymerization temperature, 30°C; polymerization time, 60 min.

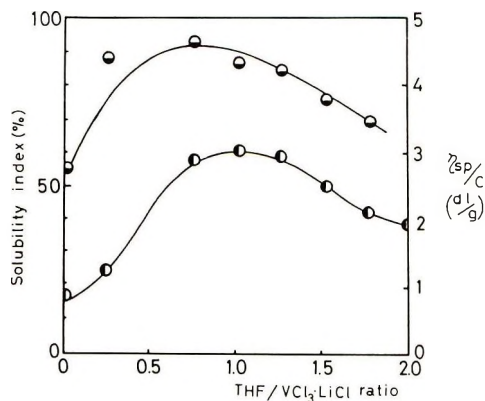


Fig. 10. Influence of THF/VCl₃·LiCl ratio on the polymerization: (●) solubility index; (○) η_{sp}/c ($C = 1.0$) measured for the acetone-insoluble fractions. Polymerization conditions are as in Fig. 9.

Polymerization by $\text{VCl}_3 \cdot \text{LiCl} \cdot \text{THF}(1:1)$

When the polymerizations were run with $\text{THF} \cdot \text{VCl}_3 \cdot \text{LiCl}$ (1:1), no appreciable temperature elevation was observed after the addition of monomer. With the $\text{VCl}_3 \cdot \text{LiCl} \cdot \text{THF}$ (1:1) catalyst, the influence of

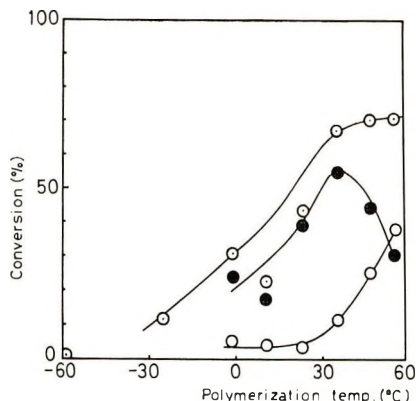


Fig. 11. Influence of the polymerization temperature on the polymerization of isobutyl vinyl ether by $\text{VCl}_3 \cdot \text{LiCl} \cdot \text{THF}$ (1:1): (○) total conversion; (●) acetone-insoluble; (○) acetone-soluble. Polymerization conditions: $\text{VCl}_3 \cdot \text{LiCl}$, 0.0005 mole; *n*-heptane, 30 ml; monomer, 3 g; polymerization time, 60 min. No temperature elevation on addition of monomer was observed in this catalytic system.

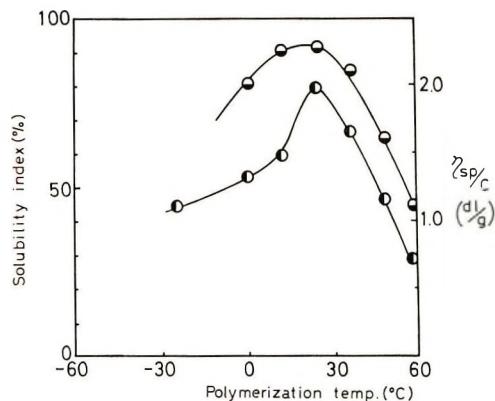


Fig. 12. Influence of polymerization temperature on the polymerization of isobutyl vinyl ether by $\text{VCl}_3 \cdot \text{LiCl} \cdot \text{THF}$ (1:1): (●) solubility index; (○) η_{sp}/c ($c = 1.0$) measured for the acetone-insoluble fractions. Polymerization conditions are as in Fig. 11.

polymerization temperature on the polymerization of isobutyl vinyl ether was studied. The results are shown in Figures 11 and 12. The polymerization behavior was quite similar to that by $\text{VCl}_3 \cdot \text{LiCl}$ alone. The optimum polymerization temperature from the conversion and the solubility index was around 20–30°C.

Polymerization of Isobutyl Vinyl Ether by Various Kinds of VCl_3 and $TiCl_3$

The polymerization of isobutyl vinyl ether was carried out by using several kinds of VCl_3 and $TiCl_3$. The results are summarized in Table III.

When we used a commercial VCl_3 which had been previously ballmilled to a finely divided form, the polymerization activity for isobutyl vinyl ether was approximately comparable to that with $VCl_3 \cdot LiCl$ or by the reaction product between $AlEt_3$ and VCl_4 (1:2). However, the solubility index as well as the molecular weight of the resulting polymer was extremely low.

TABLE III
Polymerization of Isobutyl Vinyl Ether by
Various Kinds of VCl_3 and $TiCl_3$ ^a

Catalyst		Conversion, %	Solubility index,	[η], dl/g ^b
Kind	Mole		%	
VCl_3 ^c	0.0005	96.7	3	0.17
VCl_3 ^d	0.0005	83.3	2	0.15
VCl_3 ^e	0.0005	97.5	59	0.81
VCl_3 ^f	0.0005	93.5	39	0.64
$TiCl_3(HA)$	0.0063	32.5	29	0.26
$TiCl_3(H)$	0.0097	96.6	36	0.59
$TiCl_3(AA)$	0.0094	87.7	61	1.27
$TiCl_3$ ^g	0.0005	90.8	55	0.72

^a Polymerization conditions: *n*-heptane, 30 ml; monomer, 3 g; polymerization temperature, 30°C; polymerization time, 60 min.

^b Measured at 30°C in benzene.

^c Ballmilled commercial product.

^d Produced by thermal decomposition of VCl_4 in heptane under N_2 .

^e Reaction product of $VCl_4/BuLi$ (1:1).

^f Reaction product of $VCl_4/AlEt_3$ (1:2).

^g Reaction product of $TiCl_4/BuLi$ (1:1).

Similar results were obtained with VCl_3 prepared by a thermal decomposition of VCl_4 .

When $TiCl_3$ of HA or H type was used as catalyst, the solubility index and the molecular weight of the resulting polymers were lower than those of the polymers obtained with AA type or with $TiCl_3$ prepared from $BuLi$ and $TiCl_4$ (1:1).

This fact strongly suggests that the stereospecific polymerization is certainly related to the catalyst structure, and $LiCl$ or $AlCl_3$ which probably coexists with VCl_3 or $TiCl_3$ as a solid solution in the crystal lattice will act advantageously for the stereospecific polymerization.

When ethers were used as solvent, $VCl_3 \cdot LiCl$ dissolves in the solvent. In such a case no stereospecific polymerization took place as shown in Table I.

This fact also supports the dependence of the stereospecific polymerization on the crystal structure of the catalysts.

Stereospecificity

We have used the solubility index, which is expressed as the per cent of the acetone-insoluble portion to total polymer, as one measure of the stereospecificity of polymerization. The index is a measure for the insoluble part which is certainly related to the stereoregularity of the polymer, but does not strictly represent the stereoregularity of the polymer. We have examined the solubility index in some detail. Some relations between the solubility and the molecular weight of the polymer are listed in Table IV. Concerning polymer HP21, there is a great difference in viscosity between the acetone-insoluble fraction and the acetone-soluble fraction.

TABLE IV
Relation of Stereospecificity to the Percentage of the
Acetone-Insolubles to Total Yield

Polymer	Fraction	$[\eta]$, dl/g
HP21	Original polymer	0.778
	Acetone-insoluble fraction	1.200
	Acetone-soluble fraction	0.330
HP26	Original polymer	0.325
	Acetone-insoluble fraction	0.350
	Acetone-soluble fraction	0.315

It would seem that a major factor which determines the solubility in acetone is the molecular weight of polymer. However, for polymer HP26, there is very little difference in intrinsic viscosity values of the acetone-insoluble and the soluble fractions. There is also no appreciable difference between the intrinsic viscosity of the acetone-soluble fraction of polymer HP-21 and that of the acetone-insoluble fraction of the polymer HP26. As has been reported in the literature,^{7,9} both stereoregularity and molecular weight of polymer are controlling factors in fractionation; the former is no doubt a

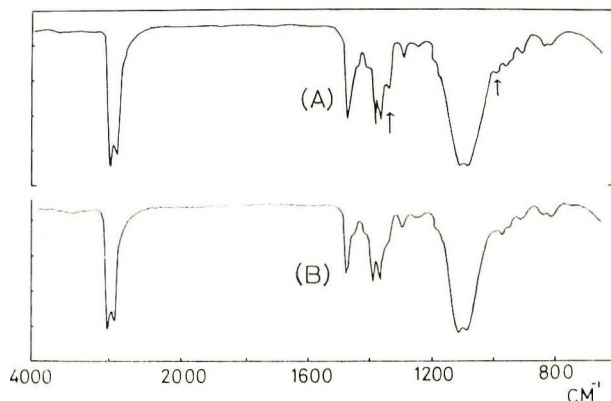


Fig. 13. Infrared spectra for the poly(isobutyl vinyl ether) obtained with $VCl_3 \cdot LiCl$:
(A) acetone-insoluble portion; (B) acetone-soluble portion.

major factor affecting the insolubility of the polymer. Obviously, it is not pertinent to have an entire discussion on the stereoregularity of the polymer in terms of the solubility index; however, the index is useful for investigating the stereospecific catalytic activity of the catalyst.

In the infrared spectra shown in Figure 13, the crystalline bands at 1335 and 988 cm^{-1} characteristic for the isotactic poly(isobutyl vinyl ether)⁴ were clearly observed for the acetone-insoluble fraction, but these bands are not sufficiently developed for the acetone-soluble fraction.

Vandenberg¹⁰ proposed a coordinated cationic polymerization mechanism for the polymerization of alkyl vinyl ether with his catalyst. It is speculated that the stereospecific polymerization of isobutyl vinyl ether by $\text{VCl}_3 \cdot \text{LiCl}$ proceeds by a similar mechanism.

References

1. Y. Joh, H. Yuki, S. Murahashi, *J. Polym. Sci.*, **8**, 2775 (1970).
2. Y. Joh, H. Yuki, S. Murahashi, *J. Polym. Sci.*, **8**, 3311 (1970).
3. R. B. Hodgdon, *J. Polym. Sci.*, **47**, 259 (1960).
4. K. Iwasaki, *J. Polym. Sci.*, **56**, 27 (1962).
5. S. A. Mosley, U. S. Pat. 2,549,921 (1951).
6. S. Okamura, T. Higashimura, and T. Watanabe, *Makromol. Chem.*, **50**, 137 (1961).
7. J. Lal, J. E. McGrath, and G. S. Trick, *J. Polym. Sci. A-1*, **5**, 795 (1967).
8. S. Murahashi, H. Yuki, Y. Joh, K. Harada, paper presented at 12th Annual Meeting of the Society of Polymer Science, Japan, 1963; *Preprints*, p. 30.
9. H. W. Coover, Jr., in *Macromolecular Chemistry, Paris 1963* (*J. Polym. Sci. C*, **4**) M. Mogat, Ed., Interscience, New York, 1963, p. 1151.
10. E. J. Vandenberg, in *First Biannual American Chemical Society Polymer Symposium* (*J. Polym. Sci. C*, **1**), H. W. Starkweather, Ed., Interscience, New York, 1963, p. 207.

Received June 1, 1970

Revised August 31, 1970

Synthesis and Polymerization of Some Optically Active 2- and 1,2-Substituted Butadienes

Z. JANOVIĆ* and D. FLEŠ,
Research Institute, INA, Zagreb, Yugoslavia

Synopsis

Dehydration of (S)-3,5-dimethyl-1-hepten-3-ol gave: (3E)- (I) and (3Z)-(5S)-3,5-dimethyl-1,3-heptadienes (II) and 2-[(S)- 2-methylbutyl]-1,3-butadiene (III). 2-[(S)-1-Methylpropyl]-1,3-butadiene (IV) was also prepared similarly by dehydration of (S)-3,4-dimethyl-1-hexene-3-ol. Monomers I-IV were polymerized in the presence of the $\text{TiCl}_4\text{-Al}(i\text{-C}_4\text{H}_9)_3$ catalyst system and in emulsion with $\text{K}_2\text{S}_2\text{O}_8$ as initiator. Monomer IV was also polymerized in the presence of butyllithium. Specific rotations of polymers are of the same order of magnitude as that of monomers, with exception of polymers prepared by stereospecific polymerization of (S)-I and (S)-II. The acetone-soluble fraction of these polymers has a molar rotation similar to that of monomer, while the acetone-insoluble part has a lower rotation ($[M]_D$ of monomer $+53.2^\circ$; $[M]_D$ of polymer, $+5.9^\circ$).

INTRODUCTION

Although a great deal of work has been done on the synthesis and polymerization of substituted butadienes, very little information is available on the use of optically active butadiene derivatives. As far as we know, the only optically active substituted butadienes described so far are 1-, and 2-[(S)-1-methylpropyl]-1,3-butadienes synthesized by Rossi and Benedetti.¹ The last compound was polymerized to optically active polymer by Benedetti et al.² Several optically active polybutadiene derivatives have been prepared by asymmetric induction. By stereoselective polymerization of alkylsorbate, methyl 5-phenylpenta-2,4-dienoate and 1,3-dimethyl-1,3-butadiene, Natta and his co-workers^{1,3} have prepared optically active polymers of low optical purity. Similarly, Aliev et al.⁴ have polymerized *trans*-1-phenyl-1,3-butadiene in the presence of optically active catalyst and prepared optically active poly-1-phenyl-1,3-butadiene.

The present work deals with the synthesis and polymerization of (3E)-(5S)-3,5-dimethyl-1,3-heptadiene (I), (3Z)-(5S)-3,5-dimethyl-1,3-heptadiene (II),⁵ 2-[(S)-2-methylbutyl]-1,3-butadiene (III), and 2-[(S)-1-methylpropyl]-1,3-butadiene (IV). While this work was in progress, Rossi and Benedetti¹ have described the synthesis of compound IV by a method different than the one used in our work.

* Present address: The University of Arizona, Tucson, Arizona 85721.

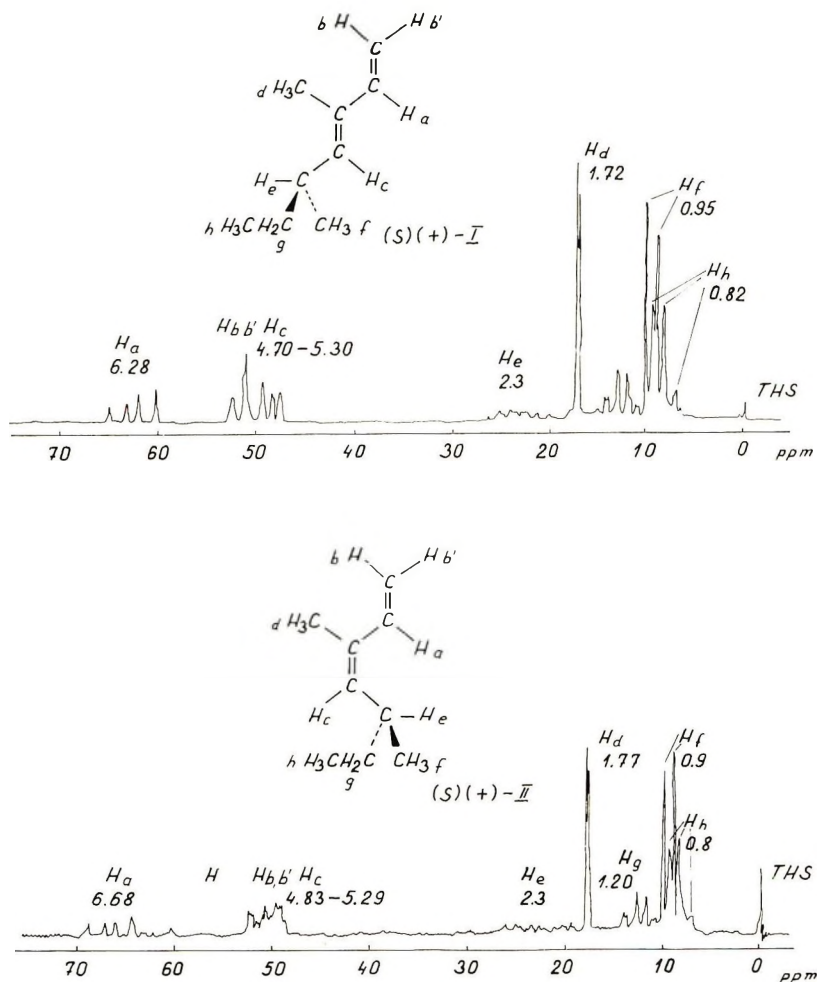
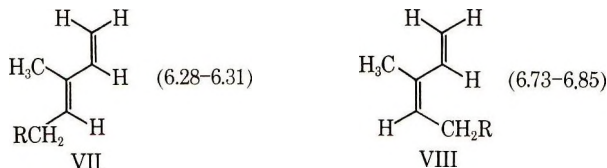


Fig. 1. The 60-MHz spectra of I and II as a 10% solutions in CCl_4 .

Compounds I and II do not react with maleic anhydride under the conditions of Diels-Alder addition, while under the same experimental conditions compounds III and IV readily form the Diels-Alder adduct. These findings are in accordance with the experiments published by Craig and his co-workers,⁶ who have found that 2-alkyl dienes are unhindered in the form of *cisoid* conformation of the diene and react readily with maleic anhydride. The same workers have established that in adducts of 1-substituted dienes, the alkyl groups in the 3-position of the tetrahydrophthalic anhydride are hindered and that the effect increases with size of alkyl group. The presence of large *sec*-butyl group at C-1 atom in I and II explains the lack of reactivity with maleic anhydride.

The stereochemistry of the double bond in butadienes I and II was assigned from the chemical shifts of the internal vinyl hydrogens at δ 6.28 and

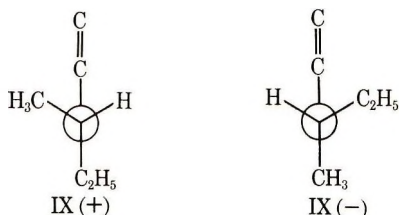
6.68. (Fig. 1). By analogy with several 1,2-disubstituted butadienes of the type VII and VIII,⁷ I and II have the configurations shown in Scheme I.



It has been noted by Forbes et al.⁸ that compounds like *cis*-1,3-pentadiene absorb at wave lengths ca. 5 $m\mu$ longer than the corresponding *trans* isomers, and as I has λ_{max} at 230 $m\mu$ and II at 234.5 $m\mu$, the ultraviolet data support the above assignments.

The infrared spectra of I and II exhibit two bands characteristic for C=C stretching in conjugated double bonds at 1613 and 1653 cm^{-1} for isomer I and 1592 and 1639 for isomer II. The out-of-plane deformations of vinyl —CH are located at 990 cm^{-1} for I and 980 cm^{-1} for isomer II. The spectra are different in the fingerprint region.

The molar rotation of I and II was calculated by the conformational dissymmetry method described by Brewster.⁹ It was first assumed that both dienes are planar, and that *s-cis* and *s-trans* isomers do not influence $[M]_D$. The rotation will in the first approximation be controlled by the conformational dissymmetry of the ethyl group. Using the empirical value of $+130^\circ$ for the methyl-olefin skew system, and -60° for the methyl-methyl-system, the calculated value for $[M]_{D(I \text{ and } II)} = +35^\circ$, compared with the observed value of $[M]_{D(I)} +53.1^\circ$, $[M]_{D(II)} +51.6^\circ$. Considering further the effect of conformational variation about the C-3 and C-4 bond of heptadienes I and II (IX), one can assume the staggered form IX



(+) to be preferred, thus increasing the dextrorotation of I and II. In any event the conformational dissymmetry method would predict similar and positive rotation for both I and II.

Isomers I and II were oxidized by potassium permanganate to (S)(+)-2-methylbutyric acid ($[\alpha]_D^{25} +17.0^\circ$),* which is an additional prove of geometric isomerism of the two butadiene derivatives. 2-[(S)-(1-methylpropyl)]-1,3-butadiene (IV) was obtained in a yield of 42% by dehydration of 3,4-dimethyl-1-hexene-3-ol (VII) which was prepared from 3-methyl-2-pentanone, by condensation with vinylmagnesium bromide.

* Reported¹⁰ for optically pure 2-methylbutyric acid, $[\alpha]_D^{25} +19.8^\circ$.

Polymerization of (3E) and (3Z)-(5S)-3,5-Dimethyl-1,3-heptadienes

Polymerization was performed with an $\text{TiCl}_4\text{-Al}(i\text{-C}_4\text{H}_9)_3$ catalytic system in benzene or in *n*-heptane as solvent, or in emulsion with $\text{K}_2\text{S}_2\text{O}_8$ as catalyst. The polymerization conditions and the pertinent properties of polymers are shown in Table I. It is evident that the molar rotation of polymers prepared in emulsion are similar to the rotation of monomer, while there is a significant difference in the rotation of polymers prepared in the presence of stereospecific catalysts ($[M]_D + 5.9^\circ$) and monomers ($[M]_D + 53.2^\circ$). Polymers prepared by stereospecific catalysts were fractionated by acetone extraction and it was found that acetone soluble fraction (12% of the total) has the molar rotation similar to monomer, while acetone insoluble part has much lower rotation.

The infrared spectra of poly-(3E)- and poly-(3Z)-(5S)-3,5-dimethyl-1,3-butadienes prepared by stereospecific and emulsion polymerization were interpreted according to the data published by Porri and Gallazzi¹¹ and Hart and Meyer.¹² It is evident (Fig. 2), that the polymers prepared by either method have low stereochemical purity and contain the mixture of 1,4-*cis* (band at 770 cm^{-1}), 1,4-*trans* (band at 960 cm^{-1}) and 3,4-structure (band at 850 cm^{-1}). The latter structure was predominant in the case of emulsion polymerization. From the ratio of intensities of bands at 960 cm^{-1} (1,4-*trans* configuration) and 850 cm^{-1} (3,4 structure), it was found that the amount of 3,4 structure in polymers prepared by emulsion technique was increased by a factor of five in comparison with the amount of 3,4 structure in polymers prepared by stereospecific catalyst.

The acetone-soluble fraction (sample I, Table I) shows infrared spectra very similar to *c* in Figure 2, thus indicating the presence of large amount of 3,4 structure. The fraction insoluble in acetone shows infrared spectra similar to *a* and *b* in Figure 2.

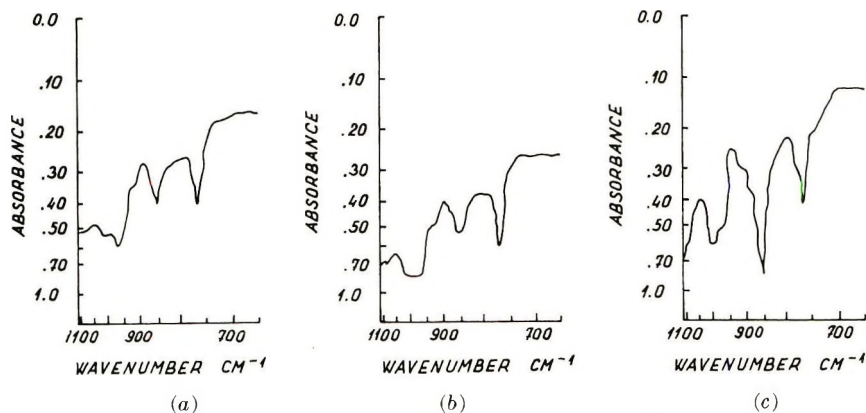


Fig. 2. Infrared spectra of poly-(5S)-3,5-dimethyl-1,3-heptadienes: (a) (5Z) derivative polymerized with $\text{TiCl}_4\text{-Al}(i\text{-C}_4\text{H}_9)_3$; (b) (5E) derivative polymerized with $\text{TiCl}_4\text{-Al}(i\text{-C}_4\text{H}_9)_3$; (c) (5E) derivative polymerized with $\text{K}_2\text{S}_2\text{O}_8$.

TABLE I
 Polymerization of (3E) and (3Z)-(5S)-3,5-Dimethyl-1,3-butadienes

Sam- ple	Monomer		Solvent and catalyst ^a	Tem- pera- ture, °C	Yield, %	$[\eta]^b$	$[M]_D^{20c}$	Extraction of polymers					
	Con- figura- tion	$[M]_D$						Acetone-soluble		Benzene-soluble			
								$\zeta\%$	$[\eta]^b$	$[M]_D^{20c}$	$\zeta\%$	$[\eta]^b$	$[M]_D^{20c}$
1	(3Z)	+51.7 ^d	Benzene, TiCl ₄ / Al(<i>i</i> -C ₄ H ₉) ₃	25	32	0.30	+9.4	12	0.24	+31.7	88	0.47	+6.4
2	(3E)	+53.2 ^e	Benzene, TiCl ₄ / Al(<i>i</i> -C ₄ H ₉) ₃	"	37	0.302	+8.6	11	0.28	+33.2	89	0.42	+5.9
3	(3Z)	+51.7	<i>n</i> -Heptane, TiCl ₄ / Al(<i>i</i> -C ₄ H ₉) ₃	"	28	0.346	+9.1	13	0.22	+30.5	87	0.44	+6.2
4	(3E)	+53.2	<i>n</i> -Heptane, TiCl ₄ / Al(<i>i</i> -C ₄ H ₉) ₃	"	33	0.30	+8.9	9.5	0.27	+28.8	90.5	0.39	+5.5
5	(3Z)	+51.7	Aq. emulsion, K ₂ S ₂ O ₈	50	43	0.218	+41.4	—	—	—	—	—	—
6	(3E)	+53.2	Aq. emulsion, K ₂ S ₂ O ₈	"	37	0.25	+44.0	—	—	—	—	—	—

^a Al/Ti molar ratio = 1.

^b In toluene at 30 ± 0.05°C.

^c In benzene; $[M]$ refers to one repeating unit.

^d Optical purity 86.5%.

^e Optical purity 88.0%.

**Polymerization of 2-[(+)-(S)-1-Methylpropyl]-1,3-butadiene
(IV), 2-[-(S)-2-Methylbutyl]-1,3-butadiene and (\pm)-2-
(1-Methylpropyl)-1,3-butadiene**

The results of polymerization performed with three different catalyst systems are summarized in Table II. Polymerization of (\pm)-IV was carried out in benzene or in *n*-heptane as solvent with a monomer/TiCl₄ ratio of 50 and Al/Ti ratio of 0.6–1.2. The best results regarding the yield and intrinsic viscosity, were obtained at a Ti/Al ratio of 1. Polymerization of (S)-IV in the presence of TiCl₄-Al(*i*-C₄H₉)₃ catalyst, gave optically active products, the molar rotation of which was similar to the rotation of monomer. While our work was in progress, Benedetti et al.² came to the same conclusion in polymerizing (S)-IV with the same catalyst.

Similar results were also obtained in the polymerization of (S)-IV with *n*-butyllithium catalyst in *n*-heptane and in emulsion polymerization. Polymerization of (S)-III was performed with TiCl₃-Al(*i*-C₄H₉)₃ and K₂S₂O₈ catalyst systems. It is interesting to note that in both cases the sign of rotation of poly-(S)-III was opposite to that of monomers. The same phenomenon was observed by Pino and co-workers¹³ in the case of polyolefins.

The infrared spectra of poly (S)-III and poly (S)-IV were very similar and show that all polymers regardless to the catalytic system used, contain 1,4-*cis*, 1,4-*trans*, and 3,4 structures, as evident by the presence of various bands. The bands at 850 cm⁻¹ present in all samples with different intensities (Fig. 3) could be related to the 840 cm⁻¹ band in isoprene.¹⁴ The intensity of this band is stronger in polymers prepared by stereospecific catalysts than in polymers prepared in emulsion. The band at 1657 cm⁻¹ was attributed to —C=C— stretching of an internal double bond, while the band at 893 cm⁻¹ (vinylidene —CH deformation) shows the presence of 3,4 structure by analogy to poly-3-*n*-propyl-1,3-butadiene¹⁵ and poly-2-*sec*-

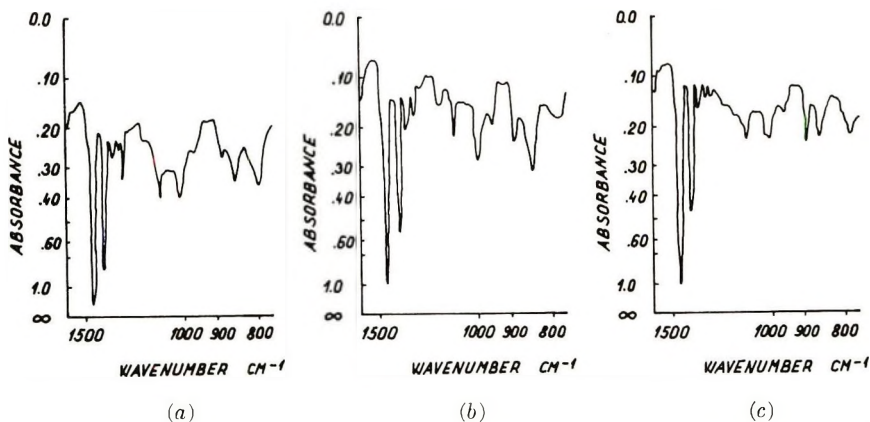


Fig. 3. Infrared spectra of poly-(S)-IV: (a) polymerized with TiCl₄-Al(*i*-C₄H₉)₃; (b) polymerized with *n*-butyllithium; (c) polymerized with K₂S₂O₈.

TABLE II
 Polymerization of (\pm) and $2-[(+)(S)-1\text{-Methyl-propyl}]-1,3\text{-butadienes}$ and $2-[-(S)-2\text{-Methyl-butyl}]-1,3\text{-butadiene}$.

Sam- ple	$\text{CH}_2=\text{C}(\text{R})-\text{CH}=\text{CH}_2$		Solvent	Catalyst	Al/Ti	Temp, °C	Yield, %	$[M]_0^B$	$[\eta]^a$
	R	$[M]_0^B$							
1	(\pm) -1-Methylpropyl	—	Benzene	$\text{TiCl}_4\text{-Al}(i\text{-C}_4\text{H}_9)_3$	0.6	25	8	—	0.62
2	"	—	"	"	0.8	25	34	—	0.89
3	"	—	"	"	1.0	25	56	—	1.12
4	"	—	"	"	1.2	25	38	—	1.02
5	$(+)(S)$ -1-Methylpropyl	+34.7 ^b	<i>n</i> -Heptane	"	1.0	25	35	+31.2	0.75
6	"	"	Benzene	"	1.0	25	63	+30.8	1.18
7	"	"	<i>n</i> -Heptane	<i>n</i> -Butyllithium	—	25	60	+31.3	0.56
8	"	"	Aq. emulsion	$\text{K}_2\text{S}_2\text{O}_8$	—	50	49	+29.3	0.48
9	$(-)(S)$ -2-Methylbutyl	-10.9 ^a	Benzene	$\text{TiCl}_4\text{-Al}(i\text{-C}_4\text{H}_9)_3$	1.0	25	52	+9.8	0.68
10	"	"	Aq. emulsion	$\text{K}_2\text{S}_2\text{O}_8$	—	50	44	+8.9	0.35

^a In toluene at $30 \pm 0.05^\circ\text{C}$.

^b Optical purity 89.3%.

^c Optical purity 87.3%.

TABLE III
Molar Rotations of (S)(-)-IV and Poly-(S)-IV

λ , $m\mu$	$[M]_{\lambda}^{25}$		
	(S)(-)-IV ^a	Poly-(S)-IV ^b	Poly-(S)-IV ^c
250	—	—	483.8
255	—	—	444.7
260	864.6	422.3	391.3
270	641.0	—	—
280	492.5	303.1	280.732
290	390.0	—	—
300	323.2	—	210.2
320	240.7	186.3	168.2
340	183.6	153.8	137.9
420	91.8	85.3	78.3
600	37.6	35.8	33.3

^a $c = 0.0825\%$ in isoctane.

^b Prepared with catalytic system $TiCl_4/Al(i-C_4H_9)_3$, $c = 0.125\%$ in isoctane.

^c Prepared in emulsion with $K_2S_2O_8$, catalyst, $c = 0.127\%$ in isoctane.

butyl-1,3-butadiene.¹⁵ The intensity of the band at 893 cm^{-1} was stronger in polymers prepared in emulsion. The band at 1150 cm^{-1} is attributed to 1,4-*trans*-configuration and that at 1082 cm^{-1} to 1,4-*cis*.¹⁶ The =CH—out-of-plane vibration of *cis*-C-(2-methylbutyl)=CH and *cis*-C-(1-methylpropyl)=CH appears at 1320 cm^{-1} . The same band was found in polyisoprene at 1315 cm^{-1} .¹⁴ From the ratio of intensities of bands at 893 cm^{-1} (3,4 structure) and 850 cm^{-1} (1,4-*cis* configuration), it was found that the amount of 3,4 structure in poly-(S)-IV prepared by emulsion polymerization was increased by a factor of two in comparison with the amount of 3,4 structure in polymers prepared by stereospecific catalyst (Fig. 3). In poly-(S)-III* prepared by emulsion polymerization the increase of 3,4-structure was by a factor of three.

Tabulation of the molar rotations at different wavelengths of (S)(-)-IV and poly-(S)-IV prepared with $TiCl_4-Al(i-C_4H_9)_2$ catalytic system and in emulsion is presented in Table III.

Monomer (S)(-)-IV and polymers prepared stereospecifically and in emulsion show plain ORD curves, which closely fit the single-term Drude equation; $\lambda_0 = 200\text{ m}\mu$ for poly-(S)-IV prepared by both catalytic systems; $K = 9.1 \times 10^5$ for polymer prepared with $TiCl_4-Al(i-C_4H_9)_3$ and 8.4×10^5 for polymer prepared in emulsion.

EXPERIMENTAL

Physicochemical Measurements

The infrared spectra were measured with Perkin-Elmer Model 147 and 421 spectrophotometers on films of polymers obtained by slow evaporation

* The infrared spectra of poly-(S)-III were almost identical to that of poly-(S)-IV in the range of $800-900\text{ cm}^{-1}$.

of benzene. Ultraviolet spectra of monomers were determined in isoctane on a Perkin-Elmer 202 recording spectrophotometer. NMR spectra were determined in CCl_4 on a Varian A-60 instrument.

Preparative and analytical GLC were performed on a Varian Aerograph, 1502 B with flame ionization detector.

Specific rotations were measured on a Rudolph, Model 70 polarimeter and on Bendix Ericsson ETL-NPL automatic polarimeter. Optical rotatory dispersion was measured on a recording Cary Model 60 spectropolarimeter in the range of 230–600 $m\mu$ in isoctane.

Intrinsic viscosities were measured in a Cannon-Fenske capillary viscometer, No. 100 in toluene at $30 \pm 0.05^\circ\text{C}$.

Preparation of (S)(+)-3,5-Dimethyl-1-heptane-3-ol (VI)

To a suspension of 14.9 g (0.62 mole) of Mg in 500 ml of THF was added gaseous vinyl bromide (70 g, 0.65 mole) at room temperature. The Dry-Ice-cooled condenser was replaced by a dropping funnel and 63 g (0.55 mole) of (S)(+)-4-methylhexanone-2 (V)¹⁷ ($[\alpha]_{\text{D}}^{25} + 6.67^\circ$) in 200 ml of THF was added at such a rate as to maintain the slow refluxing of solvent. The stirring was continued for an additional 60 min, the reaction mixture treated with 200 ml of saturated aqueous NH_4Cl , the organic layer was separated, dried, and after the removal of THF, the carbinol VI was purified by fractional distillation. The yield was 53.2 g (68%); bp $48^\circ\text{C}/1$ Torr; n_{D}^{20} 1.4408; d_{20} 0.841; $[\alpha]_{\text{D}}^{20} + 9.1^\circ$ (smear).

ANAL. Calcd. for $\text{C}_9\text{H}_{18}\text{O}$: C, 75.99%; H, 12.76%. Found: C, 75.87%; H, 12.91%.

Preparation of Dienes I, II, and III

Dehydration of (S)(+)-VI was performed in a 100-ml three-necked flask fitted with a stirrer, dropping funnel, and a 30 cm Vigreux column. Freshly prepared KHSO_4 (20 g) and 0.4 g of di-*tert*-butylcatechol were placed into the flask, which was immersed in an oil bath at a temperature of 180–185°C. Under constant stirring 50 g of (S)-IV was added during the course of 6 hr. Water was removed from the distillate, and the oily residue was dried and fractionated over the Vigreux column in the presence of di-*tert*-butylcatechol under a stream of N_2 . The yield of crude dienes boiling at 118–145°C was 32.0 g. A sample was analyzed by GLC by using a column $l = 5$ m, $d = 6$ mm packed with 10% tetracyano-ethylated pentaerythritol (TCPE) on Chromosorb P; 60–80 mesh, temp. 80° , carrier gas N_2 at 40 ml/min. The crude mixture of dienes was separated into five fractions by means of preparative GLC column ($l = 30$ m, $d = 18$ mm, with 10% TCPE on Chromosorb P, 30–70 mesh; 80°C ; He carrier gas, 200 ml/min).

The first and fourth fractions were minor unidentified impurities. The second fraction (29.0% of the crude mixture) was identified as (S)(+)-II; n_{D}^{20} 1.4558; $[\alpha]_{\text{D}}^{25} + 41.6^\circ$ ($c = 3.340\%$ in C_6H_6); λ_{max} 234.5 $m\mu$ ($\log \epsilon$ 4.360); IR (neat) 3067 (CH of $=\text{CH}_2$), 1639, 1592 (C=C) 980 cm^{-1} (vinyl

—CH); NMR δ 6.68, H_a; 4.83–5.29, H_{b,b}, H_c; 1.77, H_d; 2.3, H_e; 0.9, H_f; 1.20, H_g; 0.8, H_h.

ANAL. Calcd. for C₉H₁₆: C, 87.02%; H, 12.89%. Found: C, 87.05%; H, 13.14%.

The third fraction (33.7%) was (S)(-)-III: n_D^{20} 1.4476; $[\alpha]_D^{25}$ -8.75° (*c*, 5.45% in C₆H₆); λ_{max} 266 m μ (log ϵ 4.306). IR (neat) 3090, 1632, 1594, 990 cm⁻¹. NMR δ 6.30 (internal H of diene); 4.8–5.4 (=CH₂ groups); 2.1 (CH₂ attached to C-2 of diene); 1.4 (—CH—); 0.9 (CH₃ and C₂H₅).

ANAL. Found: C, 87.15%; H, 13.15%.

Condensation of (S)(-)-III (0.248 g) with 0.245 g maleic anhydride in 6 ml of benzene at 60°C for 12 hr gave 0.4 g (90.2%) of (S)(+)-4-(2-methylbutyl)- Δ^4 -tetrahydrophthalic anhydride; bp 150°C/1 Torr (air bath temperature); yield, 0.4 g (90.2%); mp 67°C; $[\alpha]_D^{20}$ +11.5° (*c* = 6.9% in C₆H₆).

ANAL. Calcd. for C₁₃H₁₈O₃: C, 70.25%; H, 8.10%. Found: C, 70.46%; H, 8.26%.

The fifth fraction (35.2%) was (S)(+)-I: n_D^{20} 1.4581; $[\alpha]_D^{25}$ +42.8° (*c* = 9.69% in C₆H₆); λ_{max} 230 m μ (log ϵ 4.346); IR (neat) 3106, 1653, 1613, 990 cm⁻¹; NMR δ 6.28, H_a; 4.70–5.30, H_{b,b}, H_c; 1.72, H_d; 2.3, H_e; 0.95, H_f; 1.25, H_g; 0.82, H_h.

ANAL. Found: C, 86.91; H, 13.29%.

Oxidation of Dienes I and II

Oxidation of (S)(+)-I (0.5 g) was performed with 5.0 g of KMnO₄ and 1 g of KOH in 50 ml of H₂O under reflux for 10 hr. The precipitate formed during the oxidation was filtered off, the aqueous layer extracted with two 5-ml portions of ether, acidified with HCl, and the 2-methylbutyric acid was extracted with two 5-ml portions of CHCl₃. Evaporation of solvent gave 0.3 g of (S)(+)-2-methylbutyric acid: n_D^{20} 1.4061; $[\alpha]_D^{25}$ +17.1° (*c*, 5.3% in C₆H₆).

ANAL. Calcd. for C₅H₁₀O₂: C, 58.80%; H, 9.87%. Found: C, 58.35%; H, 9.68%.

Oxidation of (S)(+)-II under the same conditions gave identical product: n_D^{20} 1.4060; $[\alpha]_D^{25}$ +17.2° (*c* = 4.4% in C₆H₆).

ANAL. Found: C, 58.68%; H, 9.93%.

Preparation of (S)(-)-3,4-Dimethyl-1-hexene-3-ol (VII)

The carbinol VII was prepared in a 67% yield from 40 g (0.4 mole) of (S)(+)-3-methylpentanone-2¹⁸ and vinylmagnesium bromide prepared from 46 g (0.43 mole) of vinyl bromide and 9.75 g (0.41 mole) of Mg according to the procedure used in the preparation of carbinol VI: Bp 41°C/1 Torr; n_D^{20} 1.4415; d^{20} 0.8452; $[\alpha]_D^{20}$ -22.1° (smear).

ANAL. Calcd. for C₈H₁₆O: C, 74.94%; H, 12.58%. Found: C, 74.60%; H, 12.66%.

Preparation of 2-[(S)-(1-Methyl-propyl)-1,3-butadiene (IV)

The butadiene derivative IV was prepared by dehydration of the carbinol VII (33.5 g) under the conditions described for the preparation of dienes I, II, and III. The crude dehydrated product (26.8 g) was purified by fractional distillation over a spinning band column and gave 12 g (42%) of diene IV; bp 112–113°C; $[\alpha]_D^{20} + 31.5^\circ$ ($c = 4.28\%$ in isoctane); λ_{\max} 226 m μ ($\log \epsilon$ 4.20).*

ANAL. Calcd. for C₈H₁₄: C, 87.19%; H, 12.81%. Found: C, 87.29%; H, 12.94%.

Condensation of (S)(+)-IV with maleic anhydride gave corresponding Δ^4 -tetrahydrophthalic anhydride derivative; mp 39–40°C; $[\alpha]_D^{25} + 2.07$ ($c = 13.4\%$ in C₆H₆).

ANAL. Calcd. for C₁₂H₁₆O₃: C, 69.20%; H, 7.67%. Found: C, 69.40%; H, 7.90%.

Polymerization Procedure

Monomers and Solvents. Monomers were purified by distillation over calcium hydride and stored at low temperature. Just before the polymerization, monomers were redistilled over sodium and kept at –78°C under an inert atmosphere.

Titanium tetrachloride was a commercial product and was used without further purification. Triisobutylaluminum produced by Ethyl Co. was used.

Reagent-grade *n*-heptane (or benzene) was refluxed over sodium and calcium hydride, passed through a column packed with 4A molecular sieves, and distilled over triethylaluminum under the atmosphere of pure nitrogen.

Polymerization with TiCl₄–Al(*i*-C₄H₉)₃ Catalyst System. The polymerizations were carried out in a 50-ml jacketed glass reactor at temperature of 25°C under continuous stirring with a magnetic stirrer. The reactor was fitted with serum-cap and all reagents were introduced by means of syringes. The order of addition of materials to the reactor was: 15 ml of solvent, 0.83 ml of a 10% solution of TiCl₄ in solvent, 3 g of monomer, 0.87 ml of a 10% solution of Al(*i*-C₄H₉)₃ in solvent. The polymerization was terminated after 72 hr by addition of 10 ml methanol. The reaction mixture was then poured into 50 ml of a 0.2% solution of *N*-phenyl- β -naphthylamine in methanol containing 1 ml of concentrated HCl. The polymer which separated as white powder, was dried at room temperature in vacuum, dissolved in benzene and precipitated with methanol.

Polymerization of (S)(+)-IV with Butyllithium as Catalyst. A glass reactor of 30 ml was dried for 1 hr at 110°, cooled in dry-box under a stream of purified nitrogen, and closed with serum cap. The order of addition of materials was: 10 ml of dry *n*-heptane, 2.5 g (0.02 mole) of (S)(+)-IV, and 1.5 ml of *n*-butyllithium in heptane (0.9 mmole). The reaction mix-

* Reported¹ bp 113°C; $[\alpha]_D^{25} + 33.18^\circ$; λ_{\max} 225 m μ ($\log \epsilon$ 4.19).

ture was stirred with a magnetic stirrer for 40 hr, and terminated with 50 ml of a 0.2% solution of *N*-phenyl- β -naphthylamine in methanol. Crude polymer was purified by precipitation of benzene solution with methanol.

Emulsion Polymerization. A mixture of 9 ml of a 3% aqueous solution of sodium dodecylbenzene sulfonate, 0.105 g. $K_2S_2O_8$, and 3 g of monomer, was placed into a double-jacketed 30-ml glass reactor. The reactor was connected to a thermostat and under a constant stream of purified nitrogen was kept for 24 hr at 55°C under vigorous stirring with a magnetic stirrer. The reaction mixture was poured into 50 ml of a 0.2% solution of *N*-phenyl- β -naphthylamine in methanol. The rubbery polymer was separated, dried under vacuum, dissolved in benzene, and precipitated with methanol.

The authors are grateful to Dr. D. Deur-Siftar for help in performing the GLC separations and to Mrs. H. Kveder and Mrs. J. Mühl for ultraviolet, infrared, and NMR measurements. The microanalyses were performed by Dr. Z. Sliepčević. Thanks are also due to Dr. J. E. Mulvaney from the University of Arizona for reviewing the manuscript. Special thanks are due to Prof. J. H. Brewster of Purdue University for his help in interpretation of stereochemistry of monomers.

This paper was taken in part from the PhD. thesis of Z. Janović submitted to the University of Zagreb, 1969.

References

1. R. Rossi and E. Benedetti, *Gazz. Chim. Ital.*, **96**, 483 (1966).
2. E. Benedetti, F. Ciardelli, O. Pieroni, and R. Rossi, *Chim. Ind. (Milan)*, **50**, 550 (1968).
3. G. Natta, L. Porri, and S. Valenti, *Makromol. Chem.*, **67** 225 (1963).
4. A. D. Aliev, B. A. Krenzel and T. N. Fedomova, *Vysokomol. Soed.*, **7**, 1442 (1965).
5. *Information Bulletin*, No. 35, IUPAC, XXVth Conference, Cortina, Italy, 30 June-8 July 1969, p. 36.
6. D. Craig, J. J. Shipman, and R. B. Fowler, *J. Amer. Chem. Soc.*, **83**, 2885 (1961).
7. L. M. Jackman and S. Sternhell, in *Application of Nuclear Magnetic Resonance Spectroscopy in Organic Chemistry*, Vol. II Ed., Pergamon Press, New York-London 1969, p. 225.
8. W. F. Forbes, R. Shilton, and A. Balasubramanian, *J. Org. Chem.*, **29**, 3527 (1964).
9. J. H. Brewster, *J. Amer. Chem. Soc.*, **81**, 5475, 5483, 5493 (1959).
10. L. Lardicci, C. Botteghi, and E. Belgodere, *Gazz. Chim. Ital.*, **97**, 610 (1967).
11. L. Porri and M. C. Gallazzi, *Europ. Polymer J.*, **2**, 189 (1966).
12. E. J. Hart and A. W. Meyer, *J. Amer. Chem. Soc.*, **71**, 1980 (1949).
13. P. Pino, F. Ciardelli, G. P. Lorenzi, and G. Montagnoli, *Makromol. Chem.*, **61**, 207 (1963).
14. J. L. Binder, *J. Polym. Sci. A*, **1**, 37 (1963).
15. W. Marconi, A. Mazzei, S. Cucinella, M. Cesari, and E. Pauluzzi, *J. Polym. Sci. A*, **3**, 123 (1965).
16. W. Marconi, A. Mazzei, S. Cucinella, and M. Cesari, *J. Polym. Sci. A*, **2**, 4261 (1964).
17. M. S. Newman and W. T. Booth, Jr., *J. Amer. Chem. Soc.*, **67**, 154 (1945).
18. P. D. Bartlett and C. H. Stauffer, *J. Amer. Chem. Soc.*, **57**, 2580 (1935).

Received July 22, 1970

Revised October 7, 1970

Polyimides Based on Pyrazinetetracarboxylic Dianhydride and Some Related Model Compounds

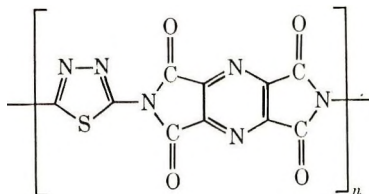
GEORGE B. VAUGHAN,* JERRY C. ROSE, and G. P. BROWN,†
*Mellon Institute, Carnegie-Mellon University,
 Pittsburgh, Pennsylvania 15213*

Synopsis

A study was made of polyimides based on pyrazinetetracarboxylic dianhydride (PTDA) plus heterocyclic diamines different from the one previously reported by Hirsch. It was postulated that thermal properties might be improved if the diamine portion did not contain the N-N linkage. The results indicate that these heterocyclic-based polyimides are in fact of lower thermal stability and of less molecular weight buildup than their corresponding polypyromellitimides. Thermal failure, outlined by their TGA curves, is shown not to be due to an inherent lack of stability for such polymers, but rather, to synthesis problems arising from both the anhydride and amine precursors. The synthetic problems are twofold: (1) the heterocyclic diamines used in this study display low reactivity; (2) pyrazinecarboxylic acids readily decarboxylate. These conclusions were drawn from a correlation of the relative basicity values of the diamines of consideration and from study of a series of model compounds prepared from an appropriate amine or diamine with PDTA, pyrazinedicarboxylic anhydride, phthalic anhydride, or pyromellitic dianhydride. An accumulation of infrared and mass spectra data for these models relate that the proposed pyrazine polyimides are not of complete polyimide structure, but rather resemble recurring amide-imide units.

INTRODUCTION

Polymers devoid of any hydrogen or other pendent groups were shown in a recent publication¹ to possess excellent thermal properties. The study was based on a polyimide prepared from pyrazinetetracarboxylic dianhydride (PTDA) and 2,5-diamino-1,3,4-thiadiazole (DATA-2,5).‡



* Present address, University of New South Wales, Sydney, Australia.

† To whom inquiries may be directed.

‡ Throughout this paper, condensation polymers prepared from PTDA and a diamine will be referred to as pyrazine polyamic acids and pyrazine polyimides.

A sequel to this work was our investigation into non-hydrogen containing polyimides. We believed the thermal properties of Hirsch's polymer might be improved if the diamine portion did not contain the N-N linkage. Accordingly, measures were taken to synthesize analogous polyimides based on PTDA and other heterocyclic diamines.

Our expectations fell short, in that polymers of significant thermal stability could not be obtained. However, the problem was not due to an inherent lack of stability for such polymers, but rather, to synthesis problems arising from both the anhydride and amine precursors.

RESULTS

Pyrazinetetracarboxylic Dianhydride

Pyrazinetetracarboxylic Acid (PTCA). Pyrazinetetracarboxylic acid was prepared from the permanganate oxidation of pure phenazine and then recovered from the lead salt.² Three recrystallizations from 20% HCl were necessary to completely liberate the tetracid from its potassium salt contaminate. The pure acid melts in the range 193–210°C, depending on the rate of heating.

Pyrazinetetracarboxylic Acid Dianhydride (PTDA). The dianhydride, PTDA, was crystallized twice from acetic anhydride with mild heating (less than 70°C). Allowing prolonged heating yielded pyrazinetetracarboxylic acid anhydride.

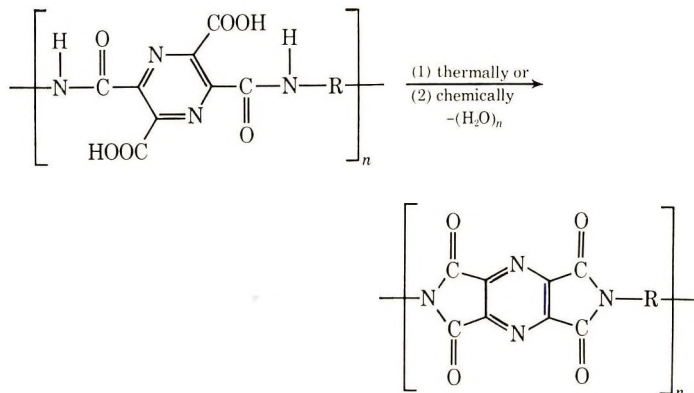
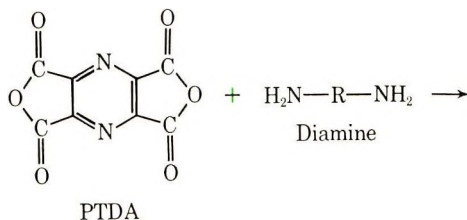
Polymerization

All solvents used in the polymerization procedures were distilled over a suitable drying agent and stored in the absence of moisture. The preparation of a polyamic acid was generally carried out by the addition of the dianhydride to a solution or slurry of the diamine in a polar solvent such as dimethylacetamide (DMAC), dimethylformamide (DMF), or *N*-methylpyrrolidone (NMP); total solute concentration ranged from 7 to 15%. In most cases, the polymerization was complete after 1½–2 hr as indicated by a leveling off of viscosity. Temperature was maintained below 40°C in order to minimize hydration to low molecular weight chains.

Thin layers (20–30 mils) of the polyamic acid solutions were doctored onto glass plates pretreated with a fluorochemical-silicone releasing agent (Minnesota Mining and Manufacturing Co.). The films were dried for 12 hr under pump vacuum at 40°C and then easily peeled from the glass plate.

Conversion of the polyamic acid film to the corresponding polyimide was performed both thermally (T) and chemically (C).

Thermal. The thin film was clamped by magnets to metal frames and cured in a forced draft oven using the following heating schedule: 12 hr at 50°C in vacuum, 1 hr at 100°C in N₂, 1 hr at 150°C in N₂, 1 hr at 200°C



in air, 1 hr at 250°C in air, 20 min at 300°C in air. As imidization proceeds, the color of the film darkens from a yellow-orange to a deep red.

Chemical. A portion of the film was allowed to soak in a 1:1:1 benzene-acetic anhydride-pyridine mixture for 12 hr at ambient temperature and 15 min at 60°. The film was washed with benzene, air-dried for 1 hr, and then heated in an oven to 150°C for 1 hr.

Characterization

Infrared Spectra. All infrared work was carried out on a Beckman IR-9 recording spectrophotometer. Solutions of 1% concentration of the polyamic acid were cast onto NaCl plates and cured according to the above thermal procedure. In each case, the imidization could be followed by the disappearance of N-H bands at 3.05 μ and 6.55 μ . Appearance of bands at 5.65 and 5.85 μ (imide carbonyl), 7.35 μ (imide ring), and 13.8 μ (imide) confirmed the final form.

Viscosity. Viscosity data was obtained from a Hewlett-Packard Model 5901B Auto-Viscometer equipped with Ubbelohde viscometers. All determinations were obtained on the solutions of the polyamic acid.³ A computer program extrapolated the inherent and reduced viscosities to a common intercept: the intrinsic viscosity at infinite dilution.

Constants in the Mark-Houwink equation were, for comparative purposes, assumed to approximate those calculated for similar polypyromellitimide systems,⁴ where $K = 1.85 \times 10^{-4}$ and $a = 0.80$:

$$[\eta] = KM^a$$

Model Reactions and Compounds

The synthetic pathways and infrared spectra of the compounds shown in Table I (I–XIII) demonstrate the properties of pyrazine polyimides. Preparation of the precursor amic acids involved reacting an appropriate amine or diamine versus PTDA, pyrazinedicarboxylic acid anhydride (PDA), phthalic anhydride or pyromellitic dianhydride (PMDA). A *p*-dioxane–DMF solvent system was generally employed.

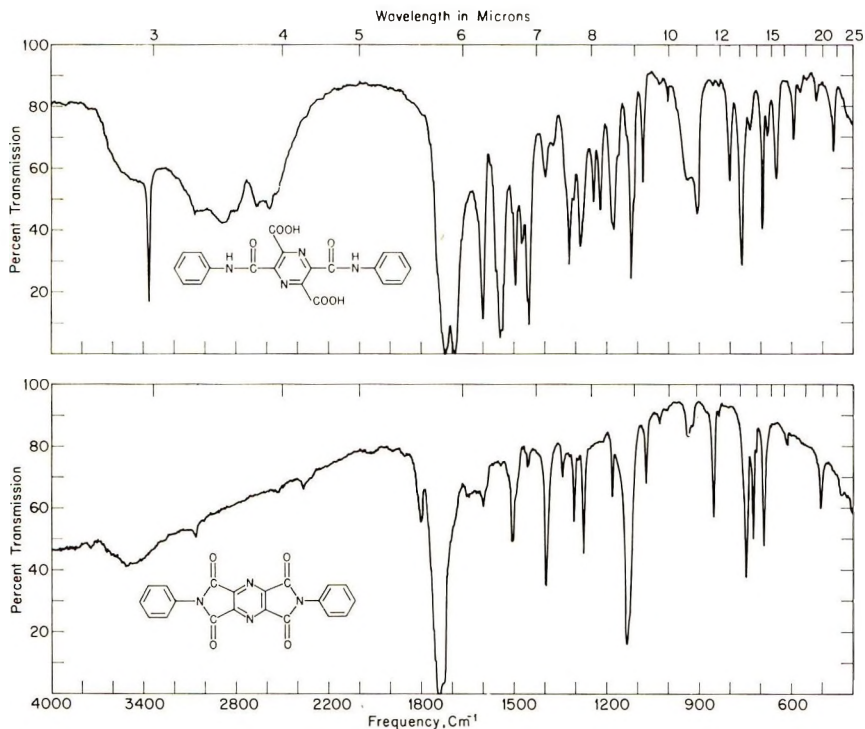


Fig. 1. Infrared spectra of (top) 2,5-pyrazinedicarboxanilide-3,6-dicarboxylic acid (KBr) and (bottom) *N,N'*-diphenyl pyrazinetetracarboxydiimide (KBr).

The chemical or thermal imidization of the product obtained from phthalic anhydride and a diamine or from PMDA plus aniline, proceeded without difficulty to yield imides I, IV, and X (Table I). In the pyrazine series, however, unexpected results occurred. When the amic acid product from PDA and aniline was heated under prescribed imidization conditions, pyrazinecarboxanilide (II) was isolated. Similarly, the direct preparation of the imide from 1 part PTDA and 2 parts aniline resulted in a mixture of products which were identified by mass measuring as the mono- and di-decarboxylated products (V and VI). The product obtained from the reaction of 2 parts PDA and 4,4'-oxydianiline (ODA) decarboxylated to VIII. The decarboxylation was avoided, however, if chemical imidiza-

tion was employed. In this manner, the expected imide products, III, VII, and IX, were prepared. Typical infrared patterns are shown in Figures 1 and 2.

The diamines XIV–XXV (see Table II) were suggested for polyimide formation from PTDA. Except for those described in the experimental section, they were obtained commercially and recrystallized to a 1°C melting point range. Purity was checked by elemental analysis, GLPC, and mass spectra (m^+).

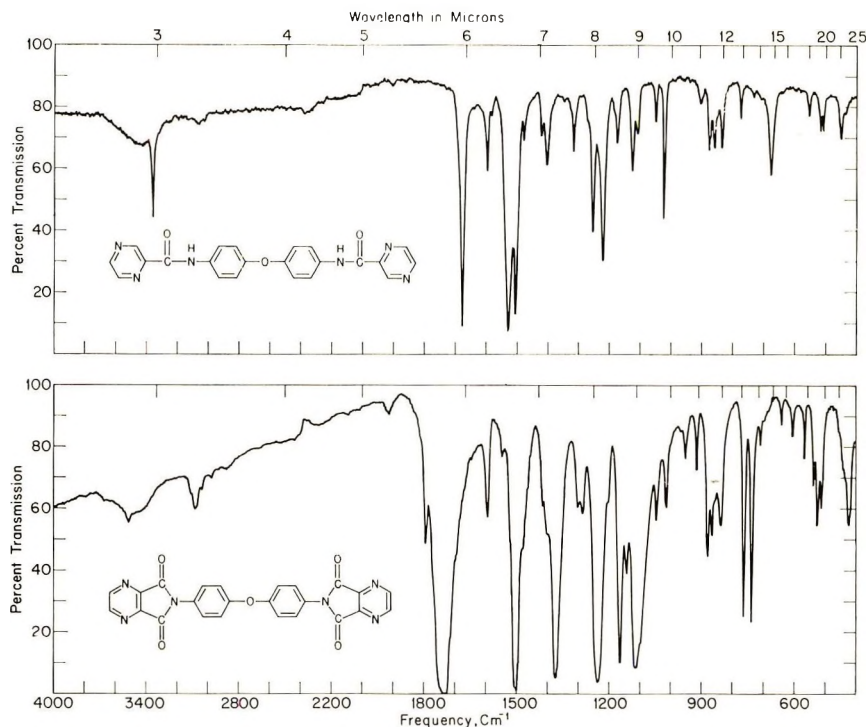
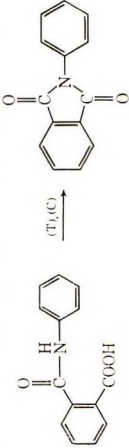
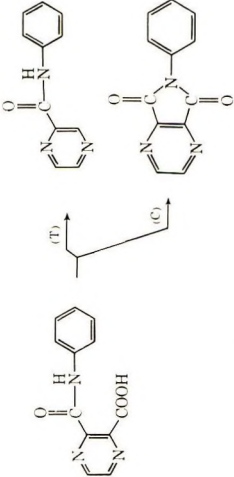
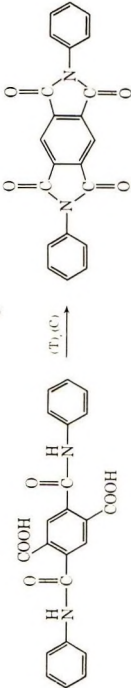
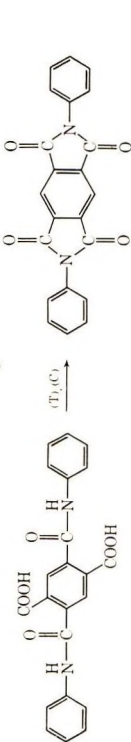
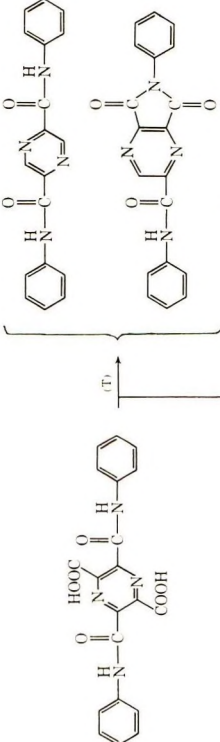
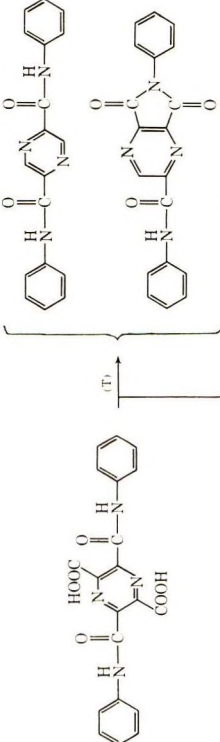
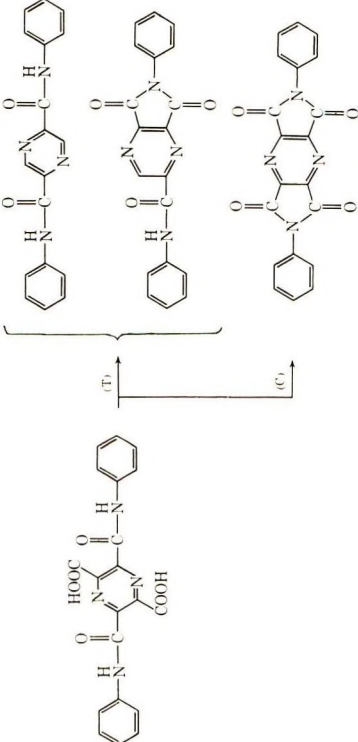


Fig. 2. Infrared spectra of (top) bis(pyrazinecarboxyimino-*p*-phenylene) ether and (bottom) *N,N'*-*p*-oxydiphenyl bis(pyrazine-2,3-dicarboxyimide) (KBr).

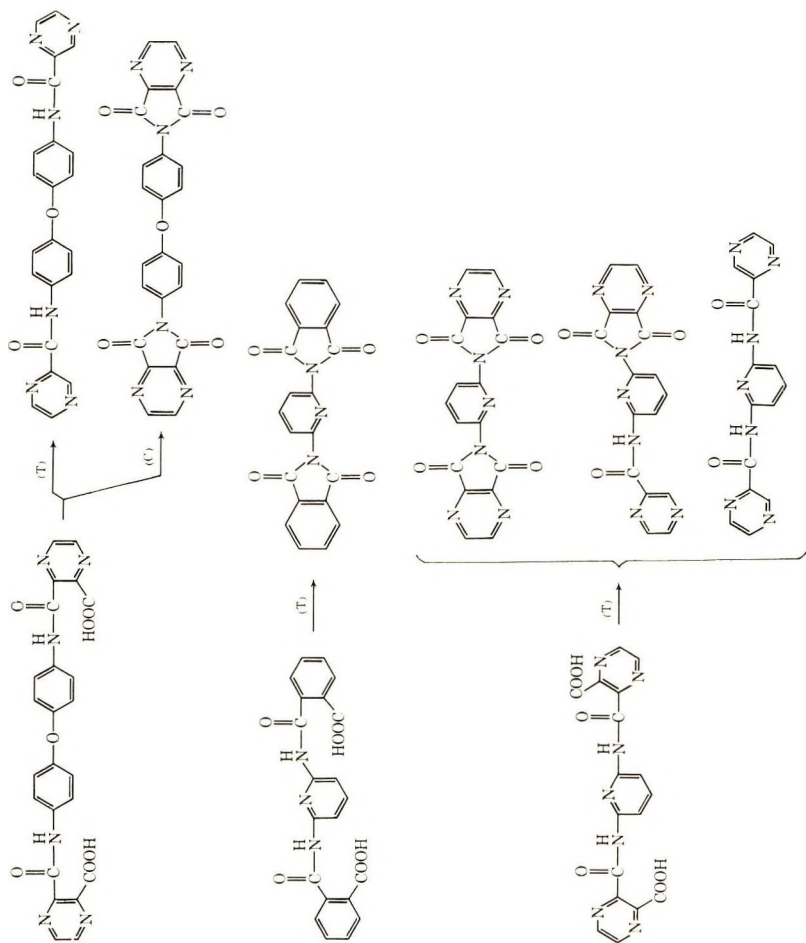
The reactions of the diaminophenylene derivatives XIV–XVIII with PMDA have been well studied⁵ and shown to result in viscous polyamic acid solutions. For comparative purposes, PTDA was allowed to react with these diamines and, as expected, gave comparable solution properties.

Because of the expense involved in preparing PTDA, heterocyclic diamines XIX–XXV were first reacted with PMDA. Only DATA-2,5¹ (XX) and diaminotriazole (XXIV) gave indication of polymer formation. The reaction of PMDA with 3,5-diamino-1,2,4-thiadiazole (DATA-3,5) (XXI) yielded a red precipitate which was identified by mass spectra

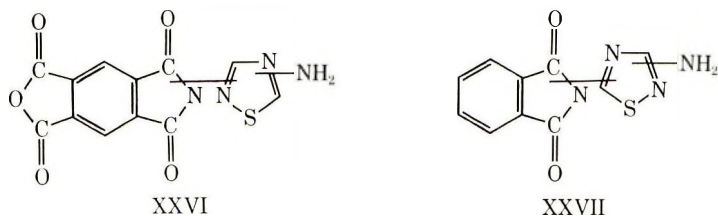
TABLE I. Summary of Model Compounds Obtained from Imidization by (I) Thermal and (C) Chemical

Compound	Identification
	I M.p. 208°C (lit. ¹² mp, 210°C)
	II ANAL. Calcd. for $C_{11}H_{13}N_3O_2$: C, 65.99%; H, 5.03%; N, 20.99%; O, 7.99%. Found: C, 66.05%; H, 5.20%; N, 21.08%; O, 8.14%.
	III ANAL. Calcd. for $C_{12}H_{11}N_3O_2$: C, 64.00%; H, 3.13%; N, 18.66%. Found: C, 63.18%; H, 3.13%; N, 18.44%. M.s., p = 225
	IV ANAL. Calcd. for $C_{13}H_{11}N_3O_2$: C, 71.74%; H, 3.28%; N, 7.60%; O, 17.38%. Found: C, 71.58%; H, 3.26%; N, 7.80%; O, 17.61%.
	V M.s., parent ion = 318
	VI M.s., parent ion = 344
	VII ANAL. Calcd. for $C_{16}H_{10}N_4O_2$: C, 64.86%; H, 2.72%; N, 15.13%; O, 17.28%. Found: C, 62.13%; H, 2.19%; N, 14.34%. M.s., parent ion = 370

VIII	ANAL. Calcd. for $C_{22}H_{16}N_4O_4$: C, 64.07%; H, 3.91%; O, 11.64%; N, 20.38%. Found: C, 64.07%; H, 4.05%; O, 11.68%; N, 20.17%.
IX	ANAL. Calcd. for $C_{23}H_{12}N_4O_5$: C, 62.07%; H, 2.61%; N, 18.10%. Found: C, 61.65%; H, 2.63%; N, 17.95%.
X	ANAL. Calcd. for $C_{22}H_{11}N_5O_4$: C, 68.27%; H, 3.00%; N, 11.38%. Found: C, 68.78%; H, 3.23%; N, 11.28%.
XI	M.s., parent ion = 373
XII	M.s., parent ion = 347
XIII	M.s., parent ion = 321



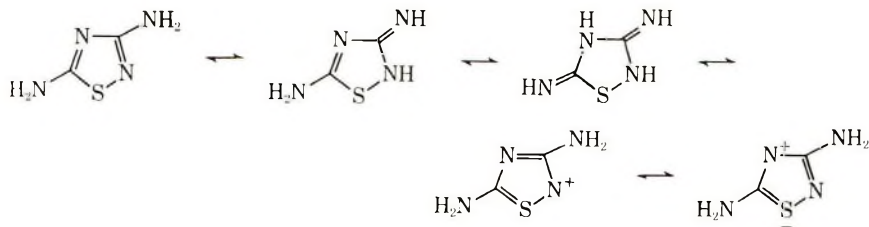
and elemental analysis as the mono-imide (XXVI). In similar manner, the



reaction between 2 parts phthalic anhydride and 1 part DATA-3,5 yielded the monoaddition product XXVII, even under severe conditions.

Attempted polymerization of PMDA with either 3,4- or 3,5-diaminofurazan (XXII and XXIII) resulted in no viscosity buildup or other indications of reaction. The insolubility⁶ of diaminomethyl-*s*-triazine (XXV) precluded normal polymerization procedures in a dry organic solvent; a very low molecular weight polymer was obtained in a water-pyridine solvent system.

The above evidence indicate that low reactivity might be explained on the basis of a combination of inductive and tautomeric effects.



Structures similar to those illustrated can be drawn for the other heterocyclic diamines of this work.


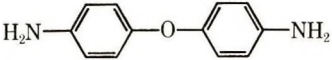
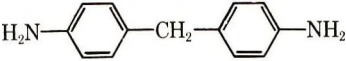
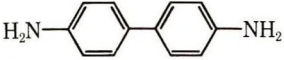
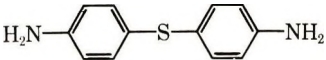
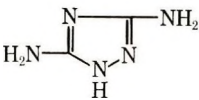
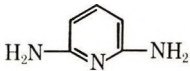
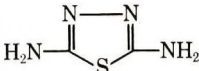
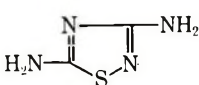


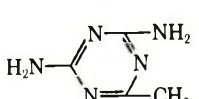
The equilibrium of these forms should affect a decrease in basicity, which, according to a proposed mechanism,⁷ will influence the reactivity for aminolysis of an anhydride.

Although a detailed study of the diamines is not the intention of this paper, observations pertaining to their relative basicities were considered of importance to our work. To establish a correlation between basicity and reactivity, two approaches were taken.

First, pK_{a1} and pK_{a2} constants were determined in aqueous media for each of the diamines of consideration.⁸ In some cases, pK_{a2} values were unobtainable due to the characteristic low pH (high H^+) values encountered.

Secondly, shifts in the NMR for the amine protons were determined in $DMSO-d_6$ and recorded in terms of τ . Factors which result in increasing pK_a values also yield a downfield shift in the NMR spectra due to local diamagnetic deshielding effects. The spectra also demonstrate the magnetic nonequivalence of the two amino groups in compounds XXI and XXIII.

TABLE II
 Correlation of Basicities

	Diamine	pK_{a1}^a	pK_{a2}^a	τ^b
XIV		6.08	3.29	5.75
XV		°		5.23
XVI		°		5.22
XVII		4.70	3.63	5.05
XVIII		°		4.54
XXIV		4.22	2.02	4.72
XIX		6.43	1.67	4.66
XX		3.98	1.85	3.75
XXI		2.57	1.54	4.35 2.50
XXII		1.05	d	4.20
XXIII		1.78	d	4.42 2.73
XXV		4.46	1.93	e

^a Arithmetic mean of ten values.

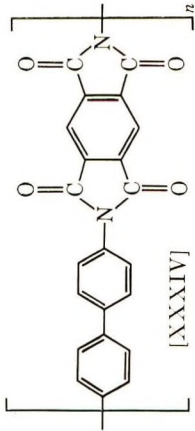
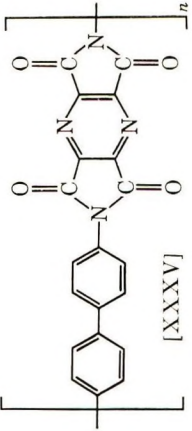
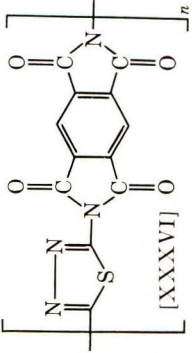
^b Tau values recorded as singlets for amine protons.

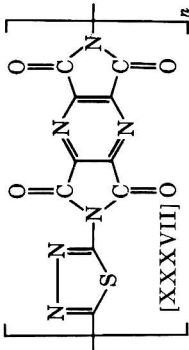
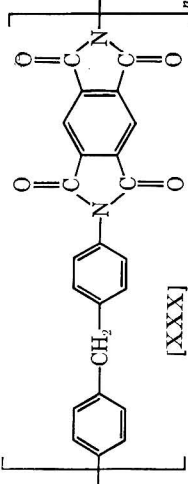
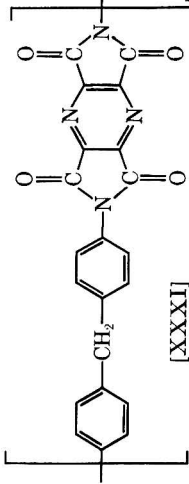
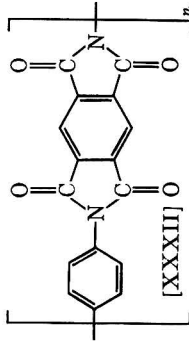
° Insoluble in water.

^d Too acidic to obtain value.

^e Insoluble in DMSO.

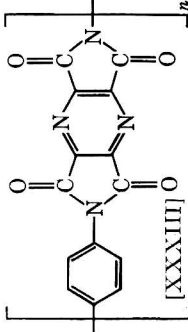
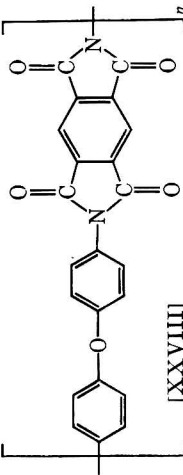
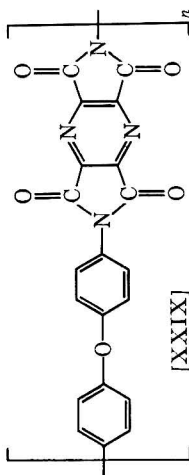
TABLE III
Data on Preparation, Structure, Inherent Viscosity, and Approximate MW of Polyamic Acids

Starting material (total solid conc.)	Solvent	Properties of imidized products	Repeating unit	Identity	Inherent viscosity ($c = 0.5\text{g}/\text{dl}$) $\times 10^{-3}$	MW $\times 10^{-3}$
PMDA + ODA (8.8 g/dl)	DMAC	Tough film, v. flexible	 <p>[XXXIV]</p>	XXXVIII	2.078	114.5
PTDA + ODA (10 g/dl)	DMAC	Tough film, v. flexible	 <p>[XXXV]</p>	XXIX	0.7657	33.2
PMDA + MDA (5 g/dl)	DMAC DMF	Tough film, v. flexible	 <p>[XXXVI]</p>	XXX	2.792	171.8

PTDA + MDA (10 g/dl) DMAC	Tough film, v. flexible		XXXVI 0.9111 41.3
PMDA + PPD (14.5 g/dl) DMF	Film, tough v. flexible		XXXVII 2.043 113.3
PTDA + PPD (7.5 g/dl) DMF	Film, s. flexible		XXXVIII 0.4789 18.5
PMDA + DBZ (7.5 g/dl) DMAC	Film, s. brittle		XXXIX 1.3562 67.8

(continued)

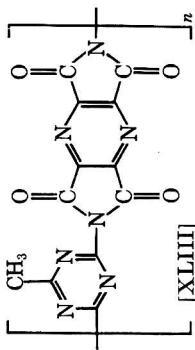
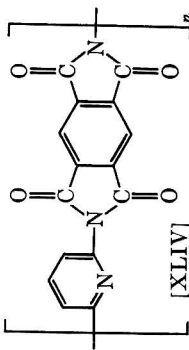
TABLE III (continued)

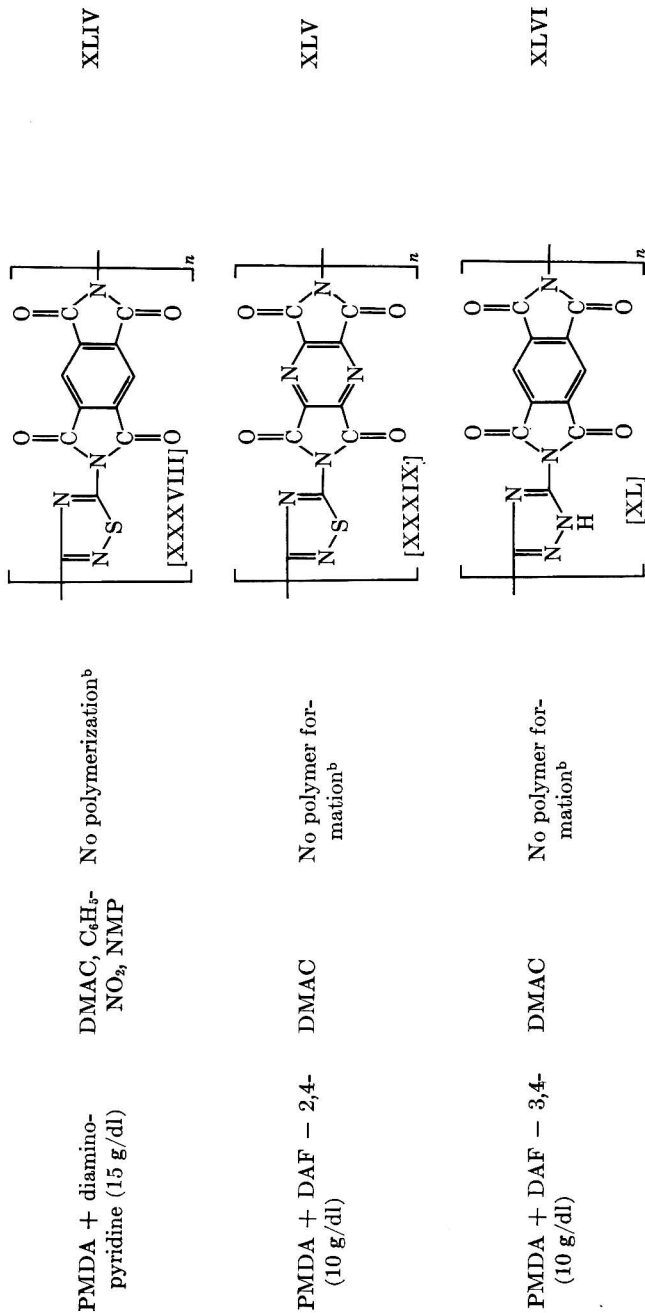
Starting material (total solid conch)	Solvent	Properties of imidized products	Repeating unit	Identity	Inherent viscosity ($c = 0.5\text{g}/\text{dl}$) $\times 10^{-3}$ MW
PTDA + DBZ (10 g/dl)	DMAC	Film splintered on imidization, very brittle	 [XXXVIII]	XXXV	0.3312 11.6
PMDA + DATA - 2,5- (6.67 g/dl)	DMAC	Film, s. brittle	 [XXVIII]	XXXVI	0.5659 22.7
PTDA + DATA - 2,5- (10 g/dl)	DMAC	Film, s. flexible	 [XXIX]	XXXVII	0.6638 27.8

<p>PMDA + DATA - 3,5- (10 g/dl)</p>	<p>DMAC, NMP, DMF (+ LiCl) inter- facial HMT,^a DMSO</p>	<p>No polymer for- mation isolated red precipitate</p>	<p>[XXXVIII]</p>	<p>XXXVIII</p>
<p>PTDA + DATA - 3,5- (10 g/dl)</p>	<p>DMAC</p>	<p>No polymer for- mation</p>	<p>[XXXIX]</p>	<p>XXXIX</p>
<p>PMDA + diamino-s- triazole (10 g/dl)</p>	<p>NMP</p>	<p>Film, v. brittle</p>	<p>[XL]</p>	<p>XL 0.0700 2.0</p>
<p>PTDA + diamino-s- triazole (10 g/dl)</p>	<p>NMP</p>	<p>Film, v. brittle</p>	<p>[XLI]</p>	<p>XLI 0.0700 2.0</p>

(continued)

TABLE III (continued)

Starting material (total solid conc.)	Solvent	Properties of imidized products	Repeating unit	Identity	Inherent viscosity ($c =$ $0.5\text{g}/$ $\text{dl}) \times$ 10^{-3}	MW \times 10^{-3}
PMDA + diaminomethyl- <i>s</i> -triazine (15 g/dl)	Pyridine-water interfacial	Precipitate	 <p>[XLIII]</p>	XLII	0.054	1.2
PTDA + diaminomethyl- <i>s</i> -triazine (15 g/dl)	Pyridine-water	Precipitate	 <p>[XLIV]</p>	XLIII	0.050	1.0



^a Hexamethylphosphoric triamide

^b Based on no viscosity build-up

In order to attempt a correlation, the diamines were first listed in the order of their observed viscosity buildup on reaction with PMDA as an estimate of reactivity. A general correlation between ranking achieved in this manner and decreasing pK_a and/or τ values does exist and is illustrated in Table II.

Since shifts in the NMR reflect the sum of all local diamagnetic and paramagnetic effects, a linear relation between pK_a and τ does not exist.

Polyimides

The series of polyimides which were prepared are summarized in Table III. Inability to obtain a high molecular weight polymer of structure (XXXVIII-XLVI) based on PMDA appears to be related to the properties of the diamine. Thermal stability was determined for polyimide

TABLE IV
Thermogravimetric Analysis of Polymers

Polyimide	Temperature, °C, at various degrees of weight loss			
	5%	10%	20%	50%
PMDA-ODA (XXVIII)	500	520	541	565
chemically imidized	510	527	543	563
PTDA-ODA (XXIX)	265	365	439	502
chemically imidized	375	415	455	505
PMDA-MDA (XXX)	472	503	528	553
PTDA-MDA (XXXI)	320	391	452	535
chemically imidized	394	420	454	506
PMDA-PPD (XXXII)	502	535	560	582
PTDA-PPD (XXXIII)	285	360	430	500
chemically imidized	378	407	445	495
PMDA-DBZ (XXXIV)	505	542	565	590
PTDA-DBZ (XXXV)	330	360	400	475
PMDA-DATA-2,5 (XXXVI)	339	374	435	523
PTDA-DATA-2,5 (XXXVII)	342	365	430	539
chemically imidized	167	178	196	331
PMDA-diaminotriazole (XL)	400	437	460	535
PTDA-diaminotriazole (XLI)	380	432	470	505
PMDA-DMT (XLII)	297	315	395	492
PTDA-DMT (XLIII)	225	232	240	309

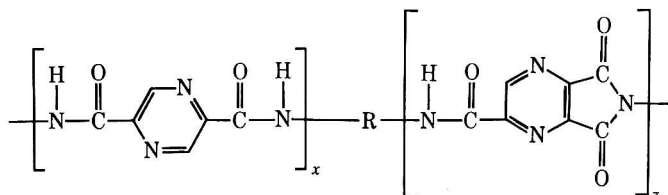
films by thermal gravimetric analysis and is reported in Table IV as percentage weight loss versus temperature. (All TGA data were obtained on a Du Pont 950 Thermogravimetric Analyzer. Samples were heated at 10°C/min under an oxygen atmosphere.) No case was found in which the thermal properties for a pyrazine polyimide was greater than that of the corresponding polypyromellitimide.

DISCUSSION

The objective of this work was to investigate polyimides not containing hydrogen, similar to the one previously reported¹ but without the N-N bond. It was postulated that polymers of such modification would display an enhanced thermal stability. The results presented clearly indicate that these heterocyclic-based polyimides present extreme difficulties in synthesis and are in fact of lower thermal stability than the corresponding polypyromellitimides.

The synthetic problems are twofold: (1) the heterocyclic diamines used in this study displayed low reactivity; (2) pyrazinecarboxylic acids readily decarboxylate. The facile decarboxylation of PTDA is noted in low yields in the preparation of PTDA, in the model compound studies, and is implicated in the spectral data of the polymers.

The infrared spectra of the imidized polymers prepared from PTDA did not exhibit a characteristic imide spectra, but instead, retained the amine absorption pattern. This suggests that the pyrazine polyimides are not of complete polyimide structures but also contain amide-imide recurring units of x and z as shown. Additional evidence for this occurrence was provided by elemental analysis which showed a maximum hydrogen content of 3-5%.



R = Diamine

Consequently, thermal stability of such structures is, as a limit, no better than that of a polyamide-imide.

The decarboxylation incurred during thermal imidization was circumvented by a chemical method for dehydration. The infrared spectra of some arbitrarily chosen chemically cured pyrazine polyimides give imide bands, but only after warming the acetic anhydride-pyridine mixture, contacting the film, to 60°C for 15 min (see Fig. 3). As indicated by a later inflection point and lower weight loss, the TGA curves of the pyrazine polyimides XXIX, XXXI, and XXXIII cured by this method actually showed better thermal stability than previously (Figs. 4 and 5). However, the TGA data of polymer XXXVII (PTDA-DATA-2,5) showed an early inflection point followed by an overall diminution of thermal stability. Apparently, for low molecular weight polymers, as in the latter case, excess acetylation of the numerous available free amines accounts for early weight loss. This effect would become less of a factor with polymers of higher molecular weight.

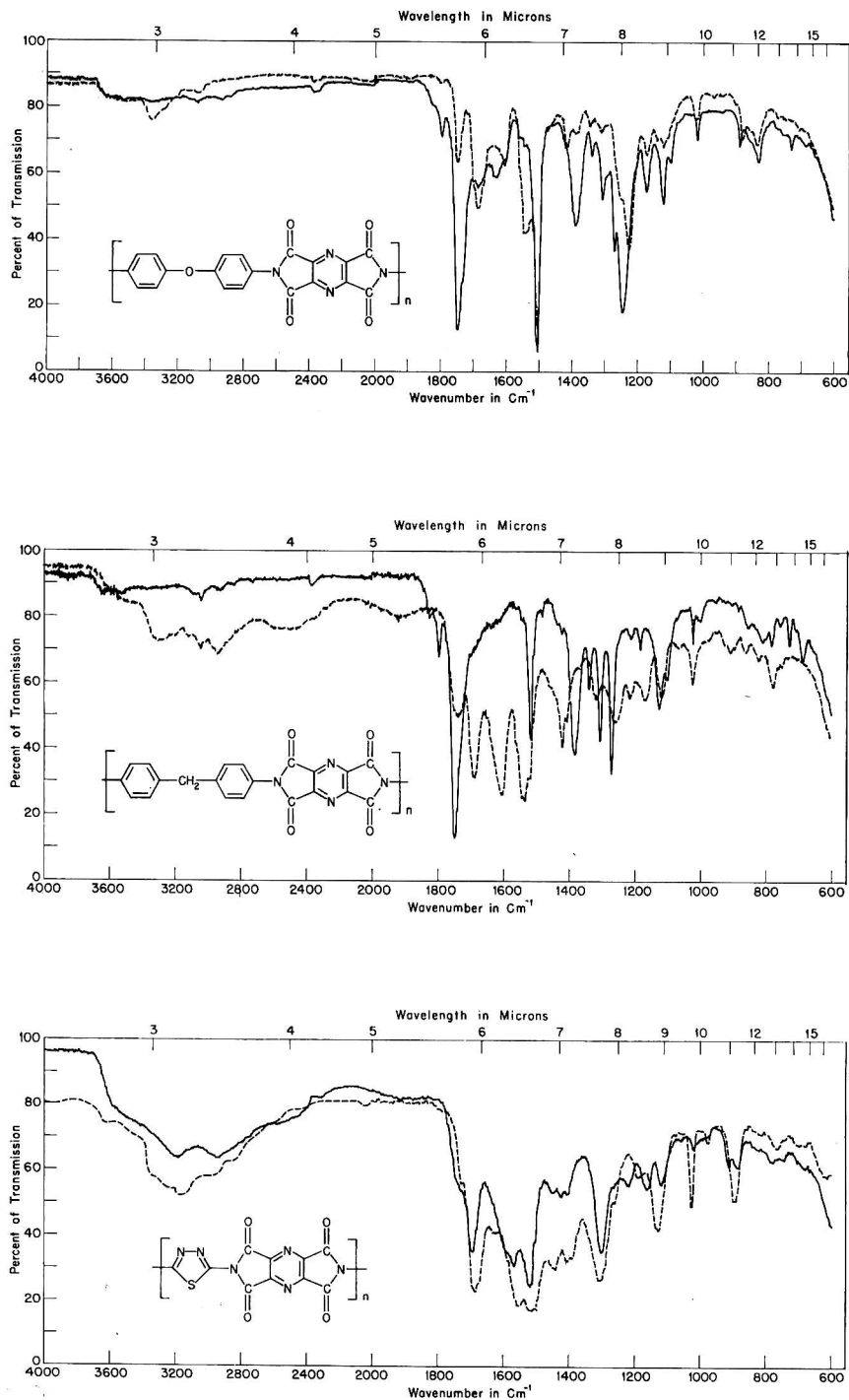


Fig. 3. Infrared spectra of various pyrazine polyimides: (—) thermally cured; (---) chemically cured.

In conclusion, the evidence presented is not intended to discourage the investigation of polymers devoid of hydrogen as a unique class of thermally stable polymers. The experimental results of this work do indicate that polyimides prepared from PTDA plus a diamine contain inherent problems which preclude this pathway as a practical route.

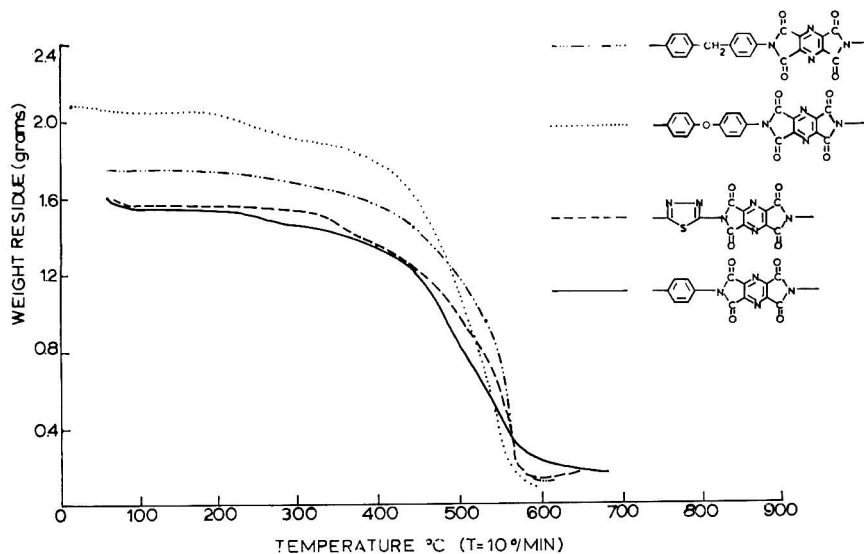


Fig. 4. Thermogravimetric analysis of thermally cured pyrazine polyimides.

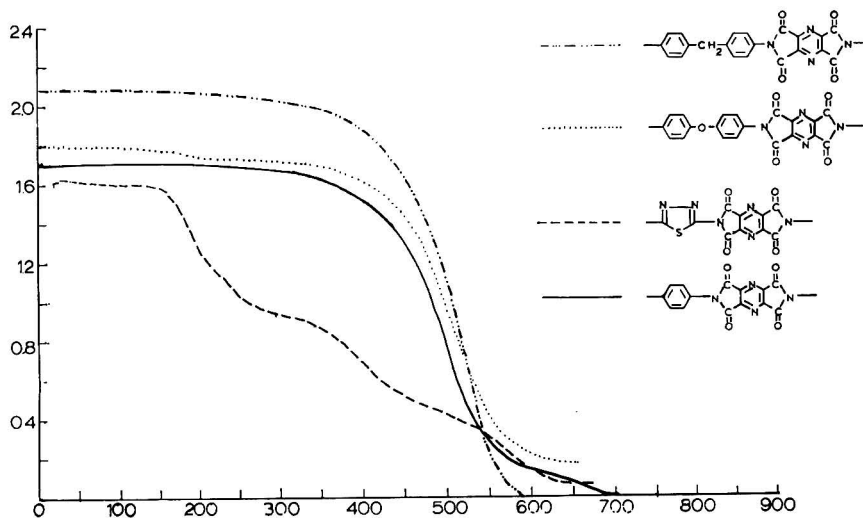


Fig. 5. Thermogravimetric analysis of chemically cured pyrazine polyimides.

EXPERIMENTAL

3,5-Diaminofurazan (XXIII)

This compound was prepared⁹ from the reaction of 0.5 mole $\text{NH}_2\text{OH} \cdot \text{HCl}$ with 0.5 mole sodium dicyanamide in 250 ml of MeOH. After the initial temperature rise, the mixture was refluxed for 30 min, cooled, and the NaCl filtered off. Evaporation of the filtrate gave 45% yield of white needles which were recrystallized from water to mp 166–167°C; mass spectra parent ion = 100.

ANAL. Calcd for $\text{C}_2\text{H}_4\text{N}_4\text{O}$: C, 24.00%; H, 4.03%; N, 55.98%; O, 15.99%. Found: C, 24.06%; H, 4.01%; N, 55.95%; O, 16.04%.

3,4-Diaminofurazan (XXII)

A pressure bomb was charged with 11.8 g (0.10 mole) diaminoglyoxime and 50 ml of a 8% NaOH solution. The container was sealed and heated for 4 hr at 170°C. After cooling in an ice bath, the solid was filtered. The product, 3,4-diaminofurazan, was crystallized from water as white needles, mp 179°C (lit.¹⁰ 180°C); yield 17%; mass spectra parent ion = 100.

3,5-Diamino-1,2,4-thiadiazole (XXI)

Guanyl thiourea (8.0 g, 0.067 mole) was dissolved in a solution of 200 ml EtOH and 9 ml HCl. While heating at reflux temperature, 25 ml of 30% hydrogen peroxide was added over an interval of 30 min. The solution was cooled and 16 g of tolylsulfonic acid was added. After concentrating to a small volume, the thiadiazole tosylate was isolated from a methanol–water mixture, mp 237–238°C (lit.¹¹ 238–240°C). The free base was obtained by passing the tosylate through a weakly basic ion-exchange resin. 3,5-Diamino-1,2,4-thiadiazole was crystallized from dioxane as white needles, mp 168–169°C (lit.¹¹ 168–171°C); mass spectra parent ion = 116. The overall yield was 24%.

ANAL. Calcd for $\text{C}_2\text{H}_4\text{N}_4\text{S}$: C, 20.68%; H, 3.47%; N, 48.24%; S, 27.61%. Found: C, 20.96%; H, 4.13%; N, 47.75%; S, 27.23%.

N-Aminothiadiazole-1,2,4-diyl-3,5-phthalimide (XXVII)

In a 100 ml round-bottomed flask, 0.40 g DATA-3,5 (3.38×10^{-3} mole) was dissolved in 50 ml DMF plus 5 ml pyridine. Then 1.0 g of phthalic anhydride (6.76×10^{-3} mole) was added, and the solution was heated at reflux temperature for 2 hr. Upon cooling, 1.30 g (61% yield) of yellow crystals was collected; mass spectra parent ion = 246. No melting point was observed below 300°C. The position of attack was not ascertained.

ANAL. Calcd for $\text{C}_{10}\text{H}_6\text{N}_4\text{O}_2\text{S}$: C, 48.78%; H, 2.46%; N, 22.75%. Found: C, 48.50%; H, 2.66%; N, 22.87%.

Pyrazinecarboxyanilide-2-carboxylic Acid

A 5.0-g portion (0.033 mole) of pyrazinedicarboxylic anhydride, recrystallized twice from acetic anhydride, was added with stirring to a solu-

tion of 3.1 g (0.033 mole) aniline in 25 ml THF. The solution was heated at 50°C for 40 min and then concentrated to dryness. A quantitative yield of white product was recrystallized from EtOH, mp 140.1°C.

ANAL. Calcd for $C_{12}H_9N_3O_3$: C, 59.26%; H, 3.73%; N, 17.28%; O, 19.73%. Found: C, 59.20%; H, 4.03%; N, 16.96%; O, 19.84%.

Pyrazinecarboxyanilide (II)

A 0.5-g sample of the previous acid was heated under N_2 to 180°C in the melt state, cooled to solid, and recrystallized from EtOH as white needles, mp 127.1°C.

ANAL. Calcd for $C_{11}H_{10}N_3O$: C, 65.99%; H, 5.03%; N, 20.99%; O, 7.99%. Found: C, 66.05%; H, 5.20%; N, 21.08%; O, 8.14%.

Pyrazine-2,3-dicarboxy-*N*-phenylimide (III)

A 1.0-g sample of the previous acid anilide was dissolved in a mixture of 30 ml acetic anhydride plus 15 ml pyridine. After setting for 30 min, the darkened solution was concentrated to dryness under reduced vacuum. The residue was charcoaled and crystallized from a mixture of 45 ml EtOH plus 5 ml DMF as white plates, mp 229.4°C.

ANAL. Calcd for $C_{12}H_7N_3O_2$: C, 64.00%; H, 3.13%; N, 18.66%. Found: C, 63.18%; H, 3.13%; N, 18.44%.

N,N'-Diphenylpyromellitimide (IV)

To a solution of 5.5 g (0.025 mole) of pyromellitic dianhydride in 50 ml THF was added 4.75 ml (0.05 mole) aniline. The mixture was heated at reflux temperature for 14 hours, cooled, and the precipitate filtered. The yellow plates were recrystallized from boiling nitrobenzene, yield 8.4 g (91%), does not melt below 300°C.

ANAL. Calcd for $C_{22}H_{12}N_2O_4$: C, 71.74%; H, 3.28%; N, 7.60%; O, 17.38%. Found: C, 71.58%; H, 3.26%; N, 7.80%; O, 17.61%.

2,5-Pyrazinedicarboxyanilide-3,6-dicarboxylic Acid

To a solution of pyrazinetetracarboxylic dianhydride (0.243 g, 1.1×10^{-3} mole) in 10 ml *p*-dioxane plus 3 ml DMF was added 0.28 g (3.0×10^{-3} mole) of aniline. After stirring for 3 hr, the solution was refrigerated and filtered, yield 0.110 g (25%), mp 178°C.

N,N'-Diphenylpyrazinetetracarboxydiimide (VII)

A 0.05-g sample of the previous acid dianilide was treated in a 10 ml acetic anhydride-pyridine, 5:1, solution for 2.5 hr and filtered. The filtrate was washed twice with diethyl ether to give a quantitative yield of the imidized product, which decomposes at 260°C.

ANAL. Calcd for $C_{20}H_{10}N_4O_4$: C, 64.86%; H, 2.72%; N, 15.13%; O, 17.28%. Found: C, 62.13%; H, 2.19%; N, 14.34%.

Bis(pyrazinecarboxyimino-*p*-phenylene) Ether (VIII)

A mixture of pyrazinedicarboxylic anhydride (4.0 g, 0.027 mole), oxydianiline (2.7 g, 0.014 mole), and 25 ml of redistilled nitrobenzene was heated at 200°C for 5 hr. The crystals which precipitated upon cooling were filtered and recrystallized from boiling nitrobenzene after treatment with charcoal. A quantitative yield of yellow-green plates was obtained, mp 300°C (dec.).

ANAL. Calcd for $C_{22}H_{16}N_6O_3$: C, 64.07%; H, 3.91%; N, 20.38%; O, 11.64%. Found: C, 64.07%; H, 4.05%; N, 20.17%; O, 11.68.

***N,N'*-*p*-Oxydiphenylbis(pyrazine-2,3-dicarboximide) (IX)**

To a solution of 2.7 g (0.0133 mole) oxydianiline in 35 ml THF plus 5 ml DMF was added a solution of 4.0 g (0.0267 mole) of pyrazinedicarboxylic anhydride in 35 ml THF plus 8 ml DMF. A slight exothermic reaction occurred. After stirring for 6 hr, the solvent was removed under reduced pressure to yield a yellow solid material. This was dissolved in 100 ml of acetic anhydride-pyridine, 1:1 and stirred for 30 min. The solution was again concentrated under reduced pressure to yield a yellow precipitate. The product was charcoaled and crystallized from nitrobenzene, washed with ether to give 3.1 g (66% yield) of product, mp 321°C (TGA).

ANAL. Calcd for $C_{24}H_{12}N_6O_5$: C, 62.07%; H, 2.61%; N, 18.10%. Found: C, 61.65%; H, 2.63%; N, 17.95%.

The assistance of Mrs. Doris Haarr for the thermogravimetric analysis work is acknowledged with thanks.

This work was sponsored by Essex International, Inc.

References

1. S. S. Hirsch, *J. Polym. Sci. A-1*, **7**, 15 (1969).
2. S. S. Hirsch, private communication.
3. M. L. Wallach, paper presented at American Chemical Society Meeting, Chicago, September 1967; *Polym. Preprints*, **8**, No. 2, 1170 (1967).
4. M. L. Wallach, *J. Polym. Sci. A-2*, **5**, 653 (1967).
5. H. Lee, D. Stoffey, and K. Neville, *New Linear Polymers*, McGraw-Hill, New York, 1967.
6. E. A. Hoess and E. L. O'Brien, A.D. 433, 664 (1964).
7. W. Wrasidlo, P. M. Hergenrother, and H. H. Levine, paper presented at American Chemical Society Meeting, Philadelphia, April 1964; *Polym. Preprints*, **5**, No. 1, 141 (1964).
8. A. Albert and E. P. Sergeant, *Ionization Constants of Acids and Bases*, J. Wiley, New York, 1962.
9. D. W. Kaiser (American Cyanamid), U.S. Pat. No. 2,648,669 (August 11, 1953).
10. M. D. Coburn, *J. Heterocyclic Chem.*, **5**, 83 (1968).
11. F. Kurzer, *J. Chem. Soc.*, **1955**, 1.
12. L. Kurosaki and P. R. Young, in *Macromolecular Chemistry Tokyo-Kyoto 1966* (*J. Polym. Sci. C*, **23**), I. Sakurada and S. Okamura, Eds., Interscience, New York, 1968, p. 57.

Received September 8, 1970

Optical Properties of Inherently Dissymmetric Polyamides*†

C. G. OVERBERGER, A. OHNISHI, and A. S. GOMES,‡
*Department of Chemistry and the Macromolecular Research Center,
University of Michigan, Ann Arbor, Michigan 48104*

Synopsis

A study of the optical rotatory dispersion (ORD), circular dichroism (CD), and ultraviolet spectra (UV) of polyamides derived from optically active biphenyl acid chlorides, and aromatic, and aliphatic diamines, was made. The optically active monomers were (-)-(S)-2,2'-dinitro-6,6'-dimethylbiphenyl-4,4'-dicarbonyl chloride and (-)-(S)-2,2'-dichloro-6,6'-dimethylbiphenyl-4,4'-dicarbonyl chloride. The diamines were *o*-, *m*-, and *p*-phenylenediamine, piperazine, *trans*-2,5-dimethylpiperazine, and 1,2-pyrazolidine. The ORD spectra of the *o*-phenylenediaminepolyamide taken in different solvents indicated the existence of some ordered structure in the least polar solvent. All other polyamides existed in a random coil conformation in the solvents employed.

INTRODUCTION

Recently, the optical rotatory properties of polymers containing atropisomers have been investigated. Overberger and Yoshimura² have prepared rigid and asymmetric polyamides by incorporation of optically active biphenyls into the polymer backbone. These polymers, together with their model compounds, have been investigated by visible optical rotatory dispersion (ORD). Their polyamides derived from 2,2'-dinitro-6,6'-dimethylbiphenyl-4,4'-dicarbonyl chloride, and *o*-phenylenediamine showed a complex ORD curve in dichloroacetic acid while the curves of the *m*- and *p*-phenylenediamine polymers were simple, using a single term Drude equation. Schulz and Jung³ have prepared several esters⁴ including a polyvinyl ester of (+)-2-methyl-6-nitrobiphenyl 2'-carboxylic acid and investigated their optical properties. Schulz and Jung⁵ later studied the rotatory power of a polyamide obtained from (+)-2,2'-diaminobinaphthyl and terephthaloyl chloride and its model compound. In this case, an enhancement of rotatory strength and red-shifted bands were observed for the polymer with respect to its model. However, they did not find any

* In honor of Professor W. Kern on the occasion of his 65th birthday.

† This is the 22nd in a series of papers concerned with the syntheses and properties of asymmetric polymers; for the previous paper in this series see Overberger et al.¹

‡ Fellow of the Brazilian National Research Council and the National Academy of Science overseas research fellowship program.

enhancement of rotatory power nor red-shifted bands when they studied the ORD and circular dichroism (CD) of the optically active polyamide derived from 2,2'-dimethoxy-6,6'-dicarboxylic acid and piperazine in comparison with the model compound prepared from piperidine.⁶ It should be mentioned that in the above-mentioned cases, the ORD and CD curves were obtained from the aromatic chromophore groups and in no cases were they able to observe the amide absorption, mainly because of the lack of solubility in an appropriate solvent which does not cut off in that ultra-violet region.

With these problems in mind, we decided to restudy the polyamides, previously prepared by Overberger and Yoshimura,² hoping to be able to observe some of the amide absorptions in the far ultraviolet spectrum. In order to study the effect of hydrogen bonding and rigidity in these polyamides, we decided also to prepare some polyamides derived from (-)-(S)-2,2'-dinitro-6,6'-dimethylbiphenyl-4,4'-dicarbonyl chloride and (-)-(S)-2,2'-dichloro-6,6'-dimethylbiphenyl-4,4'-dicarbonyl chloride and secondary cyclic diamines such as piperazine (PIP), *trans*-2,5-dimethylpiperazine (DMP) and 1,2-pyrazolidine (PD) (Table I).

TABLE I
Polyamides and Model Compounds Derived from
(-)-(S)-2,2'-Dinitro-6,6'-dimethylbiphenyl-4,4'-dicarbonyl chloride and
(-)-(S)-2,2'-Dichloro-6,6'-dimethylbiphenyl-4,4'-dicarbonyl chloride

R	R' = NO ₂	R' = Cl
	POA PMA PPA	— — —
	Model A I	—
	—	PIPB
	DMPA	DMPB
	PDA	PDB
	Model A II	Model B

Since the method for preparation of these monomers described in the literature^{2,7} gave poor yields, we decided to improve the overall yield by using a modified procedure, which is described in a separate paper.¹

The ORD, CD, and ultraviolet spectra of the optically active aromatic polyamides were taken in trimethyl phosphate (TMP), tributyl phosphate (TBP) and methanesulfonic acid. In these solvents we were able to observe the beginning of a Cotton effect (ORD), which we believe is associated with the $n-\pi^*$ and $\pi-\pi^*$ transition of the amide chromophore.

Recently, Steigman and co-workers⁸ studied the behavior of poly(γ -ethyl L-glutamate) and its model diamide in strong acid-water mixtures. They were able to show, by CD measurements, that the polymer was in the coil conformation in methanesulfonic acid and sulfuric acid solutions. The addition of water produced the α -helical form of the polymer. In a later publication, Steigman and co-workers⁹ also showed that poly(γ -ethyl L-glutamate) exists in the coil conformation in dichloroacetic acid solution because of strong solvation rather than protonation. The coil-to-helix transition could be observed by using several cosolvents. The order of decreasing efficiency of these cosolvents in effecting the transition was: triethylamine > acetic acid \simeq methanol > water \simeq nitrobenzene > nitroethane > formic acid > carbon tetrachloride. The hypothesis was made that dichloroacetic acid in the liquid phase consists of monomers, cyclic dimers, other cyclic forms and open-chain polymers and that the order of the cosolvents represented the abilities of the various donors to form hydrogen bonds with either dichloroacetic acid monomeric molecules or with the nonhydrogen-bonded terminal carboxyl group of an open-chain solvent polymer. In either event, a shift in solvent polymer-dimer-monomer proportions would take place, reducing the concentration of the chain polymer, and reducing the solvation of the peptide groups of the polymer.

RESULTS AND DISCUSSION

Optical Rotatory Properties of the Aromatic Polyamides and the Model Compound from

(-)-(S)-2,2'-Dinitro-6,6'-Dimethylbiphenyl-4,4'-Dicarbonyl Chloride

The ORD and CD curves of the model compound, AI, in trimethyl phosphate (TMP) are shown in Figure 1.

There are four Cotton effects: two negative ones centered around 305 and 260 $m\mu$, and two positive ones centered around 282 and 230 $m\mu$. The positive CD maximum at 231 $m\mu$ corresponds to an ultraviolet maximum at 235 $m\mu$, and two Cotton effects of opposite signs centered at 282 and 260 $m\mu$ are related to an ultraviolet inflection at about 270 $m\mu$ and a negative CD maximum at 305 $m\mu$ corresponds to another ultraviolet inflection at 310 $m\mu$.

The ultraviolet spectrum of nitrobenzene contains the maximum at 255 $m\mu$ and an apparent inflection at 305 $m\mu$, whereas 2,2'-dinitrophenyl

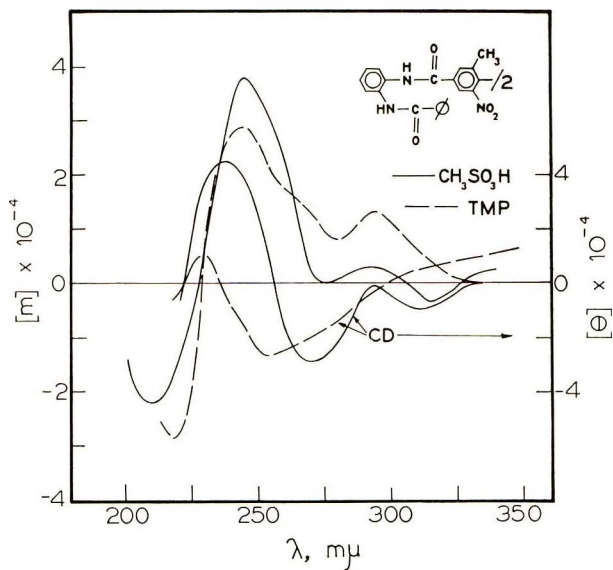


Fig. 1. ORD and CD spectra of the model compound, AI, in trimethyl phosphate and methanesulfonic acid.

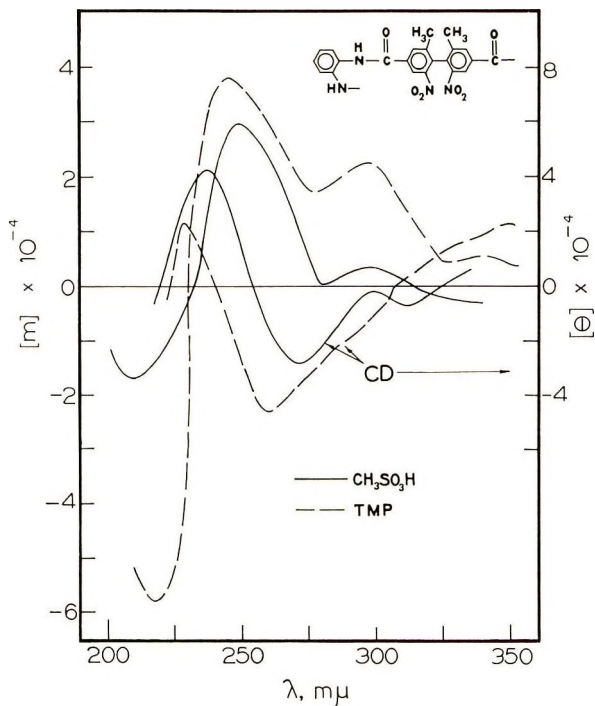


Fig. 2. ORD and CD spectra of the POA polymer in trimethyl phosphate and methanesulfonic acid.

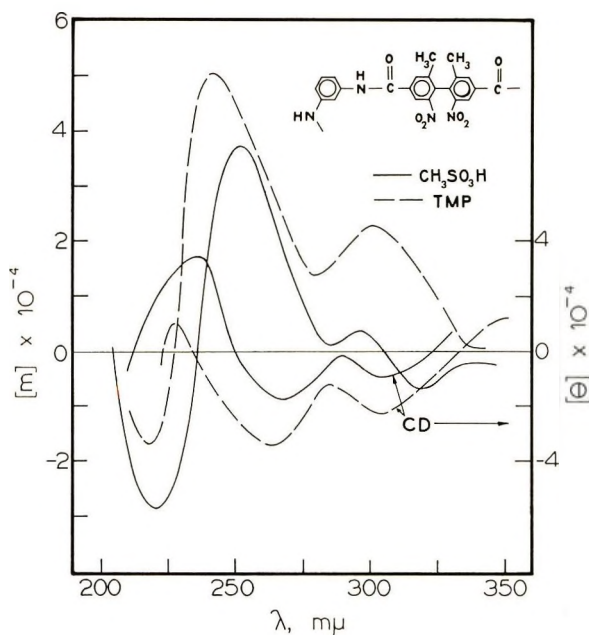


Fig. 3. ORD and CD spectra of the PMA polymer in trimethylphosphate and methanesulfonic acid.

has shown the maximum at 257 $m\mu$ and no such an inflection at all.¹⁰ Mislow et al.^{11,12} have found that optically active 2,2'-dinitro-6,6'-dimethylbiphenyl exhibits two Cotton effects of opposite signs at 260 and 330 $m\mu$. They estimated that the effect at 260 $m\mu$ corresponds to the $\pi-\pi^*$ transition of the nitrobenzene B-band which is a formally forbidden band in a symmetrical aromatic system. They also assigned another masked nitrobenzene transition near 330 $m\mu$, which does not appear in the ultraviolet spectrum. Recently, Schulz and Jung^{3,4} have found similar optical rotatory phenomena in the studies of the ethyl and polyvinyl esters of (+)-2-methyl-6-nitrophenyl-2'-carboxylic acid.

Although the CD extremum at 330 $m\mu$ is not observed in Figure 1, some evidences of the positive extremum are shown in the figures of the polyamides. The ORD tail and CD in the far-ultraviolet region indicate that there is another Cotton effect centered at around 210 $m\mu$.

The ORD and CD curves of the polyamide (POA) in TMP are shown in Figure 2. There are noticeable differences between the curves of the polyamide (POA) and those of its model compound. The former shows a marked enhancement of rotatory strength and red-shifted absorption bands in both ORD and CD spectra, although there is no particular difference in their ultraviolet spectra.

The spectra of the polyamide (PMA) in TMP are shown in Figure 3. A comparison between this polymer (PMA) and POA reveals that the ORD spectrum of the POA polymer is red-shifted with respect to that of PMA.

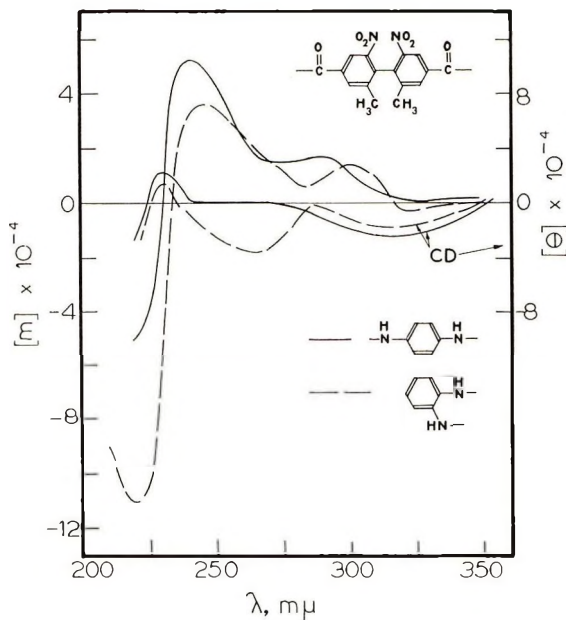


Fig. 4. ORD and CD spectra of the POA and PPA polymers in tributyl phosphate.

The most noticeable difference in their ultraviolet spectra (not shown) is that the broad shoulder evident in the POA spectrum becomes a distinguishable ultraviolet maximum at 272 $m\mu$ in the PMA polymer, together with a shift of the negative CD maximum from 260 to 265 $m\mu$.

The ORD and CD curves of the polyamides derived from *o*-phenylenediamine (POA) and *p*-phenylenediamine (PPA) in tributyl phosphate are shown in Figure 4. Here again, the former polyamide is slightly red-shifted in the ORD spectrum. The ultraviolet spectrum of the polyamide PPA shows two independent absorption maxima at 235 and 315 $m\mu$. Similarly, the CD spectrum shows two Cotton effects of opposite signs, a positive one centered at 230 $m\mu$ and a negative one at 315 $m\mu$.

It is summarized that the polyamide (POA) shows a noticeable enhancement of rotatory strength and red-shifted absorption bands compared with that of the model compound, AI, when TMP is the solvent used. The ultraviolet spectra of the polymers show the appearance of another maximum in addition to the original one at about 235 $m\mu$; the shoulder at 260 $m\mu$ in the polymer POA, and maxima at 272 and 315 $m\mu$ in the polymers PMA and PPA, respectively. At the same time, the negative CD maximum is moved from 260 to 265 and 315 $m\mu$, respectively. The rotatory strength of the strongest band of the polymer is enhanced, to some extent, upon changing the diamine component from *o*- to *m*- and *p*-phenylenediamine. According to the nature of the diamine component of the polyamide (*p*-, *m*-, or *o*-phenylenediamine), the negative CD maximum at about 265 $m\mu$ appears and increases in rotational strength as the intensity of another negative maximum at about 310 $m\mu$ decreases.

In order to study the behavior of these polyamides in a stronger polar medium in which the polymers are expected to be in a random coil conformation, we decided to use methanesulfonic acid as the solvent.

Beforehand, one can predict that if all polymers exist in a random conformation in the TMP and TBP solvents, no major changes, caused by a helix-coil transition in the ORD, CD, and ultraviolet absorptions of these polymers will occur in the methanesulfonic acid solution, except for the expected changes due to the change in the solvent. These effects (solvation or some protonation of the amide) are, however, expected to be similar for all polymers and model compounds.

The ORD and CD curves for the model compound, AI, in methanesulfonic acid are shown in Figure 1. A red shift in the ultraviolet from 235 to 251 $m\mu$ was observed. This shift in ultraviolet band is due to both protonation and medium effects.⁸ A red shift in the ORD and CD absorptions was also observed. A negative CD band, centered at 313 $m\mu$ appeared; this band was not present in the spectra taken in TMP. An increase in the molar ellipticity of the CD band centered at 238 $m\mu$ ($\Delta[\theta] = 35,000$) took place.

The ORD and CD curves for the polyamide POA in methanesulfonic acid are shown in Figure 2. A large decrease in the molar rotation ($\Delta[m] = 42,000$ in TMP and $\Delta[m] = 94,000$ in TBP) of the ORD trough centered at 218 $m\mu$ took place when methanesulfonic acid was used. At the same time, an increase in the molar ellipticity and a red shift of the CD maximum centered at 231 $m\mu$ took place ($\Delta[\theta] = 30,000$ in TMP and $\Delta[\theta] 25,000$ in TBP). A red shift in the ultraviolet maximum from 236 $m\mu$ to 245 $m\mu$ and the appearance of a new peak in the CD spectrum, centered at 313 $m\mu$, were also observed.

The ORD and CD curves for the polymers PMA and PPA in methanesulfonic acid are shown in Figures 3 and 5. A decrease in the intensity of the ORD curves, a red shift in the ultraviolet maximum were observed in both polyamides. A new CD absorption centered at 271 $m\mu$ appeared in the spectrum of the polyamide PPA.

In brief, the following changes in the spectra of these polyamides and model compounds could be observed when methanesulfonic acid was used instead of trimethyl phosphate and tributyl phosphate: a red shift and decrease in the absorptions of the ultraviolet band at 235–236 $m\mu$ of all polymers (in the case of the model compound, an increase in the ultraviolet absorption was observed instead); a decrease in the intensity of the ORD peaks at 238–245 $m\mu$ of all polymers; a decrease in the CD peak at 238 $m\mu$ of all compounds. The most remarkable result was observed in the ORD spectrum of the polyamide POA, in which a drastic decrease in the ORD trough occurred at 218 $m\mu$.

The red shift in the ultraviolet maximum of all compounds could be explained by solvation in the stronger dielectric medium and by some protonation of the amide. However, the fact that an increase in the ultraviolet coefficients of the model while a decrease in the ultraviolet coefficients

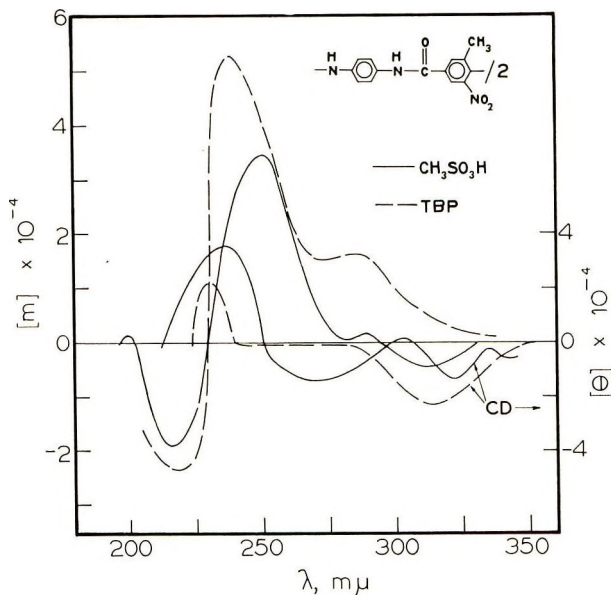


Fig. 5. ORD and CD spectra of the PPA polymer in tributyl phosphate and methanesulfonic acid.

for all polymers took place, is still open to discussion. In general, a red shift and increase in the ultraviolet coefficients are a common rule for the behavior of amides in strong acidic medium.⁸

The large decrease in the molar rotation of the ORD trough, centered at 218 $m\mu$, of the polyamide POA, in comparison with the other compounds, can be explained in terms of relative rigidity or flexibility of a polymer chain. If a polymer is composed of conformationally rigid monomer units, portions of the polymer chain will have a fixed molecular geometry. This allows the coupling of identical chromophores to take place, with consequent enhancement of the rotatory strength.¹³ In the case of polyamides, with dipoles aligned in the same direction, one also expects to observe for the amide band, some of the features displayed by polypeptides in the helical form: high rotatory strength, splitting of $\pi-\pi^*$ transition, and shifts of ultraviolet bands.¹⁴ On the other hand, if the polymer backbone is somewhat flexible, allowing several conformational arrangements, the effects mentioned above should be minimized, and eventually loss of intensity because of different geometrical dispositions along the chain should be observed. Scale models of the POA polymer indicate that its most stable conformation may be an ordered structure which may allow the amide chromophores to couple. On the other hand, models of the PMA and PPA polymers indicate that they should exist in extended forms in which each amide chromophore may be randomly ordered.

We suggest that the ORD trough centered at 218 $m\mu$ is associated with an $n-\pi^*$ transition of the amide chromophore; hence the large molar rota-

tion of the ordered POA polymer is observed. Since the PMA and PPA polymers exist in a random conformation in TMP and TBP, no such large change in their molar rotations is observed when a more polar solvent is employed.

Optical Rotatory Properties of the Polyamides and the Model Compound Derived from (–)-(*S*)-2,2'-Dinitro-6,6'-Dimethylbiphenyl-4,4'-Dicarbonyl Chloride and Cyclic Diamines

The ORD and CD curves for these polyamides are shown in Figures 6 and 7. There are five Cotton effects: Three negative ones centered around 305, 265 and 205 $m\mu$, and two positive ones centered around 285 and 230 $m\mu$. The positive CD maximum at 225 $m\mu$, and two Cotton effects of opposite signs centered at 285 and 265 $m\mu$ are related to an ultraviolet inflection at about 290 $m\mu$. The magnitude of the optical rotation of these compounds in TFE was of the same order of that obtained from the above-mentioned aromatic polyamides taken in methanesulfonic acid. No noticeable change could be detected in the ORD, CD, and ultraviolet absorptions of the PDA and DMPA polyamides in comparison with the spectra of the model compound AII. These results indicated that the most probable conformation of these polymers in TFE solution is a random coil.

Trifluoroethanol is known to stabilize poly-L-proline II in solution, by hydrogen bonding with the amide carbonyl, while pyridine stabilizes poly-

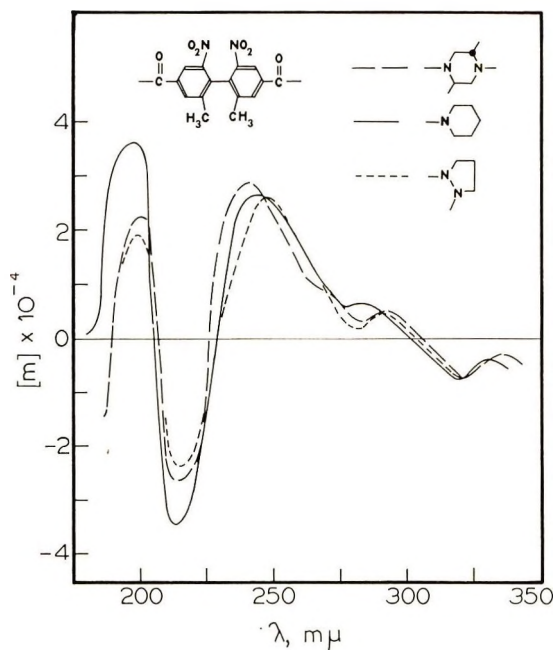


Fig. 6. ORD spectra of the DMPA and PDA polymers and the model compound AII in trifluoroethanol.

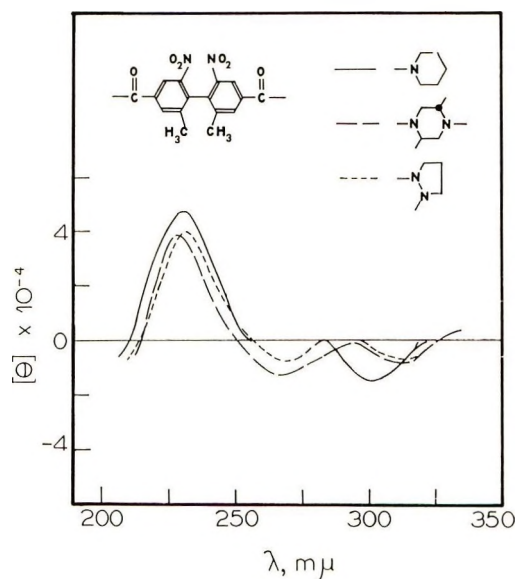


Fig. 7. CD spectra of the DMPA and PDA polymers and the model compound AII in trifluoroethanol.

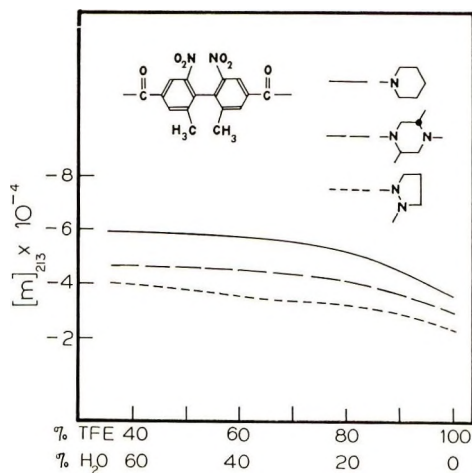


Fig. 8. Variation of the molar rotation of the ORD trough centered at 213 $m\mu$ with the mole fraction of trifluoroethanol in water.

L-proline I.¹⁵ The interaction of proteins in water-organic solvent mixtures has been recently investigated, and preferential binding of either one or the other solvent has been recognized.^{16,17}

In order to study the solvation effect of TFE upon these polyamides, we decided to add a nonsolvent into these solutions and measured the variation of the molar rotation of the ORD trough centered at 213 $m\mu$ with the mole fraction of TFE. The results are shown in Figure 8. An increase in the

rotation of these compounds was observed, but no unequal behavior for the polymers in comparison with the model could be found. At a concentration lower than 35% TFE the polymers precipitated. In brief, we can conclude that the polymers derived from *trans*-2,5-dimethylpiperazine and 1,2-pyrazolidine also exist in a random-coil conformation in a trifluoroethanol-water mixture.

Optical Rotatory Properties of the Polyamides and the Model Compound Derived from (–)-(*S*)-2,2′-Dichloro-6,6′-Dimethylbiphenyl-4,4′-Dicarbonyl Chloride and Cyclic Diamines

In order to further characterize the exact position and type of the amide absorptions in the polyamides above described, we decided to prepare some

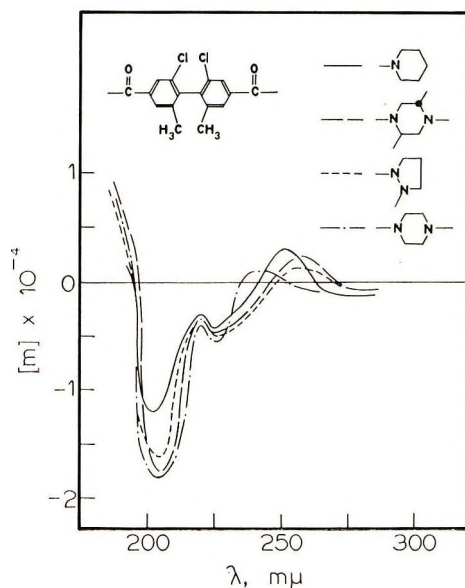


Fig. 9. ORD spectra of the PIPB, DMPB, and PDB polymers and the model compound B in trifluoroethanol.

polyamides and a model compound derived from (–)-(*S*)-2,2′-dichloro-6,6′-dimethylbiphenyl-4,4′-dicarbonyl chloride in which the chloro atoms replaced the nitro groups.

The ORD and CD curves for these polyamides are shown in Figures 9 and 10. There are four Cotton effects: three negative ones centered around 272, 225, and 205 $m\mu$ and one positive centered around 245 $m\mu$. The CD maximum at 241 $m\mu$ corresponds to an ultraviolet maximum at 245 $m\mu$. Mislow et al.¹¹ have found that optically active 2,2′-dichloro-6,6′-dimethylbiphenyl exhibits two Cotton effects of opposite signs at 255 and 270 $m\mu$.

The ultraviolet bands of the polymers were red-shifted in comparison with those of the model compound.

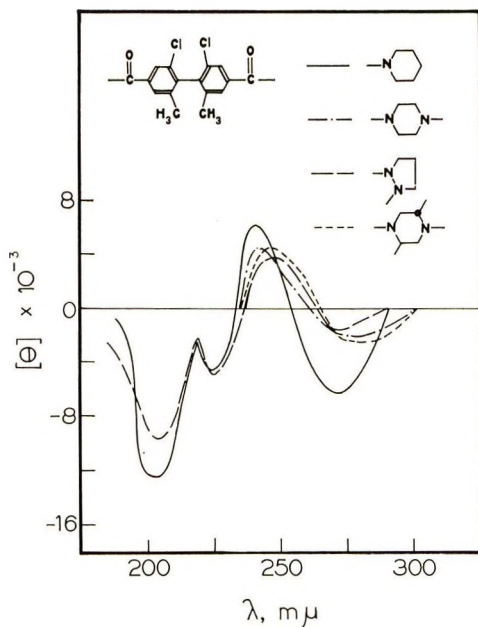


Fig. 10. CD spectra of the PIPB, DMPB, and PDB polymers and the model compound B in trifluoroethanol.

The position of the ORD troughs around 205 $m\mu$ in these polyamides confirmed our previous assignments of an amide absorption for these troughs (beginning of a Cotton effect resulting from an $n-\pi^*$ transition).

The magnitude of the optical rotations of these polyamides and the model compound was the same. No data could be found to support the existence of an ordered structure for any of the polyamides in solution of trifluoroethanol at room temperature.

One of us (ASG) expresses appreciation to the Conselho Nacional de Pesquisa do Brasil and Macromolecular Research Center of The University of Michigan for support of this work. The authors are also grateful for financial support by the U. S. Army, Research Office-Durham, under Grant DAHCO4-69-C-0050.

References

1. C. G. Overberger, T. Yoshimura, A. Ohnishi, and A. S. Gomes, *J. Polym. Sci. A-1*, **8**, 2275 (1970).
2. C. G. Overberger and T. Yoshimura, paper presented at IUPAC Symposium, Tokyo, 1966; Preprint 2.3.02.
3. R. C. Schulz and R. H. Jung, *Makromol. Chem.*, **96**, 295 (1966).
4. R. C. Schulz and R. H. Jung, *Angew. Chem.*, **79**, 422 (1967); *Angew. Chem. Internl. Ed.*, **6**, 461 (1967).
5. R. C. Schulz and R. H. Jung, *Makromol. Chem.*, **116**, 190 (1968).
6. R. C. Schulz, private communication.
7. H. Mix, *Ann.* **592**, 146 (1955).
8. J. Steigman, E. Peggion, and A. Cosahi, *J. Amer. Chem. Soc.*, **91**, 1822 (1969).

9. J. Steigman, A. S. Verdini, C. Montagner, and L. Strasorier, *J. Amer. Chem. Soc.*, **91**, 1829 (1969).
10. B. Williamson and W. H. Rodebush, *J. Amer. Chem. Soc.*, **63**, 3018 (1941).
11. K. Mislow, M. A. W. Glass, R. E. O'Brien, P. Rutkin, D. H. Steinberg, J. Weiss, and C. Djerassi, *J. Amer. Chem. Soc.*, **84**, 1455 (1962).
12. K. Mislow, E. Bunnenberg, R. Records, K. Wellman, and C. Djerassi, *J. Amer. Chem. Soc.*, **85**, 1342 (1963).
13. M. Kasha, *J. Radiation Res.*, **20**, 55 (1963).
14. J. T. Yang, in *Poly- α -Amino Acids*, G. D. Fasman, Ed., Dekker, New York, 1967.
15. H. Strassmair, J. Engel, and G. Zundel, *Biopolymers*, **8**, 237 (1969).
16. H. Inoue, *J. Amer. Chem. Soc.*, **90**, 1890 (1968).
17. G. Conio and E. Patrone, *Biopolymers*, **8**, 57 (1969).

Received June 11, 1970

Revised October 14, 1970

Kinetics of Vinyl Acetate Emulsion Polymerization

PETER HARRIOTT, *School of Chemical Engineering,
Cornell University, Ithaca, New York 14850*

Synopsis

The emulsion polymerization of vinyl acetate has generally been considered a special type of reaction that is not covered by the Smith-Ewart theory. Although the number of particles depends on coalescence rates and can not be predicted by this theory, the polymerization rate data are consistent with the general concepts of Smith and Ewart, including reaction primarily inside swollen polymer particles, escape of radicals from particles, and termination of chains inside the particles. Allowing for rapid exchange of radicals following chain transfer leads to a simple equation which fits much of the published data for cases of both very low and very high values of \bar{n} , the average number of radicals per particle.

$$r_p = k_p[M]_p(2k_d[I]_wV_wV_p/k_t)^{1/2}$$

Background

The emulsion polymerization of vinyl acetate does not follow the simplest form of the Smith-Ewart theory,¹ which predicts that the polymerization rate is proportional to the number of particles, with each particle having a free radical about half of the time. In the batch tests by Patsiga et al.,² the particle concentration N was varied three fold by using different amounts of seed particles, and the polymerization rate was almost unchanged. In similar tests by Netschey and Alexander,³ N was varied 130-fold with at most a twofold increase in the rate of reaction. Other authors^{4,5} have changed N by varying the emulsion stability and have found about the same maximum rate, except when N was very low and the particles very large. In the recent study of semi-batch polymerization by Gulbekian,⁶ N varied from 10^{16} to 2×10^{18} particles per liter, and the rate actually decreases as N increased, as shown by an increasing level of unreacted monomer at the end of the feed period.

Further evidence of abnormal kinetics comes from the effects of initiator [I] and emulsifier concentration [E], but the results must be examined carefully to separate the effects on N and on the rate per particle. One form of the Smith-Ewart equation predicts that N and the polymerization rate vary with $[I]^{0.4}[E]^{0.6}$. In some studies the rate did vary with a fractional power of [I], yet measurements showed that N was constant, so such results would not support the Smith-Ewart theory even if the exponent were close to 0.4. For typical recipes, N varies with the 1 to 3 power of emulsifier concentration, yet the reaction rate is nearly the same, sometimes increasing

and sometimes decreasing. Many of these studies are reviewed by Lindemann.⁷

Because of the small or zero effect of N on rate, some authors^{2,6} concluded that polymerization takes place mainly in the aqueous phase, and they cited the moderate solubility of vinyl acetate in water (3% at 50°C) as an explanation. Dunn and Chong⁸ could not explain their results by either an aqueous-phase or a polymer-phase reaction and suggested that Medvedev's theory⁹ of a surface reaction might apply. Napper and Parts,¹⁰ working with dilute emulsions of large particles, explained their results by assuming reaction in swollen particles, with more than one radical per particle, which is case 3 of the Smith-Ewart theory. However no general treatment has been proposed which explains the effects of reaction variables for small and large particle emulsions.

In this paper, published rate data are compared with the cases considered by Smith and Ewart, including case 1, for which the particles have a radical less than half of the time. The Smith-Ewart theory of particle formation is not examined, since it obviously does not apply to vinyl acetate. In a typical vinyl acetate polymerization, a large number of particles are formed in a short time even when micelles are absent, but the final number is determined by stabilizer concentration and other factors affecting coalescence.⁵

Polymerization in the Water Phase

The initial rate of polymerization in the water phase r_{p_w} can be estimated from the normal equation for solution polymerization [eq. (1)], assuming initiating and termination of radicals only in the water,

$$r_{p_w} = k_p[M]_w(2k_d[I]_w/k_{t_w})^{1/2} \quad (1)$$

where k_p , k_d , k_t are rate constants for propagation, initiator decomposition, and termination, respectively; $[M]_w$ and $[I]_w$ are the concentrations of monomer and initiator, respectively, in the water phase. As shown by Dunn and Taylor,⁵ eq. (1) gives a propagation rate about one twentieth of the maximum rate observed for a 2% solution of vinyl acetate. After polymer particles are formed, partition of radicals between the phases decreases the radical concentration in the water, and the predicted reaction rate in the water phase is even smaller. The rate is also lowered by the decrease in monomer concentration, and the rate in the water phase may be less than 1% of the measured rate at 50% conversion. While this is strong evidence against a significant water phase reaction, the calculation was based on the rate constants for bulk polymerization, $k_p = 3000$ and $k_t = 2.5 \times 10^7$ l./mole-sec. The rate constants might be different in a poor solvent such as water, though an order of magnitude error in the rate seems unlikely.

Experimental evidence for a negligible reaction in the water phase is the large increase in rate as the volume of polymer phase increases. This increase is most evident for runs starting with a 1-3% homogeneous solution.

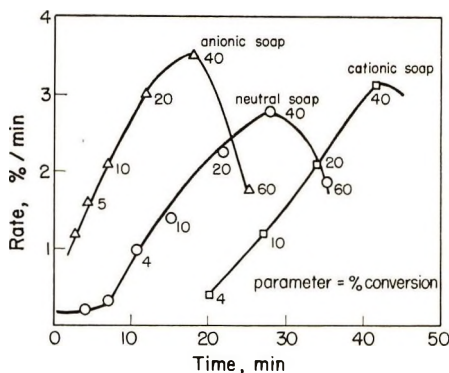


Fig. 1. Rate of polymerization in dilute emulsions $[\text{VAC}]_0 = 0.33M$, 40°C , $0.015M$ $\text{K}_2\text{S}_2\text{O}_8$; data of Napper and Alexander.⁴

Some data taken from Napper and Alexander are shown in Figure 1, and similar results were obtained by other workers.^{3,5,10} The reaction rate is small for a few minutes and then increases as polymer molecules precipitate to form a polymer phase. The initial rate of 1×10^{-5} mole/l.-sec (0.2% /min) with a neutral soap is about that predicted for aqueous-phase reaction from eq. (1). The rate increases until 40–50% conversion and then decreases, as the effect of reduced monomer concentration offsets that of increased polymer volume. The prolonged increase in rate is quite different from an induction period. When impurities are present in other polymerizations, the rate goes from zero to a maximum value in a very short time. When oxygen is present in vinyl acetate solution, there is an induction period, but the conversion–time curve still has the pronounced sigmoidal shape, with a maximum rate at about 40% conversion.⁵

In the polymerization of concentrated emulsions (20–30% VAc), the reaction starts in the water phase, and the rate must increase manyfold as the polymer phase grows. However the volume of the polymer phase is a maximum at only 14% conversion, when the monomer phase disappears, and it is more difficult to separate an increase in rate in this interval from an induction period. The data of Patsiga^{11,12} for 25% emulsions show nearly constant rates from about 15 to 85% conversion, and the maximum rates are 300–400 times those predicted from eq. (1) for water-phase polymerization.

Equilibrium Theory for Reaction in the Polymer Phase

The rate of polymerization in the polymer phase r_p , is assumed to follow the standard equation:

$$r_p = k_p[M]_p\bar{n}N/N_A \quad (2)$$

where $[M]_p$ is the monomer concentration in the polymer phase and N_A is Avogadro's number. The value of \bar{n} , the average number of free radicals per particle, is the major uncertainty in eq. (2). Applying this equation

to published data gives values of \bar{n} from 0.02 to 60 for different conditions. In studies where N was varied, \bar{n} varied nearly inversely with N . A value of $1/2$ for \bar{n} , as predicted for case 2 of the Smith-Ewart theory, occurs only by coincidence, and the more complex treatment of cases 1 and 3 must be considered.

The high values of \bar{n} are consistent with case 3, where all radicals formed in the water enter the particles, no radicals diffuse out, and particles are large enough to have more than one radical at a time. Various solutions of the recursion formula of Smith and Ewart have been presented for the region $n = 1/2$ to $n = 4$,^{13,14} but a simpler solution holds for larger values of \bar{n} . With several radicals per particle, the number of radicals per unit volume would be about the same for different particles, and simple second-order termination kinetics would apply. The rate of initiation in the water phase is set equal to the rate of termination in the polymer phase, and the polymerization rate per liter of emulsion is proportional to the volume fraction of polymer phase, V_p :

$$2k_d[I]_w V_w = k_{t_p}[R^\cdot]_p^2 V_p \quad (3)$$

$$r_p = k_p[M]_p[R^\cdot]_p V_p \quad (4)$$

$$r_p = k_p[M]_p(2k_d[I]_w V_w V_p/k_{t_p})^{1/2} \quad (5)$$

Here $[R^\cdot]$ is the radical concentration. Since eq. (2) still applies, \bar{n} varies inversely with N .

$$\bar{n} = (N_A/N)(2k_d[I]_w V_w V_p/k_{t_p})^{1/2} \quad (6)$$

The low values of \bar{n} indicate that radicals can diffuse out of the particles quite readily, which is plausible for radicals of low molecular weight. The relatively rapid chain transfer to vinyl acetate provides a source of such radicals. At 60°C with $[M]_p = 6$, $k_p = 3700$ l./mole-sec, and a rate constant for chain transfer to monomer $C_M = 2.5 \times 10^{-4}$, a growing chain adds monomer at the rate of 22,000 molecules/sec, and transfer to monomer occurs after 4000 units or 0.18 sec, on the average. A new vinyl acetate radical might add a monomer molecule to start a chain after 1/22,000 sec, but in this interval it might instead diffuse out of the particle. The mean displacement is $\sqrt{2Dt}$ or 1000 Å in 5×10^{-5} sec for a diffusivity $D = 10^{-6}$ cm²/sec and 300 Å for $D = 10^{-7}$ cm²/sec. As the radical adds monomer molecules, it will diffuse more slowly, but it still has a good chance of leaving the particle until several molecules have been added.

The escape of radicals from particles is considered in case 1 of the Smith-Ewart theory, but the equations are complex and require estimates of diffusion rates. A simpler solution can be written for the limiting case when diffusion of radicals in and out of the particles is rapid enough to establish an equilibrium between the water phase and the polymer phase and between the different polymer particles. Then the number of contacts between radicals would be the same as if all the polymer were in one mass, and the termination rate per liter of emulsion would be $k_{t_p}[R^\cdot]_p^2 V_p$, as for

suspension polymerization. Note that the radical concentration $[R^\cdot]_p$ is based on the total number of radicals and the total volume of polymer phase, and the termination rate would be independent of particle size, even though \bar{n} would be much less than $1/2$ for large values of N . Since the termination rate is the same as given in eq. (3), eq. (5) would then apply to low or intermediate values of \bar{n} as well as high values. Therefore the more general basis for eq. (5) is an equilibrium distribution of radicals which will be called the equilibrium theory in further discussion.

Although small radicals can diffuse in and out of particles readily, the large radicals cannot do so, both because of a lower diffusion rate and because of a higher distribution coefficient in favor of the polymer phase. For vinyl acetate radicals, the distribution constant K would probably be about the same as for vinyl acetate, which is 30 at 40°C.¹⁰ Oligomeric radicals would have a higher K , and radicals with more than about 50 monomer units would probably always stay in the polymer phase. (Priest¹⁵ found that polymer started to precipitate from the aqueous phase when the degree of polymerization was 53.) Since all but a few of the radicals have more than 50 units and are therefore confined inside particles, the equilibrium assumption and the mechanism of termination must be examined more carefully. With small values of \bar{n} , the main termination reaction may occur between a large radical trapped in a particle and a small, rapidly diffusing radical, but several small radicals may diffuse in and out of a growing particle before termination occurs. The termination rate is then proportional to the number of large radicals per liter of emulsion and to the equilibrium concentration of small radicals in the polymer phase, which is a small fraction α of the total radical concentration.

$$r_t = k_{t_p}(\alpha[R^\cdot]_p)V_p(1 - \alpha)[R^\cdot]_p \cong \alpha k_{t_p}[R^\cdot]_p^2 V_p \quad (7)$$

Equation (7) implies a lower termination rate than normal because α is small, but termination in bulk polymerization may also be largely between small and large radicals because of the difference in mobility, and perhaps published values of k_t really include α . Therefore the α is omitted, which leads back to eq. (5) as the proposed rate equation for the equilibrium theory.

Additional termination in the water phase can be allowed for by adding a term to eq. (3)

$$2k_d[I]_w V_w = k_{t_p}[R^\cdot]_p^2 V_p + k_{t_w}[R^\cdot]_w^2 V_w \quad (8)$$

$$[R^\cdot]_p = K_{ave}(R^\cdot)_w \quad (9)$$

$$r_p = k_p[M]_p V_p \left\{ 2k_d[I]_w V_w / [k_{t_p} V_p + (k_{t_w} V_w / K_{ave}^2)] \right\}^{1/2} \quad (10)$$

For vinyl acetate, K_{ave} is probably greater than 1000, which would make termination in the water phase negligible, even though k_{t_w} might be much greater than k_{t_p} . The last term in eq. (8) might be significant for more soluble polymers or when chain transfer has an even stronger effect in limiting the size of growing radicals. If the major termination is in the water

phase, the reaction rate in the polymer phase would vary with the first power rather than the square root of V_p .

Diffusion Effects

The transfer of radicals from the water phase, where they are formed, to the polymer phase, where most of them terminate, requires external and internal concentration gradients. The following example shows that both driving forces should be small for particles as large as 5000 Å. For polymerization at 60°C with $V_p = 0.2$, $[K_2S_2O_8] = 10^{-3}$, and $k_{t_p} = 2 \times 10^6$, the equilibrium radical concentration from eq. 3 is $[R^\cdot]_p = 4.3 \times 10^{-7}$. For particles 5000 Å in diameter, with $D = 10^{-5}$ cm²/sec, and the mass transfer coefficient $k_c = 2D/d = 0.4$ cm/sec (where d is particle diameter), the external driving force required for transfer of all radicals to the polymer particles is 1.5×10^{-12} mole/l., which is negligible. When the particles are surrounded by a 200 Å layer of surfactant molecules¹⁶ in which D might be 10^{-6} cm²/sec, the extra resistance only doubles the required driving force, which is still negligible.

The diffusion rate of radicals in the viscous polymer phase is more likely to be important. The problem is similar to that of diffusion plus reaction in porous catalysts, but the net flux of radicals into the particles is fixed, and the diffusion resistance changes the radical concentration gradient rather than the rate of termination. For very large particles, there would be high values of $[R^\cdot]_p$ near the outside of the particle, low values near the center, and a lower average value of $[R^\cdot]_p$, which would give a lower polymerization rate. The diffusion modulus ϕ for this case is based on the termination rate constant and the estimated radical concentration at the particle surface.

$$\phi = d/2(k_{t_p}[R^\cdot]_0/D)^{1/2} \quad (11)$$

For the example cited with $d = 5000$ Å, $[R^\cdot]_0 = 4.3 \times 10^{-7}$, and $D = 10^{-8}$ cm²/sec, $\phi = 0.23$, which means a negligible gradient.¹⁷ However, D for polymer radicals might be as low as 10^{-9} cm²/sec, which would make ϕ close to the critical value of 1, where the gradient becomes significant. For particles larger than 5000 Å or for very high rates of initiation, a decrease in rate with particle diameter might be expected. Dunn and Taylor⁵ did find low reaction rates when an electrolyte was added to promote particle coalescence, but the particle size was not reported.

Tests of the Equilibrium Theory

The equilibrium theory predicts that the polymerization rate varies with the square root of the volume of polymer phase if the total charge of initiator is constant ($[I]_w V_w$ constant). In Patsiga's study of seeded polymerization at 60°C,¹¹ the rate varied with the 0.35 power of the volume of organic phase added, over the range 10–50 parts of organic per 100 parts of water. This is further proof that the reaction takes place in the polymer phase, and the exponent is not far from the predicted value of 0.5.

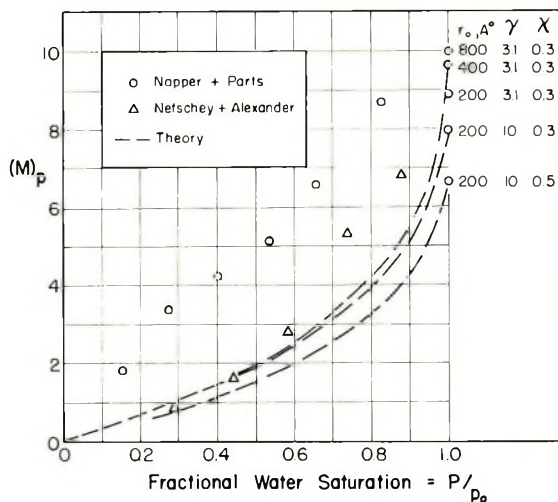


Fig. 2. Monomer concentration in polymer particles.

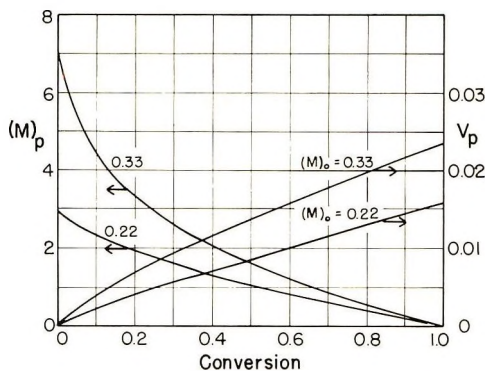


Fig. 3. Volume of polymer phase and monomer concentration for dilute emulsions.

Another check on the effect of V_p can be obtained from the studies of very dilute emulsions, where V_p increases with conversion. However the volume of polymer phase must be calculated allowing for partial swelling of the particles in an unsaturated water solution. Figure 2 shows values of monomer concentration in the polymer phase calculated by using eq. (5) of Gardon.¹⁸ For a saturated solution, there is a significant effect of particle size, but for $P/P_0 < 0.9$, the curves for 200 and 800 \AA particles are practically identical. The upper dashed line is based on an interfacial tension γ of 3.1 dynes/cm and an interaction parameter χ of 0.3, values given by Vanzo et al.¹⁹ The lower lines were included to show the slight effect of γ and the stronger effect of χ on the swelling. The experimental data of Netschey and Alexander²⁰ seem acceptable except near $P/P_0 = 0.8$, but those of Napper and Parts¹⁰ are much too high and would correspond to negative values of χ . The calculated values of V_p and $[M]_p$ in Figure 3

are based on the theoretical line in Figure 2 for 400 Å particles. The monomer and polymer volumes are assumed additive with a density ρ of 0.93 g/cm³ and 1.21 g/cm³, though the measured contraction is only 16%.⁵

By using the values of V_p and $[M]_p$ from Figure 3, the rate data of Napper and Alexander were replotted as shown in Figure 4. For the small (800 Å) and medium (2000 Å) particles formed with anionic or neutral soaps, the rate divided by $\sqrt{V_p}$ is nearly constant until the monomer concentration is less than 2. For cationic soaps ($d \cong 5000$ Å) the initial rates are lower, but the maximum rate is about the same. Similar results were obtained in recent work by Netschey and Alexander,³ who used different seed concentrations to vary the particle size. The maximum rate was about the

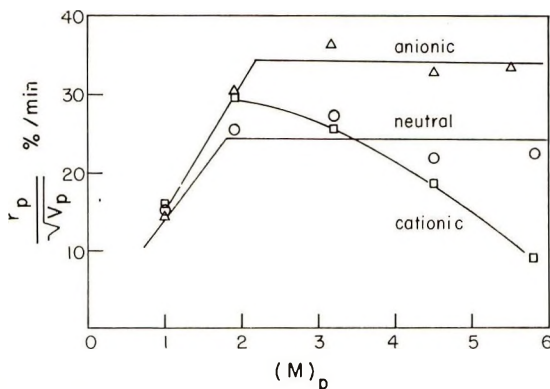


Fig. 4. Polymerization in dilute emulsions: data from Fig. 1.

same for 480 Å particles as for 4220 Å particles, though the initial rate was lower with larger particles. The lack of a particle size effect on maximum rate is good evidence for the equilibrium theory, even though the lower initial rates for large particles are not explained. If the reaction were confined to the particle surface, the rates would have been inversely proportional to particle size.

Since the rate depends on $V_p^{1/2}$ and V_p is almost proportional to the conversion for dilute emulsions (see Fig. 3), the square root of the conversion x should be approximately proportional to the reaction time.

$$dx/dt = kV_p^{1/2} \cong k'x^{1/2} \quad (12)$$

$$x^{1/2} \cong 1/2k't \quad (13)$$

Napper and Parts¹⁰ derived this equation as a limiting case for large particles with large values of \bar{n} , but their data show that it holds for small particles as well. The square-root relationship only held to a certain conversion, which ranged from 50 to 20% with decreasing monomer concentration; these critical conversions correspond to a monomer concentration of 1.4 ± 0.2 , in agreement with the breakpoint in Figure 4. For concentrated emulsions, the rate is constant to about 85% conversion or $[M]_p = 2$. The reac-

tion is assumed to be first-order to monomer, and the apparent zero-order reaction down to $[M]_p \cong 2$ is explained as a compensating decrease in termination rate as the viscosity of the polymer phase increases.

The polymerization of dilute solutions was also studied by Dunn and Taylor,⁵ who worked at 60°C and reported only the maximum rate of reaction for most runs. On going from 0.3 to 1.0% monomer in the charge, the maximum rate per liter of emulsion increased sevenfold, and between 1 and 2% monomer it increased twofold. If the rates were measured at about the same percent conversion, V_p at that point would be nearly proportional to $[M]_0$, and the term $V_p^{1/2}$ could account for only part of the increase in rate. The rest of the change in rate must come from the increase in $[M]_p$, which

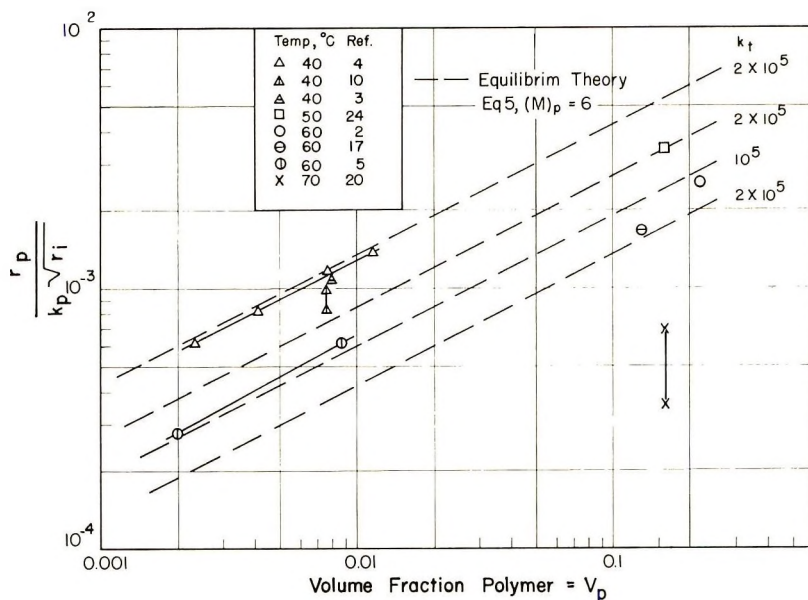


Fig. 5. Test of equilibrium theory.

varied from about 0.2 to 2.0. Analyzing the same or similar data, Dunn and Chong⁸ found a linear relation between the maximum rate and $[M]_w$, (not a proportionality as stated) and a square-root relation with $[M]_p$. However these relationships must be considered coincidental, since the change in volume of the polymer phase was not considered.

The equilibrium theory predicts that the rate varies with the square root of the initiation rate, and published data show exponents from 0.5 to 1. Patsiga et al.² found an exponent of 0.8 for persulfate initiation, Dunn and Taylor⁵ found 0.64, and Dunn and Chong give 1.0 for low concentrations and 0.6 for $[I] > 2 \times 10^{-4}$. O'Donnell²¹ also found a shift from about 1 at low concentration to 0.7. Values of 0.5 were reported by Napper and Parts¹⁰ and by Gershberg.²² Exponents greater than 0.5 may be caused by impurities, which have more effect at low persulfate levels, or by changes

in the rate constant for decomposition of persulfate. Morris and Parts²³ found an increase in the decomposition rate on adding vinyl acetate or soap, but the effect diminished after some reaction took place.

For initiation by radiation, Stannett and co-workers,²⁴ found that the rate varied with the 0.9 power of the dose rate for unseeded emulsions and the 0.26 power for seeded emulsions. No explanation is apparent for this difference.

The data for several investigators are compared by plotting $r_p/(k_p \sqrt{r_i})$ versus V_p , as suggested by eq. (5).^{*} Figure 5 shows that the data of Dunn and Taylor for a dilute emulsion at 60°C fall on about the same line as the concentrated emulsion data of Patsiga et al.² and Okamura²⁵. The theoretical lines are based on $[M]_p = 6$, which occurs at 50% conversion for concentrated emulsion. The dilute emulsion data are for $[M]_p = 5-1.5$, which does not invalidate the comparison, since the rate is independent of $[M]_p$ in this range. However the value of k_t needed to fit the data to eq. (5) changes from $\sim 10^6$ for $[M]_p = 6$ to $\sim 10^5$ for $[M]_p = 2$, since k_t must vary approximately with $[M]_p^2$ if r_p is constant.

The several results at 40°C indicate a termination constant fourfold lower than at 60°C. The point for 50°C is based on the maximum initiation rate used by Stannett, et al.²⁴ assuming a yield of 5 radicals per 100 eV. The point at 70°C is too low even after allowing for some further increase in k_t , and the low rate is attributed to loss of radicals by chain transfer to the polymeric stabilizer that was used. Others have shown that such stabilizers lower the rate even when the particle size is not changed.¹⁶

The calculated values of k_t would afford a final check on the equilibrium theory if good values from another method were available. No such data were found for 40-70°C, but the data of Bengough and Melville²⁶ for bulk polymerizations at 25°C are often cited. They found k_t to be nearly constant at low conversions and then to drop from about 10^7 at $[M] \cong 7$ to about 10^5 at $[M] \cong 4$. The computed values obtained from Figure 5 are slightly lower than these published values, in spite of the higher temperatures, and do not change as rapidly with monomer concentration. However the published values are quite uncertain, and order of magnitude agreement is perhaps all that could be expected. More work is needed to determine the termination constant as a function of temperature and monomer concentration and also the propagation constant, which may decrease at very high viscosities.

In conclusion, the rate data for emulsion polymerization of vinyl acetate indicate that growth and termination take place primarily inside the swollen polymer particles. The data support the concept of an equilibrium distribution of radicals, brought about by a high rate of interchange of radicals between polymer particles. The rapid escape of radicals from particles is possible because of the relatively high rate of chain transfer to monomer and the moderate water solubility of monomeric and oligomeric radicals.

* The initiation rates r_i were calculated by using $k_d = 1.9 \times 10^{-7} \text{ sec}^{-1}$ at 40°C and $4.6 \times 10^{-6} \text{ sec}^{-1}$ at 60°C for persulfate.

References

1. W. V. Smith and R. H. Ewart, *J. Chem. Phys.*, **16**, 592 (1948).
2. R. Patsiga, M. Litt, and V. Stannett, *J. Phys. Chem.*, **64**, 801 (1960).
3. A. Netschey and A. E. Alexander, *J. Polym. Sci. A-1*, **8**, 407 (1970).
4. D. H. Napper and A. E. Alexander, *J. Polym. Sci.*, **61**, 127 (1962).
5. A. S. Dunn and P. A. Taylor, *Makromol. Chem.*, **83**, 207 (1965).
6. E. V. Gulbekian, *J. Polym. Sci. A-1*, **6**, 2265 (1968).
7. M. K. Lindemann, in *Vinyl Polymerization*, Vol. 1, Part 1, G. E. Ham, Ed., New York, Dekker, 1967.
8. A. S. Dunn and L. C.-H. Chong, *Brit. Polym. J.*, **2**, 49 (1970).
9. S. S. Medvedev, *Proceedings of the International Symposium on Macromolecular Chemistry, Prague, 1957*, Pergamon Press, New York.
10. D. H. Napper and A. G. Parts, *J. Polym. Sci.*, **61**, 113 (1962).
11. R. Patsiga, PhD Thesis, Syracuse University, New York, 1962.
12. M. Litt, R. A. Patsiga, and V. Stannett, to be published.
13. W. H. Stockmayer, *J. Polym. Sci.*, **24**, 314 (1957).
14. J. T. O'Toole, *J. Appl. Polym. Sci.*, **9**, 1291 (1965).
15. W. J. Priest, *J. Phys. Chem.*, **56**, 1077 (1952).
16. A. Netschey, D. H. Napper, and A. E. Alexander, *J. Polym. Sci. B*, **7**, 829 (1969).
17. A. Wheeler, *Advan. Catal.*, **3**, 249 (1951).
18. J. L. Gardon, *J. Polym. Sci. A-1*, **6**, 2859 (1968).
19. E. Vanzo, R. H. Marchessault, and V. Stannett, *J. Colloid Sci.*, **20**, 62 (1965).
20. A. Netschey and A. E. Alexander, *J. Polym. Sci. A-1*, **8**, 399 (1970).
21. J. T. O'Donnell, R. B. Mesrobian, and A. E. Woodward, *J. Polym. Sci.*, **28**, 171 (1958).
22. D. S. Gershberg, *J. Polym. Sci.*, **58**, 227 (1962).
23. C. E. M. Morris and A. G. Parts, *Makromol. Chem.*, **119**, 212 (1968).
24. V. Stannett, J. A. Gervasi, J. J. Kearney, and K. Araki, *J. Appl. Polym. Sci.*, **13**, 1175 (1969).
25. S. Okamura and T. Motoyama, *J. Polym. Sci.*, **58**, 221 (1962).
26. W. I. Bengough and H. W. Melville, *Proc. Roy. Soc. (London)*, **A230**, 429 (1955).

Received September 21, 1970

Revised October 22, 1970

ANNOUNCEMENT

The 1971 International Paper Physics Conference, sponsored by the Technical Section of the Canadian Pulp & Paper Association and by TAPPI, will take place in September 1971 at Mont Gabriel Lodge, Mont Gabriel, P. Q., Canada.

Contents (continued)

YASUSHI JOH, KOICHI HARADA, HEIMEI YUKI, and SHUNSUKE MURAHASHI: Stereospecific Polymerization of Isobutyl Vinyl Ether. III. Polymerization with $VCl_3 \cdot LiCl$	1089
Z. JANOVIĆ and D. FLEŠ: Synthesis and Polymerization of Some Optically Active 2- and 1,2-Substituted Butadienes	1103
GEORGE B. VAUGHAN, JERRY C. ROSE, and G. P. BROWN: Polyimides Based on Pyrazinetetracarboxylic Dianhydride and Some Related Model Compounds . . .	1117
C. G. OVERBERGER, A. OHNISHI, and A. S. GOMES: Optical Properties of Inherently Dissymmetric Polyamides	1139
PETER HARRIOTT: Kinetics of Vinyl Acetate Emulsion Polymerization	1153
ANNOUNCEMENT	1165

The *Journal of Polymer Science* publishes results of fundamental research in all areas of high polymer chemistry and physics. The *Journal* is selective in accepting contributions on the basis of merit and originality. It is not intended as a repository for unevaluated data. Preference is given to contributions that offer new or more comprehensive concepts, interpretations, experimental approaches, and results. Part A-1 *Polymer Chemistry* is devoted to studies in general polymer chemistry and physical organic chemistry. Contributions in physics and physical chemistry appear in Part A-2 *Polymer Physics*. Contributions may be submitted as full-length papers or as "Notes." Notes are ordinarily to be considered as complete publications of limited scope.

Three copies of every manuscript are required. They may be submitted directly to the editor: For Part A-1, to C. G. Overberger, Department of Chemistry, University of Michigan, Ann Arbor, Michigan 48104; and for Part A-2, to T. G. Fox, Mellon Institute, Pittsburgh, Pennsylvania 15213. Three copies of a short but comprehensive synopsis are required with every paper; no synopsis is needed for notes. Books for review may also be sent to the appropriate editor. Alternatively, manuscripts may be submitted through the Editorial Office, c/o H. Mark, Polytechnic Institute of Brooklyn, 333 Jay Street, Brooklyn, New York 11201. All other correspondence is to be addressed to Periodicals Division, Interscience Publishers, a Division of John Wiley & Sons, Inc., 605 Third Avenue, New York, New York 10016.

Detailed instructions in preparation of manuscripts are given frequently in Parts A-1 and A-2 and may also be obtained from the publisher.

New Titles in the Polymer Sciences from Wiley-Interscience

ENCYCLOPEDIA OF POLYMER SCIENCE AND TECHNOLOGY

Plastics, Resins, Rubbers, Fibers

Volume 13: Step-Reaction Polymerization to Thermoforming

Executive Editor: NORBERT M. BIKALES, *Consultant*
Editorial Board: HERMAN F. MARK, (*Chairman*),
Polytechnic Institute of Brooklyn
NORMAN G. GAYLORD, *Gaylord Associates, Incorporated*

In recent years, the polymer concept has fused plastics, resins, rubber, fibers, and biomolecules into one body of knowledge. The *Encyclopedia of Polymer Science and Technology* presents the developments, both academic and industrial, that are a result of this fusion.

This latest volume, like the previous, is a collection of authoritative and original articles that were written and reviewed by specialists from all over the world. It comprehensively treats all monomers and polymers, their properties, methods, and processes, as well as theoretical fundamentals.

1970 843 pages (est.) Subscription: \$40.00
Single copy: \$50.00

VINYL AND DIENE MONOMERS

Parts One, Two, and Three

Edited by EDWARD C. LEONARD, *Kraftco Corporation, Glenview, Illinois*

Volume 24 of High Polymers, edited by H. Mark, C. S. Marvel, H. W. Melville, and P. J. Flory

Vinyl and Diene Monomers provides a comprehensive, systematic, and uniform treatment of vinyl and diene monomers.

- Part One describes the manufacture, chemical and physical properties, purification and polymerization behavior of some of the commercially important vinyl monomers. These include acrylonitrile, acrylamides, methacrylic acid and the related esters, vinyl acetate and the higher vinyl esters, and vinyl ethers.
- Part Two parallels the format of Part One, discussing styrene, ethylene, isobutylene, butadiene, isoprene, and chloroprene.
- Part Three similarly treats vinyl and vinylidene chloride, the fluorocarbon monomers, and certain miscellaneous monomers such as N-vinyl compounds, vinyl sulfur compounds, vinylfuran, and certain substituted styrenes.

Part One: 1970 477 pages \$19.95
Part Two: 1971 704 pages \$37.50
Part Three: 1971 432 pages \$24.95

MOLECULAR WEIGHT DISTRIBUTION IN POLYMERS

by LEIGHTON H. PEEBLES, JR., *Chemstrand Research Center, Inc., Durham, North Carolina*

Volume 18 of Polymer Reviews, edited by H. F. Mark and E. H. Immergut

Molecular Weight Distribution in Polymers deals with the question, "How do changes in the manufacturing process affect the molecular weight distribution of the polymers?" Special features include—

- distribution functions that are presented mainly without derivation and with a minimum of commentary on the assumptions used
- standardization of the nomenclature for equations which are illustrated with many examples based on computer calculations
- distributions, derived for polymers with a number-average molecular weight of 100, which may be compared with any other degree of polymerization to a good approximation
- references to the original literature that enable the reader to examine the derivation

1971 352 pages \$17.50

PHYSICAL CHEMISTRY OF ADHESION

By DAVID H. KAEUBLE, *Science Center, North American Rockwell Corporation*

This comprehensive treatment of adhesion phenomena covers thermodynamics, surface chemistry, polymer physics and rheology, as well as specialized topics in the mechanics of fracture.

Physical Chemistry of Adhesion is divided into three major sections. The first section, on surface chemistry, emphasizes the analysis of contact angle experiments. The second section, on rheology, presents the significance of thermal expansivity and compressibility measurements in defining the polymer physical state. The third section, on fracture mechanics, analyzes six basic rheological operations, and deals directly with the phenomenological and engineering aspects of adhesion and cohesion phenomena.

1971 528 pages \$27.50

wiley

WILEY-INTERSCIENCE

a division of JOHN WILEY & SONS, Inc.
605 Third Avenue, New York, New York 10016

In Canada:
22 Worcester Road, Rexdale, Ontario

1688254